

Czech Technical University in Prague

Faculty of Electrical Engineering

Doctoral Thesis



September, 2020

Ing. Ibrahim Ahmad

Czech Technical University in Prague
Faculty of Electrical Engineering
Department of Electrical Power Engineering

***Power Quality Improvement in Smart Grids Using DG
Units***

Doctoral Thesis

Ing. Ibrahim Ahmad

Prague, 2020

Ph.D. Programme: Electrical Engineering and Information Technology (P2612)

Branch of study: Electric Power Engineering (3907V001)

Supervisor: doc. Ing. Zdeněk Müller Ph.D.

Supervisor - specialist: doc. Dr. Ing. Jan Kyncl

Declaration

I hereby declare that I worked out the presented thesis independently and I quoted all used sources of information in accord with Methodical instructions about ethical principles for writing academic thesis.

.....

Ing. Ibrahim Ahmad

Acknowledgment

First of all, I would like to give my special gratitude to my supervisor, doc. Ing. Zdeněk Müller Ph.D. and my Supervisor - specialist, doc. Dr. Ing. Jan Kyncl for their supervision, guidance and advice from the beginning of this dissertation and giving me the experience throughout the work. Also, I would like to thank Professor Josef Tlustý for his support, assistance, kindness, and helpful discussions. Also, I would like to thank you for your encouragement me to work and learn new things from your experience. It is a great honor for me to work under your supervision.

I would like to thank my colleagues and all members of staff in the Department of Electrical Power Engineering for their support, assistance, and helpful discussions.

I would also like to thank my friends for their encouragement.

Finally, my greatest gratitude goes to my parents and siblings for their encouragement and support during my studies.

My research has been partially supported by the Ministry of Education, Youth and Sports of the Czech Republic, and by the Grant Agency of the Czech Technical University in Prague: (SGS17/181/OHK3/3T/13).

Abstract

Increased penetration of renewable energy sources in the electrical grid due to the rapid increase of power demand and the need of diverse energy sources; makes Distributed Generation (DG) units an essential part of the modern electrical grids. Integration of many DG units in the smart grids requires control and coordination between them and the grid to maximize the benefits of the DG units. Smart grids and modern electronic devices require high standards of power quality, especially voltage quality [118].

In this research, a new methodology has been presented to improve voltage quality and power factor in smart grids. This method depends on using voltage variation and admittance values as inputs of a controller which controls the reactive power generation in all DG units. The results show that the controller is efficient in improving voltage quality and power factor [118].

Keywords: Voltage quality; power factor; smart grids; distributed generation; renewable energy; power quality.

Abstrakt

Díky vzrůstající poptávce po obnovitelných zdrojích energie, která je vyvolaná rychlým nárůstem spotřeby energie se stává decentralizovaná výroba elektrické energie nedílnou součástí moderní elektrické sítě. Dobrá kontrola a koordinace mezi nimi a sítí zvyšuje výrazným způsobem její přínos. Chytré sítě a moderné elektronické zařízení mají vysoké nároky na kvalitu energie a to především na kvalitu napětí[118].

V této práci byla představena nová metoda pro zlepšení kvality napětí a výkon pro chytré sítě. Tato metoda závisí na využití střídání napětí na vstupu a ovladači, který kontroluje výrobu energie ve všech částech decentralizované sítě. Výsledky ukazují, že ovladač účinně zlepšuje kvalitu napětí a výkon sítě [118].

Klíčová slova: kvalita napětí, výkon sítě, chytré sítě, decentralizovaná výroba elektrické energie, obnovitelné zdroje energie, kvalita napětí.

Contents

Declaration.....	i
Acknowledgment.....	ii
Abstract.....	iii
Abstrakt.....	iv
Contents.....	v
List of figures.....	ix
List of tables.....	xiii
Chapter 1.....	14
1 Introduction.....	14
Chapter 2.....	16
2 Literature Review.....	16
2.1 Conventional electrical grid.....	16
2.1.1. Infrastructure of conventional electrical networks.....	16
2.1.2 Main characteristics of conventional electrical networks.....	17
2.1.3. Environmental impacts of conventional electrical networks.....	18
2.2 Motives and drivers of the Smart Grid concept.....	20
2.3. Smart grid.....	21
2.3.1. Background and history of Smart Grid evolution.....	21
2.3.2. Comparison between Smart Grid and conventional electrical networks.....	23
2.3.3. The main features of Smart Grid.....	25
2.3.4. Benefits of smart grids.....	27
2.3.5. Smart grid composition.....	28
2.3.6. Infrastructure of the smart grid.....	30
2.3.7. New Trends in Distribution Systems and New Types of Load.....	31
2.4. Power Quality.....	32
2.4.1. Importance of Power Quality.....	32
2.4.2. Ensuring power Quality of electrical grids.....	33
2.4.2.1. The reliability of supply.....	33
2.4.2.2. The voltage quality.....	34
2.4.2.3. The service quality.....	36

- 2.4.3. Steady State voltage 37
 - 2.4.3.1. Voltage value and power factor..... 37
 - 2.4.3.2. Long-Duration Voltage Variations..... 38
 - A. Overvoltage..... 38
 - B. Undervoltage 38
 - C. Sustained interruptions 38
- 2.5. Distributed Generation 39
 - 2.5.1 Categories of DG 40
 - 2.5.2. Specifications for DG Concepts..... 40
 - 2.5.3. DG Benefits 41
 - 2.5.4. DG policies 41
- 2.6. Wind Farms 42
 - 2.6.1. Wind Turbine types..... 43
 - 2.6.2. Concept Model of Wind Turbine Generators 46
 - 2.6.3. PMSG modeling..... 47
 - 2.6.4. Model of the Full scale converter system in wind farms..... 48
 - 2.6.5. Model structure of generator and converter 49
 - 2.6.5.1 Current Limitation..... 50
 - 2.6.5.2 DC-Link Energy Absorber 52
 - 2.6.5.3 Resulting Generator and Converter Model 53
 - 2.6.6. Control Structures for Grid Converter 53
 - 2.6.6.1 The dg Control..... 54
 - 2.6.6.2 Stationary Frame Control..... 54
 - 2.6.6.3 The abc Frame Control..... 55
 - 2.6.7 Control Structure of Wind Turbines..... 57
 - 2.6.8 Voltage profile stability in wind farms systems 59
 - 2.6.9 Voltage stability improvement and FACTS devices..... 60
 - 2.6.9.1 Static Var Compensator (SVC):..... 60
 - 2.6.9.2 Static Synchronous Compensator (STATCOM) 63
- Chapter 3..... 66
 - 3 Methodology..... 66
 - 3.1. General approach..... 66
 - 3.2. Case Study..... 73

3.2.1. Proposed mesh grid	73
3.2.2. Simulation and procedures	74
Chapter 4.....	76
4 Results.....	76
4.1 Voltage profile and $\cos\phi$	76
4.1.1 Speed 15 m/s	76
4.1.1.1 Voltage deviation % of busbars	76
4.1.1.2 Sending voltage deviation % of transmission lines	78
4.1.1.3 Receiving voltage deviation % of transmission lines	80
4.1.1.4 Voltage drop % of transmission lines.....	82
4.1.1.5 Sending $\cos(\phi)$ of transmission lines	84
4.1.1.6 Receiving $\cos(\phi)$ of transmission lines.....	86
4.1.2 Speed 10 m/s	88
4.1.2.1 Voltage deviation % of busbars	88
4.1.2.2 Sending voltage deviation % of transmission lines	90
4.1.2.3 Receiving voltage deviation % of transmission lines	91
4.1.2.4 Voltage drop % of transmission lines.....	93
4.1.2.5 Sending $\cos(\phi)$ of transmission lines	94
4.1.2.6 Receiving $\cos(\phi)$ of transmission lines.....	96
4.1.3 Speed 5 m/s	98
4.1.3.1 Voltage deviation % of busbars	98
4.1.3.2 Sending voltage deviation % of transmission lines	99
4.1.3.3 Receiving voltage deviation % of transmission lines	101
4.1.3.4 Voltage drop % of transmission lines.....	103
4.1.3.5 Sending $\cos(\phi)$ of transmission lines	104
4.1.3.6 Receiving $\cos(\phi)$ of transmission lines.....	106
4.1.4 Fault Line 2-3 (speed 5 m/s).....	107
4.1.4.1 Voltage deviation % of busbars	107
4.1.4.2 Sending voltage deviation % of transmission lines	109
4.1.4.3 Receiving voltage deviation % of transmission lines	110
4.1.4.4 Voltage drop % of transmission lines.....	112
4.1.4.5 Sending $\cos(\phi)$ of transmission lines	114
4.1.4.6 Receiving $\cos(\phi)$ of transmission lines.....	115

4.2 Power losses.....	116
4.2.1 Speed 15 m/s	116
4.2.2 Speed 10 m/s	118
4.2.3 Speed 5 m/s	119
4.2.3 Fault Line 2-3 (speed 5 m/s).....	120
4.5 Results Summary.....	121
Chapter 5.....	123
5 Conclusion.....	123
Chapter 6.....	125
6 Literatures	125
6.1 References	125
6.2 Author’s Publications	132
6.2.1 Publications in the Framework of the Thesis.....	132
6.2.1.1 Publications in Impact Factor Journals	132
6.2.1.2 Publications in Reviewed Journals	132
6.2.1.3 Patents	132
6.2.1.4 Publications in WoS and Scopus	132
6.2.1.5 Publications are not in WoS and Scopus.....	132
6.2.2 Other Publications	132
6.2.2.1 Publications in Impact Factor Journals	132
6.2.2.2 Publications in Reviewed Journals.....	133
6.2.2.3 Patents	133
6.2.2.4 Publications in WoS and Scopus	133
6.2.2.5 Publications are not in WoS and Scopus.....	133
6.2.3 Submitted Publications	133
6.2.4 Awards	133
Chapter 7.....	134
7 Appendix	134
7.1 Transformers parameters	134
7.2 Results for wind speed 15 m/s.....	134
7.3 Results for wind speed 10 m/s.....	136
7.4 Results for wind speed 5 m/s.....	138
7.5 Results for fault L 2-3, wind speed 5 m/s.....	140

List of figures

Figure 2.1 Principles of vertical structure of conventional power systems whereby the flow of electricity is unidirectional [17]	17
Figure 2.2 Architecture of the traditional electric power grid [19].	17
Figure 2.3 CO ₂ Emissions in the USA [22].....	18
Figure 2.4 Global Emissions by Gas [24]	19
Figure 2.5 Global Emissions by Economic Sector [24]	20
Figure 2.6 The reserve expectations for primary energy and the annual world demand (Sources a [27], b [28]).....	21
Figure 2.7 Key features of Smart grid [51]	25
Figure 2.8 Interaction of Roles in Different Smart Grid Domains through Secure Communication [54] ...	29
Figure 2.9 The Smart Grid basic infrastructure [17]	30
Figure 2.10 Changing conditions in the distribution networks due to DER integration [26].....	31
Figure 2.11 European benchmark of the system average interruption duration index [59].....	34
Figure 2.12 Connection of distributed generation units [63]	39
Figure 2.13 Global cumulative wind power capacity from 2001 to 2020 [65]	42
Figure 2.14 Developments of power electronics for the wind turbines between 1980 and 2020 (E); gray area inside the turbine circle indicates the power rating coverage by power electronics; D means diameter of the rotor [67].	43
Figure 2.15 Type 1 wind turbines [73].	44
Figure 2.16 Type 2 wind turbines [73].	44
Figure 2.17 Type 3 wind turbines [73].	45
Figure 2.18 Type 4 wind turbines [73].	45
Figure 2.19 WTG control blocks and dynamics [74].	46
Figure 2.20 Key components of FSC system [73].	49
Figure 2.21 Core of generator model of machine and current control [73].	50
Figure 2.22 Current limitation block model [73].	51
Figure 2.23 Aggregated generator model for Full scale converter [73].	53
Figure 2.24 (a) Representation of single-phase circuit used to derive the DB controller equation, where $LT = Li + Lg$ and $RT = Ri + Rg$ (b) Single-phase representation of the LCL filter used to calculate the gains of the controllers [80].....	55
Figure 2.25 Aggregated generator model for Full scale converter [99].	57
Figure 2.26 Control of a wind turbine with DFIG [99].....	58
Figure 2.27 Control of active and reactive power in a wind turbine with multipole PMSG [99].	59
Figure 2.28 Single-phase equivalent circuit of the shunt SVC (TCR) [111].	61
Figure 2.29 Voltage-current characteristics of the SVC [111].....	62
Figure 2.30 Equivalent circuit of the STATCOM [111].	63
Figure 2.31 Voltage-current characteristics of the STATCOM [111].....	64
Figure 3.1 General electrical system [118].	67
Figure 3.2 Control system structure [118].....	68
Figure 3.3 Proposed control algorithm of busbar No. 1 [118].....	72
Figure 3.4 Proposed algorithm for the entire system [118].	73

Figure 3.5 Proposed mesh grid [118].	74
Figure 4.1 Voltage deviation % comparison between (normal) and (controlled DG) cases for all busbars (15 m/s) [118].	77
Figure 4.2 Voltage deviation % comparison between (normal) and (DG) cases for all busbars(15 m/s) .	78
Figure 4.3 Sending voltage deviation % comparison between (normal) and (controlled DG) cases for all transmission lines(15 m/s) [118].	79
Figure 4.4 Sending voltage deviation % comparison between (normal) and (DG) cases for all transmission lines (15 m/s).	80
Figure 4.5 Receiving voltage deviation % comparison between (normal) and (controlled DG) cases for all transmission lines (15 m/s) [118].	81
Figure 4.6 Receiving voltage deviation % comparison between (normal) and (DG) cases for all transmission lines (15 m/s).	82
Figure 4.7 Voltage drop (%) comparison between (normal) and (controlled DG) cases for all transmission lines (15 m/s) [118].	83
Figure 4.8 Voltage drop (%) comparison between (normal) and (DG) cases for all transmission lines (15 m/s).	84
Figure 4.9 Sending $\cos(\phi)$ comparison between (normal) and (controlled DG) cases for all transmission lines (15 m/s) [118].	85
Figure 4.10 Sending $\cos(\phi)$ comparison between (normal) and (DG) cases for all transmission lines (15 m/s).	86
Figure 4.11 Receiving $\cos(\phi)$ comparison between (normal) and (controlled DG) cases for all transmission lines (15 m/s) [118].	87
Figure 4.12 Receiving $\cos(\phi)$ comparison between (normal) and (DG) cases for all transmission lines (15 m/s).	88
Figure 4.13 Voltage deviation % comparison between (normal) and (controlled DG) cases for all busbars (10 m/s).	89
Figure 4.14 Voltage deviation % comparison between (normal) and (DG) cases for all busbars (10 m/s).	89
Figure 4.15 Sending voltage deviation % comparison between (normal) and (controlled DG) cases for all transmission lines(10 m/s).	90
Figure 4.16 Sending voltage deviation % comparison between (normal) and (DG) cases for all transmission lines(10 m/s).	91
Figure 4.17 Receiving voltage deviation % comparison between (normal) and (controlled DG) cases for all transmission lines (10 m/s).	92
Figure 4.18 Receiving voltage deviation % comparison between (normal) and (DG) cases for all transmission lines (10 m/s).	92
Figure 4.19 Voltage drop (%) comparison between (normal) and (controlled DG) cases for all transmission lines (10 m/s).	93
Figure 4.20 Voltage drop (%) comparison between (normal) and (DG) cases for all transmission lines (10 m/s).	94
Figure 4.21 Sending $\cos(\phi)$ comparison between (normal) and (controlled DG) cases for all transmission lines (10 m/s).	95
Figure 4.22 Sending $\cos(\phi)$ comparison between (normal) and (DG) cases for all transmission lines (10 m/s).	96

Figure 4.23 Receiving $\cos(\phi)$ comparison between (normal) and (Controlled DG) cases for all transmission lines (10 m/s).....	97
Figure 4.24 Receiving $\cos(\phi)$ comparison between (normal) and (DG) cases for all transmission lines (10 m/s).....	97
Figure 4.25 Voltage deviation % comparison between (normal) and (controlled DG) cases for all busbars (5 m/s).....	98
Figure 4.26 Voltage deviation % comparison between (normal) and (DG) cases for all busbars (5 m/s).....	99
Figure 4.27 Sending voltage deviation % comparison between (normal) and (controlled DG) cases for all transmission lines(5 m/s).....	100
Figure 4.28 Sending voltage deviation % comparison between (normal) and (DG) cases for all transmission lines(5 m/s).....	101
Figure 4.29 Receiving voltage deviation % comparison between (normal) and (controlled DG) cases for all transmission lines(5 m/s).....	102
Figure 4.30 Receiving voltage deviation % comparison between (normal) and (DG) cases for all transmission lines(5 m/s).....	102
Figure 4.31 Voltage drop (%) comparison between (normal) and (controlled DG) cases for all transmission lines (5 m/s).....	103
Figure 4.32 Voltage drop (%) comparison between (normal) and (DG) cases for all transmission lines (5 m/s).....	104
Figure 4.33 Sending $\cos(\phi)$ comparison between (normal) and (controlled DG) cases for all transmission lines (5 m/s).....	105
Figure 4.34 Sending $\cos(\phi)$ comparison between (normal) and (DG) cases for all transmission lines (5 m/s).....	105
Figure 4.35 Receiving $\cos(\phi)$ comparison between (normal) and (controlled DG) cases for all transmission lines (5 m/s).....	106
Figure 4.36 Receiving $\cos(\phi)$ comparison between (normal) and (DG) cases for all transmission lines (5 m/s).....	107
Figure 4.37 Voltage deviation % comparison between (normal) and (controlled DG) cases for all busbars (fault line 2-3, 5 m/s).....	108
Figure 4.38 Voltage deviation % comparison between (normal) and (DG) cases for all busbars (fault line 2-3, 5 m/s).....	108
Figure 4.39 Sending voltage deviation % comparison between (normal) and (controlled DG) cases for all transmission lines((fault line 2-3, 5 m/s).....	109
Figure 4.40 Sending voltage deviation % comparison between (normal) and (DG) cases for all transmission lines((fault line 2-3, 5 m/s).....	110
Figure 4.41 Receiving voltage deviation % comparison between (normal) and (controlled DG) cases for all transmission lines((fault line 2-3, 5 m/s).....	111
Figure 4.42 Receiving voltage deviation % comparison between (normal) and (DG) cases for all transmission lines((fault line 2-3, 5 m/s).....	112
Figure 4.43 Voltage drop % comparison between (normal) and (controlled DG) cases for all transmission lines ((fault line 2-3, 5 m/s).....	113
Figure 4.44 Voltage drop % comparison between (normal) and (DG) cases for all transmission lines ((fault line 2-3, 5 m/s).....	113

Figure 4.45 Sending $\cos(\phi)$ comparison between (normal) and (controlled DG) cases for all transmission lines ((fault line 2-3, 5 m/s).	114
Figure 4.46 Sending $\cos(\phi)$ comparison between (normal) and (DG) cases for all transmission lines ((fault line 2-3, 5 m/s).	115
Figure 4.47 Receiving $\cos(\phi)$ comparison between (normal) and (controlled DG) cases for all transmission lines ((fault line 2-3, 5 m/s).	115
Figure 4.48 Receiving $\cos(\phi)$ comparison between (normal) and (DG) cases for all transmission lines ((fault line 2-3, 5 m/s).	116
Figure 4.49 Total power losses comparison between (normal) and (controlled DG) cases (15 m/s).	117
Figure 4.50 Total power losses comparison between (normal) and (controlled DG) cases (10 m/s).	118
Figure 4.51 Total power losses comparison between (normal) and (controlled DG) cases (5 m/s).	119
Figure 4.52 Total power losses comparison between (normal) and (controlled DG) cases (fault line 2-3, 5 m/s).	120
Figure 7.1 MATLAB Simulink model of the electrical system.	143
Figure 7.2 MATLAB Simulink model of the controller (Busbars voltage inputs).....	144
Figure 7.3 MATLAB Simulink model of the controller (Reactive power inputs).	145

List of tables

Table 2.1 Fundamental differences between the Smart Grid and conventional electrical networks [45]	24
Table 2.2 Domains and Roles/Services in the Smart Grid Conceptual Model [54]	28
Table 2.3 Globally used reliability indices [58]	33
Table 2.4 Disturbances of the voltage quality and their impact [26]	35
Table 2.5 Bandwidths and requirements of EN 50160 for voltage quality [60]	36
Table 2.6 Service quality characteristics, bandwidth of limits and penalties [58]	37
Table 3.1 Loads values for all steps [118]	75
Table 4.1 Sending active power values of lines for all steps (15 m/s) [kW]	117
Table 4.2 Receiving active power values of lines for all steps (15 m/s) [kW]	117
Table 4.3 Sending active power values of lines for all steps (10 m/s) [kW]	118
Table 4.4 Receiving active power values of lines for all steps (10 m/s) [kW]	118
Table 4.5 Sending active power values of lines for all steps (5 m/s) [kW]	119
Table 4.6 Receiving active power values of lines for all steps (5 m/s) [kW]	119
Table 4.7 Sending active power values of lines for all steps (fault line 2-3, 5 m/s) [kW]	120
Table 4.8 Receiving active power values of lines for all steps (fault line 2-3, 5 m/s) [kW]	121
Table 7.1 Parameters of the three-phase 0.575/66 kV transformer of Wind farm A [118]	134
Table 7.2 Parameters of the three-phase 0.575/66 kV transformer of Wind farm B [118]	134
Table 7.3 Parameters of the three-phase 0.575/66 kV transformer of Wind farm A [118]	134
Table 7.4 Voltage values of busbars for all steps and all cases (V) (15 m/s) [118]	134
Table 7.5 Sending voltage values of lines for all steps and all cases (V) (15 m/s) [118]	135
Table 7.6 Receiving voltage values of lines for all steps and all cases (V) (15 m/s) [118]	135
Table 7.7 Voltage drop values of lines for all steps and all cases (V) (15 m/s) [118]	135
Table 7.8 Sending $\cos(\phi)$ values of lines for all steps and all cases (15 m/s) [118]	136
Table 7.9 Receiving $\cos(\phi)$ values of lines for all steps and all cases (15 m/s) [118]	136
Table 7.10 Voltage values of busbars for all steps and all cases (V) (10 m/s)	136
Table 7.11 Sending voltage values of lines for all steps and all cases (V) (10 m/s)	137
Table 7.12 Receiving voltage values of lines for all steps and all cases (V) (10 m/s)	137
Table 7.13 Voltage drop values of lines for all steps and all cases (V) (10 m/s)	137
Table 7.14 Sending $\cos(\phi)$ values of lines for all steps and all cases (10 m/s)	138
Table 7.15 Receiving $\cos(\phi)$ values of lines for all steps and all cases (10 m/s)	138
Table 7.16 Voltage values of busbars for all steps and all cases (V) (5 m/s)	138
Table 7.17 Sending voltage values of lines for all steps and all cases (V) (5 m/s)	139
Table 7.18 Receiving voltage values of lines for all steps and all cases (V) (5 m/s)	139
Table 7.19 Voltage drop values of lines for all steps and all cases (V) (5 m/s)	139
Table 7.20 Sending $\cos(\phi)$ values of lines for all steps and all cases (5 m/s)	140
Table 7.21 Receiving $\cos(\phi)$ values of lines for all steps and all cases (5 m/s)	140
Table 7.22 Voltage values of busbars for all steps and all cases (V) (Fault line 2-3, 5 m/s)	140
Table 7.23 Sending voltage values of lines for all steps and all cases (V) (Fault line 2-3, 5 m/s)	141
Table 7.24 Receiving voltage values of lines for all steps and all cases (V) (Fault line 2-3, 5 m/s)	141
Table 7.25 Voltage drop values of lines for all steps and all cases (V) (Fault line 2-3, 5 m/s)	141
Table 7.26 Sending $\cos(\phi)$ values of lines for all steps and all cases (Fault line 2-3, 5 m/s)	142
Table 7.27 Receiving $\cos(\phi)$ values of lines for all steps and all cases (Fault line 2-3, 5 m/s)	142

Chapter 1

1 Introduction

Renewable energy sources (RES) especially wind, solar and biomass have become an important part of modern grids, and it is predicted that the number of RES units will increase rapidly within the European Union where, according to [1], the share of renewable energy sources (RES) will rise substantially, achieving at least 55% of gross final energy consumption in 2050. Further, renewables will account for almost one-third of the total electricity output in the world by 2035 [2]. According to International Energy Agency (IEA), renewable power capacity will grow by 50% between 2019 and 2024. This expected increase is 1 200 GW that is equivalent to the total installed power capacity of the United States. Wind farms will contribute 29% of this growth. Also, China will contribute for about 40% of expansion of global renewable capacity and about 50% of global distributed Photovoltaic (PV) growth over the forecast period. Moreover, heat generated from renewable energy is expected to expand by about 20% over this period. Furthermore, electrical power from renewable sources used for heat is anticipated to rise by approximately 40% [3], [118].

Due to the high penetration of renewable energy sources in the electrical systems, the electrical power system changed from centralized generation to distributed generation (DG) or decentralized generation. DG can be defined as on-site generation which is directly connected to the distribution networks in order to support the grid on distribution levels [4]. There are a lot of benefits of DG, such as reducing transmission and distribution costs and increasing the efficiency of energy [5]. Also, DG units play an important role in minimizing pollution, especially CO₂ [6]. Moreover, DG could play a big role in security and emergency energy systems for cities, as mentioned in [7]. In addition, photovoltaic energy systems in homes increases the efficiency of networks both in capital and utilization rates [8]. DG units could also be used to maximize the voltage profile and minimize power loss [9]. These units vary between non-traditional units such as wind turbines, photovoltaic farms, and fuel cells, as well as traditional generators such as micro turbines, therefore, modern grids have become more complex [10]. The increased numbers of DG units in the grids require operators and designers to deal with a greater number of power sources and more complex systems [118].

The increased complexity of electrical grids and high sensitivity of modern devices demand high quality, reliability, and flexibility in the modern electrical networks. The rapid development of technology and control systems has driven electricity companies and operators to transition from conventional grids to smart grids. The term ‘smart grid’ according to the (EU) vision, refers to the intelligent integration of all generations and consumers in order to provide a reliable, secure, economic, and sustainable energy supply [11]. In fact, many technical and business challenges have been raised with respect to the integration of the DG units in smart grids [12], [118].

Power quality is one of the essential needs of obtaining a reliable energy supply in smart grids, where the appropriate power quality maintains the extent of compatibility between all the equipment of grid parts [13]. The importance of power quality is based on serious problems that could occur when power quality is lacking-such difficulties could include, but are not limited to, troubles related to essential business applications, sensitive industrial processes, and

important public services, i.e., hospitals and traffic control [14]. Power quality issues could be classified into five categories: short duration variation, long duration variation (and power factor), transients, voltage imbalance, and waveform distortion [15]. Long duration variations have long term impacts on voltage quality, so it is important to minimize them as much as possible [118].

Voltage control and minimize its variation over the time is one of most important aspects of the voltage quality in the smart grids. DG units which are equipped with full scale converters have the capability to generate reactive power separately from active power [16]. As there is a strong relationship between voltage and reactive power, we can control full scale converters in the DG units in order to control the voltage. The topology of the electrical grid is prone to change because of adding new DG units or loads over the years. Also, the power by DG units and loads is changeable continuously. Therefore, the need to control the voltage in robust way becomes more essential [118].

The used grid in this dissertation is meshed one which has a combination of radial and loop parts. We used both of the voltage deviation values for all grid busbars and the influence of the DG unit location (i.e., admittance values) as main parameters to control the voltage, minimize voltage variations and power losses as well. Voltage deviation and admittance values have a significant impact on the reactive power flow and voltage profile. The used data in the simulation model are from a real network. We made different scenarios of loads to test the performance of the model in various cases. In this work, we focus on improving voltage quality by minimizing the long duration variations of voltage and improving power factor to achieve better voltage quality. The model is created using MATLAB Simulink software [118].

Chapter 2

2 Literature Review

2.1 Conventional electrical grid

2.1.1. Infrastructure of conventional electrical networks

In general, conventional electrical grid usually made up of many systems which include generation, transmission, distribution, and consumer (load) systems. Generation system which is the most complicated one usually consists of large-scale centralized generation plants which are combined together where the typical modern unit in these plants has rated value of over 1,000 MW. A transmission system is normally used to transfer bulk of power from the large-scale centralized generating plants to distribution systems. The used voltages in the transmission system over long distances are high, extra, and ultra-high voltage levels. Standard voltage levels which are used in transmission systems are 275 kV, 400 kV, 500 kV, 765 kV, and 1100 kV. Regarding distribution systems, their mission is to receive the supplied electric power from transmission system then deliver it to the consumers. It could be noticed clearly the passive role of the distribution network. It is therefore important to note that the role of a distribution network is passive because its work is limited by transferring electrical power from generation and transmission systems to consumers. The standard voltage levels of distribution system involve 11 kV, 20 kV, 33 kV, 66 kV, 110 kV, and 132 kV. The design and infrastructure of the traditional grid relies on the requirements which have been written in the 1950s, when the main purpose was to keep the lights on. This design based on using large-centralized power plants to supply power to the load centers over an electro-mechanical grid. This approach called producer-controlled model as there is only one way or power flow. In such grids, there is no two-way direction which allows grid and consumers to interact with each other [17],[18].

In general, conventional electrical grids have vertical structure. In such grids, the electric power which has been generated by the generation system will pass through transmission system to distribution network which in turn supply the electric power to the load centers. Vertical structure of the conventional electrical networks is illustrated in Figure 2.2 shows where electric power flows in one-way mode, starting from generation system, then going through transmission system till reaching distribution networks which feed it to the final loads. Control system which uses in such grids is a centralized one and known as Supervisory Control and Data Acquisition (SCADA) systems which will supervise energy production process and distribution. SCADA is the responsible system of visualizing and mapping any operational activity in the electrical network. Actually, SCADA systems is very useful in reducing costs and minimizing unnecessary power generation because it can control the transmission and distribution of power locally or remotely according to the current demand and peak loads as shown in Figure 2.3 [17],[19].

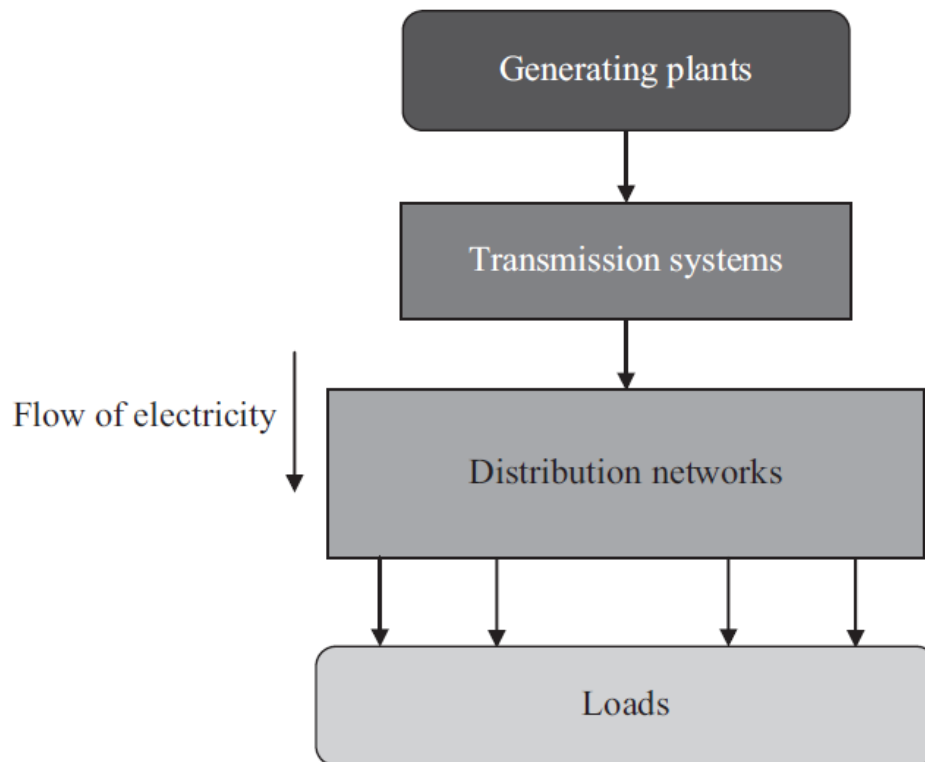


Figure 2.1 Principles of vertical structure of conventional power systems whereby the flow of electricity is unidirectional [17]

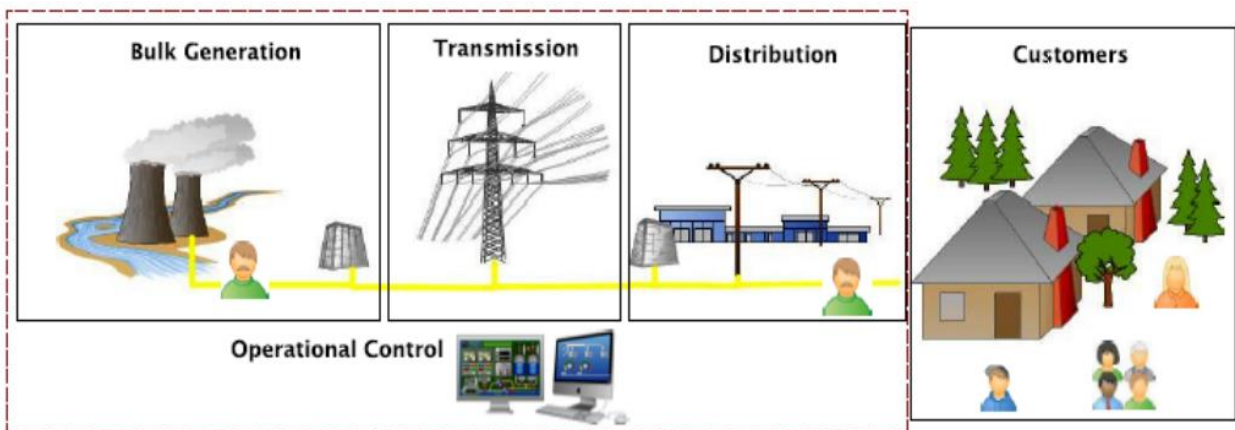


Figure 2.2 Architecture of the traditional electric power grid [19].

2.1.2 Main characteristics of conventional electrical networks

The main properties of conventional electrical grids are:

- (i) The vertical structure of conventional electrical grid.
- (ii) Power flow is one way and it is especially true for distribution networks.

(iii) The price of electric power is strongly related to which utility the consumer is linked. That means, there is no choice for consumers of choosing the company which they want to buy electricity from it, thereby, consumers play a passive role. [17]

2.1.3. Environmental impacts of conventional electrical networks

The electrical power network has been providing many useful services to the societies since a long time with some intermittent problems such as blackouts. Although, currently the used energy by the countries is only a small part in form of electricity. The harmful effects of electrical power generation due to the emissions comes not only from power plants but also from other part of its fuel chain. These emissions could be categorized into solid, liquid, gaseous and radioactive emissions. In general, power plants depend basically on energy sources in form of petroleum, coal, gas, and biomass. Furthermore, the efficiency of the electrical generation system which convert the traditional forms of energy such as petroleum or gas is relatively low. The inefficiencies of these electrical generation systems are transformed into emissions such as CO₂ which has big impact on environment especially in countries such as USA where most of the energy came from fossil fuels sources. In fact, the electrical sector is responsible for about 40% of the CO₂ emissions in USA as shown in the Figure 2.4 [20].

Actually, the real problem is not necessarily from missions themselves, but it is because of their influences on the environment. For instance, breathing in of air containing high levels of sulphates with specific other emissions can cause an increase of the premature death probability. In fact, Sulphur dioxide can has some benefits at low concentrations that it can increase growth of certain plants, but at high levels it will decrease the growth of them. If Sulphur dioxide combined with water, it forms acids which have a corrosive impact on a various material. [21]

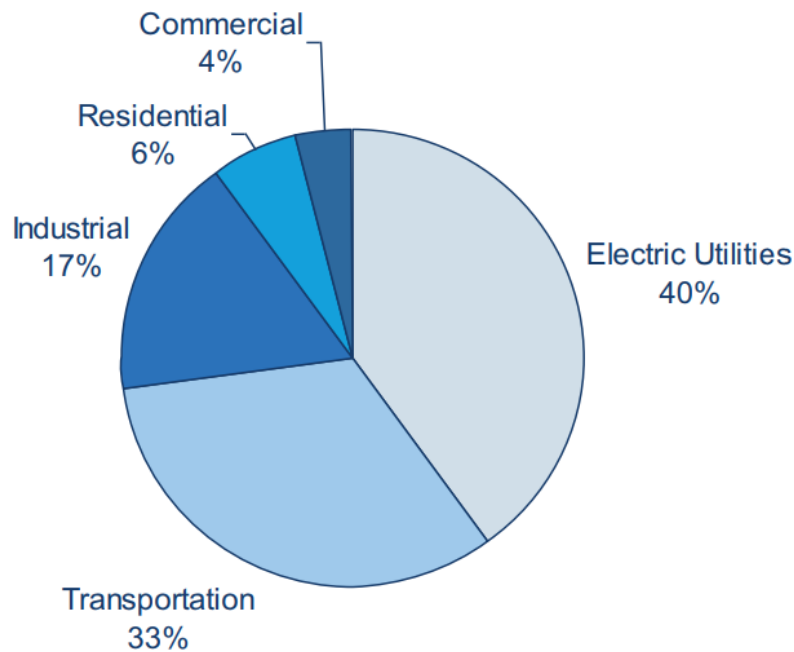


Figure 2.3 CO₂ Emissions in the USA [22].

Global Emissions by Gas

Actually, the most significant greenhouse gases which are emitted by human activities on the global scale are:

- Carbon dioxide (CO₂).
- Methane (CH₄).
- Nitrous oxide (N₂O).
- Fluorinated gases (F-gases). [23]

Figure 2.5 shows the percentage of them.

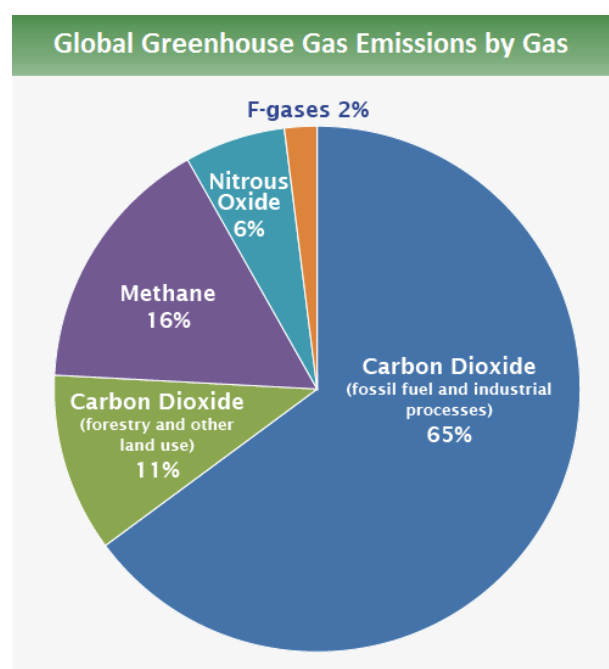


Figure 2.4 Global Emissions by Gas [24]

Global Emissions by Economic Sector

Greenhouse emissions can be divided by the economic activities the cause releasing them. We can notice in Figure 2.6 the contribution of each sector in the global emissions. The figure shows that energy sector causes about 35% of the global emissions.

- Electricity and Heat Production.
- Industry
- Agriculture, Forestry, and Other Land Use
- Transportation
- Buildings

- Other Energy [23], [24]

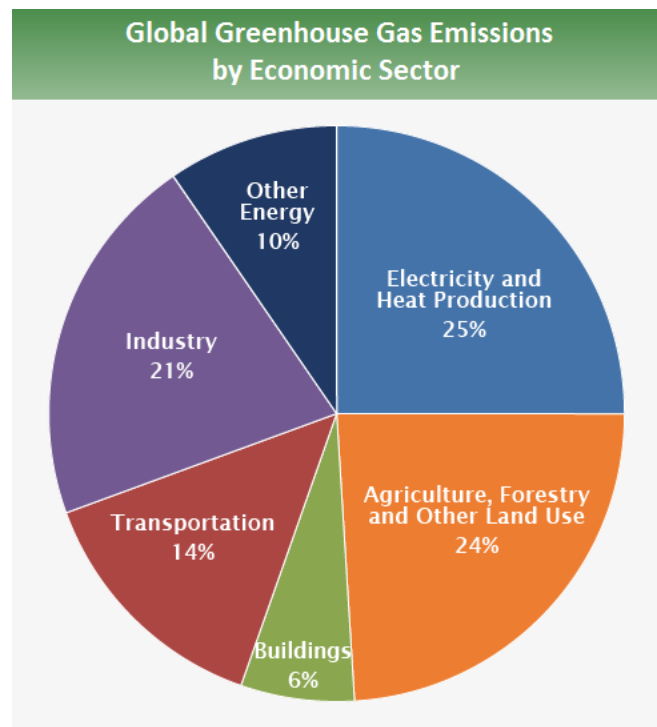


Figure 2.5 Global Emissions by Economic Sector [24]

2.2 Motives and drivers of the Smart Grid concept

Actually, achieving efficient transmission and distribution of electricity is an essential need for sustainable development and growth throughout the world. Nevertheless, electrical grids will have to face big challenges in this field in the 21st century. The most important challenges that the European Union has to deal with are [25],[26]:

- Decreasing the available primary energy sources (PES) such as nuclear, fossil fuel energy sources.
- The rapid increase of PES prices.
- The fact that Central Europe imports about 70 % of its energy needs.
- The environmental issues and the increasing influences of greenhouse emissions.

Figure 2.7 shows the expected number of years of fossil and nuclear PES production that left in the Earth with the most hopeful projected reserves. This data is according to the present information about the geological sites of production and the present demand of the world. It can be noticed that the data about the reserves that are exploitable at the current locations are close to each other in both information sources. In fact, we can notice that the main difference in the figures is related to the expected increase of energy resources which could be invested

by non-traditional technologies such as hydraulic breaking of rock for gas exploitation, in addition to, the difference in the known reserves [26].

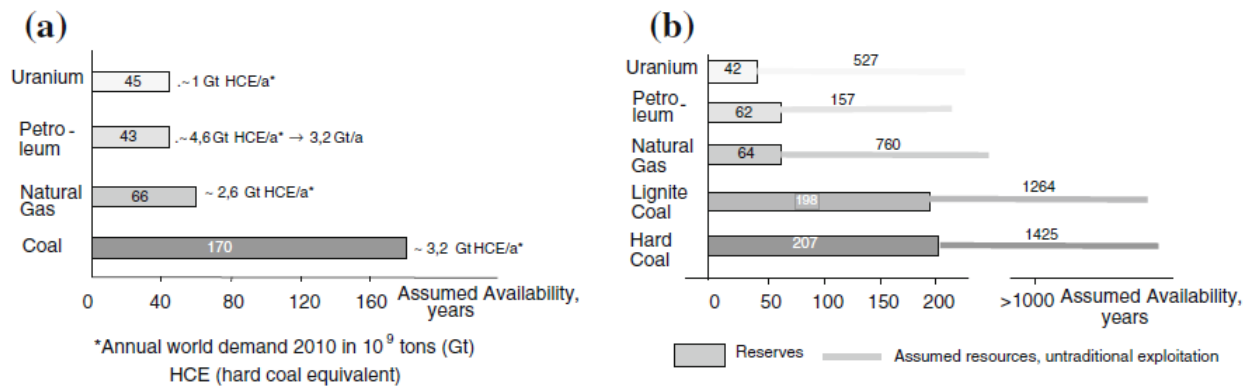


Figure 2.6 The reserve expectations for primary energy and the annual world demand (Sources a [27], b [28])

Moreover, it has been noticed that the electrical grids had many changes in the recent years that have made the present grid unable to face the challenges of the future [29]. Therefore, the modernizing of electrical networks becomes an extreme need, which has improved into the development of the Smart Grid concept. In general, this concept is widely understood as way forward to solve issues which are related to increasing energy consumption, energy efficiency, integration of distributed generation, power quality, and power supply reliability [30].

Therefore, the development and evolution of the Smart Grid concept has been induced due to the following factors:

- Aging of traditional electrical grids as well as the emanation of new applications
- Environmental issues and political factors
- Current electricity market and the liberalization of it.
- Participation and motivation of consumers as active players to support the electrical network [17]

2.3. Smart grid

2.3.1. Background and history of Smart Grid evolution

In 2001, an accurate description of the future grids has been published in Wired Magazine [31]. This description that was recognized later as a Smart Grid concept, states “The best minds in electricity R&D have a plan: Every node in the power network of the future will be awake, responsive, adaptive, price-smart, eco-sensitive, real-time, flexible, humming, and interconnected with everything else.”

The concept of Smart Grid has been evolved in the recent years in different location in the worldwide such as North America [32],[33] and Europe [34],[35],[36], as well as India, China [37],[38],[39],[40], and South Africa [41].

In Europe, the European Technology Platform for the Electricity Networks of the Future has been formed following a statement by research community and industrial stakeholders during the first International Conference which held in December 2004 on the Integration of Renewable Energy Sources and Distributed Energy Resources. After that, the development of Smart Grids was started by the Smart Grids European Technology Platform for Electricity Networks of the Future in 2005. The goal was to set up, promote and evolve a vision for the needed development of European electricity networks in 2020 and future [42],[17].

The concept of Smart Grid in USA has been evolved officially by US Energy Independence and Security Act through its publication in December 2007 by which it is specified by the following points [43]:

1. Shifting the United States toward greater energy security and independence.
2. Protecting consumers.
3. Increasing the participation and production of renewable energy sources,
4. Increasing the efficiency of vehicles, products, and buildings.
5. Encouraging research on and circulate greenhouse gas vision and possible storage options.
6. Enhancing the energy performance of the Federal Government [43].

US Energy Independence and Security Act has a title XIII-Smart Grid, Sec. 1301 in which the Smart Grid is defined by the following statement of policy:

It is the policy to assist the modernization process of the electricity transmission and distribution system in United States to maintain a secure and reliable electrical network infrastructure that can be capable to meet future growth of power demand and to attain all the following points, which together describe a Smart Grid [17]:

1. Increased use of controls technology and digital information to enhance security, efficiency, and reliability of the electrical network.
2. Incorporation and deployment of distributed generation units, including renewable energy sources.
3. Dynamic optimization of energy resources and operations in the grid as well as promoting a full cyber-security system.
4. Deployment of “smart” technologies (automated, real-time, interactive technologies which optimize and improve the physical process of devices and consumer devices) for communications, metering concerning network processes and status, and distribution automation.

5. Development and integration of demand-side resources, demand response, and energy efficiency resources.
6. Deployment and incorporation of peak shaving technologies and developed electricity storage, including hybrid electric and plug-in electric vehicles, and thermal-storage air conditioning.
7. Integration of “smart” devices and consumer devices
8. Provision to consumers of control options and timely information.
9. Identification and decreasing of unnecessary or unconscionable obstructions to adoption of smart grid services, practices, and technologies [17].
10. Advancement of standards for interoperability and communication of equipment and devices which are connected to the electrical network, including the infrastructure serving the network [17].

The definition of Smart Grid which has been mentioned above is very wide. It includes many aspects of electrical network management and operation [44]. The vision of Smart Grid involved in this definition aims at enhancing efficiency, security, reliability, and of all aspects of the electrical power system, including distribution, transmission, generation, and customer sites. Actually, many entities concentrate their vision of the Smart Grid almost on the possibility customer services authorized by evolved metering infrastructures. [17]

2.3.2. Comparison between Smart Grid and conventional electrical networks

In fact, conventional electrical networks apart from being out-of-date and old, have recently been under various changes. The most essential changes that proved to be complicated for the grids to adapt include the following [17]:

- (i) Controlling and handling the dynamic situation between electrical utilities and electricity market stakeholders because electricity market becomes liberal in the recent few years which require the implementation of new methodologies, approaches, and tools with the help of most advanced and modern technologies
- (ii) Accommodating the modern evolution in automotive industry in terms of electric vehicles (EVs) will be a new type of load that puts additional potential on the electrical grid.
- (iii) The increased integration and penetration of distributed energy resources (DERs) based-generators, particularly renewable energy sources (RESs) based-generators and energy storage systems into electrical grids, especially at distribution voltage levels [17].

However, these changes have negatively affected the protection, management, and operation of electrical grids in many ways. Additionally, in the recent years, an advancement has been happened in automatic control, communication, digital, and other technologies. This advancement has opened new opportunities, possibilities, and windows to discover new

solutions and treat electrical grid's problems efficiently. This in turn has led to firstly ruminate on modernizing traditional electrical grids and finally to the evolution of the Smart Grid concept [17].

Actually, Smart Grid is different from the current traditional grids in many points. In table 2.1 it is possible to see the main differences between the Smart Grid and conventional electrical networks, especially distribution network [17].

Table 2.1 Fundamental differences between the Smart Grid and conventional electrical networks [45]

Feature/component	Conventional network	Smart Grid
Communications	None or one-way, typically not real-time	Two-way, real-time
Customer interaction	Limited	Extensive
Metering	Electromechanical	Digital (enabling real-time pricing and net metering)
Operation and maintenance	Manual equipment checks	Remote monitoring, predictive, time-based maintenance
Generation	Centralized	Centralized and distributed
Power flow control	Limited	Comprehensive, automated
Reliability	Prone to failures and cascading outages, essentially reactive	Automated, proactive protection, prevents outages before they start
Restoration following disturbance	Manual	Self-healing
Topology of distribution networks	Radial, generally one-way power flow	Network, multiple power flow pathways

In order to tackle all challenges which have been mentioned before, developed countries in Europe and America continuously plan to develop smart grid and take it as an essential part of national energy strategy [46],[47],[48]. Furthermore, many other countries also start to design and implement smart networks successively. As a result of that, smart grid has been a new trend of power grid evolution and development in the whole world [49].

Even though, the goals and driving force of smart grid are not precisely the same in different countries, the following three features of smart grid are widely believed as the most important differences from the conventional power grid [47],[48],[50]:

1. Maximizing profits, as well as, reducing costs, energy consumption and emissions remarkably.
2. Nearly preventing all the risks of longtime and large-area blackout, except those being caused by physical damages that have large-scale.
3. Improving the acceptability and integration of renewable energy sources which have intermittent nature and give electrical power grid the ability to adapt various power sources [49].

2.3.3. The main features of Smart Grid

For the preservation of energy and to cover the energy demand by all loads including the industrial and commercial consumers, smart grid has some very significant and essential features which are needed by the utility [51]. According to EU vision, the main characteristics of the smart grid are [52]:

1. Flexible: Smart grid must fulfill the needs of customers, as well as, responding to the challenges and changes ahead.
2. Reliable: smart grid must guarantee and improve security and quality of supply, proportionate with the demands of the digital age with resilience to uncertainties and hazards.
3. Accessible: which means giving connection access to all network users, especially for renewable power sources in addition to high efficiency local generation with zero or low carbon emissions.
4. Economic: Smart grid have to provide best value through efficient energy management, innovation, and ‘level playing field’ regulation and competition [52].

Regarding US vision, the main features of the smart grid is as shown in Figure 2.8 [51].

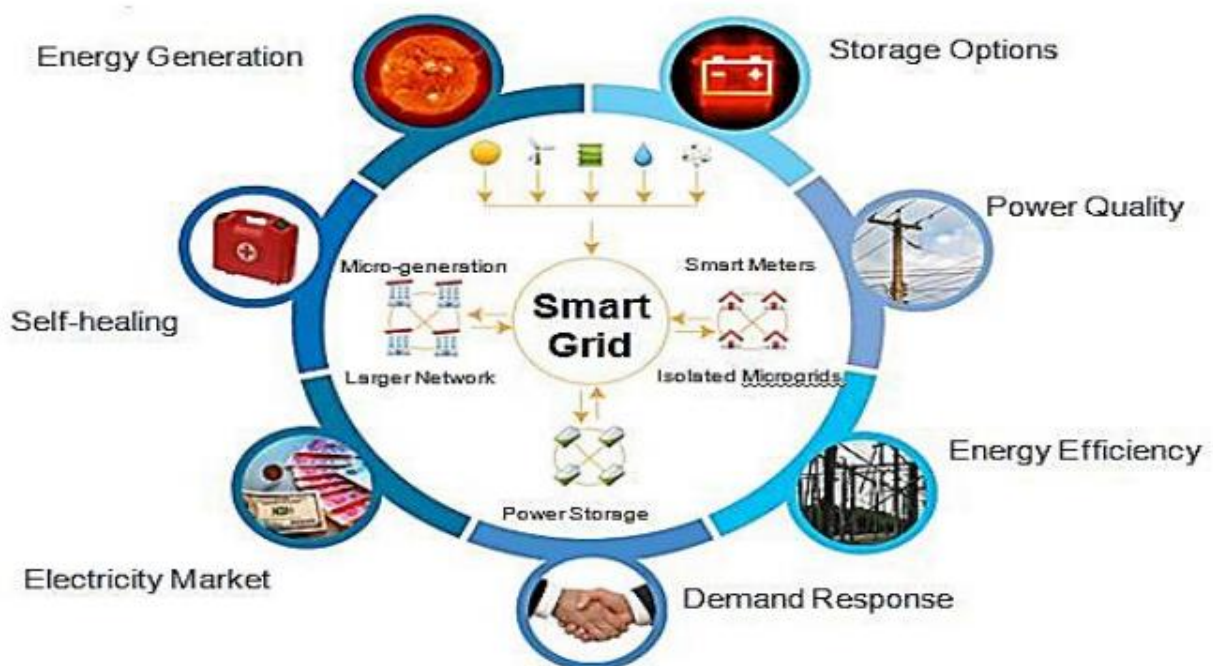


Figure 2.7 Key features of Smart grid [51]

As shown in fig 2.8, the following functions are accomplished by smart grid [51], [17]:

1. Self-healing: which means that the grid itself automatically rapidly senses, detects, analyses, responds and then restores. In other words, the grid has the capability of automatically repair

and remove potential faulty devices and disconnect them from the grid before they completely fail, and the capability of reconfiguring the electrical network system to ensure the energy continuity to all customers.

2. Integrates and empowers the consumer: it is the capability to integrate the consumer equipment and devices and behavior in electrical network regarding designing and operation. If Smart Grid concept has fully implemented, consumers will have an access to the needed control, options, and information, so they will be capable to engage in electricity markets. Furthermore, well informed consumers can modify their electrical energy consumption based on balancing their energy resources and demands with the capability of the electric system to meet their demands. In fact, when the consumers participate in the electrical grid, they help in shifting or reducing peak demand which will lead to minimize operating expenses of equipment and utilities.

3. Power quality requirements by users: the power quality in the grid is proportionate with consumer and utility needs: this will be achieved by supervision, diagnosing, and responding to power quality problems. Deficiencies in power quality will lead to business problems by consumers. The Smart Grid will supply the power with varying grades of quality at different pricing levels.

4. Fully enables and is supported by competitive electricity markets: where it will assist the creation of new markets of electricity and additional tools that ensure electricity trading in an effective way. This will give consumers and third parties ability to bid their energy into the electricity market. The reaction of consumers to price increases will automatically cause a decrease in demand and energy usage. Therefore, the market will have lower-cost solutions, which in turn will be a reason for a new technology development.

5. Optimize asset utilization and operate efficiently: It is expected that implementing the Smart Grid concept will improve significantly the performance of the electrical power system due to many reasons such as reducing power losses, improving load factors, and the big advancement in the outage management performance. It is also expected that if the Smart Grid concept has been fully implemented, the grid will be equipped with additional intelligence. Therefore, engineers and planners will have extra knowledge to build and design “what is needed when it is needed,” increase the assets’ life, repair equipment before unexpected or sudden fails, and manage the work force that is responsible for maintaining the electrical grid. This in turn will lead to reducing the maintenance, operation, and capital costs.

6. Accommodate all generation and storage options: in the smart grid, it will be easy to integrate all kinds and capacities of electrical generation systems including nuclear plants, thermal plants, and RESs, such as wind and solar farms which are environment friendly.

7. Tolerant of attack: The smart grid is able to operate resiliently and mitigate physical and cyber-attacks and has the ability of rapid recovery from disruptions. Thus, the Smart Grid will be resilient which will prevent any attack from anyone even those who are well equipped and determined. Moreover, security protocols will be designed appropriately in which they will contain elements of prevention, detection, supervision, mitigation, and response to ensure reduction the effects on the electrical grid, consumers, and economy [17],[51].

2.3.4. Benefits of smart grids

Actually, the smart grid will bring a wide variety of benefits. These benefits include the following [17],[53]:

1. Improves power reliability: This could be done by decreasing the period and frequency of faults and interruptions in the electrical grid.
2. Optimizes facility utilization and averts construction of backup (peak load) power plants: This is achieved by better demand of the management side and using advanced metering infrastructures.
3. Improving the power quality: This is achieved by keeping the magnitude of voltage in its statutory limits by advanced technologies such as various sensors in the grid, communication technologies, and two-way information system.
4. Enhances capacity and efficiency of existing electric power networks: using automation, active control and management in the distribution levels of the electrical grid. In addition, empowering the customers by home automation.
5. Automated and predictive maintenance and operation in addition to self-healing responses to system disturbances: this is achieved by network sensors which provide better monitoring of the grid in addition to distributed grid management and control.
6. Facilitates expanded deployment of renewable and distributed energy sources: by improving the integration of distributed energy sources especially renewable energy sources such as solar and wind energy. Also, by using plug in electric or hybrid cars.
7. Reduces greenhouse gas emissions: due to many reasons such as using electric vehicles, integration of renewable and distributed energy sources, and reduction of power losses in the electrical grid.
8. Presents opportunities to improve grid security and resilience to disruption by natural disasters and attacks: The improvement can be achieved by using automated operations and sensors which will lead to threats reduction of blackouts. Also, it can be done by using properly coordinating the operation of transmission and distribution with intelligent deterrent, coordinated restoration, and emergency control.
9. Reducing the consumption of fossil fuel by decreasing the need for gas turbine generation during peak usage periods and facilitating generation of electricity from renewable energy sources, such as wind, solar, and hydro sources.
10. Increases consumer choice, and enables new products, services, and markets: there will be a dynamic interaction between suppliers and consumers. The information about electricity prices from different suppliers will be available under smart grid environment which would naturally let consumers to choose the least electricity price supplier. Therefore, this will create healthy competition in the electricity market, which in turn will give benefits to consumers and play an important part in optimizing the operation of the power system network

11. Provides consumers with actionable and timely information about their energy usage: by advanced metering infrastructures so they will be able to know the consumption and generation of energy [17],[53].

2.3.5. Smart grid composition

The composition of smart grid is highly complex. The National Institute of Standard and Technology (NIST) in the USA proposed conceptual domain model. This model supports planning, requirements development, documentation, and organization of the various combinations of networks and devices which form the smart grid. As a result of the, NIST divided the smart grid into seven domains, as described in table 2.2 and shown in Figure 2.9 [54].

All domains and sub-domains include types of services, interactions, and stakeholders which set decisions and exchange information necessary for achieving desired goals, such as: outage management, distributed generation aggregation, and customer management. In general, services are done by one or more roles within a domain. For instance, corresponding services may include home automation, load control and near real time wide-area situation awareness (WASA), distributed energy resource (DER) and customer demand response [54].

Table 2.2 Domains and Roles/Services in the Smart Grid Conceptual Model [54]

	Domain	Roles/Services in the Domain
1	Customer	The end users of electricity. May also generate, store, and manage the use of energy. Traditionally, three customer types are discussed, each with its own domain: residential, commercial, and industrial.
2	Markets	The operators and participants in electricity markets.
3	Service Provider	The organizations providing services to electrical customers and to utilities.
4	Operations	The managers of the movement of electricity.
5	Generation	The generators of electricity. May also store energy for later distribution. This domain includes traditional generation sources (traditionally referred to as generation) and distributed energy resources (DER). At a logical level, "generation" includes coal, nuclear, and large-scale hydro generation usually attached to transmission. DER (at a logical level) is associated with customer- and distribution-domain-provided generation and storage, and with service-provider-aggregated energy resources.
6	Transmission	The carriers of bulk electricity over long distances. May also store and generate electricity.
7	Distribution	The distributors of electricity to and from customers. May also store and generate electricity.

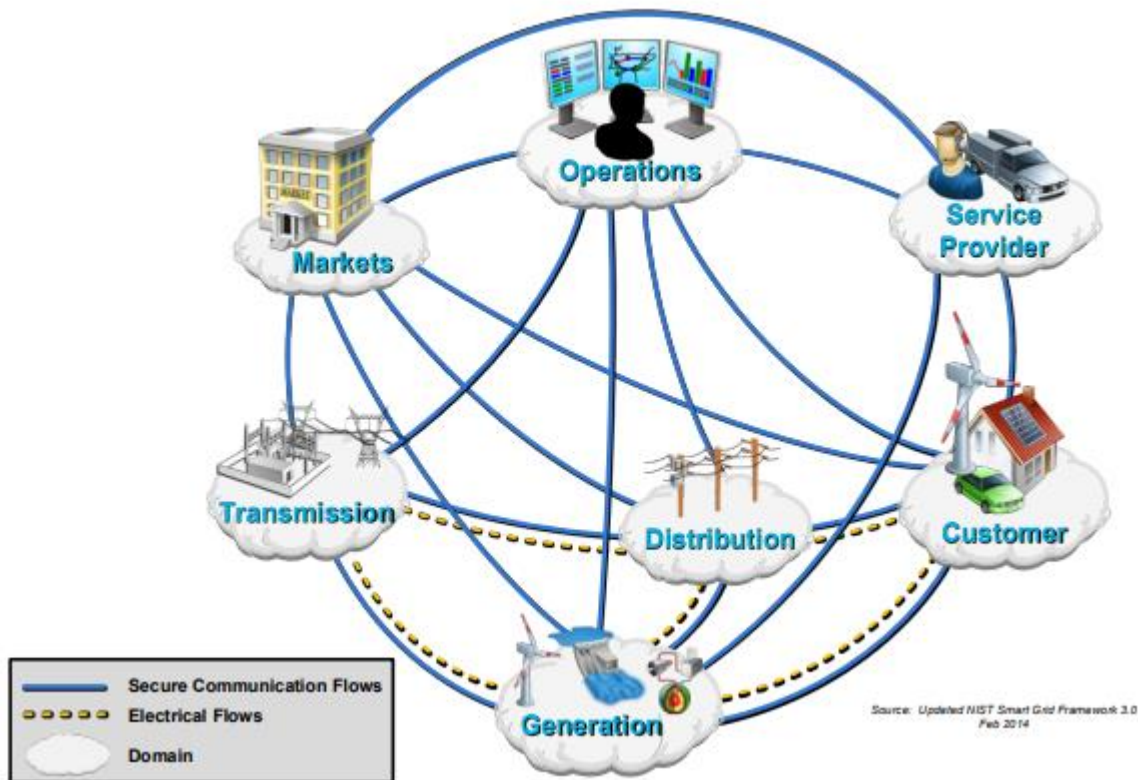


Figure 2.8 Interaction of Roles in Different Smart Grid Domains through Secure Communication [54]

Actually, roles in the same domain have similar objectives. Although, communications within the same domain could have different features and could have to meet different requirements to get interoperability [54].

For effective and functional operation of the smart grid, the roles in a specific domain often interact with roles in other domains, as described in Figure 9. Furthermore, particular domains could also contain some parts of other domains. For instance, the Regional Transmission Organizations (RTOs) and Independent System Operators (ISOs) in North America have roles in both the operations domains and markets. In the same vein, a distribution utility is not fully contained within the distribution domain where it is possible to include roles in the operations domain, such as a distribution management, and in the customer domain, such as monitoring. Moreover, a vertically integrated utility could have roles in many domains [54].

In fact, the conceptual model is prepared to be a functional tool for regulators at all levels to find the best way to achieve public policy goals, along with business objectives, encourage investments in modernizing the electric power infrastructure and building a clean energy economy [54].

2.3.6. Infrastructure of the smart grid

The basic infrastructure of Smart Grid consists of the following four systems as shown in Figure 2.10. These systems are [17]:

1. Electrical power system
2. Electricity marketing system
3. Intelligent protection, automation, and distributed control system
4. Communication and information system

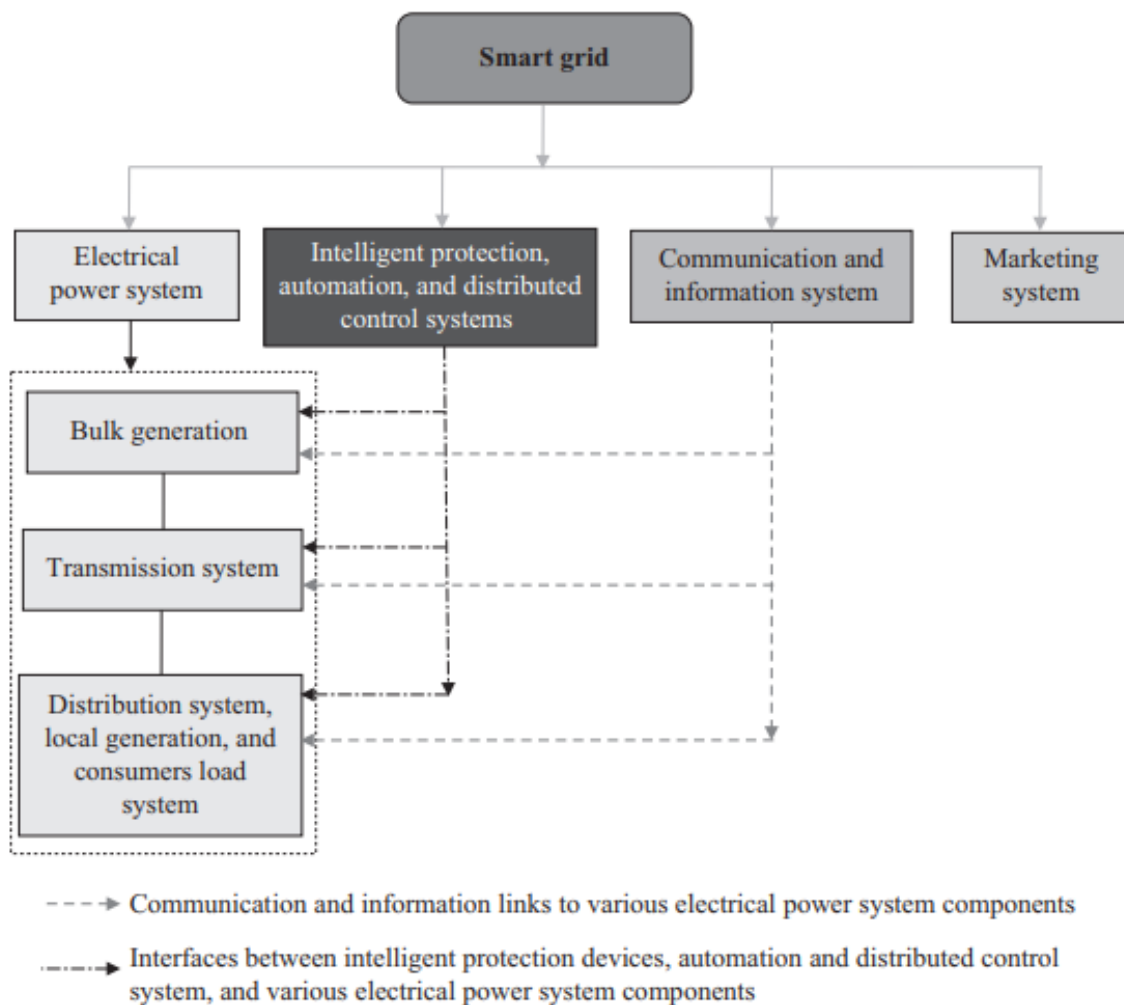


Figure 2.9 The Smart Grid basic infrastructure [17]

2.3.7. New Trends in Distribution Systems and New Types of Load

In fact, the new challenges for electrical power distribution network are related to the universal goals to reduce the CO₂ emissions and greenhouse emissions, to increase the proportion of renewable energy in the balance of energy and to improve the energy efficiency [26].

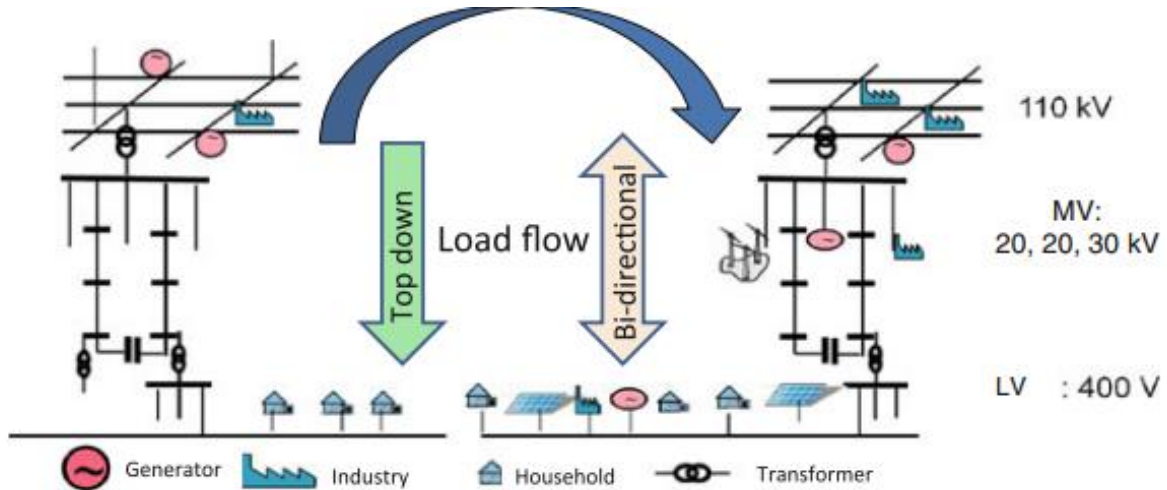


Figure 2.10 Changing conditions in the distribution networks due to DER integration [26].

Currently, in many countries, the renewable energy sources have the preference to in-feed by law. A considerable part of the renewable energy will feed into the electrical power distribution networks from a large number of small sized distributed energy resources (DER). As a result of these trends, the operation status of the electrical distribution networks will modify fundamentally. The modifying status is explained in Figure 2.11. Traditional way of flow is in a top down direction (left) is illustrated too in the figure [26].

However, due to the connection of DER in the LV and MV electrical grids, bidirectional load flows between the LV, MV and HV electrical grids will occur. Where, if the load level is lower than the generation one, a reverse power flows will occur. And, due to the meteorological status which directly impact power generation levels are volatile, the balance of load generation may change multiple times during the day. As a result, the power flow in the electrical power network changes its direction multiple times during the day and becomes volatile as well [26].

On the other hand, the targets in regard to environmental protection and energy efficiency will also be achieved through alteration of conventional combustion engine cars by electric cars (e-mobiles). Actually, the main benefit is seen that the electric fuel for the electric cars comes basically from renewable energy sources. Nevertheless, the needed electrical power for the rapid charging of one electric car may be as much as 15–20 kW. This value is up to 52–70 % of the tripping power of the 35 A fuses in the LV electrical power grids [26].

Therefore, the synchronized rapid charging of a number of electric vehicles along a LV feeder, will creates a critical state for most LV electrical power grids [26].

Moreover, the targets in regard to energy efficiency improvement will also be supported by a paradigm change regarding the heating systems for households, public buildings and small

enterprises. Recently, program have been initiated to install small power units for cogeneration of heat and power (CHP) of electric and thermal energy [26].

Furthermore, a considerable enhancement of the heating efficiency is anticipated from heat pumps installation. In the next few decades, the connection of heat pumps will increase remarkably [26].

2.4. Power Quality

In general, the problems which are related to the quality of electrical supply concerns all the actors present: network operators, network users as producers or consumers of electricity and various interacting parties such as suppliers of electrical power or services [55].

In fact, the operation and integrity of specific electrical and electronic devices and machines has always been affected by disturbances [56]. There are different paths where these disturbances can enter the sensitive equipment through [55]:

1. Electricity supply.
2. Input and output of signals, radiation, grounding.... etc.: however more localized compatibility problems are in industrial sites [55].

The electrical supply system includes a three-phase system of voltage waves that are featured by amplitude, sinusoidal waveform, frequency, and symmetry of the three-phase power system. Actually, there is no perfect supply and the four features that have been mentioned above are affected by disturbances even if they are reduced to low values which do not interfere with the sensitive devices [55].

2.4.1. Importance of Power Quality

Power quality becomes more essential in the electrical power systems due to the following reasons [57]:

1. Increase the emission of distorted current waveforms because of increased use of power electronics.
2. Decrease in immunity of some sensitive devices and equipment with increasing use of electronic power supplies with inappropriate filtering.
3. Higher integration of manufacturing processes especially in industrialized countries so that a loss of supply in one production line can lead to an economic losses and significant delays.
4. Regulator concerns and applying minimum power quality standards.
5. Electrical power consumers becoming more rights conscious [57].

2.4.2. Ensuring power Quality of electrical grids

The operators of electrical distribution grids must ensure a reliable, consumer friendly, ecologic and economically efficient electrical power supply to the community with the best possible level of power quality [26].

Power quality term is based on the following three pillars [26]:

- reliability of supply.
- voltage quality.
- service quality.

2.4.2.1. The reliability of supply

It is proved by statistical analyses of such signs as the average time of electrical supply interruptions, the frequency of electrical supply interruptions, or the electrical energy not delivered on time. By applying probabilistic methods calculation, it is possible to evaluate the reliability indicators in the planning phases which are related to new erections, enhancements or extensions of electrical distribution grids. Generally, the most used reliability indicators are presented in Table 2.3 [26].

Actually, the European benchmarks show that the highest reliability of supply (SAIDI) is achieved with 16 min/a. Figure 2.12 shows the benchmark of the European regulators. In fact, the majority of supply interruptions are occurred because of faults in the MV networks [26].

Table 2.3 Globally used reliability indices [58]

Index	Name	Definition	Unit
SAIFI	System average interruption frequency index	Interruption frequency per customer served	n/a
SAIDI	System average interruption duration index	Service unavailability per customer served	Min/a
CAIFI	Customer average interruption frequency index	Interruption frequency per customer interrupted	n/a
CAIDI	Customer average interruption duration index	Mean duration of a customer interruption	Min/a
ASAI	Average system availability index	Measured/required system availability	%
ENS	Energy not supplied on time	Sum of the energy amounts not delivered in time of all customer interruptions	MVAh/a

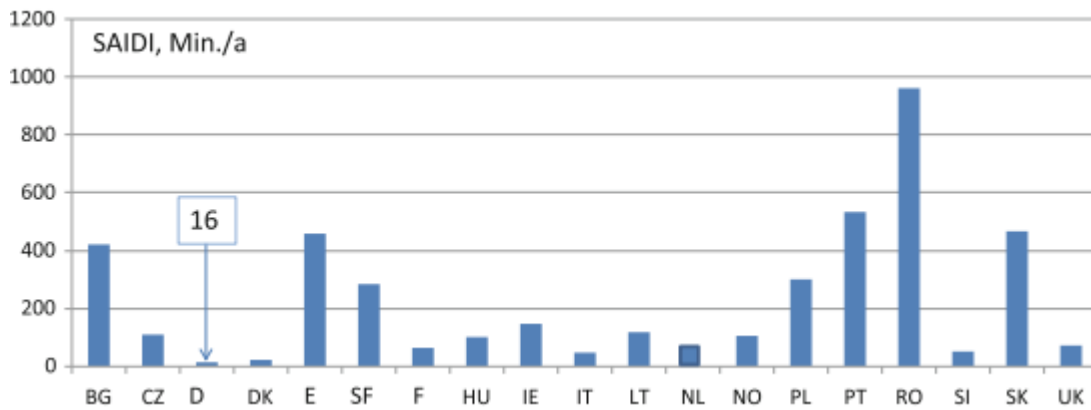


Figure 2.11 European benchmark of the system average interruption duration index [59]

2.4.2.2. The voltage quality

It is affected by the technical parameters of the electrical grid (such as network impedance value or short circuit power), the features of the electrical network assets and the technical parameters and operations of the electrical grid users [26].



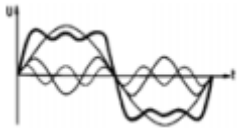
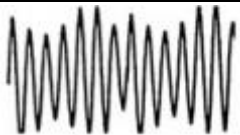
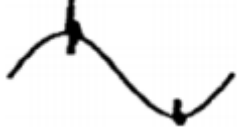

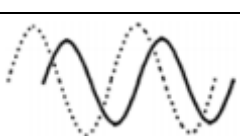
The majority of the applied electric power plants, electrical machines, devices and equipment (from powerful converter controlled motors down to small household electrical devices) more or less cause reverse impact on the electrical network voltage at the access points. The network users may affect the voltage quality on all voltage levels due to their demand processes of them. The damping magnitude of the voltage quality disturbances is related to the technical parameters of the electrical grid and its assets where the lower the impedance, the higher the damping and vice versa [26].

On the other hand, the impact of the users may also affect the frequency of the electrical grid, the voltage value with fast or slow changes that may have an sporadic character (i.e. flicker-voltage fluctuations producing the subjective effect of fluctuations in the lighting density of lighted objects by the perception chain of an electric light- eye- brain), the distortion of the sinus curve of voltage by the dissymmetry of the line to ground voltages (unbalances) or the harmonics [26].

Also, harmonics (sine-shaped oscillations where their frequency is an integral multiple of the fundamental electrical grid frequency) are produced from non-linear loads and are very intense when generated by frequency converters or inverters. The typical harmonics are specified ordinal numbers and have an odd ordinal number such as 1st, 3rd, 5th etc. by which the 5th harmonic has often the biggest impact [26].

Furthermore, some actions such as short circuits, switch operations and atmospheric lightning may cause transient over-voltages and fast voltage sags. An overview of the voltage quality disturbances, their reasons and the negative consequences is illustrated in Table 2.4 [26].

Table 2.4 Disturbances of the voltage quality and their impact [26]

Type of disturbance	Shape of disturbance	Possible causes	Consequences
Voltage dips		Successfully cleared fault Start-up of large motors	Shutdown of equipment, particularly electronic devices
Low voltages, over voltages		Uncontrolled active or reactive power in-feed	May harm equipment within adequate design margin
Harmonics, harmonic distortions		Non-linear load resonance DC/AC converter	Voltage distortion causes additional heating in motors Misoperation of electronic device
Flicker, voltage fluctuations		Start-up of large motors Electric arc furnaces	Weakening of components Malfunctions Annoyance of human
Transient over-voltages		Lightning strike Switching events	Misoperation of electronic device Reduced lifetime of equipment
Supply interruptions		Faults	Insulation failure Shutdown of equipment Misoperation of electronic device
Phase unbalances		Unbalanced loads	Risk of disconnection of the overload phase Machine overheating

In fact, the requirements of voltage quality for MV and LV networks are specified in the CENELEC standard EN 50160. This standard determines the allowable maximum bandwidths and tolerances regarding the rated voltages of public LV and MV electrical grids. This standard is included in the supply contracts between the electrical grid users and distribution grid operators. Where the distribution grid operators guarantee the voltage quality according to the requirements of EN 50160 and the network users have to ensure a convenient level reverse impact. The convenient measures have to be implemented in cases of deviations [26].

High harmonic distortions may need the installations of harmonic filters which make a resonance circuit for the related ordinal numbers of the harmonics [26].

Actually, providing a convenient voltage quality is often the precondition for the distribution of industries. The main requirements of EN 50160 are shown in Table 2.5 [26].

Table 2.5 Bandwidths and requirements of EN 50160 for voltage quality [60]

Parameter	LV	MV	Verifi-cation	Requirement
Frequency	50 Hz \pm 1 % 50 Hz + 4 %,– 6 %	50 Hz \pm 1 % 50 Hz + 4 %,– 6 %	10 s Average	99.5 % in 1 year 100 %
Rated voltage	230 V phase to ground	Network related		
Slow changes	+10 %,–15 % \pm 10 %	\pm 10 %	10 min Average	100 % 95 % during a week
Fast changes	Normal 5 %, Infrequently 10 % $P_{lt} \leq 1^*$	Normal 4 % Infrequently 6 % $P_{lt} \leq 1^*$	Sequence of 12 P_{st}^* values (600 s) within 2 h	95 % during a week
Voltage dips < 1 min	Indicative p/a a few tenth to a thousand	Indicative p/a a few tenth to a thousand		Majority < 1 s, Dip < 60 %
Harmonic distortions	Limits for $v = 5-25$ from < 6 % to < 0.4 %	Limits for $v = 5-25$ from < 6 % to < 0.4 %	10 min Average	95 % of a week
Interruptions <3 min	Indicative p/a a few tenth to several 100	Indicative p/a a few tenth to several 100		70 % <1 s
Interruptions >3 min	<10 up to \leq 50	<10 up to \leq 50	Sum of planned and unplanned minutes	Depending on the region

* P Flicker intensity, lt long term, st short term

2.4.2.3. The service quality

It describes the relationship quality between the companies of electrical power supply and the power consumers. As a consequence of the splitting of the electrical power supply processes, the consumers will be in active connection with the electrical power trader, with the distribution grid operator, and with the provider of meter service (if this function is not allocated to the distribution grid operator). As a result of that, all three players of the electricity market have to supply service quality in their consumer relations [26].

Actually, the service quality does not have a direct influence on the secure electrical power supply of the consumers and their connected plants, machines or devices. Thus, there is no general standards of the service quality yet. Nonetheless, individual countries in the European Union apply guidelines regarding the main features of service quality. It could be shown in table 4 an overview of the most common features of service quality in Europe with the bandwidth durations in addition to the possible financial penalties in case of violation [26].

The overview in Table 2.6 illustrates a wide range relying on the laws which has been determined in the various European countries. For instance, in Germany the meter and the

installations of the consumer connection have to be completed within two days, and there are generally not any penalties for such case [26].

While, in Spain and Italy, connections' establishment can take up to five days and there are penalties which may reach 30 €. Furthermore, in Ireland the installation can take three days and penalties are the highest where they may reach 50 € [26].

Regarding liberalization, any consumer can contract and choose the meter service provider and the trader himself, but he has to rely on the local acting distribution network operator [26].

Table 2.6 Service quality characteristics, bandwidth of limits and penalties [58]

Service characteristic	Time limits	Penalties, €
Appointments scheduling	2–3 h	0–35
Connection and meter installation	2–5 d	0–50
Estimation of charges for simple works	5–20 d	0–65
Response to metering problems	5–20 d	0–35
Response to queries on charges and payments	5–20 d	0–30
Number of meter readings per annum	1–6	0–30
Response to consumer letters	8–20 d	0–20
Response to consumer claims	5–20 d	0–35

2.4.3. Steady State voltage

2.4.3.1. Voltage value and power factor

In fact, the voltage decreases with increasing customer load, particularly further away from the transformer, due to the interaction between customer current and the impedance of the electrical supply system. The value of voltage reduction seen at a specific installation is related to the load current drawn by all the customers which are connected to the transformer and the position of the installation along the line. Actually, the maximum voltage drop occurs during peak loading period especially at the far end of the supply line. The voltage value at the point of connection must be in a range of $V_n \mp 10\%$. Voltages greater than the nominal voltage could cause equipment and machines insulation to degrade faster than intended and as a result of this reducing lifetime. On the other hand, if voltages are less than the nominal voltage, equipment and machines can fail to operate as intended. The equipment of motor-driven can fail to start or motors could overheat and trip or even be damaged [57].

Furthermore, wiring within a customer's installation has impedance and participates to voltage drop up to the point where customers' equipment or machine may be connected. Therefore, installations must be wired with conductor that has an adequate cross-section so that the maximum voltage drop from the point of connection is not exceeding the allowed limits [57].

Power factor is a related issue to voltage. Power factor can be improved by reactive power compensation which could be done using many methods [57].

2.4.3.2. Long-Duration Voltage Variations

Long-duration variations includes deviations of root-mean-square (rms) at power frequencies for longer than 1 min. American National Standards Institute (C84.1) determines the steady-state voltage tolerances anticipated on an electrical power system. In fact, a voltage variation will be considered as long duration when the ANSI limits are exceeded for longer than 1 min. Moreover, long-duration variations can be over voltages or under voltages. Generally, the reasons of over voltages and under voltages are not the faults of the electrical power system, but load variations on the electrical power system and switching operations in the system. These variations are displayed as plots of rms voltage versus time [61].

A. Overvoltage

Overvoltage is an increase in the rms value of voltage greater than 110% at the power frequency for a time duration longer than 1 min [61].

Generally, over voltages are usually the consequence of load switching operation. Moreover, the over voltages occurred because either the electrical power system is too weak for the required voltage regulation or voltage controls are unqualified. In addition, incorrect tap settings on electrical transformers may also lead to over voltages in the electrical system [61].

B. Undervoltage

An undervoltage can be defined as a decrease in the rms value of voltage to less than 90 percent at the power frequency for a time duration longer than 1 min [61].

Under voltages are the consequence of switching actions that are the opposite of the events that result over voltages. A load switching on can cause an undervoltage until voltage regulation device on the electrical power system can bring the voltage back to within allowance limits. Overloaded circuits may also be the reason of under voltages [61].

C. Sustained interruptions

A sustained interruption is defined as long-duration voltage variation that the supply voltage degrades to zero for a time duration longer than 1 min. Generally, voltage interruptions which are longer than 1 min are permanent and need intervention of human to repair the electrical power system for restoration. The term continued interruption indicates to determined power system phenomena and, in general, has no connection to the usage of the term outage. Moreover, utilities use interruption or outage to express phenomena of similar nature for reliability reporting studies. Although, this leads to confusion for end users who think of an electricity outage as any interruption of electrical power that shuts down an operation. This might be as little as one-half of a cycle. According to IEEE Standard 100 [62] definition of electricity outage, this term does not refer to a specific phenomenon, but indeed to the situation of a component in a system that has failed to function as anticipated. Furthermore, the usage of the term interruption in the context of power quality observation has no connection to

reliability or other statistics of continuity service. Therefore, this term has been specified to be more specific concerning the absence of voltage for long time periods [61].

2.5. Distributed Generation

Actually, distributed generation (DG) is a relatively new approach to describe the new type of generation at the customer side, that is smaller than the conventional power station in a competitive market of electricity. Regarding the term “Distributed Generation” it is synonymous and strongly connected with the terms such as embedded generation and dispersed generation. Some countries set a specific definition of distributed generation, according to the capacity of the power plant, the voltage level to which it is connected, environmental impact, power delivery area and point of connection. Though, these criteria are necessary, but they are not sufficient. In general, these definitions follow some national and technical documents that used to specify the main aspects of the management or connection of distributed generation and not from any basic consideration of its impact on the electrical system. So, the practical definition of DG unit is “an electric power source connected directly to the power network, preferably at the customer side of the meter, sufficiently smaller than the controlling generating plant.” We can notice that this definition does not specify the capacity of the distributed generation unit as the maximum capacity depends to the voltage level of electrical distribution system [63],[64].

Distributed generation units can be connected to electrical distribution system at a various voltage levels range from 120/230 V to 150 kV. Only very small units may be connected to the lowest voltage power grids, but large generation units of some hundreds of megawatts must be connected to the high voltage electrical distribution systems as shown in Figure 2.13 [63]

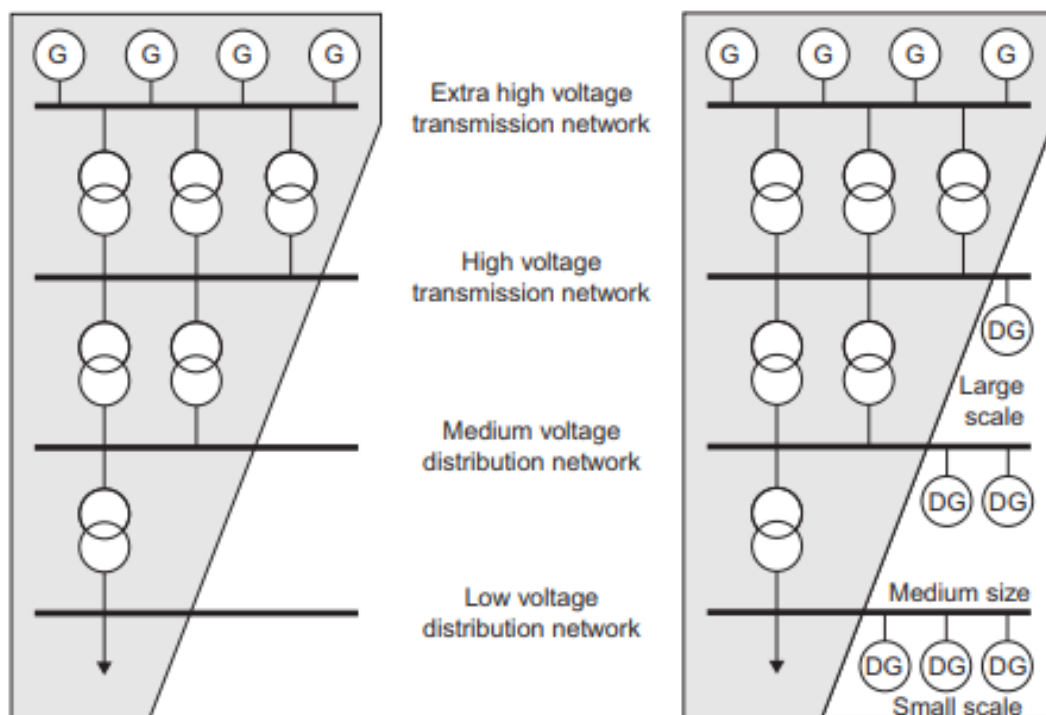


Figure 2.12 Connection of distributed generation units [63]

Actually, the connection of these DG units to the electrical distribution grids leads to many challenges because these electrical networks were designed to supply power to loads with flows from the higher to the lower voltage levels. Conventional distribution grids are passive with few measurements and very limited active control. Generally, the design of conventional distribution grids is basically to accommodate all sets of loads without any action by the operator of the system. [63]

Furthermore, due to the fact that supply and demand of electrical power must be balanced on a second-by-second basis, the power injection from distributed generation units needs an equivalent power reduction in the output of the large central power plants. Currently, central power generation supplies electrical energy but also many ancillary services, such as voltage and frequency control, reserve and black-start, which are crucial for the stability and operation of the electrical power network. Due to the increase use of distributed generation units, they have to provide the ancillary services that are required to keep the power grid functioning with fewer central power plants being operated [63].

2.5.1 Categories of DG

DG units may categorize according to capacity as follows:

- Micro DG (between 1 W and 5 kW)
- Small DG (between 3 kW and 5 MW)
- Medium DG (between 5 and 50 MW)
- Large DG (between 50 and 300 MW) [64].

We can notice that the DG definition does not determine the used technology. Therefore, DG includes all kinds of renewable sources, combined heat and power (CHP) applications are modular applications [64].

2.5.2. Specifications for DG Concepts

In order to define the DG in narrow way, the following specifications should be existed:

1. As voltage between transmission and distribution systems is different and related to country, DG units have to be closer to the loads more than high levels of voltage. Therefore, DG is limited to the distribution electrical grid.
2. Generation capacity range is pivotal in defining DG units, but there is no universal agreement on maximum generation.
3. Some DGs use renewable energy sources; some do not.
4. There are various technologies for DG units and, hence, cannot be used to narrow the definition. Also, generation mode, area, or ownership do not define DG. For instance, both traditional generators and independent power producers can own a DG.
5. DG units should be able to generate reactive power, but some DGs cannot and, hence, this may not be an adequate criterion for definition [64].

2.5.3. DG Benefits

Distributed generation units can play a vital role in reducing investments in transmission and distribution capacity. In fact, from a planning point of view, DG units can be installed close to main load, which will reduce losses in the electrical grids from an operations point of view and minimizing the costs for controls and operations. DG is preferable to help reduce power losses in electrical distribution grids and to serve as back-up and stand-alone generation [64].

We can summarize the benefits of DG by the following [64]:

1. Grid support: DG units can participate to provision of ancillary services needed to sustain stable operation of the electrical network.
2. DG combined generation and heat capacity: DG units have provided cogeneration and trigeneration that provide electricity, heat, and steam for various applications.
3. Environmental concerns: DG can have a significant impact in improving or performing environmental regulations.
4. Fuel diversity: DG units use different fuel sources at optimized prices, depending on the technology.
5. Because of fuel diversity, any shortage in fuel DG that is nonrenewable is considered to be risky and costly. So, it may not help in mitigation blackouts and degrades the security of the electrical power system, therefore asserting the need for higher regulating power of backup generation
6. DG moves the electricity markets to Liberalization to form a new environment within a competitive market and because of different technologies makes it hard to generalize.
7. Power quality and system frequency: Policies are very important to ensure that DG units adhere to quality of power supply and be able to sustain frequency of the electrical system. Also, high voltage levels approved for DG connections relative to the utility companies have to be suitably controlled in order to obtain voltage security to respond to the changes in electricity markets. Moreover, DG market is economically attractive due to the flexibility in construction of centralized generation and transmission lines [64].

2.5.4. DG policies

The main policy issues regarding DG include the following [64]:

1. High cost of implementing and installing different DG technologies, a concern of stakeholders and policy makers.
2. A policy to verify economic efficiency of DG to liberalize the electricity market.
3. Less choice between more expensive DG units and expensive fuel, a fact that has discouraged choosing of DG units when we want to compare with the central generation costs.

2.6. Wind Farms

By the end of twentieth century, most countries started big investments in the field wind energy systems. This is due to the fact that wind generation depends on renewable energy source and instability of fuel prices. The cumulative installation of wind turbines has grown very fast over the last two decades. The capacity of installed wind power generation is expected to exceed 760 GW by 2020, making this type of renewable energy a pivotal portion of the new and smart energy supply systems. Figure 2.14 shows the total capacity installed from the end of 2011 till the end of 2016 [65]. The participation of wind generation in the total power generations differs from one country to another according to many reasons such as wind availability and fossil fuel costs. Statistics and information of World Wind Energy Association (WWEA) show that China, USA, Germany, India and, Spain, produce about 67% of total global wind capacity. The increase of wind farms utilization is due to many reasons especially rapid progress in wind technology. The wind turbine rating can be taken as an example of this progress; where in 1980 wind turbine rating began with 50 MW and reached 10 MW by 2012 [65],[66],[67], [68],[59],[70].

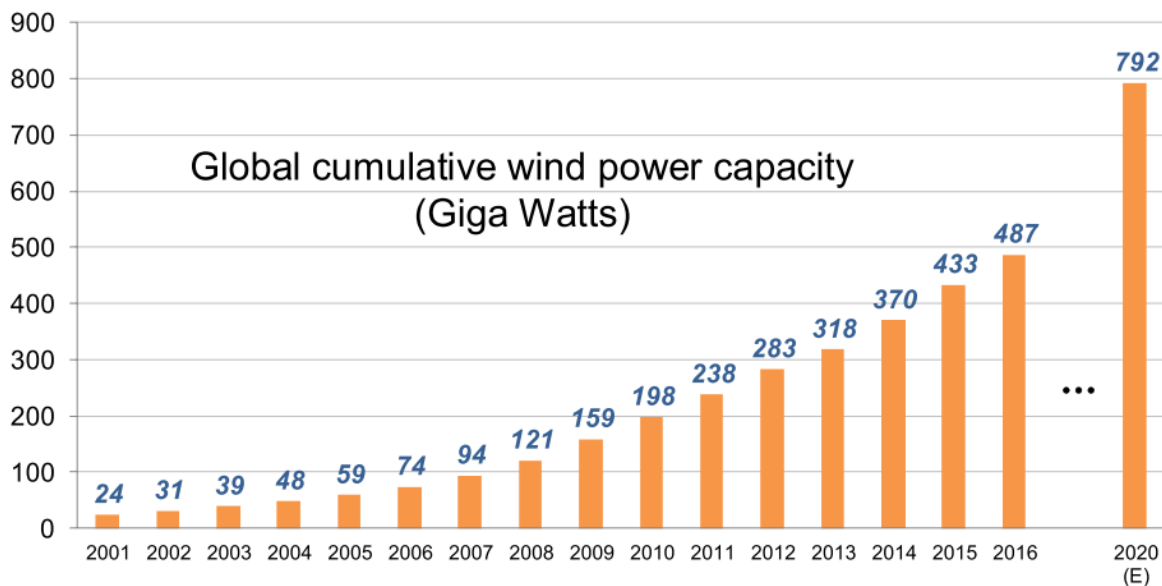


Figure 2.13 Global cumulative wind power capacity from 2001 to 2020 [65]

In fact, power electronics have become more developed with growing capacity coverage, and have added considerable improvements to wind turbines performance. The effect is not only reducing mechanical stress and increasing energy production, but also enabling the wind turbine to act as a controllable power source that is much more suitable for power network integration [67].

The individual size and the power capacity of wind turbines have also increased significantly. Figure 2.15 [67] shows the increased sizes of wind turbines between 1980 and 2020. The figure shows the development of power electronics with its functional role and capacity coverage are also illustrated. The average capacity of wind turbines installed in Europe was 2.7 MW for onshore and 4.2 MW for offshore in 2015. At present, cutting-edge 8 MW wind turbines with a diameter of 164 m are on the market [67], [71]. Currently, most of wind turbine manufacturers

have issued their products in the range of 4–6 MW, and it is anticipated that more wind turbines above 4 MW will be installed in the next decade. This trend is mainly induced by the need to reduce the cost of electrical energy per kilowatt hour [67],[72].

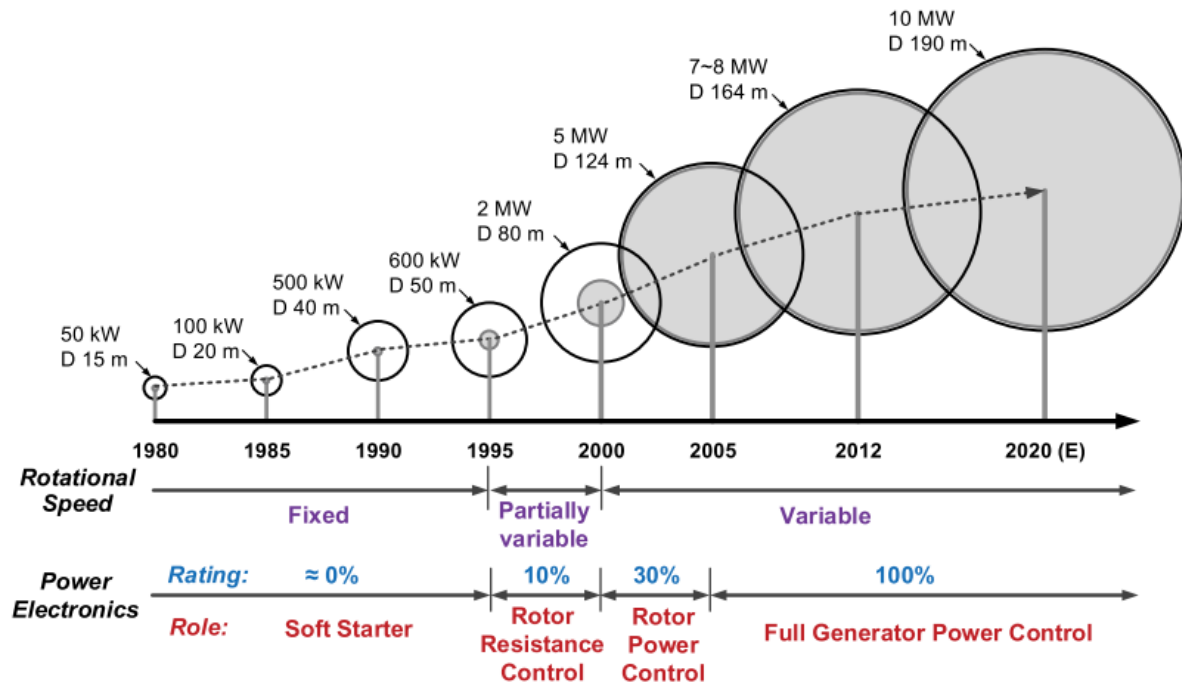


Figure 2.14 Developments of power electronics for the wind turbines between 1980 and 2020 (E); gray area inside the turbine circle indicates the power rating coverage by power electronics; D means diameter of the rotor [67].

2.6.1. Wind Turbine types

We can classify wind turbine types according to their electrical connection to the network. Nevertheless, there are more combinations such as fixed speed pitch or variable speed active stall control, but they do not have a role in practice any more [73]. The types are as following:

Type 1 wind turbines: This type operates at fixed speed using squirrel cage induction generators as shown in Figure 2.16. The control of aerodynamic power is achieved using passive aerodynamic stall or active stall blade control. The control of reactive power is done using capacitor banks or active power electronics [73].

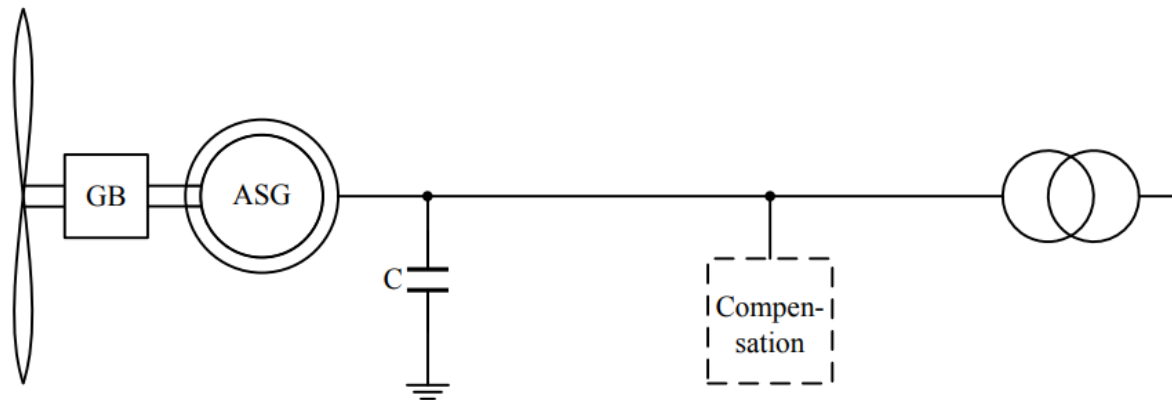


Figure 2.15 Type 1 wind turbines [73].

Type 2 wind turbines: This type uses a wound rotor induction generator instead of squirrel cage and work within a limited operating range as shown in Figure 2.17. Speed control is done using controlled resistors in the rotor circuit. Generally, for aerodynamic power limitation pitch control is used. Reactive power control is achieved using capacitor banks or additional active power electronics [73].

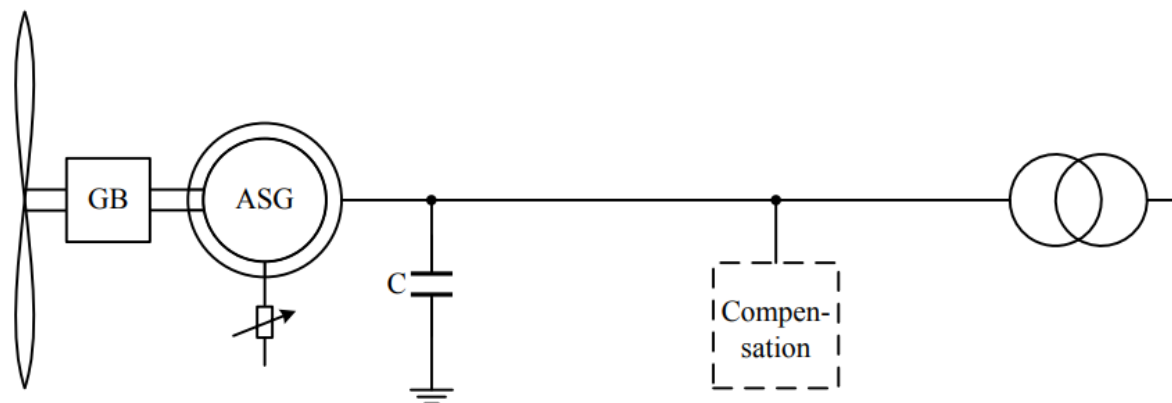


Figure 2.16 Type 2 wind turbines [73].

Type 3 wind turbines: This type uses a wound rotor induction generator in addition to a converter on the rotor side which is rated for partial load as shown in Figure 2.18. Therefore, it is possible to control of active and reactive power independently within a wide speed operating range. Also, pitch control is generally used for aerodynamic power limitation. This turbine type is also called doubly fed generator system (DFG) because both rotor and stator can supply power to the network [73].

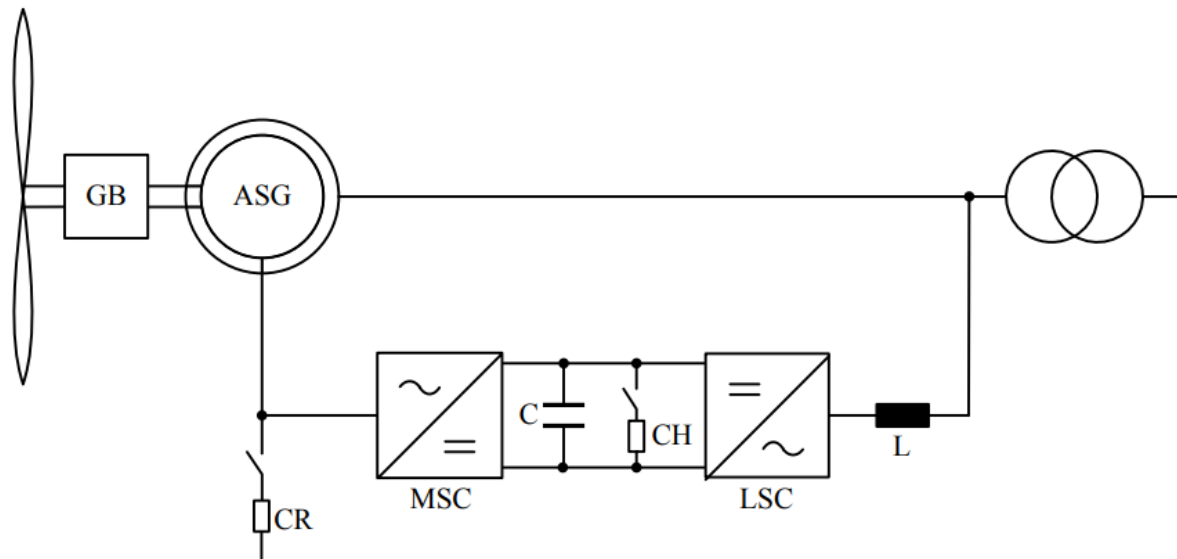


Figure 2.17 Type 3 wind turbines [73].

Type 4 wind turbines: This type is based on converters connected to the stator side of the generator which are rated at full turbine power as shown in Figure 2.19. This type is called a full size converter (FSC) turbines. Pitch control is used for aerodynamic power limitation. Various types of generators might be used for this wind farm such as permanent magnet synchronous generators, wound rotor synchronous generators, and squirrel cage induction generators. Usage of a gearbox is related to the type of generator [73].

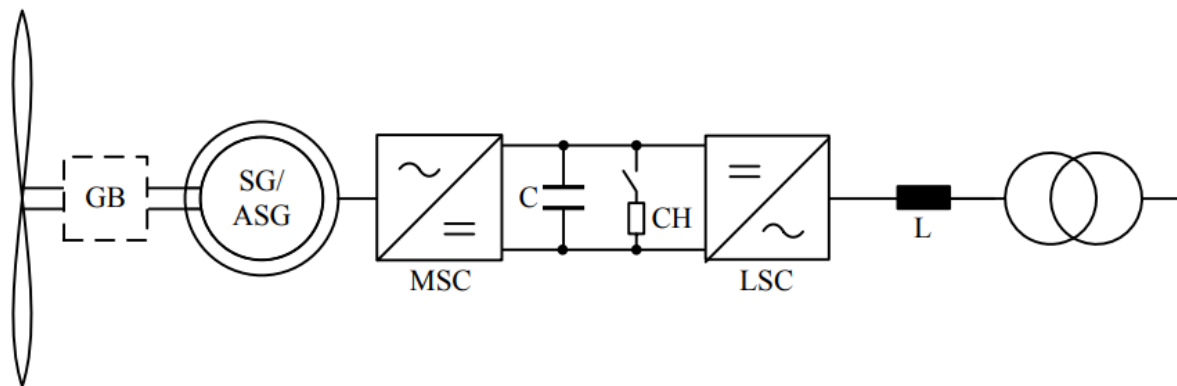


Figure 2.18 Type 4 wind turbines [73].

2.6.2. Concept Model of Wind Turbine Generators

In this section, a generic model that is in time domain will be introduced. Also, it explains the different controls in WTGs. Figure 2.20 shows the control model of WTG [74].

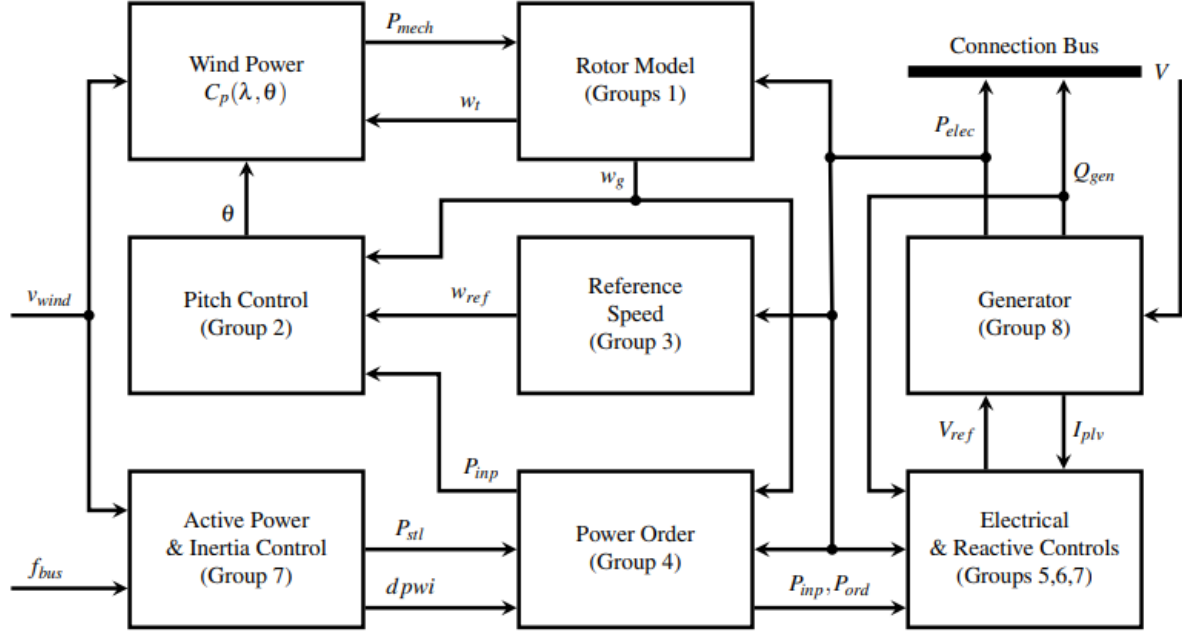


Figure 2.19 WTG control blocks and dynamics [74].

Main parts of the Model:

1. Wind power model: The power in the air streams is given by [75]:

$$P_{wind} = \frac{1}{2} \rho A_r v_{wind}^3 \quad (2.1)$$

This part expresses how a WTG extracts power from the air. The model's main goal is to introduce the C_p curves such that the extracted power from the air is:

$$P_{mech} = \frac{1}{2} C_p \rho A_r v_{wind}^3 \quad (2.2)$$

2. Rotor model: This part explains the dynamics of the generator and turbine speeds owing to the mechanical and electrical torques [74].

3. Reference speed: This section expresses reference speed calculation. The reference speed dynamics are relying on the generated electric power such that at steady state $w_{ref} = f(P_{elec})$. This speed is fundamental to control the turbine and generator speeds [74].

4. Pitch control and compensation: This block models the dynamics of the Pitch. This control calculates the Pitch angle according to the differences between the rated power and the ordered power, and between the generator speed and the reference speed. Actually, the Pitch angle has big effect on the efficiency of power extraction. This control is essential to keep the WTG generating the rated power for a wider range of wind speeds [74].

5. Reactive power control: This model controls the generated reactive power from the WTG, and it can be done in the power factor setup or the supervisory voltage setup. The first condition occurs when the WTG is considered as one unit, while the second condition is used when the WTG is working as one part of many units [74].

6. Electrical control: Unlike the previous control block where the control was for the reactive section that supplies the generator, the electrical control shows how the active current can be generated and controlled [74].

7. Active power and inertia controls: In general, these controls are not activated. The main objective of these two controls is to control the power order generated by the WTG. This management is related to the changes in bus frequency. Both of these controls provide additional power when the frequency is lower than normal bus frequency (reference frequency) and vice versa. Whereas, the active power control supplies additional power by setting up the maximum rated power and cutting out the available power to the WTG if needed. Also, inertia control does the same, but by supplying additional power from the rotor inertia [74].

8. Converter and Generator model: This model explains how the output of the WTG is delivered to the electrical power network. This block is feeding the electrical network by active and reactive power using one branch for each power [74].

9. Terminal voltage and electrical network model: The terminal voltage is the connection between the network model and the converter and generator model. The wind turbine is connected to the electrical network in order to work. Therefore, the network should be modeled so we can have an algebraic equation (the network equation) from Kirchhoff's law, that relates the dynamics of the WTG to the network. The terminal voltage will be given as following [74] [76]:

$$(V^2)^2 - [2(P_{elec} \cdot R + Q_{gen} \cdot X) + E^2] \cdot V^2 + (R^2 + X^2)(P_{elec}^2 \cdot Q_{gen}^2) = 0 \quad (2.3)$$

2.6.3. PMSG modeling

The dynamic modelling of PMSG can be illustrated in d-q reference system as in the following equations [77],[78]:

$$v_{gq} = (R_g + pL_q) \cdot i_q + \omega_e L_d i_d + \omega_e \psi_f \quad (2.4)$$

$$v_{gd} = (R_g + pL_q) \cdot i_d + \omega_e L_q i_q \quad (2.5)$$

Where [77]:

R_g is the stator resistance.

L_q and L_d are the inductances of the generator on the d and q axis.

ψ_f is the permanent magnetic flux and ω_e is the rotating speed of the generator which could be described by [77]:

$$\omega_e = p_n \omega_m \quad (2.6)$$

Where [77]:

p_n is the number of pole pairs of the generator.

ω_m is the mechanical angular speed.

The electromagnetic torque of the PMSG can be described as [77],[78]:

$$T_e = \frac{3}{2} p_n [\psi_f i_q (L_d - L_q) i_d i_q] \quad (2.7)$$

If $i_d = 0$, the electromagnetic torque is described as in [77]:

$$T_e = \frac{3}{2} p_n \psi_f i_q \quad (2.8)$$

The dynamic equation of the wind turbine is expressed by [77]:

$$J \frac{d\omega_m}{dt} = T_e - T_m - F\omega_m \quad (2.9)$$

Where [77]:

J is the moment of inertia.

T_m is the mechanical torque developed by the turbine.

F is the viscous friction coefficient.

2.6.4. Model of the Full scale converter system in wind farms

Full scale converter (FSC) systems have been used in wind turbines since more than two decades. Currently, there is a wide variety of generators such as, asynchronous machines, synchronous wound rotors or permanent magnet synchronous machines, with gearbox, with a higher number of poles and a reduced gearbox and without gearbox. A typical structure of the model is shown in Figure 2.12. But from a network connection point of view, choosing the generator and the machine side converter does not have impact on the behavior in terms of the electrical network if machine side converter and line side converter are not connected by a DC link which is very common in modern wind turbine. Therefore, the generator and machine side converter are represented as controllable current source [73].

The FSC works as a fast-acting voltage source and the impedance Z can be defined as [73]:

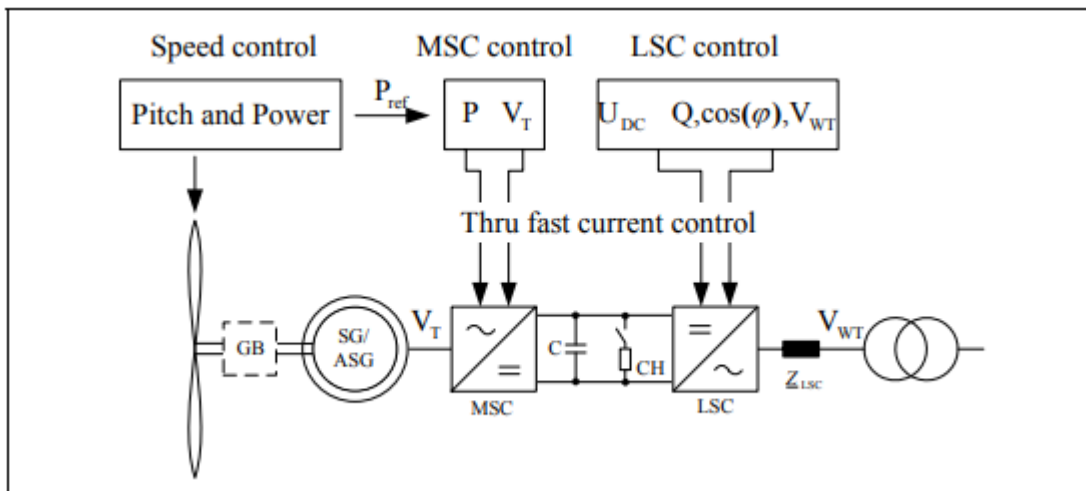


Figure 2.20 Key components of FSC system [73].

$$Z = Z_{LSC} + Z_{Tr} \quad (2.10)$$

Where:

Z_{LSC} : choke impedance

Z_{Tr} : transformer impedance

2.6.5. Model structure of generator and converter

Figure 2.22 shows the generator model implementation using active, reactive current and turbine voltage as input, and real and imaginary parts of the current as output [73].

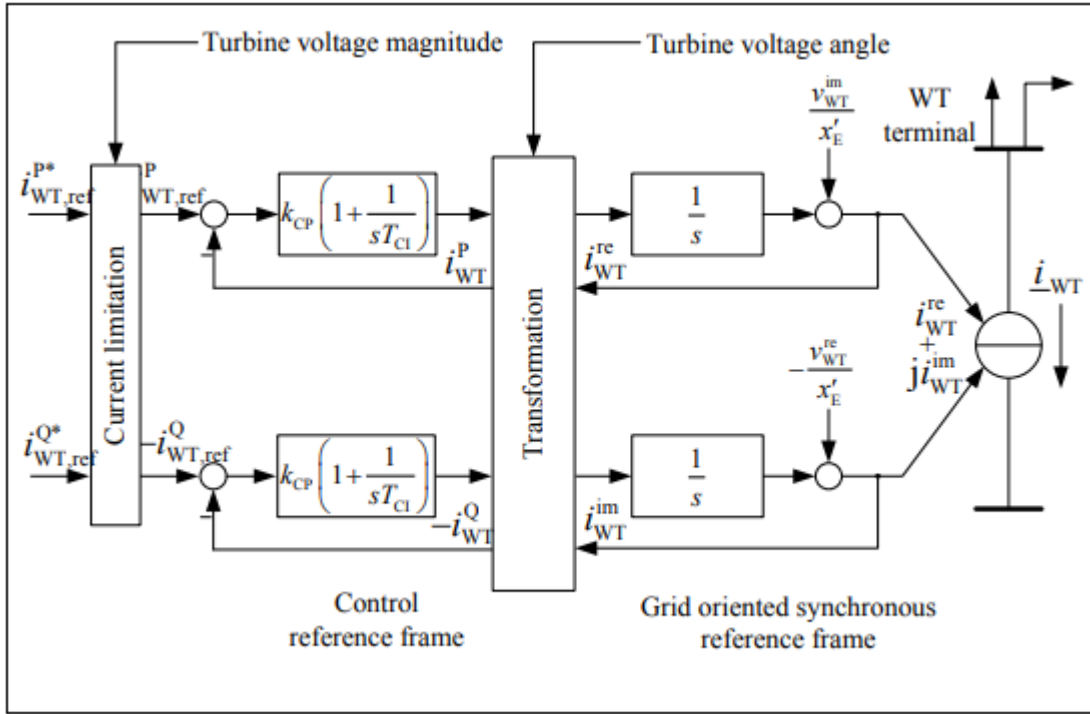


Figure 2.21 Core of generator model of machine and current control [73].

2.6.5.1 Current Limitation

Figure 2.23 shows the output current limitation of the generator model. In fact, current limitation can be divided into three main sections [73]:

A. Control Limits

Generally, active and reactive current output limitations can be expressed as a function of the voltage. Even though, the actual implementation could be different, a good approximation can be accomplished by specifying the limits of active and reactive currents as function of voltage [73]:

$$i_{WT}^P' = \max(i_{WT}^{P*}, f_P(v_{WT})) \quad (2.11)$$

$$|i_{WT}^Q'| = \max(|i_{WT}^{Q*}|, f_Q(v_{WT})) \quad (2.12)$$

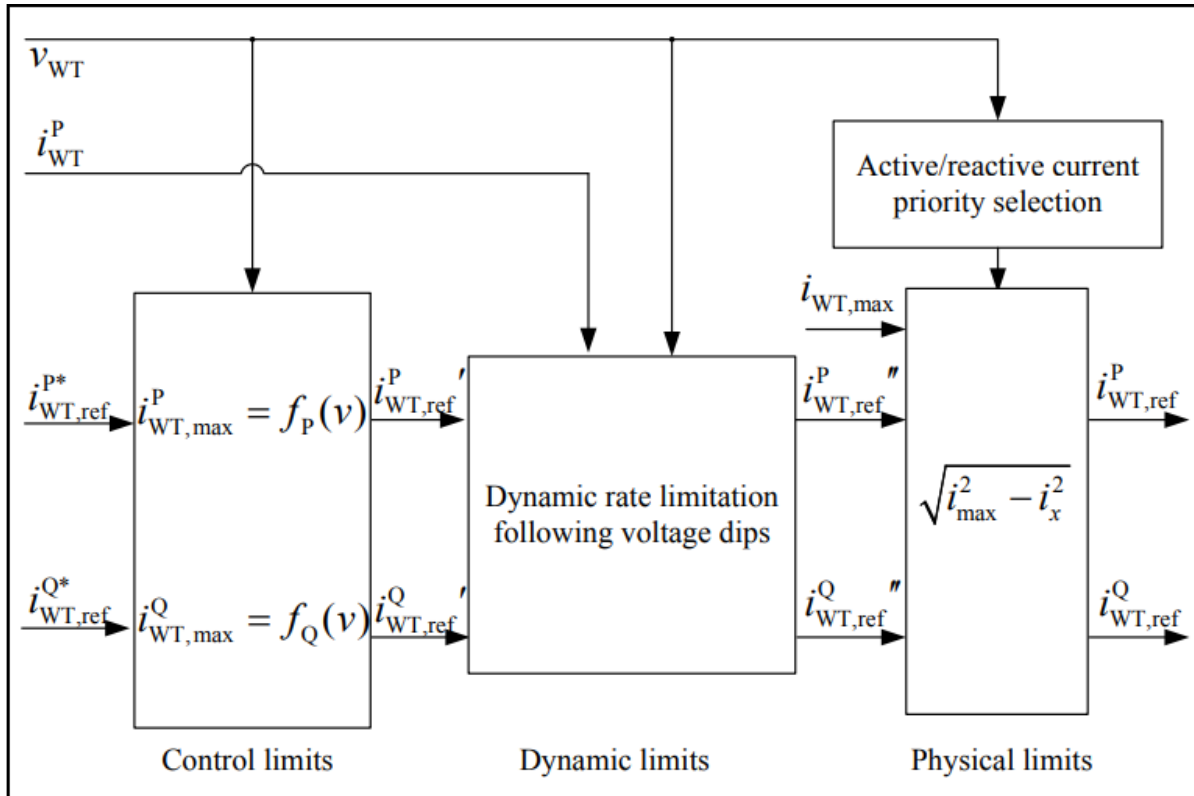


Figure 2.22 Current limitation block model [73].

Where i_{WT}^{P*} and i_{WT}^{Q*} are the active and reactive current reference values from the turbine controller [73].

There are main causes for implementing an active current limitation as function of voltage. There reasons are [73], [79]:

1. Active current limitation to fulfill specific network codes.
2. Implementing a reactive current priority during faults of the electrical network.
3. Network stability limits at weak network connection points.

Whereas the causes for reactive current limitations as function of voltage are:

1. Emulating a specific reactive current control during grid faults.
2. Implementing specific converter limits

B. Dynamic Limits

Dynamic control limits are important for an improved representation of active power recovery after faults in the electrical network. After network faults, a slow recovery of active and reactive

power or currents could be required. Figure 2.23 shows these currents $i_{WT,ref}^P$ and $i_{WT,ref}^Q$ [73].

The main causes of the dynamic control limits are [73].:

1. Limiting voltage changes to restrain overvoltage following network faults.
2. Limiting DC-link voltage variations because of very fast changes of active power.
3. Limiting gearbox and shaft loads.

Moreover, a delay may be happened after the voltage starts rising until the active power increases. The reason of this is the control delays in the converter, phase angle jumps after fault clearance and a settling time needed by the phase locked loop to synchronize after voltage dips to very low voltages [73].

C. Physical Limits

In fact, the physical limits for the maximum current which the system can feed into the electrical network is defined by short term thermal current limitations. These current limits of the doubly feed generator and full scale converter are always defined by the converter because it has far shorter time constants than the generator. Generally, active current has the priority during steady state operation while a reactive current has the priority during very low or high voltage states to reduce the voltage changes in the grid. If we considered that maximum allowed current for the wind turbine is $i_{WT,max}$ the limitations of active and reactive current according to the priority will be as follows [73]:

$$i_{WT,ref}^P = i_{WT,ref}^P \quad (2.13)$$

$$i_{WT,ref}^Q = i_{WT,ref}^Q \quad (2.14)$$

$$i_{WT,ref}^Q = \sqrt{(i_{WT,max})^2 - (i_{WT,ref}^P)^2} \quad (2.15)$$

$$i_{WT,ref}^P = \sqrt{(i_{WT,max})^2 - (i_{WT,ref}^Q)^2} \quad (2.16)$$

Commonly, converters are designed to have a very short overloading capability which allows to feed higher currents for a limited time period, particularly during faults [73].

2.6.5.2 DC-Link Energy Absorber

The electrical energy that can be supplied into the electrical network when faults occur is limited both for physical causes and limited maximum current of converters. As the supplied electrical energy by the wind may not necessarily change, a network fault with voltage below 90% of the nominal voltage will cause an increase of the rotor speed. It's possible to reduce the input power from the wind by changing the blade pitch angle, but the duration of network faults is small compared to the time constants of the pitch system [73].

Wind turbines that use full scale converter are generally equipped with a controlled resistor in the DC-link or another technique to absorb at least a part of the energy supplies by the generator that cannot be injected into the network in the case of grid faults [73].

2.6.5.3 Resulting Generator and Converter Model

The resulting generator model of the full-scale converter model including current limitation, transformer and DC-link energy absorber is shown in Figure 2.24. In fact, this model does not exactly represent the real turbines where functionality may be implemented either in the wind plant control, the converter or the turbine control. However, it allows a modular model design [73].

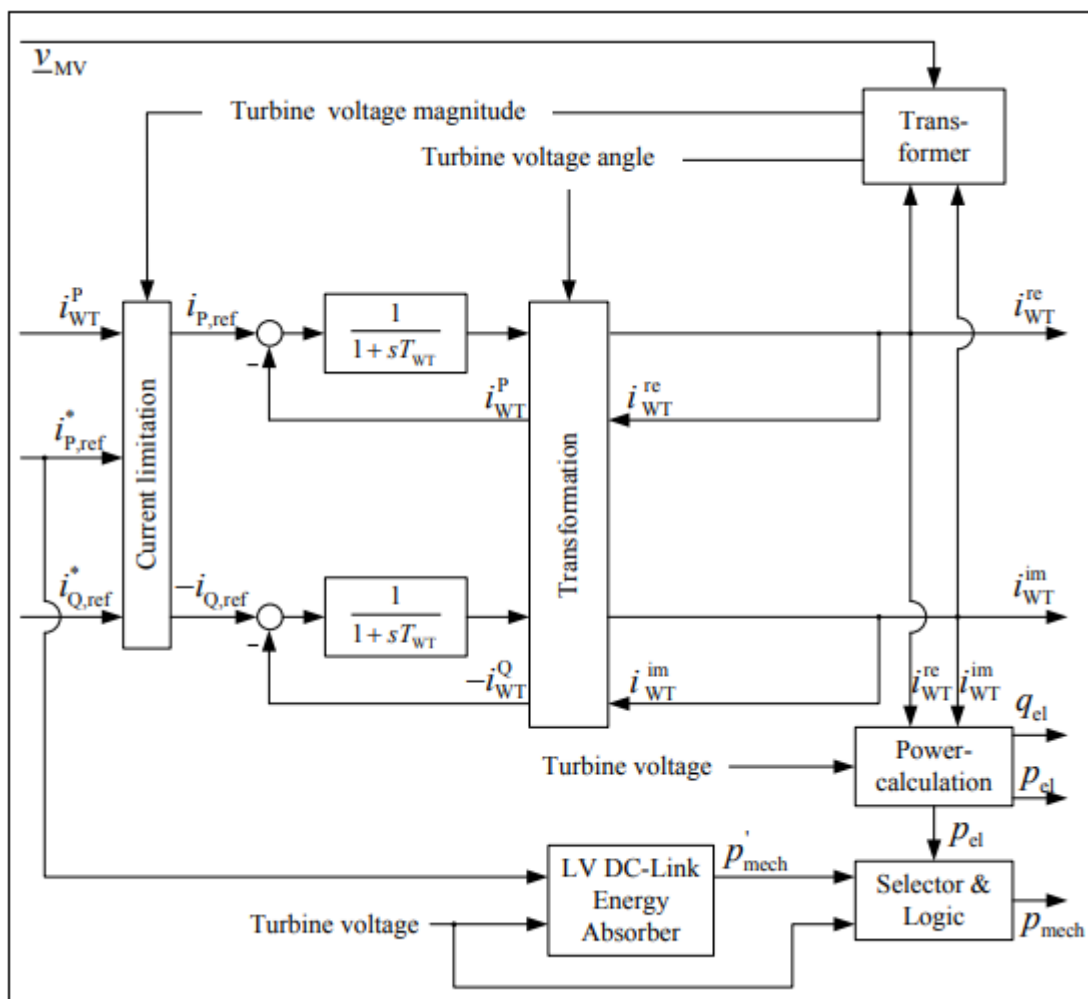


Figure 2.23 Aggregated generator model for Full scale converter [73].

2.6.6. Control Structures for Grid Converter

In the following, a few control structures for the grid side converter are discussed. Control strategy for distributed generation can be implemented in various reference frames like synchronous rotating frame (dq), stationary frame ($\alpha\beta$), or reference frame (abc) [80].

2.6.6.1 The dg Control

This control structure uses the abc→dq transformation module in order to transform the control variables from their main frame (abc) to another frame which rotates synchronously with the frequency of the network voltage. Therefore, the control variables become dc signals. For this control structure, there is a need for the information about the phase angle of utility voltage to perform the abc→dq transformation. Generally, proportional integral controllers (PI) controllers are used with this control structure. Normally, a transfer function of a (PI) controller is given by [80]:

$$G_{PI}(s) = K_p + \frac{K_i}{s} \quad (2.17)$$

Where [80].:

K_p is the proportional gain of the controller.

K_i is the integral gain of the controller.

The dq control structure involves cross coupling and feedforward of the network voltage values. As network voltage feedforward is used, the dynamics of this control structure is expected to be high when the network faces voltage fluctuations. Each deviation of the voltage amplitude of the network will be transformed and reflected into d and q axis components of the voltage, which will lead to a fast response of the control system [80].

2.6.6.2 Stationary Frame Control

Generally, the control variables of the stationary reference frame control such as network currents are time varying waveforms. Therefore, (PI) controllers face many difficulties in removing the steady state error. So, this situation needs another type of controller that should be used [80].

The proportional resonant (PR) controller [81],[82],[83],[84] got a large popularity because of its ability of removing the steady state error during the regulation process of sinusoidal signals, as is the case of $\alpha\beta$ or abc control structures. Furthermore, this controller is suitable for on-grids systems because it is easy to implement a harmonic compensator for low-order harmonics without affecting the controller dynamics [85]. The typical transfer function of resonant controller is as follows [80]:

$$G_{PR}(s) = K_p + K_i \frac{s}{s^2 + \omega^2} \quad (2.18)$$

This controller works on a very narrow band around its resonant frequency ω . Therefore, it is possible to use harmonic compensator for low-order harmonics without affecting the behavior of the current controller [85]. The harmonic compensator has a transfer function that is defined by [80]:

$$G_{HC}(s) = \sum_{h=3,5,7} K_{ih} \frac{s}{s^2 + (\omega h)^2} \quad (2.19)$$

Where h indicates the harmonic order that the compensator is designed for.

Both equations of the resonant controller and harmonic compensator use information about the resonant frequency that the controller works with it. In order to get the best performance of the resonant controller, this frequency must be the same as the network frequency. Therefore, there is a necessity to perform adaptive adjustment of the controller frequency if network frequency variations are registered in the utility grid [80], [86].

2.6.6.3 The abc Frame Control

Actually, the abc frame control is one of the first control structures which are used for pulse width modulation (PWM) driven converters [87], [88]. The biggest disadvantage of this type of controllers was the need of high sampling rate to achieve high performance. At present, the fast development of digital devices such as microcontrollers and digital signal processors, made the implementation of nonlinear controllers for on-grid systems very actual [80].

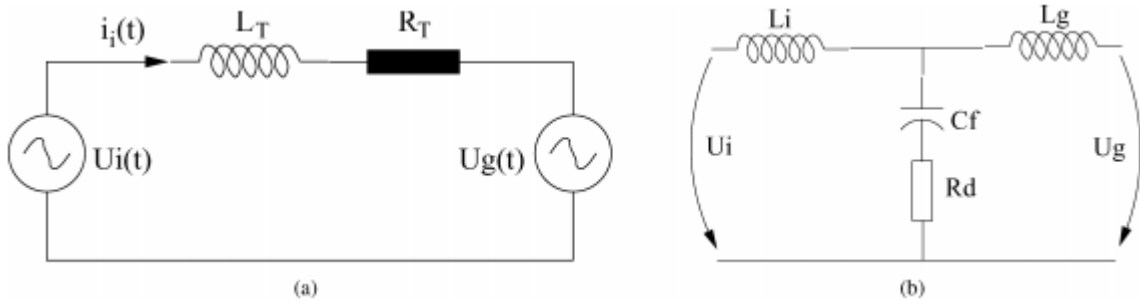


Figure 2.24 (a) Representation of single-phase circuit used to derive the DB controller equation, where $L_T = L_i + L_g$ and $R_T = R_i + R_g$ (b) Single-phase representation of the LCL filter used to calculate the gains of the controllers [80].

In such type of frame control and when an isolated neutral transformer is used, as is the case of distributed generation using a Δ transformer as network interface, only two of the network currents can be controlled in an independent way. The third current is the negative sum of the other two currents according to Kirchhoff current law. Therefore, it is necessary to implement only two controllers in this case [89]. In the following, there is a description of the implementation of PI, PR, and deadbeat (DB) controllers in stationary abc frame [80].

1. PI Controller

The portability of the PI controller to another reference frame using transformation modules between the frames has been derived in [89]. Furthermore, the equivalent of PI controller in abc frame has been derived in [90] as shown (4). The complexity of the controller matrix is due to the off diagonal terms because of the cross coupling terms between the phases [80].

$$G_{PI}^{(abc)}(s) = \frac{2}{3} \begin{bmatrix} K_p + \frac{K_i s}{s^2 + \omega_0^2} & -\frac{K_p}{2} - \frac{K_i s + \sqrt{3} K_i \omega_0}{2(s^2 + \omega_0^2)} & -\frac{K_p}{2} - \frac{K_i s - \sqrt{3} K_i \omega_0}{2(s^2 + \omega_0^2)} \\ -\frac{K_p}{2} - \frac{K_i s - \sqrt{3} K_i \omega_0}{2(s^2 + \omega_0^2)} & K_p + \frac{K_i s}{s^2 + \omega_0^2} & -\frac{K_p}{2} - \frac{K_i s + \sqrt{3} K_i \omega_0}{2(s^2 + \omega_0^2)} \\ -\frac{K_p}{2} - \frac{K_i s + \sqrt{3} K_i \omega_0}{2(s^2 + \omega_0^2)} & -\frac{K_p}{2} - \frac{K_i s - \sqrt{3} K_i \omega_0}{2(s^2 + \omega_0^2)} & K_p + \frac{K_i s}{s^2 + \omega_0^2} \end{bmatrix} \quad (2.20)$$

2. Resonant Controller

The PR controller is already defined in stationary frame, therefore, its portability to the main frame is a straight solution. So, the controller matrix is expressed as showing in the following equation [80]:

$$G_{PR}^{(abc)}(s) = \begin{bmatrix} K_p + \frac{K_i s}{s^2 + \omega_0^2} & 0 & 0 \\ 0 & K_p + \frac{K_i s}{s^2 + \omega_0^2} & 0 \\ 0 & 0 & K_p + \frac{K_i s}{s^2 + \omega_0^2} \end{bmatrix} \quad (2.21)$$

In such case, there is no cross-coupling terms for phases interaction. Therefore, the previous equation cannot be used when the neutral of the transformer is isolated. Hence, only two controllers are necessary in this case [80], [89].

3. DB Controller

DB controller has high dynamic response so it is widely implemented for sinusoidal current regulation in many systems and applications [80],[91],[92],[93],[94],[95],[96],[97],[98]. The main principle of DB controller is to calculate the derivative of the controlled variable in order to anticipate the influence of the control action. This type of controllers has theoretically a very high bandwidth, therefore, tracking of sinusoidal signals is very effective. Nevertheless, if the saturation of the control action and PWM are considered, the DB controller shows slower response [80].

Using Kirchoff's law, it is possible to derive the equation of DB controller for a single-phase circuit that is shown in figure 2.24 (a). In such situation, the equation for the current through the inverter i_i is defined as follows [80]:

$$\frac{di_i(t)}{dt} = -\frac{R_T}{L_T} i_i(t) + \frac{1}{L_T} (U_i(t) - U_g(t)) \quad (2.22)$$

Where [80]:

L_T is the total inductance upstream of the grid converter.

R_T is the total resistance upstream of the grid converter.

$U_i(t), U_g(t)$ are the inverter and grid voltages, respectively.

The discretized form of (6) is defined by [80]:

$$i_i((k+1)T_s) = e^{-(R_T/L_T)T_s} \cdot i_i(kT_s) - \frac{1}{R_T} (e^{-(R_T/L_T)T_s} - 1) (U_i(kT_s) - U_g(kT_s)) \quad (2.23)$$

By solving (7), the controller equation will be as follows [80]:

$$G_{DB}^{(abc)} = \left(\frac{1}{b}\right) \left(\frac{1-az^{-1}}{1-z^{-1}}\right) \quad (2.24)$$

Where a and b can be calculated by [80]:

$$a = e^{-(R_T/L_T)T_s} \tag{2.25}$$

$$b = -\frac{1}{R_T}(e^{-(R_T/L_T)T_s} - 1) \tag{2.26}$$

Eventually, the controller equation can be described as [80]:

$$U_i((k + 1)T_s) = U_i((k - 1)T_s) + \frac{1}{b}\Delta i(kT_s) - \frac{a}{b}\Delta i((k - 1)T_s) + U_g((k + 1)T_s) - U_g((k - 1)T_s) \tag{2.27}$$

In this case, the controller equation also has been derived taking into account a single-phase circuit. Hence, it is necessary to implement only two controllers in the case of an isolated neutral transformer where the third grid current is calculated by the Kirchhoff's law [80].

2.6.7 Control Structure of Wind Turbines

Figure 2.25 shows control structure of wind turbines which includes both fast and slow control dynamics, where it illustrates the general control structure for a wind turbines, including turbine, generator, converter, and filter. In fact, power flow in and out of the wind farm generation system must be controlled carefully. Therefore, the generated power by the wind turbines has to be managed using mechanical parts such as pitch angle of blade. At the same time, the whole control system must follow the power generation commands that are given by distribution system operator DSO or transmission system operator TSO [99],[100],[101],[102],[103],[104],[105],[106].

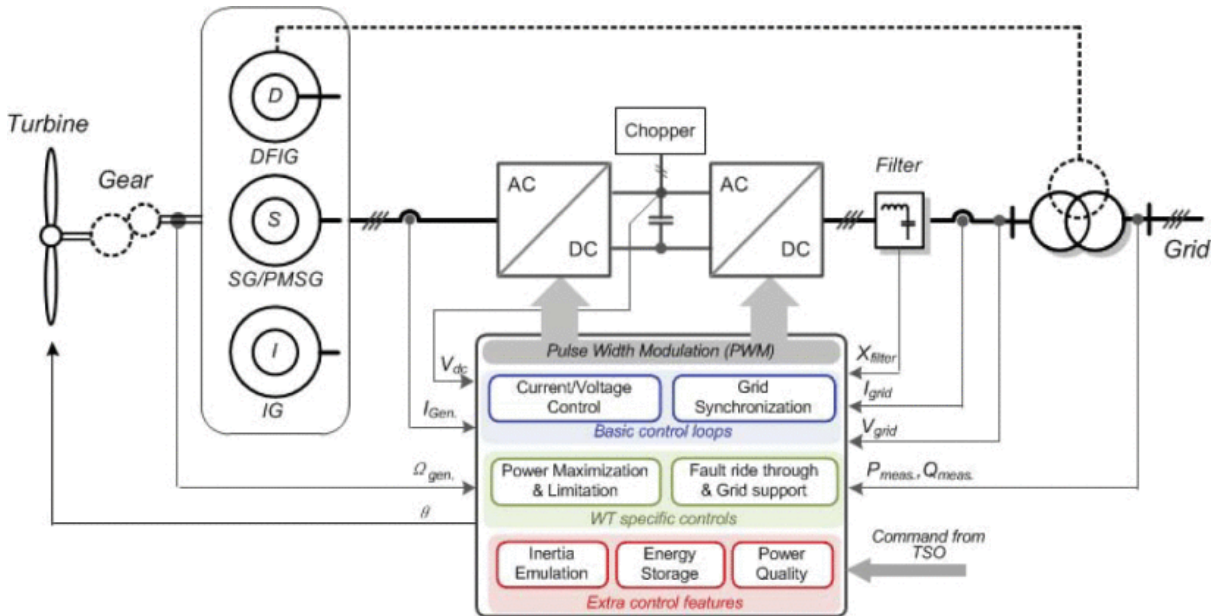


Figure 2.25 Aggregated generator model for Full scale converter [99].

More developed features of wind turbine control could be considered such as the maximization of the generated electric power, providing network supporting functions in normal and

link in case of network faults, when the additional turbine power must be dissipated due to the quick drop of network voltage [99].

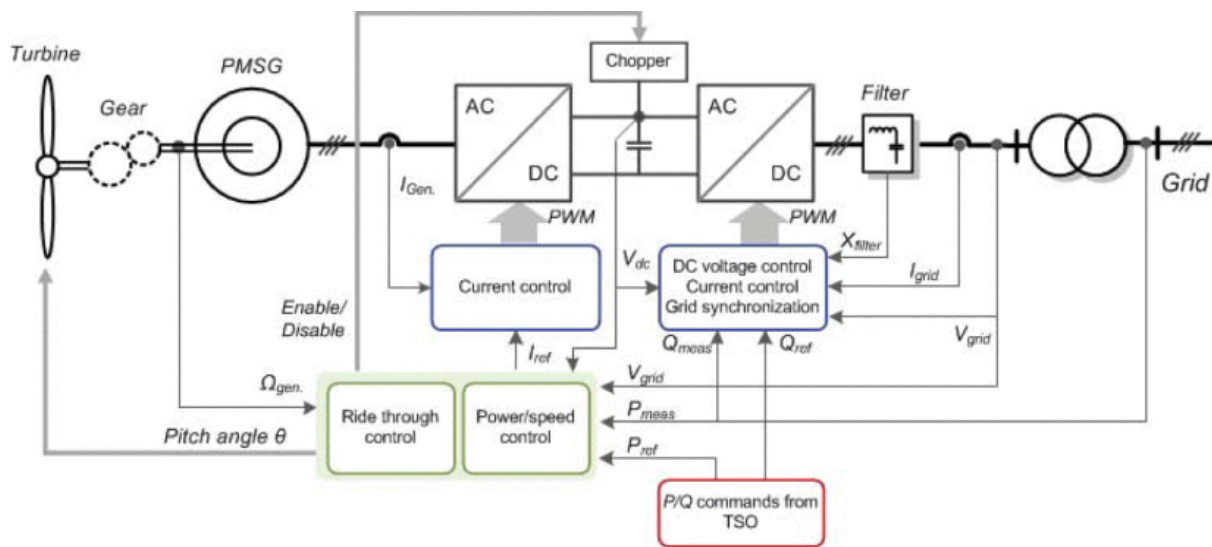


Figure 2.27 Control of active and reactive power in a wind turbine with multipole PMSG [99].

2.6.8 Voltage profile stability in wind farms systems

Voltage stability, which also called load stability, is strongly related to reactive power shortage in the electrical grid. Reactive power compensation was usually performed by combining var compensators, like capacitor banks. Nevertheless, power electronics are used now to improve voltage stability and this type of equipment is called as Flexible Alternative Current Transmission Systems (FACTS). These devices are used in addition to traditional capacitor banks. The main features of these devices include their capacities to improve voltage profile of the electrical grid and dynamic behavior of the whole electrical system in addition to enhance power quality. The implementation of FACTS devices is basically justified because of their dynamic contribution of voltage control, reactive power, and quick response of these devices [111].

Reactive power sources protrude as the best devices for enhancing voltage stability in the electrical networks. Thus, the impact of wind energy on electrical networks is concentrated on several points related to stability, power quality, security, and operation of electrical systems [111].

- All the devices must work together to feed stable and reliable voltage supply stable within particular limits of magnitude and frequency. Connecting of many wind farms could lead to voltage changes. Therefore, some countries have determined a higher short-circuit level at the connection point, generally between 20 and 25 times the wind farm capacity. Although, there are some examples with a lower short circuit level and successful operation of electrical systems [111] [112].

- Power quality is connected to the voltage variation and harmonic distortion in the electrical grid. Nevertheless, combining wind energy in electrical networks may affect the supplied electrical power to the customers. In order to reduce this influence, wind energy conversion

systems which composed of variable speed wind turbines are equipped with power electronics. Power electronics are capable of improving power quality because electronics converters can be controlled to reduce voltage fluctuation, harmonic distortion, or Flicker [111].

- The protection system of electrical system is affected by wind farms because of wind power injection which will change power flow, therefore traditional protection systems could fail under faults [111].
- The electrical grid was passively operated and kept stable under most cases. Nevertheless, if an increase in wind energy penetration is considered, the electrical grid can not be operated passively anymore. Lately, new specifications for wind farm units have been designed to keep electrical systems stable under different types of disturbances like low voltage ride-through capability [111].

2.6.9 Voltage stability improvement and FACTS devices

2.6.9.1 Static Var Compensator (SVC):

Static Var Compensator (SVC), according to the IEEE, is a shunt connected static var generator or absorber which has an output can be adjusted to exchange capacitive or inductive current to control particular parameters of the electrical network basically the bus voltage [111] [113].

SVCs can be divided to:

1. Thyristor-Controlled Reactor (TCR).
2. Thyristor-switched capacitors (TSCs).
3. Thyristor-Switched Reactor (TSR).

Figure 2.28 shows a single-phase equivalent circuit of TCR. In this device, shunt reactor is dynamically controlled from a minimum value (zero) to a maximum value using conduction control of the bidirectional thyristors. In this way, SVC works like a variable shunt reactance that build by the parallel connection of the inductive reactance X_L that is controlled by the bidirectional controlled thyristors and the shunt capacitive reactance X_C [111].

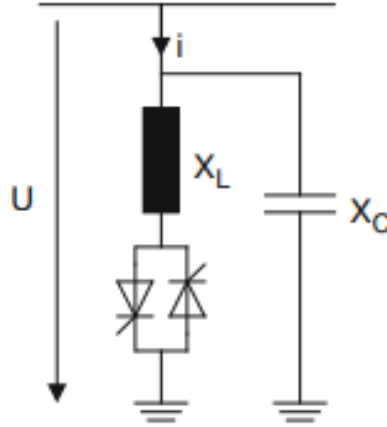


Figure 2.28 Single-phase equivalent circuit of the shunt SVC (TCR) [111].

The value of the instantaneous current supplied by SVCs is calculated using the following equation [111]:

$$I = \begin{cases} \frac{U}{X_L} (\cos \alpha_{SVC} - \cos \omega t) & \alpha_{SVC} \leq \omega t \leq \alpha_{SVC} + \varepsilon \\ 0 & \alpha_{SVC} + \varepsilon \leq \omega t \leq \alpha_{SVC} + \pi \end{cases} \quad (2.28)$$

Where:

U is the voltage of SVC at the Point of Common Coupling (PCC).

X_L is the total inductance of SVC.

α_{SVC} is the firing delay angle [111].

ε is the conduction angle of the SVC which is calculated using [111]:

$$\varepsilon = 2(\pi - \alpha_{SVC}) \quad (2.29)$$

It could be noticed that when the delay angle α_{SVC} increases, the conduction angle ε [111]. The control of the output current using the SVC device is based on the control of the firing delay angle of thyristors. Therefore, the maximum current is injected when the firing delay of 90 degrees. At the same time, a partial current contribution occurs when the firing angle delays is between 90 and 180 electrical degrees. This is a factor of improving the inductance of the SVC device and makes it possible; in addition to decrease its share of reactive power and current [111].

Using Fourier analysis, it is possible to get the fundamental component of current as shown in the following equation [111]:

$$I_1 = \frac{2(\pi - \alpha_{SVC}) + \sin 2\alpha_{SVC}}{\pi X_L} U \quad (2.30)$$

Which can be reduced to be [111]:

$$I_1 = B_{SVC}(\alpha_{SVC})U \quad (2.31)$$

Where [111]:

$$B_{SVC}(\alpha_{SVC}) = \frac{2(\pi - \alpha_{SVC}) + \sin 2\alpha_{SVC}}{\pi X_L} \quad (2.32)$$

The maximum value of B_{SVC} is $1/X_L$, which gets along with a conduction angle of 180 and represents the maximum conduction of the thyristors. The lowest value of B_{SVC} is 0 and it corresponds to a conduction angle of zero or firing angle equals to 180. It's not allowed to use thyristor firing angles lower than 90 because they lead to an asymmetric current that composed of high component of continuous current [111].

Voltage-current characteristics could be defined as the ratio between the voltage variation and the variation of the SVC compensating current over the full control range [111]:

$$U = U_{ref} + X_{SL}I \quad (2.33)$$

Generally, the typical values of X_{SL} range from 0.02 to 0.05 p.u., referring to the base value of the SVC. The SVC will work as a fixed reactance under limit conditions. Figure 2.29 shows the characteristic curve of an SVC. Therefore, the supplied reactive power by the TCR might be calculated using the following equation [111]:

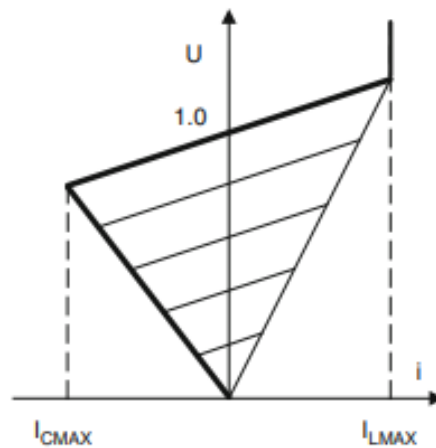


Figure 2.29 Voltage-current characteristics of the SVC [111].

$$Q_{SVC}(\alpha_{SVC}) = \frac{U^2}{X_C} - U^2 B_{SVC}(\alpha_{SVC}) \quad (2.34)$$

Optimum location and sizing of FACTS devices are the most important points for power grids operation especially grids with high wind power penetration in addition to keep the efficiency and security of the electric power system [111].

2.6.9.2 Static Synchronous Compensator (STATCOM)

According to IEEE definition, a STATCOM is a static synchronous generator operated as a shunt-connected static var compensator which has capacitive or inductive output current that could be controlled independently of the AC electrical system [111].

STATCOM device is a static compensator which is connected in parallel to the electrical network in order to compensate the reactive power. This device is capable to absorb or inject reactive power in the grid in a controlled way regardless of the network voltage [113],[114]. The main part is the Voltage Source Converter (VSC) that can convert the DC input voltage to an AC output voltage at the fundamental frequency with a controllable phase and a specific amplitude. The AC output voltage is controlled in dynamical way to inject or absorb the needed reactive power to the electrical grid [111].

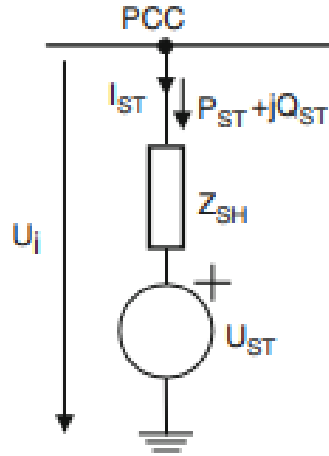


Figure 2.30 Equivalent circuit of the STATCOM [111].

The VSC generates a voltage $\vec{U}_{st} = U_{st} \angle \delta_{st}$ at the fundamental frequency with controllable voltage magnitude and phase. The VSC is connected to the electrical network that has a voltage $\vec{U}_i = U_i \angle \delta_i$ by means of an inductive impedance Z_{sh} which represents the impedance of the coupling transformer and the filters. Figure 2.30 shows the equivalent circuit of the STATCOM [111].

The interchange of active and reactive power between the STATCOM and the electrical network could be illustrated as following [111]:

$$P_{st} = U_i^2 \cdot g_{sh} - U_i U_{st} [g_{sh} \cdot \cos(\delta_i - \delta_{st}) + b_{sh} \cdot \sin(\delta_i - \delta_{st})] \quad (2.35)$$

$$Q_{st} = -U_i^2 \cdot b_{sh} - U_i U_{st} [g_{sh} \cdot \sin(\delta_i - \delta_{st}) - b_{sh} \cdot \cos(\delta_i - \delta_{st})] \quad (2.36)$$

Where [111]:

$$Y_{sh} = \frac{1}{Z_{sh}} = g_{sh} + jb_{sh} \quad (2.37)$$

The ability of STATCOM to inject reactive power into the network is related to the maximum voltage and the maximum current which is allowed by the semiconductors, as illustrated in figure 2.31 [111] that shows voltage-current characteristics of the STATCOM.

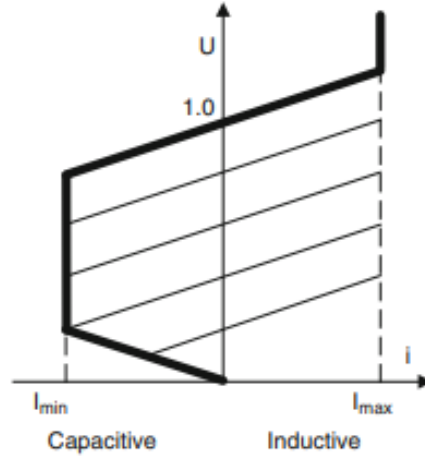


Figure 2.31 Voltage-current characteristics of the STATCOM [111]

The operation principle of the VSC-based STATCOM is related to the control technique for managing the power interchange between the network and the converter and it depends also on the output voltage of the converter. If the amplitude of the voltage converter equals to the network voltage, the interchange of reactive power between the STATCOM and the network is zero too. But, if the STATCOM is controlled in a way that converter voltage is less than the network voltage at the PCC, $U_{st} < U_i$, the STATCOM will absorb reactive power which will draw lagging current. In contrast, if the converter voltage is higher than the grid voltage $U_{st} > U_i$, reactive power will be injected into the network [111] [115].

Practically, it is very important to control also the active power interchange between the STATCOM device and the network by controlling the phase angle $\delta_{i,st} = \delta_i - \delta_{st}$ between the converter voltage ($\vec{U}_{st} = U_{st} \angle \delta_{st}$) and the PCC voltage ($\vec{U}_i = U_i \angle \delta_i$) so that the converter absorbs active power from the network to keep a constant voltage for the DC-link [111].

There are many control strategies of STATCOM devices [116]. The most typical ones are two that are listed below [111]:

- Voltage local control at the PCC voltage: The main objective of this control technique is to regulate the PCC voltage U_i to be constant and equal to its reference value U_i^{ref} . This condition is illustrated mathematically as a restriction of operation [111]:

$$U_i - U_i^{ref} = 0 \quad (2.38)$$

- Reactive Power control at the PCC: There are many cases which require the STATCOM to inject reactive power into the network according to the needs and orders of the TSO. Such type of control can be applied when a coordinated control is needed for FACTS devices and wind

farms deliver reactive power to the whole electrical network [117]. The restriction of operation for this control strategy can be expressed as follows [111]:

$$Q_{st} - Q_{st}^{ref} = 0 \quad (2.39)$$

Chapter 3

3 Methodology

3.1. General approach

There are a lot of factors that affect the voltage profile and power factor of the electrical grid such as topology of the electrical grids, location of the DG units, length of the transmission lines, load changes over the time, generated active power and faults occurrence. These factors will be studied and included in the methodology and results section [118].

The new approach involves a new important parameter in the proposed controller which is the admittance value between the DG unit and the busbars in addition to the voltage variations of busbars. These two parameters have a significant impact on the reactive power flow and voltage profile. The used data in the simulation model are from a real network. We will use different scenarios and cases to check the efficiency of the controller by changing loads values, wind speeds and under fault conditions. In this work, we focus on improving voltage quality by minimizing voltage variations and improving power factor to achieve better voltage quality. The model is created using MATLAB Simulink software [118].

The new technique depends on the admittance's values between DG units and busbars, in addition to the voltage deviation values of busbars as an input of the controller which will control the reactive power generation from all DG units in order to improve the voltage quality and power factor in the grid. In fact, controlling voltage in far busbars is a very hard mission if we do not have close control tools to these busbars. As DG units become an essential part of the smart grid, we can use them as a voltage control tool. DG units could be equipped with full scale converter, so they are capable to generate reactive power separately from active power. Moreover, there is a strong relation between the voltage profile and reactive power. Technically, we will get better a voltage profile when the reactive power is generated closer to the busbars. The admittance values between DG units and busbars give us a very good parameter for how far the DG unit is from the busbars, so we will be able to identify the suitable reactive power which must be generated [118].

Let's assume that we have a simple electrical system that consists of only generator, transmission line and load. The net reactive power at the load side will be:

$$Q_N = Q_L - Q_G = \left| \frac{V_S V_n}{X_L} \right| \cos \delta - \left| \frac{V_n^2}{X_L} \right| \quad (3.1)$$

Where:

Q_L : The demanded reactive power.

Q_G : The supplied reactive power.

V_S : Sending voltage (nominal voltage).

V_n : Measured voltage at receiving end.

X_L : Reactance of the transmission line.

δ : Load angle

If we assumed that $\delta \approx 0 \Rightarrow \cos \delta = 1$ therefore:

$$Q_N = \left| \frac{V_S \cdot V_n}{X_L} \right| - \left| \frac{V_n^2}{X_L} \right| \quad (3.2)$$

This will lead to the following equation:

$$V_n = \frac{V_S + \sqrt{V_S^2 - 4Q_N \cdot X_L}}{2} \quad (3.3)$$

This equation shows that if we controlled the net reactive power at each node, we can control the voltage values of nodes.

The ideal case will be when $V_R = V_S$ and it occurred when $Q_N = 0$. Therefore, we have to increase supplied reactive power.

In our methodology, we assume that we have a general electrical system, as shown in Figure 3.1, which consists of many generators, G1, G2, G3, etc. which feed many loads through transmission lines between busbars. These loads are connected to n busbars. In this electrical system, there are also many DG units equipped with converters [118].

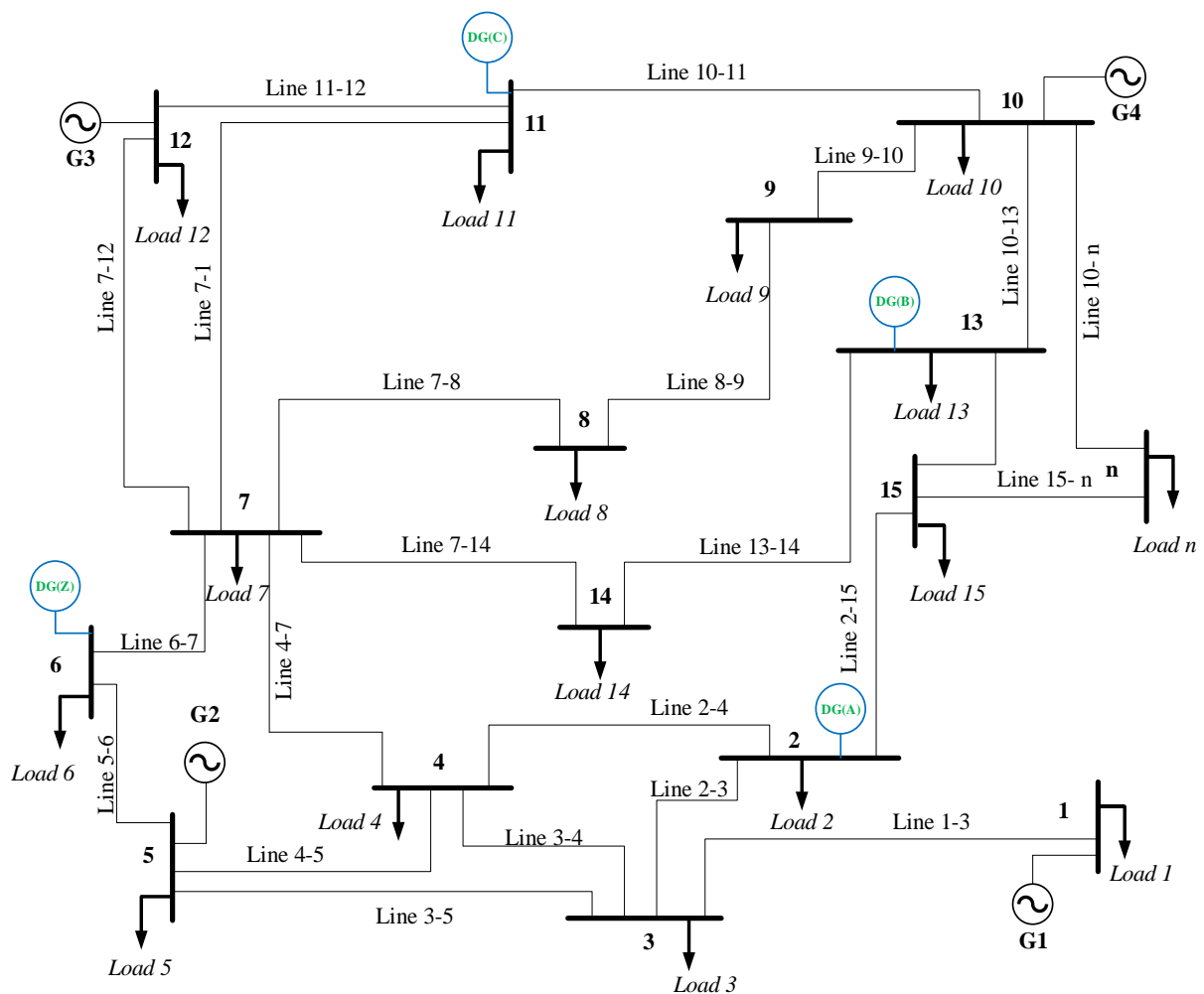


Figure 3.1 General electrical system [118].

The DG units used in this research are wind farms type 4, which consist of a permanent magnet synchronous generator PMSG and have a full-scale converter. These wind farms are capable of generating both active and reactive power separately. The structure of the control system is illustrated in Figure 3.2. The input signals of the controller are the measured values of voltage and admittance, and the output control signal is Q_{ref} [118].

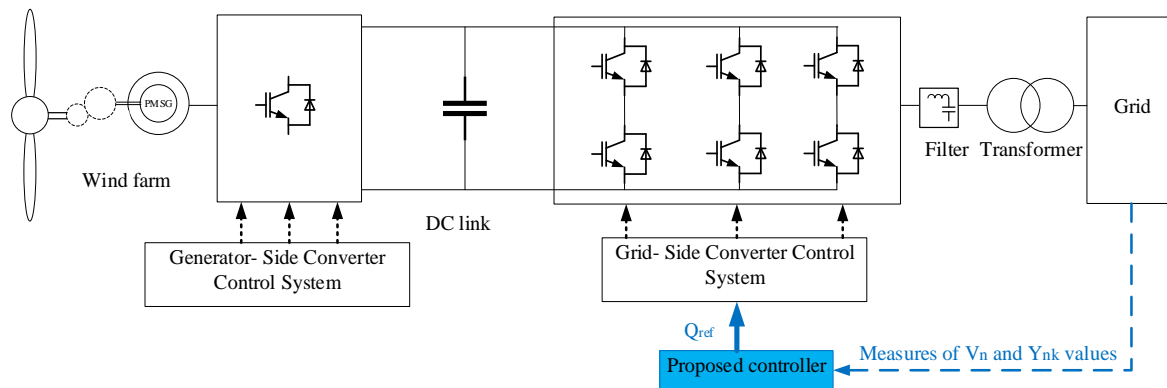


Figure 3.2 Control system structure [118].

Due to the impedance of transmission lines and load changes, we will not obtain nominal voltage at the busbars and there will be voltage deviations. Therefore, we will assume that voltage values at busbars are $V_1, V_2, V_3, \dots, V_n$, voltage deviations are $dV_1, dV_2, dV_3, \dots, dV_n$ and voltage deviations percentages are $dV_1\%, dV_2\%, dV_3\%, \dots, dV_n\%$. The voltage deviation percentage is defined as in the following equation [118]:

$$dV_n\% = \frac{V_S - V_n}{V_S} \times 100 \quad (3.4)$$

where V_S represents the nominal voltage and V_n represents the measured voltage of busbar n [118]. Using equation (3.3), we will get:

$$dV_n\% = \frac{V_S - \frac{V_S + \sqrt{V_S^2 - 4Q_N \cdot X_L}}{2}}{V_S} \times 100 = 1 - \frac{V_S + \sqrt{V_S^2 - 4Q_N \cdot X_L}}{2V_S} \times 100 \quad (3.5)$$

Therefore:

$$dV_n\% = \frac{1}{2} - \frac{\sqrt{V_S^2 - 4Q_N \cdot X_L}}{2V_S} \times 100 \quad (3.6)$$

First, we will measure the impedance values Z and, by inverting them (as $Y = \frac{1}{Z}$), we can get admittance values between each busbar and the DG units, where for the first busbar the admittance between it and DG units will be $Y_{1A}, Y_{1B}, Y_{1C}, \dots, Y_{1Z}$. These values represent the admittance between busbar 1 and DG unit A, B, C, ..., Z respectively, as well as the same for other busbars. So, we will obtain the end result of all admittance values according to the following equation [118]:

$$y = \begin{bmatrix} Y_{1A} & Y_{1B} & \cdots & Y_{1Z} \\ Y_{2A} & Y_{2B} & \cdots & Y_{2Z} \\ \cdots & \cdots & \cdots & \cdots \\ Y_{nA} & Y_{nB} & \cdots & Y_{nZ} \end{bmatrix} \quad (3.7)$$

Now, we will identify a new factor which we will call admittance factor y' . The admittance factor for the first DG unit is [118]:

$$y'_{1A} = \frac{Y_{1A}}{Y_{1A} + Y_{1B} + Y_{1C} + \cdots + Y_{1Z}} = \frac{Y_{1A}}{\sum_{k=A}^Z Y_{1k}} \quad (3.8)$$

where k represents DG unit (A, B, C, ..., Z) [118].

As well as the same for other busbars and DG units.

Obviously, the admittance factor will be bigger for the closer DG unit and vice versa. So, we will get the admittance factors matrix as shown in the following equations [118]:

$$y' = \begin{bmatrix} \frac{Y_{1A}}{\sum_{k=A}^Z Y_{1k}} & \frac{Y_{1B}}{\sum_{k=A}^Z Y_{1k}} & \cdots & \frac{Y_{1Z}}{\sum_{k=A}^Z Y_{1k}} \\ \frac{Y_{2A}}{\sum_{k=A}^Z Y_{2k}} & \frac{Y_{2B}}{\sum_{k=A}^Z Y_{2k}} & \cdots & \frac{Y_{2Z}}{\sum_{k=A}^Z Y_{2k}} \\ \cdots & \cdots & \cdots & \cdots \\ \frac{Y_{nA}}{\sum_{k=A}^Z Y_{nk}} & \frac{Y_{nB}}{\sum_{k=A}^Z Y_{nk}} & \cdots & \frac{Y_{nZ}}{\sum_{k=A}^Z Y_{nk}} \end{bmatrix} \quad (3.9)$$

$$y' = \begin{bmatrix} y'_{1A} & y'_{1B} & \cdots & y'_{1Z} \\ y'_{2A} & y'_{2B} & \cdots & y'_{2Z} \\ \cdots & \cdots & \cdots & \cdots \\ y'_{nA} & y'_{nB} & \cdots & y'_{nZ} \end{bmatrix} \quad (3.10)$$

DG units are equipped with converters so, they are capable of changing the angle between voltage and current consequently the generated reactive power. In smart grids, obtaining a steady and stable voltage with small voltage variation from the nominal voltage is very important, especially for highly sensitive electronic devices. In our methodology, DG units have been controlled to produce reactive power according to the voltage deviations of busbars and the varying admittance factors between busbars and DG units. To compensate for any increase in voltage deviation, we need to increase the generated reactive power. In the same vein, the generated reactive power must come from the closest DG unit which will have the highest value of the impedance factor. For the first busbar, the voltage deviation percentage is $dV_1\%$ thus, the generated reactive power as a percentage value is given according to the following equation [118]:

$$Q_{1A}\% = \frac{dV_1}{dV_{Allowed}} \cdot y'_{1A} = \frac{\frac{1}{2} \sqrt{V_S^2 - 4Q_{N1} \cdot X_{L1}}}{2V_S} \cdot y'_{1A} \quad (3.11)$$

where $dV_{Allowed}$ is the maximum allowed voltage deviation in the electrical grid [118].

The same was done for other busbars and DG units. Therefore, we obtain the matrix of reactive power percentages for all DG units as shown in the following equations [118]:

$$Q\% = \begin{bmatrix} \frac{1}{2} - \frac{\sqrt{V_S^2 - 4Q_{N1} \cdot X_{L1}}}{2V_S} \cdot y'_{1A} & \frac{1}{2} - \frac{\sqrt{V_S^2 - 4Q_{N1} \cdot X_{L1}}}{2V_S} \cdot y'_{1B} & \dots & \frac{1}{2} - \frac{\sqrt{V_S^2 - 4Q_{N1} \cdot X_{L1}}}{2V_S} \cdot y'_{1Z} \\ \frac{1}{2} - \frac{\sqrt{V_S^2 - 4Q_{N2} \cdot X_{L2}}}{2V_S} \cdot y'_{2A} & \frac{1}{2} - \frac{\sqrt{V_S^2 - 4Q_{N2} \cdot X_{L2}}}{2V_S} \cdot y'_{2B} & \dots & \frac{1}{2} - \frac{\sqrt{V_S^2 - 4Q_{N2} \cdot X_{L2}}}{2V_S} \cdot y'_{2Z} \\ \dots & \dots & \dots & \dots \\ \frac{1}{2} - \frac{\sqrt{V_S^2 - 4Q_{Nn} \cdot X_{Ln}}}{2V_S} \cdot y'_{nA} & \frac{1}{2} - \frac{\sqrt{V_S^2 - 4Q_{Nn} \cdot X_{Ln}}}{2V_S} \cdot y'_{nB} & \dots & \frac{1}{2} - \frac{\sqrt{V_S^2 - 4Q_{Nn} \cdot X_{Ln}}}{2V_S} \cdot y'_{nZ} \end{bmatrix} \quad (3.12)$$

$$Q\% = \begin{bmatrix} Q_{1A}\% & Q_{1B}\% & \dots & Q_{1Z}\% \\ Q_{2A}\% & Q_{2B}\% & \dots & Q_{2Z}\% \\ \dots & \dots & \dots & \dots \\ Q_{nA}\% & Q_{nB}\% & \dots & Q_{nZ}\% \end{bmatrix} \quad (3.13)$$

Next, we can find the total reactive power which must be generated by DG units. For the DG unit (A) we find [118]:

$$Q_A\% = Q_{1A}\% + Q_{2A}\% + \dots + Q_{nA}\% = \sum_{i=1}^n Q_{iA}\% \quad (3.14)$$

where i represents busbar number.

The same applies to other DG units. Therefore, the total needed reactive power for all DG units are obtained by the following equation [118]:

$$Q_T\% = \begin{bmatrix} Q_A\% \\ Q_B\% \\ \dots \\ Q_Z\% \end{bmatrix} = \begin{bmatrix} \sum_{i=1}^n Q_{iA}\% \\ \sum_{i=1}^n Q_{iB}\% \\ \dots \\ \sum_{i=1}^n Q_{iZ}\% \end{bmatrix} \quad (3.15)$$

The generated reactive power as a real value [Var] will be [118]:

$$Q_A = Q_A\% \cdot Q_{TA} \quad (3.16)$$

where Q_{TA} is the maximum reactive power of the DG unit (A).

The same applies as well for other DG units. Therefore, the total required reactive power for all DG units is [118]:

$$Q_T = \begin{bmatrix} Q_A \\ Q_B \\ \dots \\ Q_Z \end{bmatrix} = \begin{bmatrix} Q_A\% \cdot Q_{TA} \\ Q_B\% \cdot Q_{TB} \\ \dots \\ Q_Z\% \cdot Q_{TZ} \end{bmatrix} \quad (3.17)$$

Consequently,

$$Q_{N1(new)} = Q_{N1} - (Q_{1A} + Q_{1B} + \dots + Q_{1Z}) = Q_{N1} - \sum_{i=1}^Z Q_{1i} \quad (3.18)$$

So, we will get a new values of Q_{N1} as shown in the following equation:

$$Q_{N(new)} = \begin{bmatrix} Q_{N1} - (Q_{1A} + Q_{1B} + \dots + Q_{1Z}) \\ Q_{N2} - (Q_{2A} + Q_{2B} + \dots + Q_{2Z}) \\ \dots \\ Q_{Nn} - (Q_{nA} + Q_{nB} + \dots + Q_{nZ}) \end{bmatrix} = \begin{bmatrix} Q_{N1} - \sum_{i=1}^Z Q_{1i} \\ Q_{N2} - \sum_{i=1}^Z Q_{2i} \\ \dots \\ Q_{Nn} - \sum_{i=1}^Z Q_{ni} \end{bmatrix} \quad (3.19)$$

Therefore, the new voltage deviation for bus No.1 will be:

$$dV_{1(new)} = \frac{1}{2} - \frac{\sqrt{V_S^2 - 4(Q_{N1} - \sum_{i=1}^Z Q_{1i}) \cdot X_{L1}}}{2V_S} \quad (3.20)$$

For the rest busbars, the values of voltage deviation will be:

$$dV_{(new)} = \begin{bmatrix} \frac{1}{2} - \frac{\sqrt{V_S^2 - 4(Q_{N1} - \sum_{i=1}^Z Q_{1i}) \cdot X_{L1}}}{2V_S} \\ \frac{1}{2} - \frac{\sqrt{V_S^2 - 4(Q_{N2} - \sum_{i=1}^Z Q_{2i}) \cdot X_{L2}}}{2V_S} \\ \dots \\ \frac{1}{2} - \frac{\sqrt{V_S^2 - 4(Q_{Nn} - \sum_{i=1}^Z Q_{ni}) \cdot X_{Ln}}}{2V_S} \end{bmatrix} \quad (3.21)$$

The active power losses for a line x-y for instance will be:

$$\Delta P_{x-y} = \frac{(V_x - V_y)^2}{R_{x-y}} = \frac{(-dV_x + dV_y)^2}{R_{x-y}} = \frac{(-dV_x + dV_y)^2}{R_{x-y}} \quad (3.22)$$

$$\Delta P_{x-y} = \frac{(\sqrt{V_S^2 - 4Q_{Nx} \cdot X_{Lx}} - \sqrt{V_S^2 - 4Q_{Ny} \cdot X_{Ly}})^2}{4 \cdot R_{x-y} \cdot V_S^2} \quad (3.23)$$

$$\Delta P_{x-y} = \frac{Q_{Ny} \cdot X_{Ly} - Q_{Nx} \cdot X_{Lx}}{R_{x-y} \cdot V_S^2} - \frac{1}{2 \cdot R_{x-y} \cdot V_S^2} \cdot \sqrt{V_S^4 - 4Q_{Nx} \cdot X_{Lx} + 4Q_{Ny} \cdot X_{Ly} + 16Q_{Nx}Q_{Ny}X_{Lx}X_{Ly}} \quad (3.24)$$

Thus, active power losses after reactive power compensation will be:

$$\Delta P_{x-y(new)} = \frac{(Q_{Ny} - \sum_{i=1}^Z Q_{yi}) \cdot X_{Ly} - (Q_{Nx} - \sum_{i=1}^Z Q_{xi}) \cdot X_{Lx}}{R_{x-y} \cdot V_S^2} - \frac{1}{2 \cdot R_{x-y} \cdot V_S^2} \cdot (V_S^4 - 4(Q_{Nx} - \sum_{i=1}^Z Q_{xi}) \cdot X_{Lx} + 4(Q_{Ny} - \sum_{i=1}^Z Q_{yi}) \cdot X_{Ly} + 16(Q_{Nx} - \sum_{i=1}^Z Q_{xi})(Q_{Ny} - \sum_{i=1}^Z Q_{yi})X_{Lx}X_{Ly})^{\frac{1}{2}}$$

In terms of $\cos \varphi$, the new value of it will be:

$$\cos \varphi_{x-y} = \frac{P_{x-y} + \sum_{i=1}^Z P_{(x-y)i}}{\sqrt{(P_{x-y} + \sum_{i=1}^Z P_{(x-y)i})^2 + (Q_{x-y} + \sum_{i=1}^Z Q_{1i} + \dots + \sum_{i=1}^Z Q_{ni})^2}}$$

The proposed control algorithm of busbar 1 is shown in Figure 3.3 [118]:

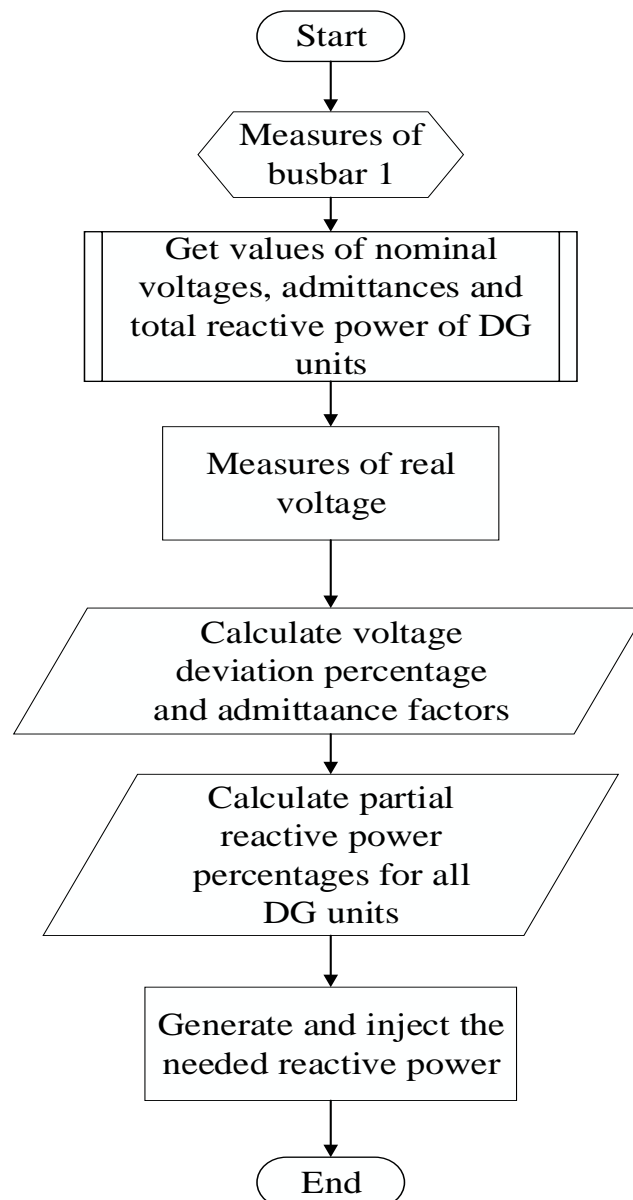


Figure 3.3 Proposed control algorithm of busbar No. 1 [118].

The proposed control algorithm for the entire system is shown in Figure 3.4 [118]:

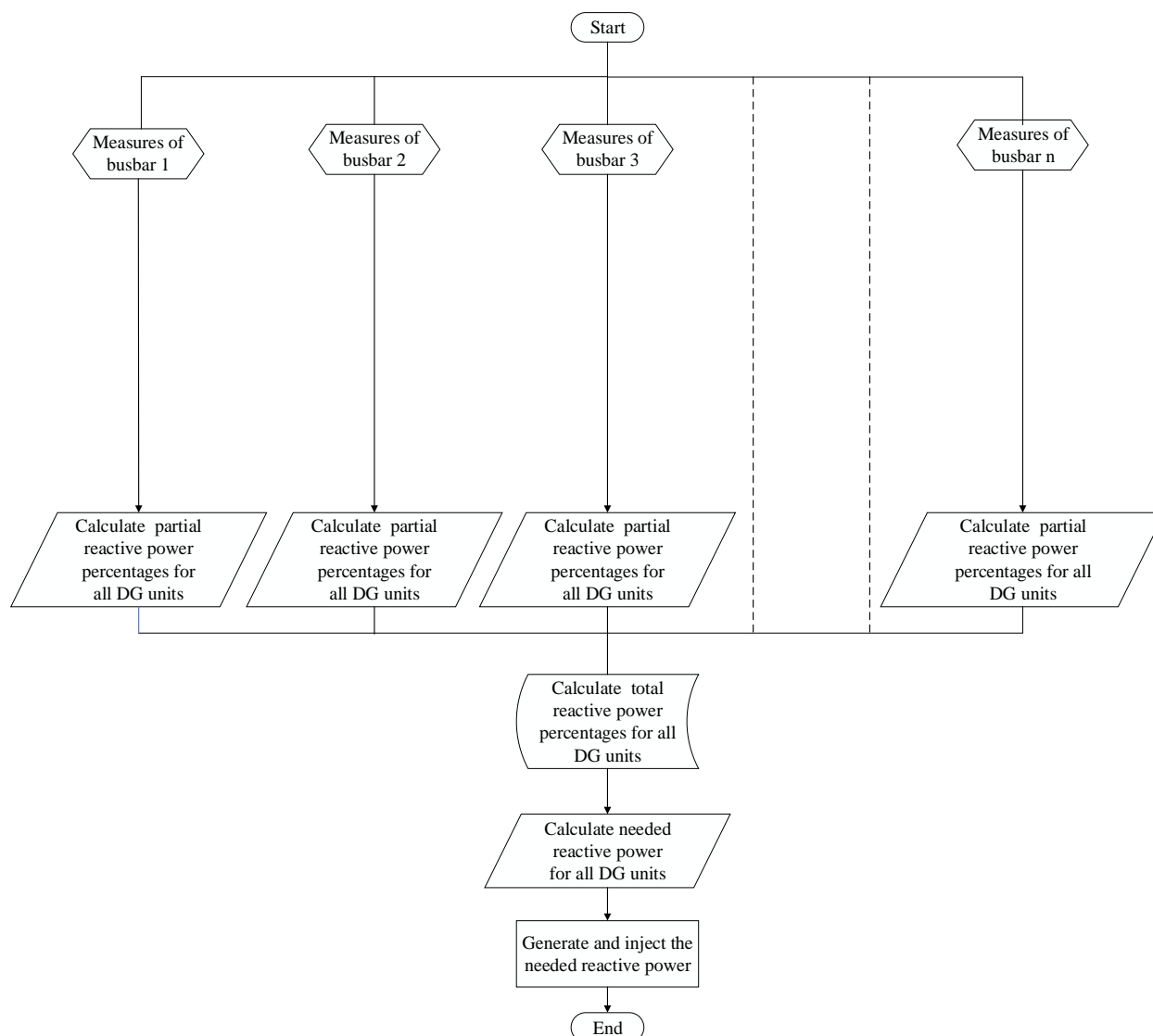


Figure 3.4 Proposed algorithm for the entire system [118].

The whole system and controller made using MATLAB Simulink. Figure 7.1 shows the whole electrical system. Figure 7.2 and 7.3 shows the controller model according to the input data (Voltage or reactive power value).

3.2. Case Study

3.2.1. Proposed mesh grid

The methodology has been applied to the real electrical system which is shown in Figure 3.5. The electrical system consists of the following [118]:

1. Two power sources (G1 and G2) which supply electrical energy to the system through two power transformers 230/66 kV.
2. Eight transmission lines which form the mesh grid. The length of lines is:
 $(L_{0-2} = 50 \text{ km}, L_{2-3} = 20 \text{ km}, L_{3-5} = 25 \text{ km}, L_{0-1} = 30 \text{ km}, L_{1-2} = 60 \text{ km},$
 $L_{3-4} = 50 \text{ km}, L_{1-4} = 35 \text{ km}, L_{4-6} = 30 \text{ km}).$
3. Six power transformers 66/20 kV which supply power to six loads.

4. Six loads with different values ($S_1 = 20 + j6$ MVA, $S_2 = 22 + j7$ MVA, $S_3 = 18 + j4$ MVA, $S_4 = 14 + j4$ MVA, $S_5 = 12 + j3$ MVA, $S_6 = 12 + j4$ MVA).
5. Three DG units which are connected to three different locations (Busbar 1, Busbar 2, and Busbar 4) with different capacities ($S_A = 15.56$ MVA, $S_B = 26.67$ MVA, $S_C = 35.56$ MVA.) [118].

These DG units are equipped with a full scale converter. These DG units are connected to the grid using three transformers which have the parameters as in Tables 7.1, 7.2, and 7.3 [118].

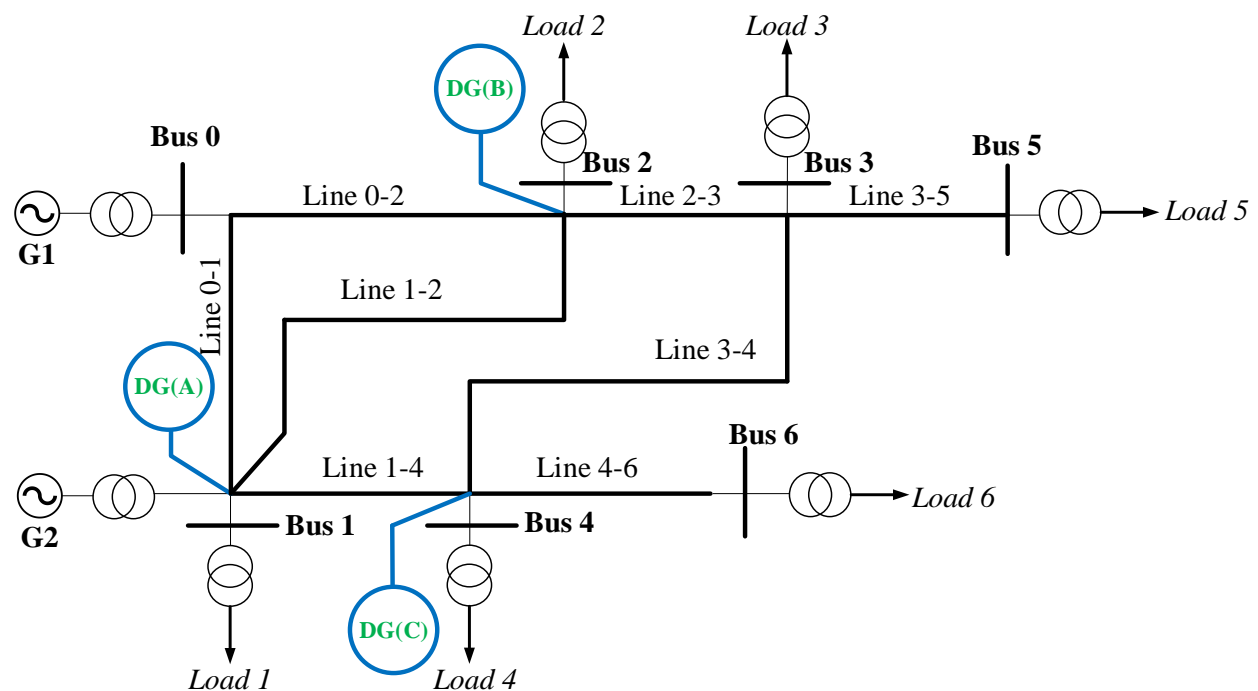


Figure 3.5 Proposed mesh grid [118].

3.2.2. Simulation and procedures

First, we built the Simulink model of the electrical grid then the Simulink model of the controller that accords to our methodology containing six busbars and three DG units. In order to construct the controller, we needed to measure admittance values and admittance factors because they are constant inputs of the controller. Measuring these values could be done by measuring the impedance between the DG units and busbars and then inverting the impedance value as $Y = \frac{1}{Z}$ and we got these values from the real grid. Admittance values include transmission lines and transformers. After measuring the admittance values, we can calculate admittance factors using equation (3.3). The following constant values have been obtained [118]:

$$y' = \begin{bmatrix} y'_{1A} & y'_{1B} & y'_{1C} \\ y'_{2A} & y'_{2B} & y'_{2C} \\ y'_{3A} & y'_{3B} & y'_{3C} \\ y'_{4A} & y'_{4B} & y'_{4C} \\ y'_{5A} & y'_{5B} & y'_{5C} \\ y'_{6A} & y'_{6B} & y'_{6C} \end{bmatrix} = \begin{bmatrix} 0.9748 & 0.0135 & 0.0131 \\ 0.0061 & 0.9900 & 0.0045 \\ 0.2566 & 0.4826 & 0.2622 \\ 0.0038 & 0.0029 & 0.9936 \\ 0.2967 & 0.4030 & 0.3003 \\ 0.2688 & 0.2340 & 0.4972 \end{bmatrix} \quad (3.13)$$

After building the whole Simulink model, we then divided the results into three groups. The first group was the (Normal) group which operated the model without DG units. The second was the (Controlled DG) group which operated the model after integrating the DG units that were equipped with our controller. The third group was the (DG) group which operated the model after integrating the DG units but without the proposed controller. Each group was examined under different values of loads using four ascending values of loads as shown in Table 3.1 [118].

This controller uses voltage deviation and admittance values as input values in order to improve the voltage quality in the network. The obtained results from both groups were compared to specify the proposed controller's capability of improving the voltage quality and power factor of the electrical grid [118].

Table 3.1 Loads values for all steps [118].

Load No.	Step 1 (MVA)	Step 2 (MVA)	Step 3 (MVA)	Step 4 (MVA)
Load 1	20 + j6	22 + j7	24 + j8	26 + j9
Load 2	22 + j7	24 + j8	26 + j9	28 + j10
Load 3	18 + j4	20 + j5	22 + j6	24 + j7
Load 4	14 + j4	16 + j5	18 + j6	20 + j7
Load 5	12 + j3	14 + j4	16 + j5	18 + j6
Load 6	12 + j4	14 + j5	16 + j6	18 + j7

These groups will be tested in four cases to check the performance of the controller. These cases are as following:

1. Wind speed 15 m/s.
2. Wind speed 10 m/s.
3. Wind speed 5 m/s.
4. Fault line 2-3 and wind speed 5 m/s.

Chapter 4

4 Results

4.1 Voltage profile and $\cos\varphi$

4.1.1 Speed 15 m/s

4.1.1.1 Voltage deviation % of busbars

Figure 4.1 shows the percentage of voltage deviation for each busbar, 1,2,3,4,5, and 6, in two cases (Normal) and (Controlled DG), and for four steps of load values. We concluded the following [118]:

1. For busbar No.1: Voltage deviation percentage in the (Normal) case ranges between -1.7% and -2.7% whereas, in the (Controlled DG) case, the range is between -0.3% and -0.5%. Moreover, we observed that the controller was able to maintain the voltage values to within a very narrow range of change (only 0.2%) during the ascent of load values, whereas the range in the (Normal) case is 1% [118].
2. For busbars No. 2,3,4,5, and 6: The voltage deviation percentage attitude is similar to that for bus No.1, but with different values and ranges whereby all values of the voltage deviation percentage, and change ranges of it, are noticeably smaller and narrower for the (Controlled DG) case compared to (Normal) case [118].
3. We also noticed that the highest voltage deviation percentages are for bus bar No. 5 and 6 because these busbars are radial and connected to radial branches of the mesh grid, so they obtain power through one transmission line. For these busbars, the voltage deviation percentage reaches over -10% in the (Normal) case, which is the maximum allowed limit of voltage deviation percentage [118].
4. Although there is a high voltage deviation percentage for busbars No. 5 and 6, the controller was able to decrease it remarkably, up to -5.5% for busbar No. 5 and -3.5% for busbar No. 6, even for the highest load value [118].
5. The percentage values of voltage deviation are smaller, the change ranges are narrower, and the controller is more efficient for busbars 1,2 and 6. This is due to the fact that they are closer to the DG units and the power sources G1 and G2 [118].

Figure 4.1 illustrates the voltage deviation percentages for all buses in the two cases (Normal) and (Controlled DG). For four steps of load values, we can notice the significant impact of the controller in decreasing the voltage deviation percentages and thus improving voltage quality and profile [118].

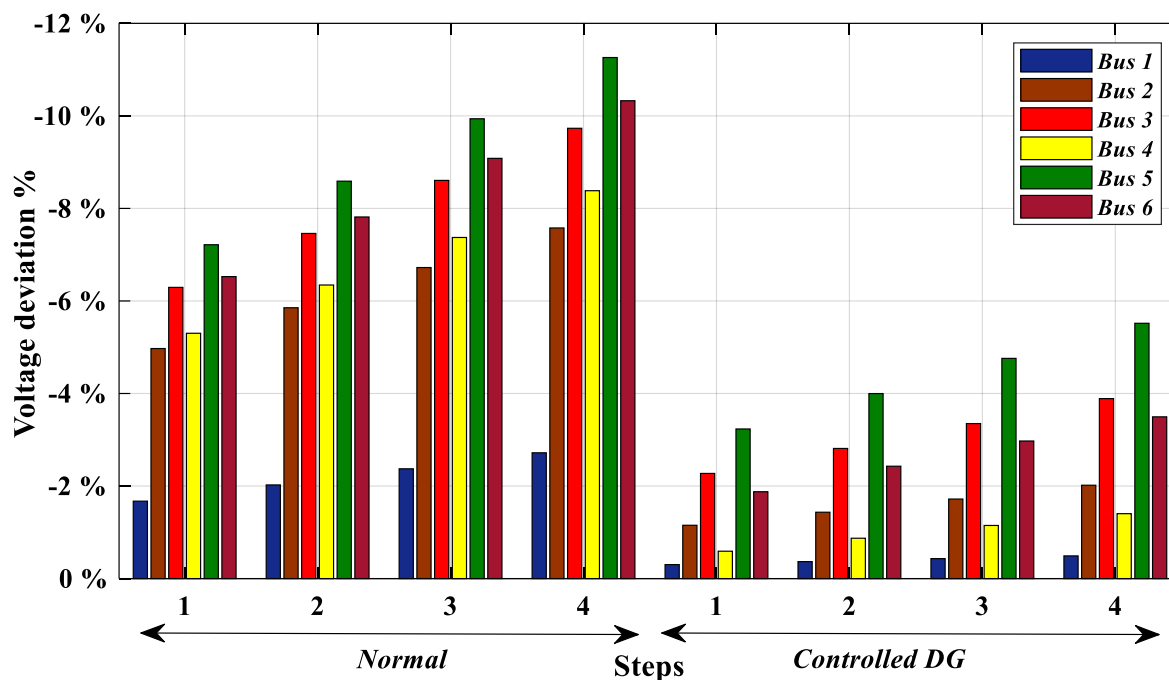


Figure 4.1 Voltage deviation % comparison between (normal) and (controlled DG) cases for all busbars (15 m/s) [118].

Figure 4.2 shows the results of voltage deviation % comparison between (normal) and (DG) cases for all busbars where the controller is not activated in this case. We can notice here that voltage deviation in the DG case is less than normal case for all busbars. But results that we got for controlled DG case in the last figure is much better than these results. For instance, voltage deviation for bus No.1 in step 4 changed from -2.7% in the normal case to -2.23% in the DG case and -0.5% in the controlled DG case and for bus No.5, voltage deviation were -11.3% in the normal case and it became -9.4% in the DG case and -5.5% in the controlled DG case. Moreover, changes ranges are narrower for controlled DG case with respect to DG case. The changes ranges for bus 1 changed from 1% in the normal case to 0.95% in the DG case while it is 0.3% for controlled DG case. For bus 5, it changed from 4% in the normal case to 3.9% and 2.3% in the DG case and controlled DG case respectively. We can figure out that effect of load changes was less in the controlled DG case with respect to DG case which shows that the controller was able not only to reduce the voltage deviation of the buses in more efficient way but also with narrower range.

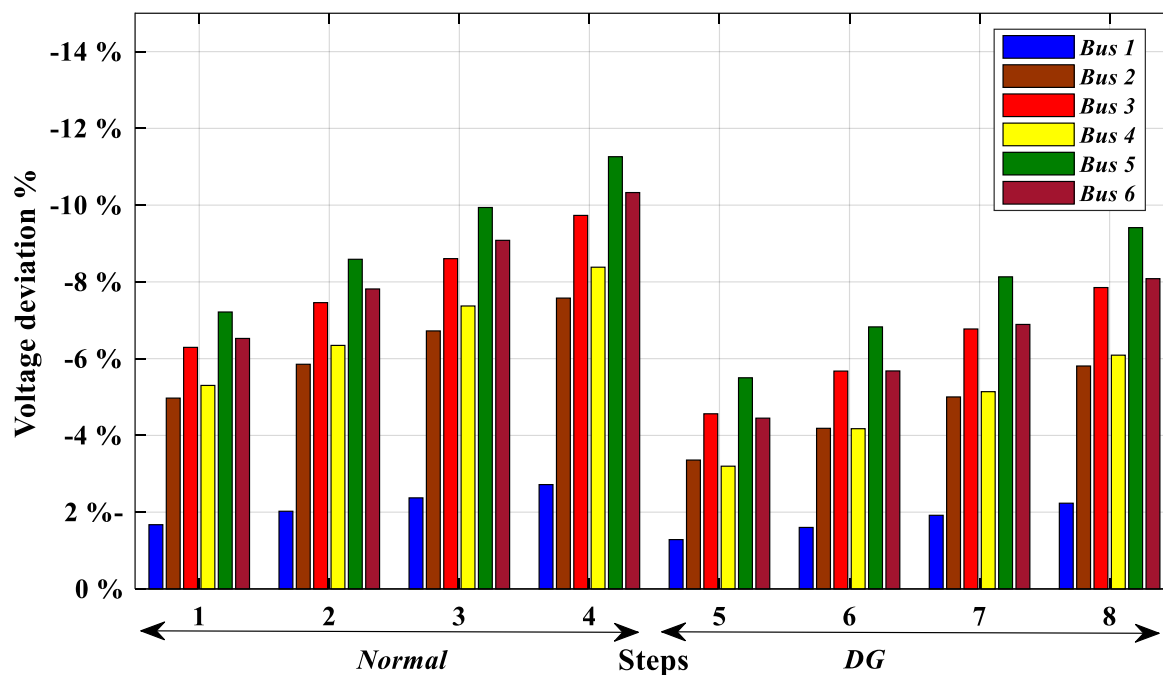


Figure 4.2 Voltage deviation % comparison between (normal) and (DG) cases for all busbars(15 m/s) .

4.1.1.2 Sending voltage deviation % of transmission lines

Figure 4.3 shows the percentage values of the sending voltage deviation for all transmission lines in both cases (Normal and Controlled DG) and for four steps of load values. It is obvious that the lowest percentage values of voltage deviations are for lines 0–1 and 0–2 as they are the closest lines to busbar 0 which is the slack bus. Further, voltage deviations for lines 1–2 and 1–4 are relatively low because they are located between two DG units. We can also notice that the highest percentage values of voltage deviations are for lines 3–5, 3–4, 2–3, and 4–6 because they are the farthest lines from the slack bus and main generators G1 and G2. In addition to that, lines 3–5 and 4–6 are radial branches. In fact, the most important thing in these results is that the impact of the DG unit's controller is still clear as it was able to decrease the percentage values of voltage deviations significantly, even for the farthest and radial transmission lines like 3–5, 3–4, and 4–6. For lines 3–5, the highest voltage deviation in the (Normal) case is about -10%, while for the (Controlled DG) case, it decreases to less than -4%. Also, for line 4–6 step 4, the deviation decreased from -8.4% to -1.4%. We can also notice that the changes ranges are narrower where for line 3-5 the range of changes is about 3.5% for normal case and 1.6% for controlled DG case. For line 4-6, the changes range decreased from 3% to 0.8% [118].

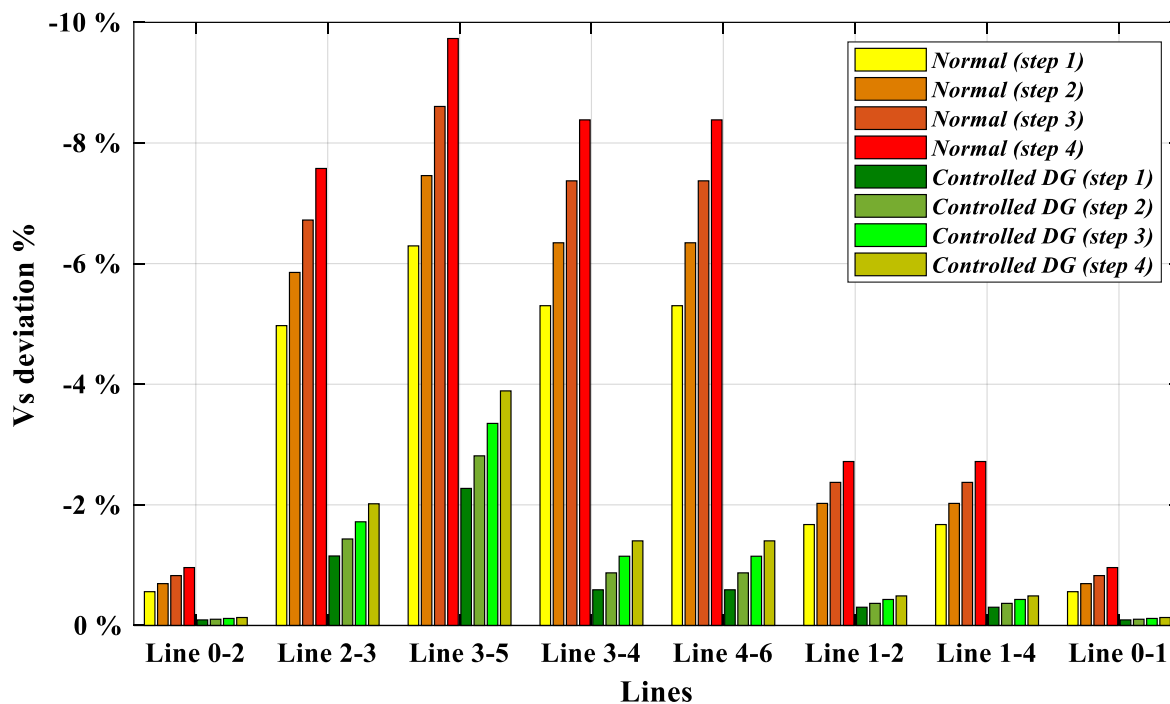


Figure 4.3 Sending voltage deviation % comparison between (normal) and (controlled DG) cases for all transmission lines(15 m/s) [118].

Figure 4.4 illustrates the results of sending voltage deviation % comparison between (normal) and (DG) cases for all transmission lines. These results show a decrease in voltage deviation% in the DG case with respect to normal case for all steps and transmission lines. Although, these results for DG case is not good as the controlled DG case. For instance, the deviation for line 3-5 step 4 changed from about -10% in the normal case to about -8% for DG case and -4% for the controlled DG case. Moreover, the changes ranges become narrower such as for line 3-5 where the range changed from 3.5% for the normal case to 3.3% in the DG case and 1.6% for the controlled DG case.

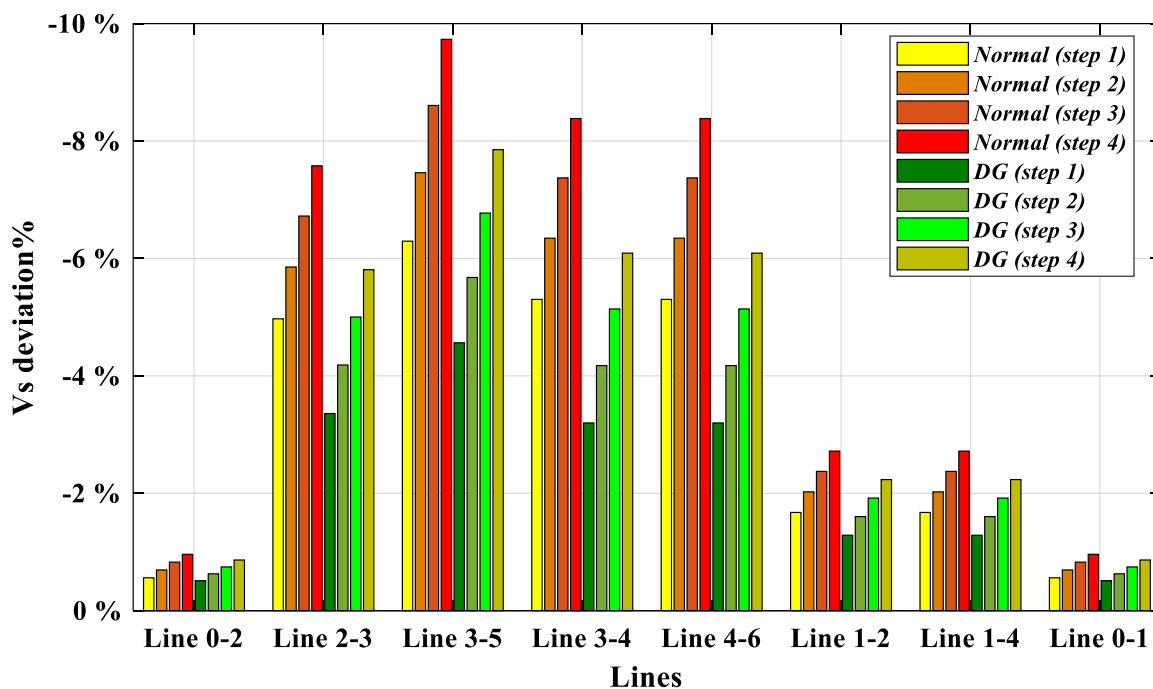


Figure 4.4 Sending voltage deviation % comparison between (normal) and (DG) cases for all transmission lines (15 m/s).

4.1.1.3 Receiving voltage deviation % of transmission lines

In Figure 4.5, we can see the percentage values of receiving voltage deviation for all transmission lines in both cases (Normal and Controlled DG) and for four steps of load values. In general, the results of sending and receiving voltage deviation are similar to each other, but with some differences in which the voltage deviations are higher for all lines because these values are for the receiving ends. The impact of the DG unit's controller is still obvious for all transmission lines even for the highest step of line 3–5 where it was able to reduce the voltage deviation from -11.2% to about -5.5%. Also, the changes ranges are narrower in controlled DG case with respect to normal case [118].

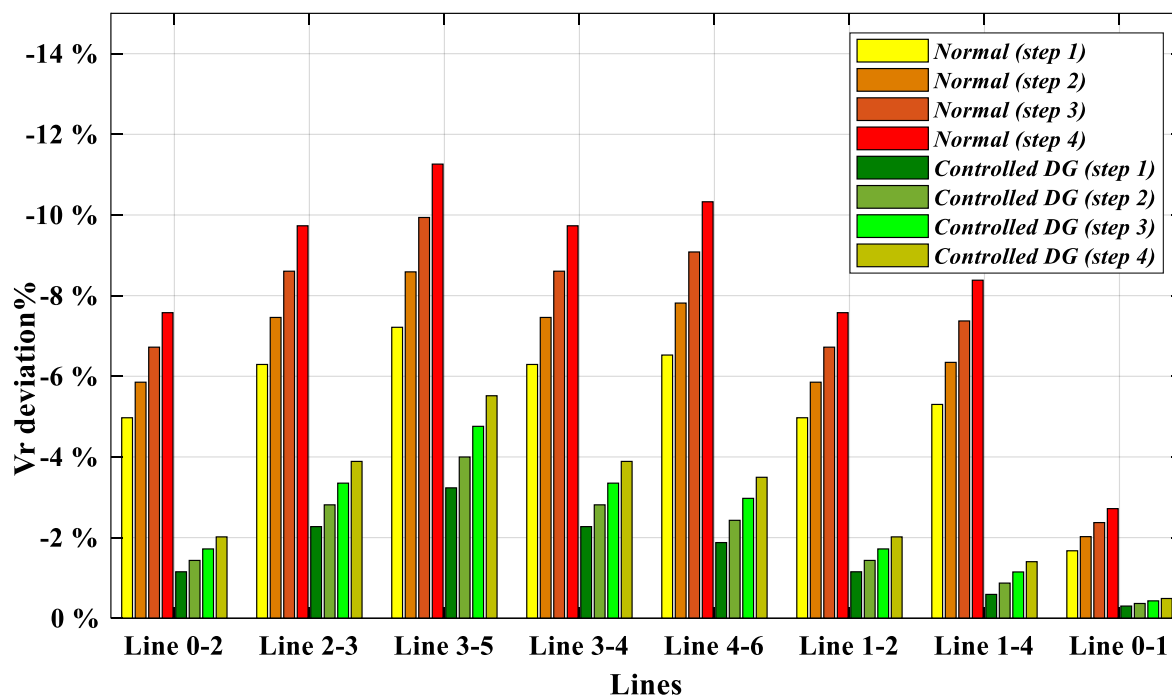


Figure 4.5 Receiving voltage deviation % comparison between (normal) and (controlled DG) cases for all transmission lines (15 m/s) [118].

Figure 4.6 shows comparison between normal and DG cases for receiving voltage deviation%. Results for this comparison are also similar to the results of the sending voltage but with a higher deviations as they are for receiving ends. Similar to what we mentioned for the sending end, deviations for controlled DG case are lower than DG case where for line 3-5 the voltage deviation decreased from -11.2% in normal case to -5.5% in the controlled DG case and -9.4% in the DG case. Also, the changes range due to load increase are narrower for controlled DG case where the range changes from 4% in the normal case to 3.9% and 2.3% in the DG and controlled DG cases respectively.

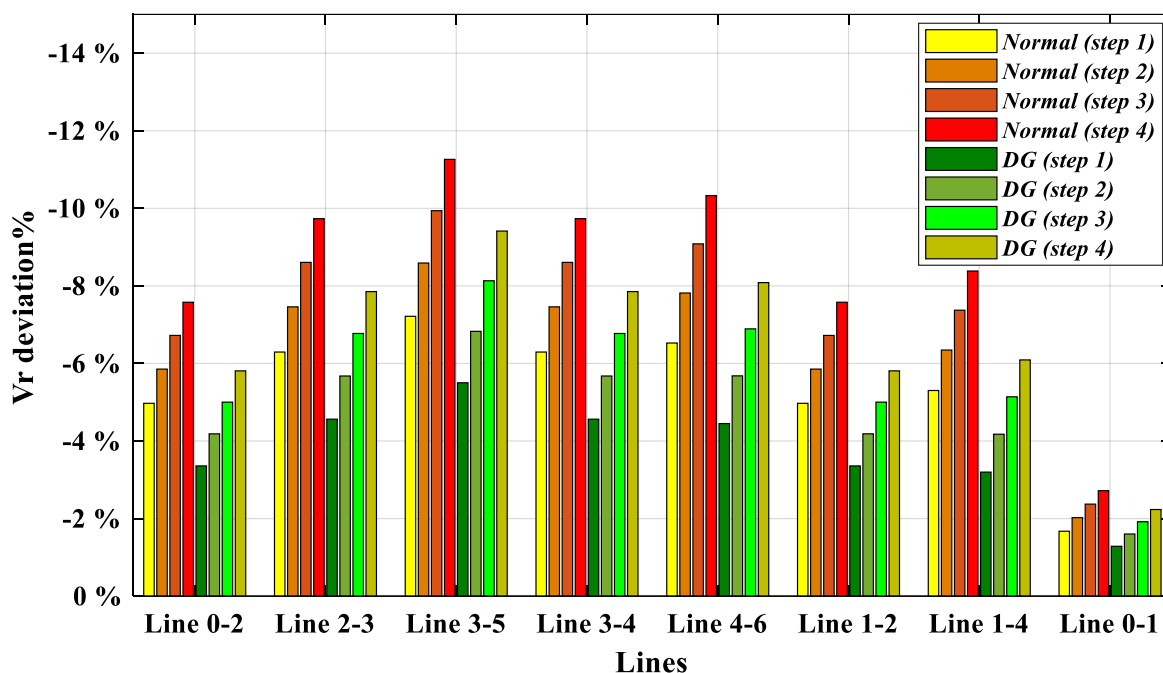


Figure 4.6 Receiving voltage deviation % comparison between (normal) and (DG) cases for all transmission lines (15 m/s).

4.1.1.4 Voltage drop % of transmission lines

Figure 4.7 shows voltage drop percentage values for all transmission lines in both cases (Normal and Controlled DG) and for four steps of load values. The most noticeable impact of the DGs unit's controller is for lines 0–1, 0–2, 1–2, and 1–4, as these lines are located between two DG units or one DG unit and the slack bus. Despite this, we can notice that the voltage drop for lines 3–5 and 4–6 in the (Controlled DG) case is slightly higher than (Normal) case and relatively higher for line 3–4 but this does not mean that the (Controlled DG) case for these lines is worse than the (Normal) case because these differences between voltage drop values in the two cases are due to the differences in the improvements of sending and receiving voltage values for these lines, where the controller improves the sending voltage more than receiving voltage. For example, for line 3–4, step 4, the sending voltage was 60.467 kV in the (Normal) case and it becomes 65.074 kV in the (Controlled DG) case with an improving value (4.607 kV), whereas the receiving voltage was 59.576 kV in the (Normal) case and it became 63.432 kV, so the improving value is 3.956 kV [118].

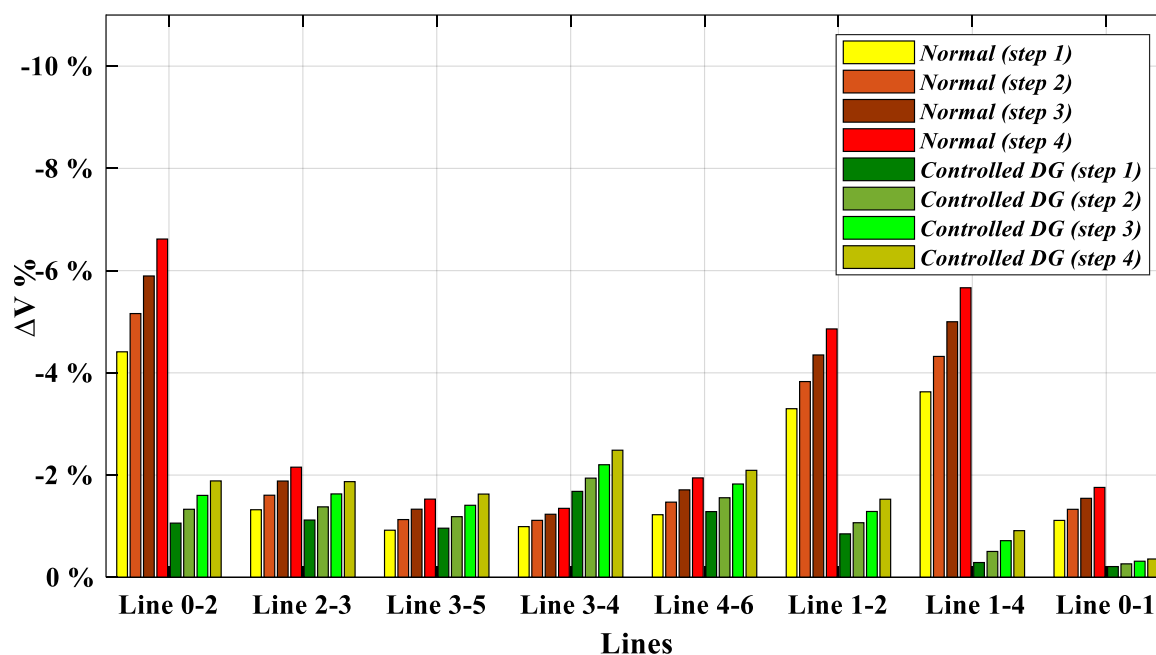


Figure 4.7 Voltage drop (%) comparison between (normal) and (controlled DG) cases for all transmission lines (15 m/s) [118].

In Figure 4.8, we can see results for voltage drop comparison between normal and DG case. In general, we can also notice a decrease in voltage drop% in the DG case comparing to the normal case. But, the amount of decrease is less than the controlled DG case which shows the effectively of the used controller in improving voltage profile. For instance, at step 4 of line 1-4 the voltage drop decreased from 5.6% in the normal case to 3.9% and 0.9% in the DG and controlled DG cases respectively.

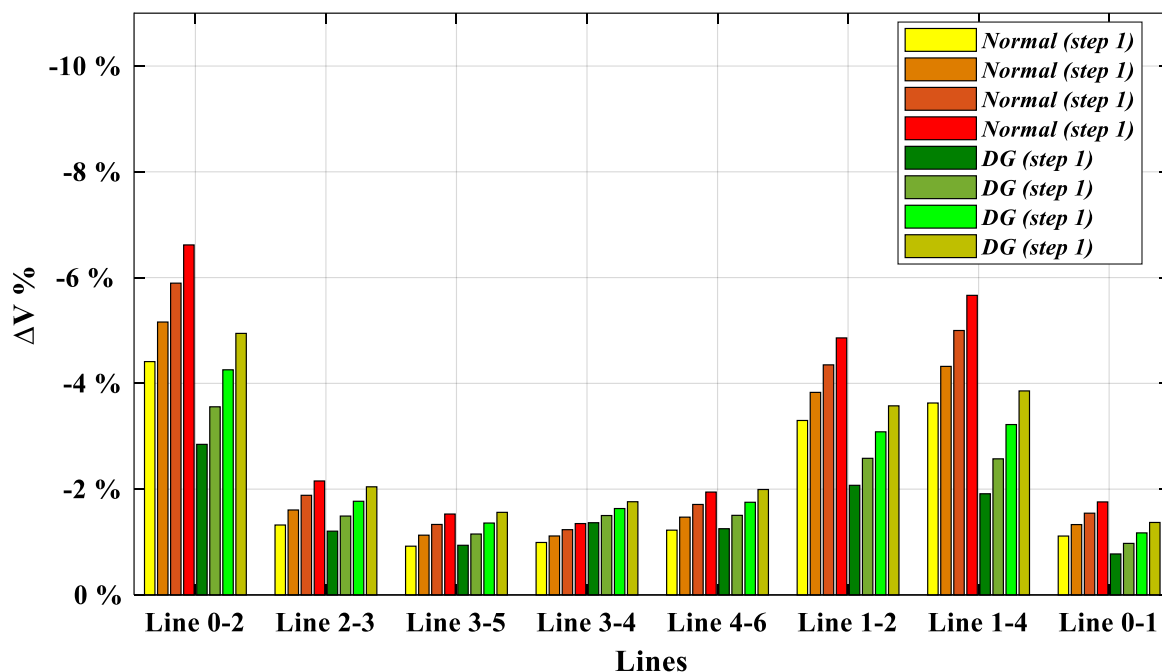


Figure 4.8 Voltage drop (%) comparison between (normal) and (DG) cases for all transmission lines (15 m/s).

4.1.1.5 Sending $\cos(\varphi)$ of transmission lines

In Figure 4.9, we can see the sending $\cos(\varphi)$ values for all transmission lines in both cases (Normal) and (Controlled DG) and for four steps of load values. We can notice the considerable influence of the DG unit's controller compared with the (Normal) case specifically for lines 0–2, 1–2, 1–4, and 0–1 where the sending $\cos(\varphi)$ values are remarkably better than the (Normal) case, also very close to 1, while $\cos(\varphi)$ for line 0–2 is (0.92–0.96) and for line 1–2 is (0.91–0.95). Moreover, the change's range during the ascending process of the load is very narrow. For example: $\cos(\varphi)$ values for line 0–2 ranges between 0.928 and 0.952 in the (Normal) case, while in the (Controlled DG) case, all the values are about 0.998. The great improvement of $\cos(\varphi)$ values for these lines is due to the fact that all of them are located close to the controlled DG units which have controller to regulate the generated reactive power. For the rest of the lines, we can notice that the sending $\cos(\varphi)$ values are relatively close to each other [118].

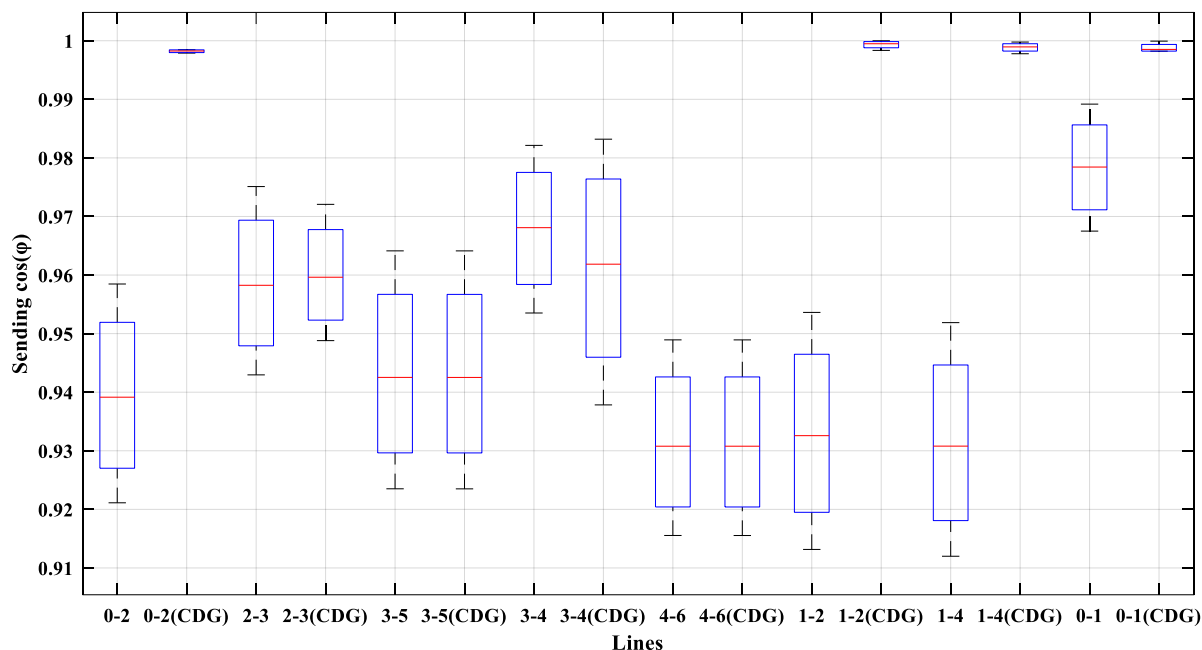


Figure 4.9 Sending $\cos(\phi)$ comparison between (normal) and (controlled DG) cases for all transmission lines (15 m/s) [118].

Figure 4.10 shows comparison of sending $\cos(\phi)$ between normal and DG cases. Results shows that $\cos(\phi)$ becomes lower for lines 0–2, 1–2, 1–4, and 0–1 in the DG case with respect to the normal case. This decrease is due to absence of the controller for the DG units and the decrease of the drawn active power from the main generators G1 and G2 because DG units feed the loads with active power too. For the rest of lines, we can notice similar results for normal and DG cases. But we can also notice that results of sending $\cos(\phi)$ are better in the controlled DG comparing to the DG case where $\cos(\phi)$ values for line 0–2 increased from (0.928 -0.952) in normal case to 0.998 in the controlled DG case while it decreased to (0.7-0.73) in the DG case.

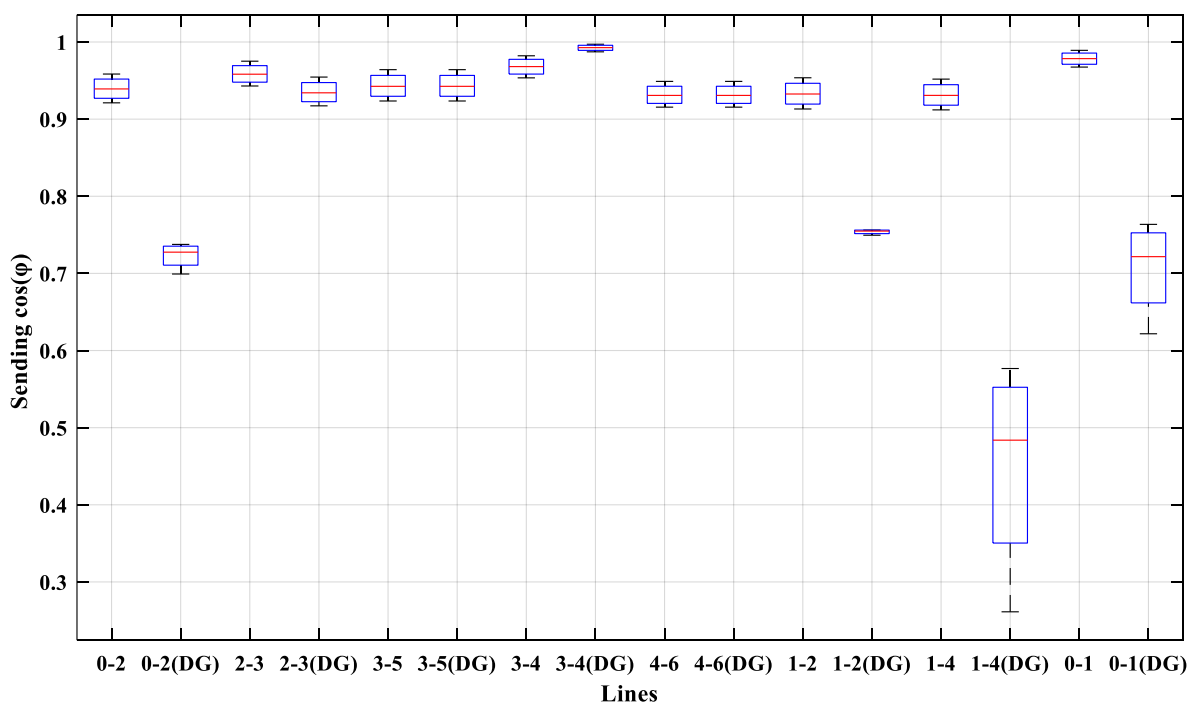


Figure 4.10 Sending $\cos(\varphi)$ comparison between (normal) and (DG) cases for all transmission lines (15 m/s).

4.1.1.6 Receiving $\cos(\varphi)$ of transmission lines

Figure 4.11 shows the receiving $\cos(\varphi)$ values for all transmission lines in both cases (Normal and Controlled DG) and for four steps of load values. The results for the receiving end are similar to the sending end where we can observe the same improvements of receiving $\cos(\varphi)$ for the same lines 0–2, 1–2, 1–4, and 0–1 where for line 0-2 $\cos(\varphi)$ is (0.94-0.96) in the normal case and it becomes (0.98-0.995) in the controlled DG case. But the range of changes is relatively wider and the values are relatively lower than sending end results. For the remaining lines, the results are also close to each other for both cases, except line 3–4 where the receiving $\cos(\varphi)$ values for the Controlled DG case are better than the Normal case [118].

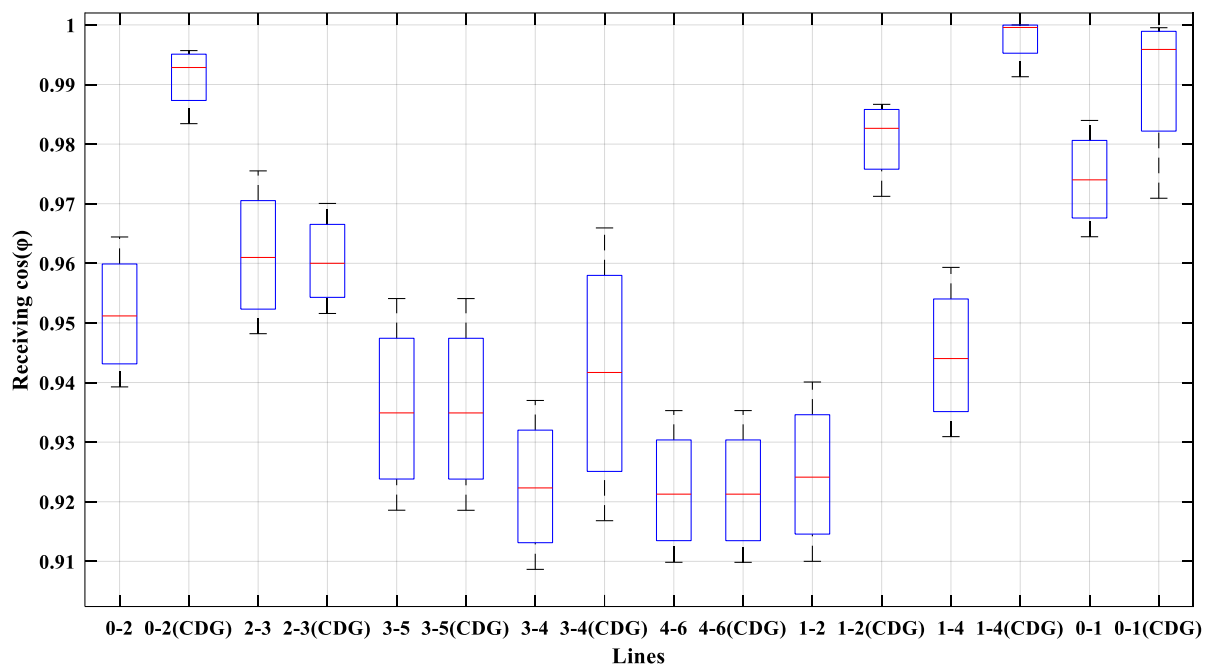


Figure 4.11 Receiving $\cos(\varphi)$ comparison between (normal) and (controlled DG) cases for all transmission lines (15 m/s) [118].

Figure 4.12 shows comparison of receiving $\cos(\varphi)$ between normal and DG cases. These results are similar to the sending end but with lower values and wider ranges of changes. Similarly, to the results of the sending $\cos(\varphi)$, results here shows that $\cos(\varphi)$ becomes lower for lines 0–2, 1–2, 1–4, and 0–1 in the DG case with respect to the normal case. Also, for the rest of lines, the results are close to each other relatively.

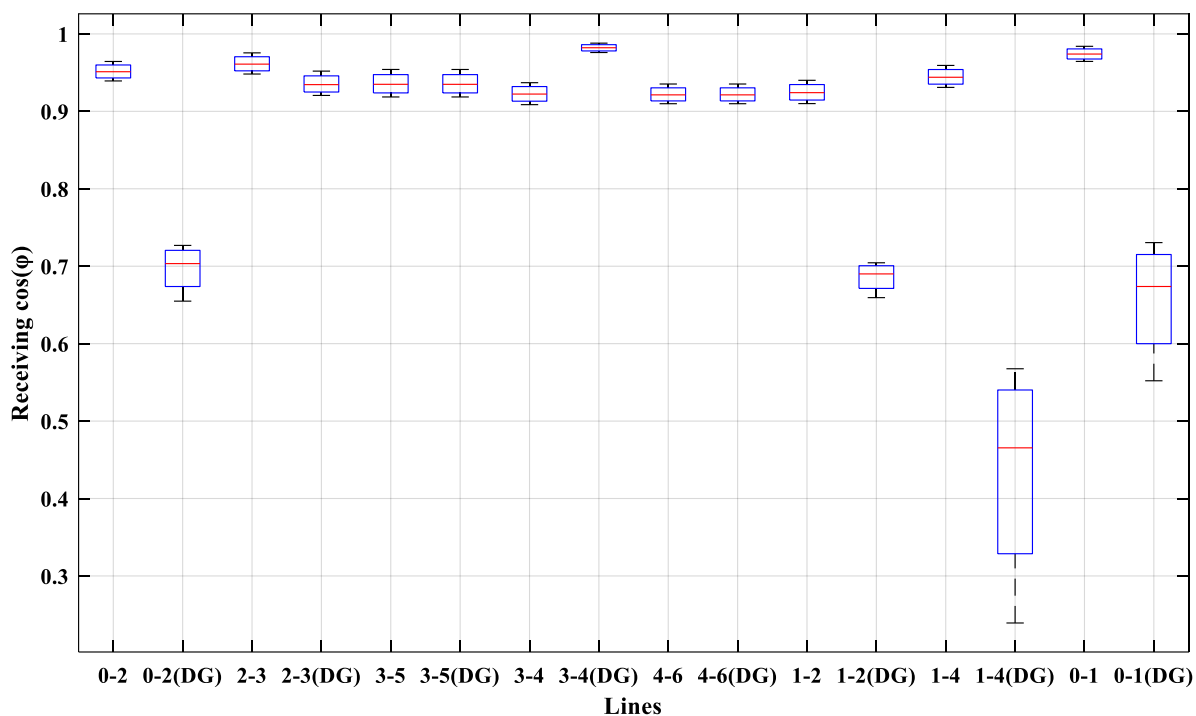


Figure 4.12 Receiving $\cos(\varphi)$ comparison between (normal) and (DG) cases for all transmission lines (15 m/s).

4.1.2 Speed 10 m/s

4.1.2.1 Voltage deviation % of busbars

Figure 4.13 shows results of voltage deviation % for normal and controlled DG cases but for speed 10 m/s. These results are very similar to the results of 15 m/s where the voltage deviation decreased remarkably for all buses in the controlled DG case compared to the normal case. Actually, numerical results from simulation shows that the voltage deviation for 10 m/s is slightly higher than 15 m/s and the difference is small about 0.3% for most busbars.

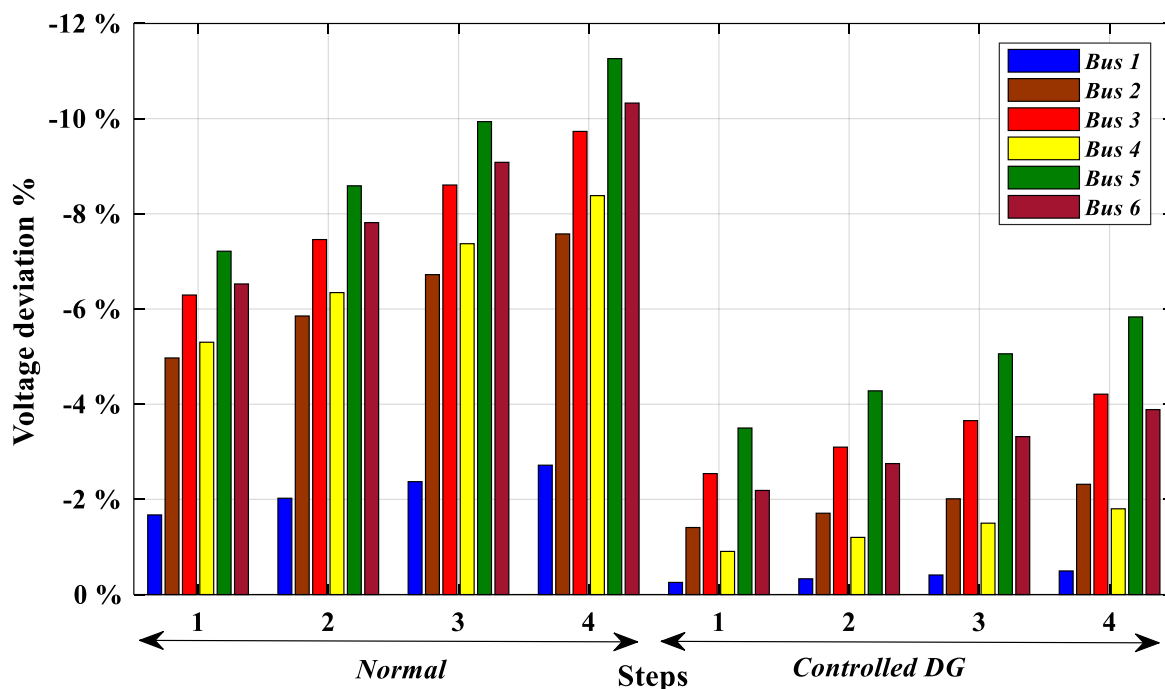


Figure 4.13 Voltage deviation % comparison between (normal) and (controlled DG) cases for all busbars (10 m/s).

Figure 4.14 shows comparison of voltage deviation % between normal and DG cases. Results in this figure are also similar to what we got for 15 m/s where voltage deviation in DG case is lower and controlled DG case is better than DG case because of lower voltage deviation. Similarly, to figure 4.13, the voltage deviation for 10 m/s case is slightly higher than 15 m/s but the magnitude of difference is higher here (0.6%-0.8%) for most busbars.

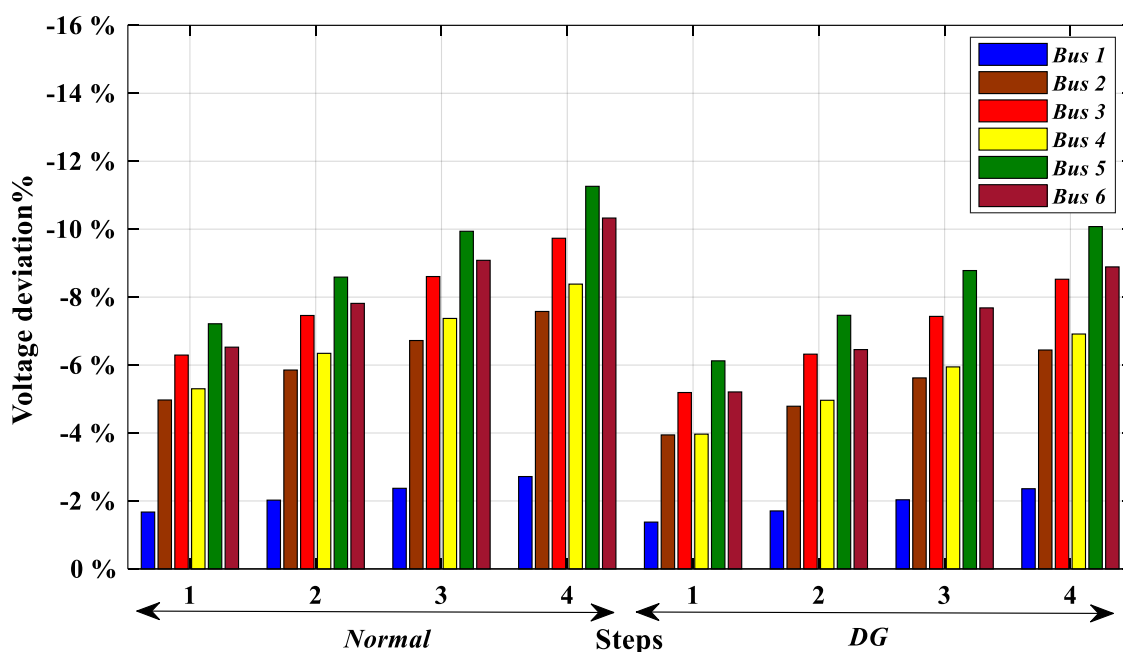


Figure 4.14 Voltage deviation % comparison between (normal) and (DG) cases for all busbars (10 m/s).

4.1.2.2 Sending voltage deviation % of transmission lines

In figure 4.15 we can see the results of sending voltage comparison between normal and controlled DG case for wind speed 10 m/s where we can notice significant improvement in voltage profile and remarkable decrease in voltage deviation for all transmission lines in all steps. These results are very similar to the results that we got for speed 15 m/s. For lines 2-3, 3-4, 3-5, and 4-6, voltage deviation is slightly higher in case of 10 m/s with respect to case 15 m/s due to the difference of active power generation. This difference ranges between 0.25 and 0.4%.

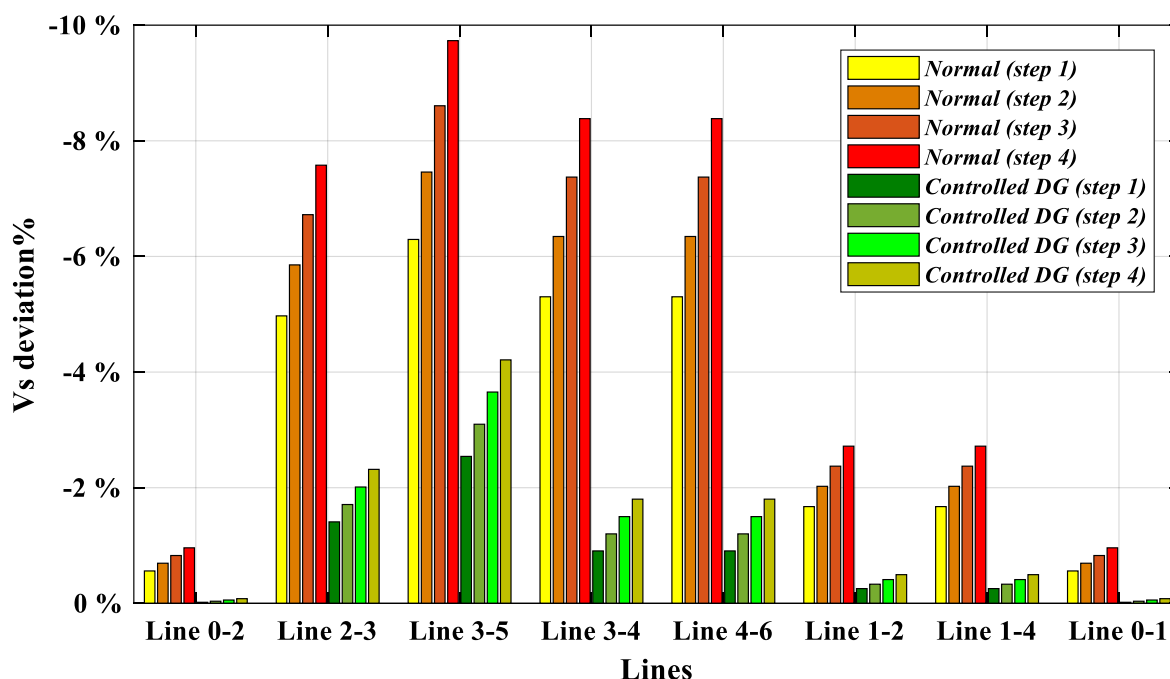


Figure 4.15 Sending voltage deviation % comparison between (normal) and (controlled DG) cases for all transmission lines(10 m/s).

In figure 4.16, we can notice the comparison between normal and DG cases for wind speed 10 m/s. The obtained results are very close to the results of wind speed 15 m/s where the voltage deviation in the DG case is less than the normal case. Also, if we compared these results with the results in the controlled DG case in figure 4.15, we can notice also that the controller played an important role in decreasing voltage deviation. The results for this speed (for lines 2-3, 3-4, 3-5, and 4-6) show also slightly higher voltage deviation compared with speed 15 m/s and this amount of increase is higher in this case compared with controlled DG case is between 0.6% and 0.8%.

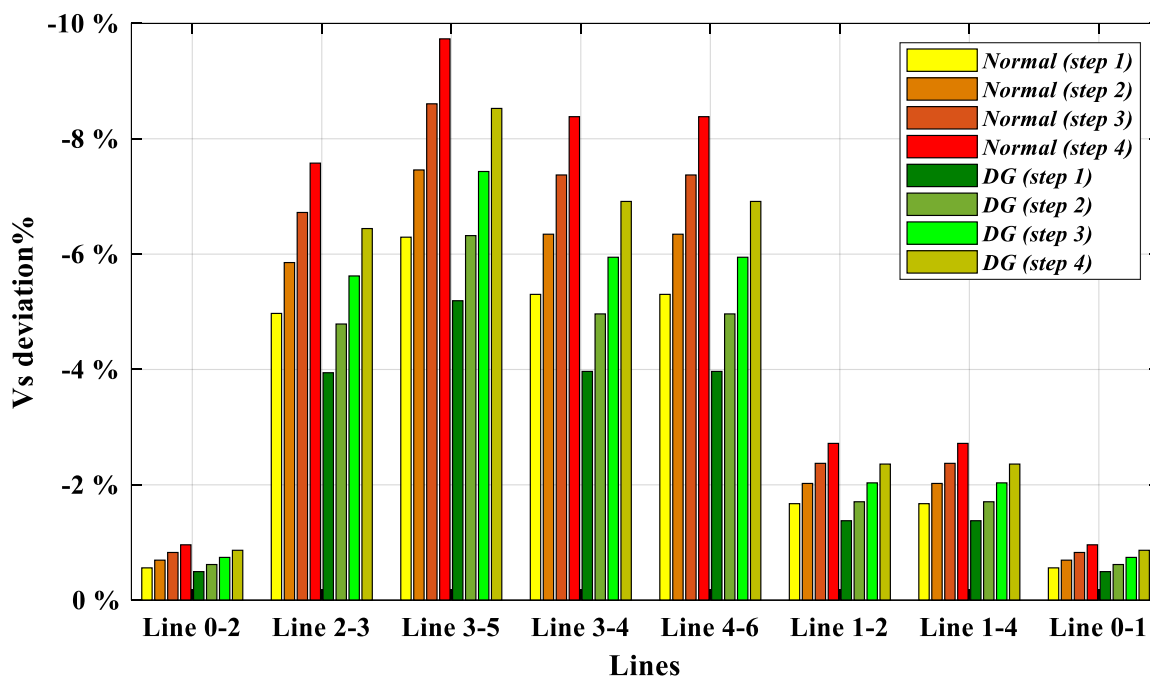


Figure 4.16 Sending voltage deviation % comparison between (normal) and (DG) cases for all transmission lines(10 m/s).

4.1.2.3 Receiving voltage deviation % of transmission lines

In figure 4.17 we can see the results of receiving voltage deviation in controlled DG case with respect to normal case for wind speed 10 m/s. The obtained results are very similar to what we got for speed 15 m/s where we are able to reduce voltage deviation using the added controller. Also, these values are higher than sending values. Anyway, if we checked the numerical results, we can notice that voltage deviation for all lines except line 0-1 is slightly higher in 10 m/s case than 15 m/s case and the difference is (0.25% - 0.3%).

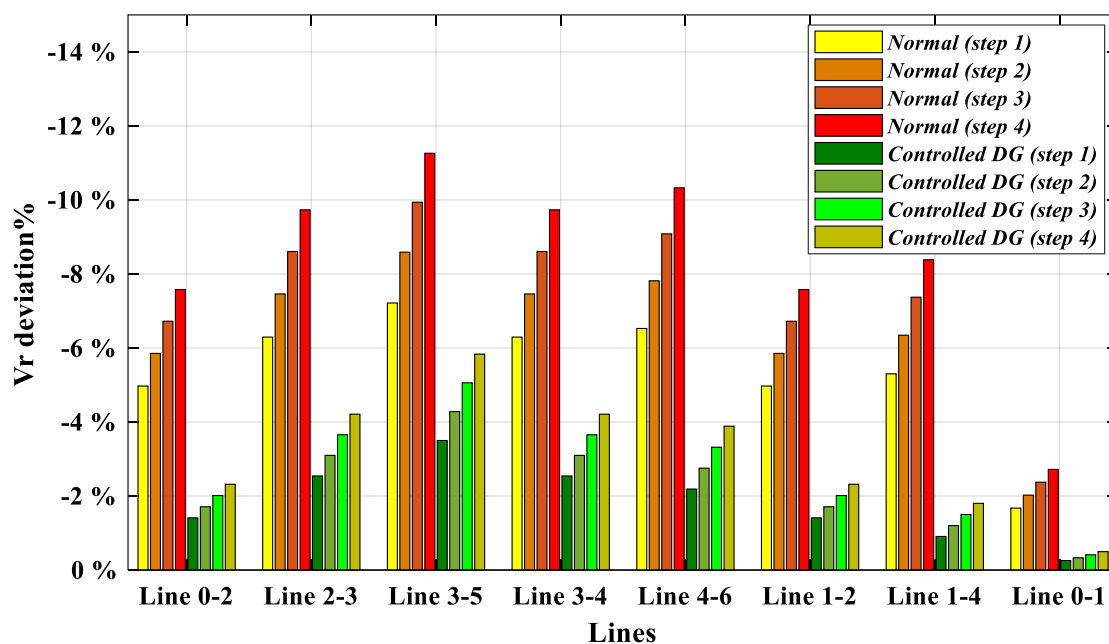


Figure 4.17 Receiving voltage deviation % comparison between (normal) and (controlled DG) cases for all transmission lines (10 m/s).

In figure 4.18, we can see receiving voltage comparison between normal and DG cases for wind speed 10 m/s. In similar way to the sending end we can notice that these results are very close to the obtained results for the case of 15 m/s. It's obvious that the results in DG case is better than normal case but controlled DG case shows far better impact on reducing voltage deviation. These results are slightly higher than the results of 15 m/s where that difference is about (0.6% - 0.8%) except for line 0-1 where the difference is about 0.1%.

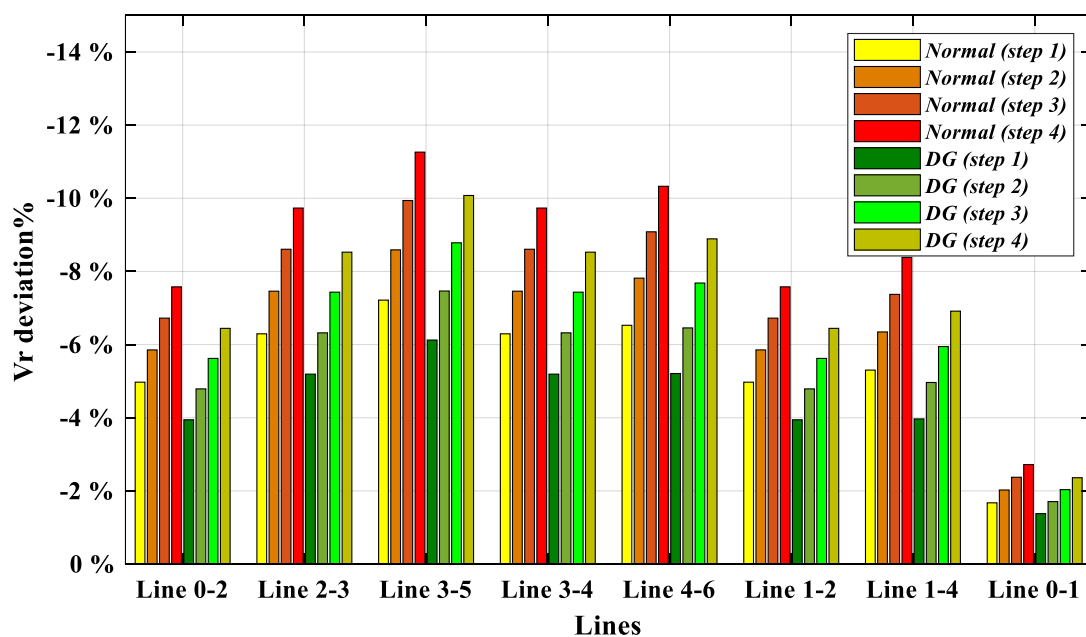


Figure 4.18 Receiving voltage deviation % comparison between (normal) and (DG) cases for all transmission lines (10 m/s).

4.1.2.4 Voltage drop % of transmission lines

Figure 4.19 shows voltage drop comparison between normal and controlled DG cases for wind speed 10 m/s. Shown results are very similar to the results of 15 m/s where we are capable to reduce voltage drop using the controller and getting better voltage profile. The values of voltage drop are very close to the case of 15 m/s for lines 2-3, 3-5, 3-4, 4-6, and 0-1. But for lines 0-2, 1-2, and 1-4, the values are slightly higher in case of 10 m/s and the difference is between 0.3% and 0.4%.

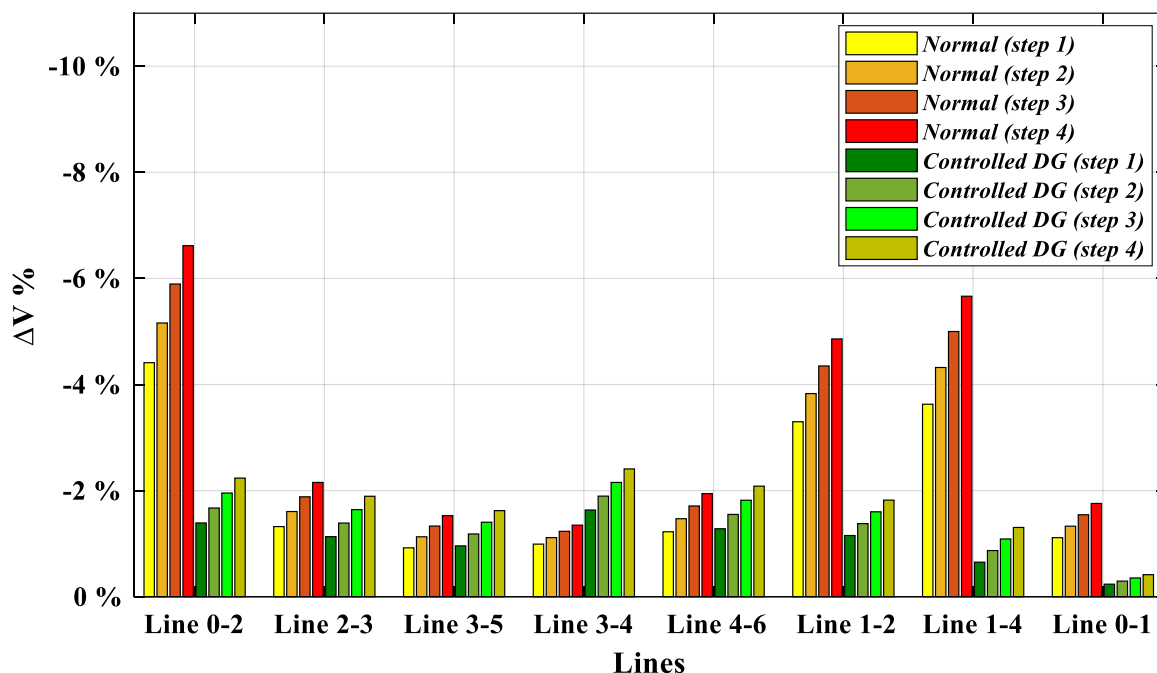


Figure 4.19 Voltage drop (%) comparison between (normal) and (controlled DG) cases for all transmission lines (10 m/s).

Figure 4.20 illustrates the results of voltage drop comparison between normal and DG cases for wind speed 10 m/s. The results are also similar to what we got for speed 15 m/s where we got better results for DG case but results for controlled DG case are still far better than these results. If we checked the numerical results, we will notice that results for all lines are close to each other except lines 0-2, 1-2, and 1-4 where the voltage drop is slightly higher in case of 10 m/s and the difference ranges between 0.5% and 0.7%.

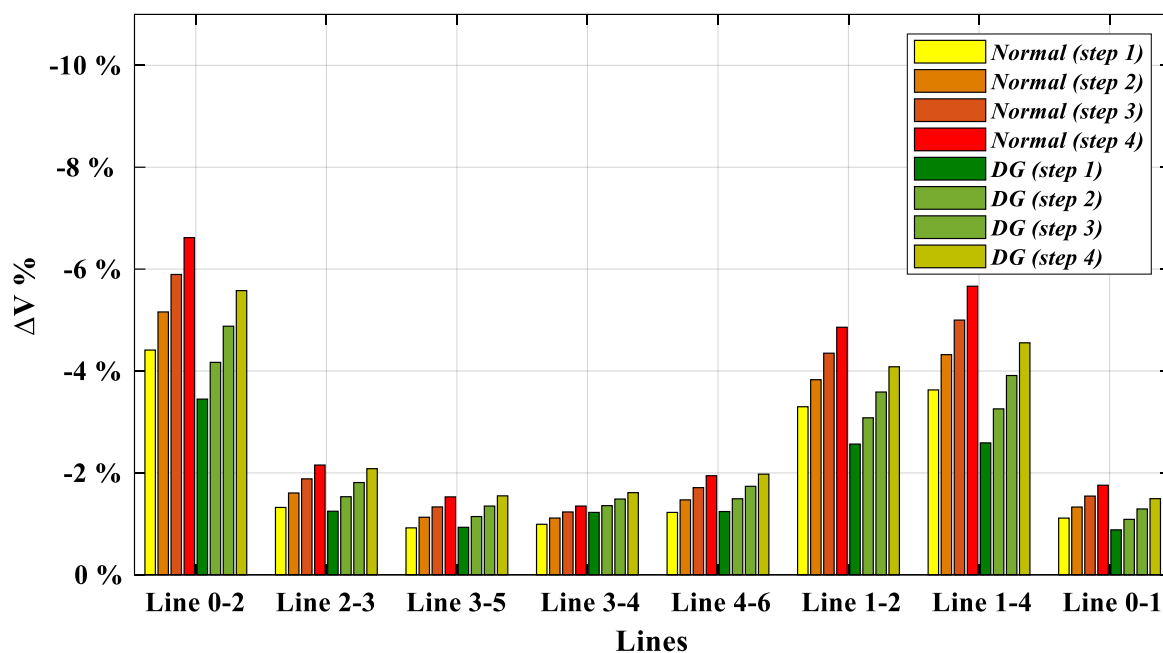


Figure 4.20 Voltage drop (%) comparison between (normal) and (DG) cases for all transmission lines (10 m/s).

4.1.2.5 Sending $\cos(\varphi)$ of transmission lines

Figure 4.21 shows sending $\cos(\varphi)$ differences between normal and controlled DG cases for wind speed 10 m/s. As what we got for speed 15 m/s, we obtained here better results in the controlled DG case and narrower range of changes especially for lines 0-2, 1-2, and 1-4 with respect to the normal case. By checking the results from MATLAB we noticed that the values are close to case of speed 10 m/s but with some small changes where $\cos(\varphi)$ decreased slightly for lines 0-1, 1-4 and 3-4. For line 0-1 $\cos(\varphi)$ values were very close to 1 for speed 15 m/s and decreased to about 0.985 for speed 10 m/s due to the small decrease of generated active power from DG units. On the other hand, it increased slightly in lines 0-2 and 2-3 due to increased generated active power from main generators G1 and G2.

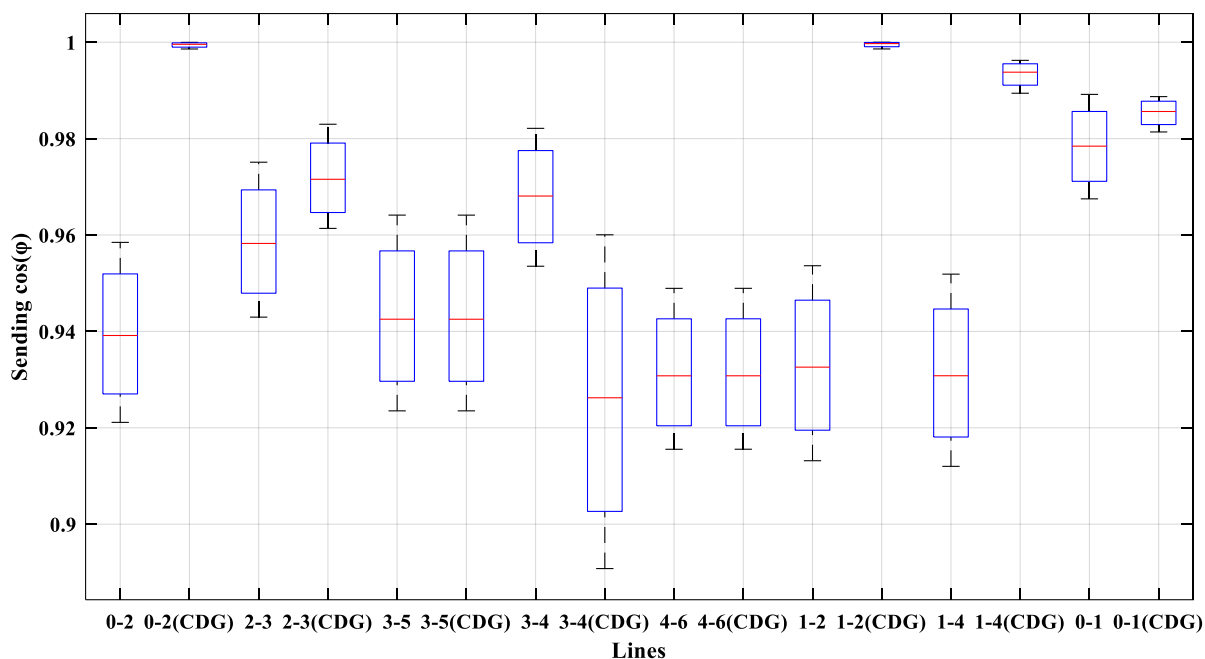


Figure 4.21 Sending $\cos(\varphi)$ comparison between (normal) and (controlled DG) cases for all transmission lines (10 m/s).

Figure 4.22 illustrates sending $\cos(\varphi)$ comparison between normal and DG cases for wind speed 10 m/s. The results are very similar to what we obtained for speed 10 m/s where we got lower values for lines 0–2, 1–2, 1–4, and 0–1 in the DG case due to the absence of the controller and generated active power from DG units but for speed 10 m/s we can see an increase in $\cos(\varphi)$ for these lines due to the decrease of active power generation from DG units when the wind speed decreased from 15 m/s to 10 m/s. For instance, $\cos(\varphi)$ for line 0-1 was (0.62-0.76) in case of speed 15 m/s and increased to (0.92-0.946) for speed 10 m/s. But, the case of controlled DG still better than DG case in case of speed 10 m/s.

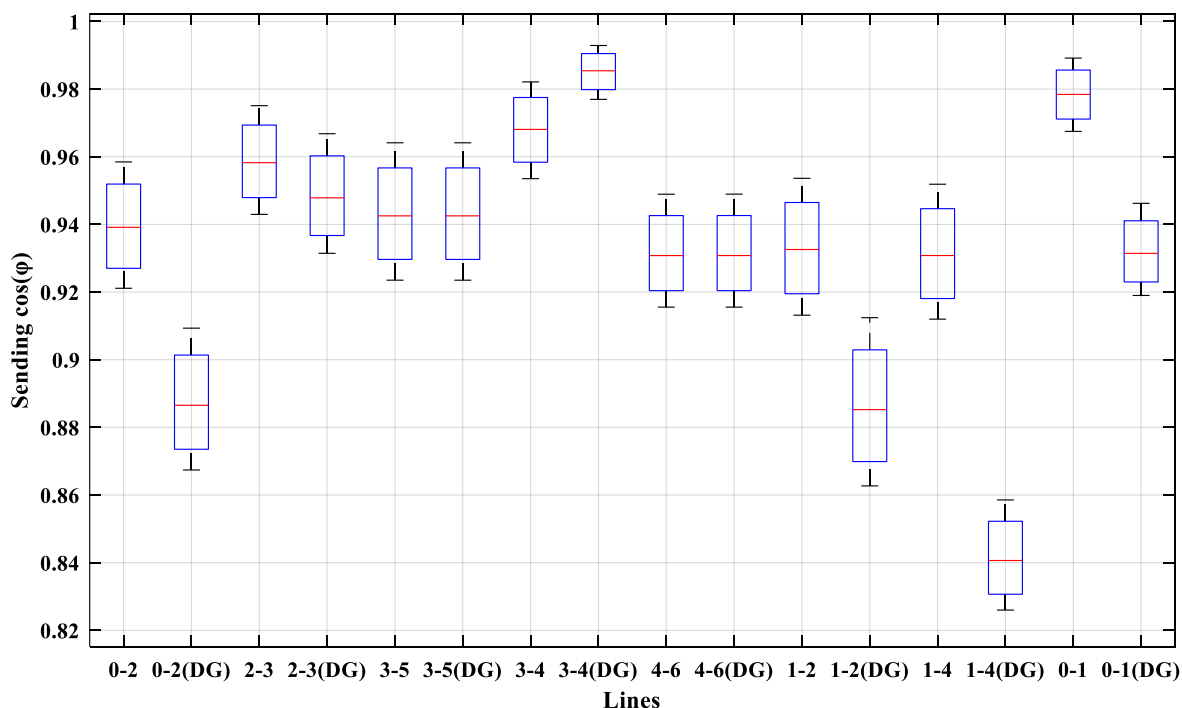


Figure 4.22 Sending $\cos(\varphi)$ comparison between (normal) and (DG) cases for all transmission lines (10 m/s).

4.1.2.6 Receiving $\cos(\varphi)$ of transmission lines

In figure 4.23, we can notice receiving $\cos(\varphi)$ comparison between normal and controlled DG cases for speed 10 m/s. The obtained results are very close to what we got for speed 15 m/s where we got better $\cos(\varphi)$ for lines 0-2, 2-3, 1-2, 1-4, and 0-1 with narrower range of change but results for speed 10 m/s is better than it for 15 m/s where values of $\cos(\varphi)$ are higher. $\cos(\varphi)$ for line 3-4 reduced for speed 10 m/s with respect to speed 15 m/s. For lines 3-5 and 4-6 the results were almost equal for normal and controlled DG cases. In general, we can say that the controller has positive impact on improving $\cos(\varphi)$ for most of lines.

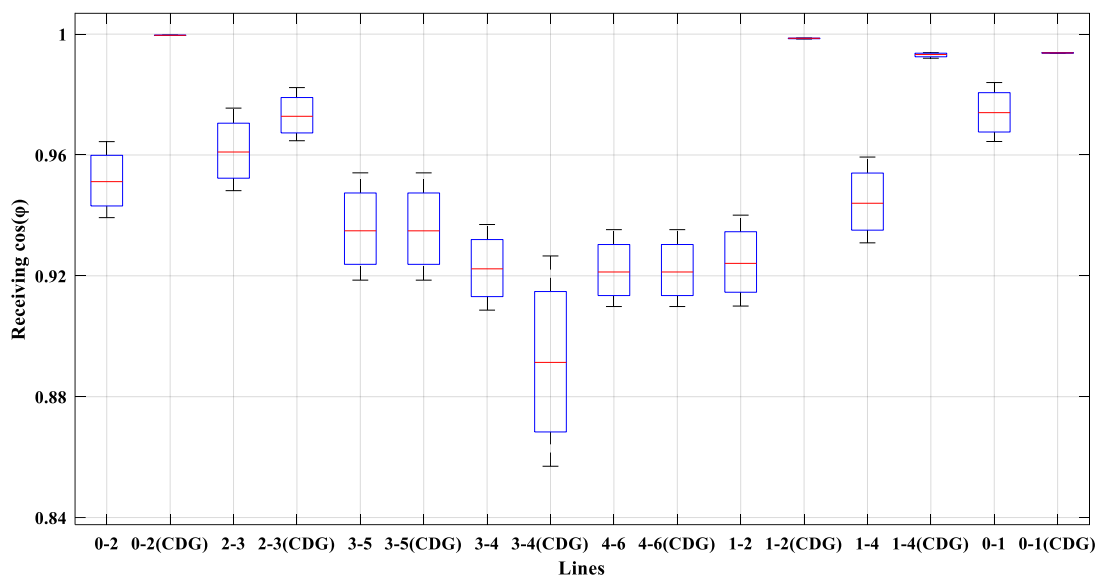


Figure 4.23 Receiving $\cos(\varphi)$ comparison between (normal) and (Controlled DG) cases for all transmission lines (10 m/s).

Figure 4.24 shows receiving $\cos(\varphi)$ comparison between normal and DG cases for wind speed 10 m/s. These results are similar to what we got for speed 15 m/s where $\cos(\varphi)$ values decreased for lines 0-2, 2-3, 1-2, 1-4 and 0-1 because of high active power generation from DG units. But when the wind speed changed from 15 m/s to 10 m/s, $\cos(\varphi)$ values increased where for line 1-4 we got (0.24-0.56) for speed 15 m/s and (0.83-0.85) for speed 10 m/s because decreased active power generation from DG units will cause more active power generation from main generators. In general, controlled DG case is still better than the DG case for this speed too.

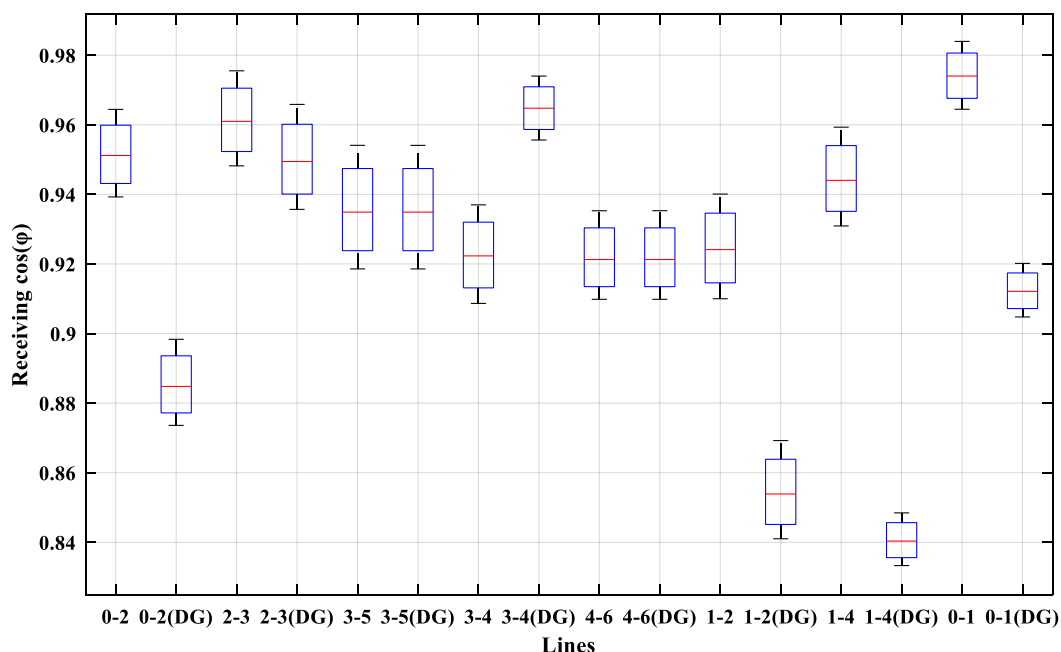


Figure 4.24 Receiving $\cos(\varphi)$ comparison between (normal) and (DG) cases for all transmission lines (10 m/s)

4.1.3 Speed 5 m/s

4.1.3.1 Voltage deviation % of busbars

Figure 4.25 shows voltage deviation % comparison between normal and controlled DG cases for wind speed 5 m/s. The obtained results are similar to what we got for speeds 15 m/s and 10 m/s where we got less voltage deviation for all busbars and all steps with respect to the normal case. Although, the voltage deviation for speed is higher than 15 m/s and 10 m/s wind speeds where for bus 6 (step 4) voltage deviation changed from -3.5% (15 m/s) to -3.9% (10 m/s) and -4.4% (5 m/s). This emphasizes that the controller is effective even for low wind speeds (low active power generation).

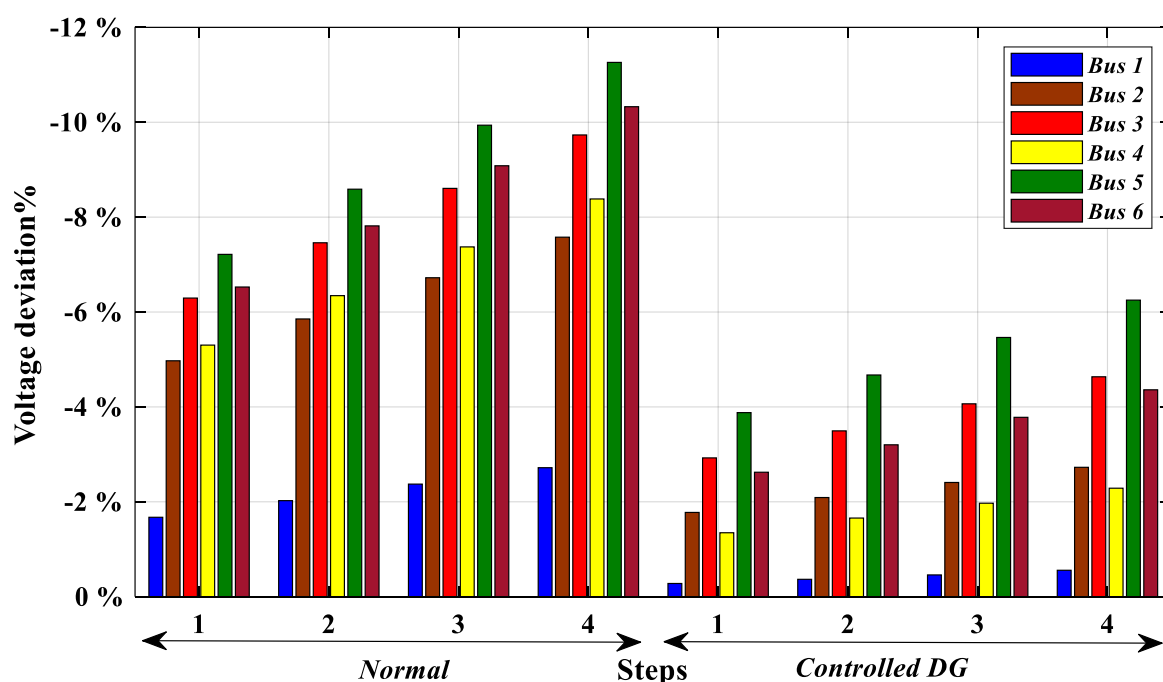


Figure 4.25 Voltage deviation % comparison between (normal) and (controlled DG) cases for all busbars (5 m/s).

Figure 4.26 illustrates the differences of voltage deviation between normal and DG cases for speed 5 m/s. Voltage deviation values increased for this speed in compared with higher speeds where voltage deviation for bus 6 (step 4) increased from -8.1% (15 m/s) to -8.9% (10 m/s) and -10% (5 m/s) which is slightly lower than voltage deviation in the normal case (-10.33 %). And we got the same performance for other busbars and steps which conclude that the controller has significant impact in low speeds.

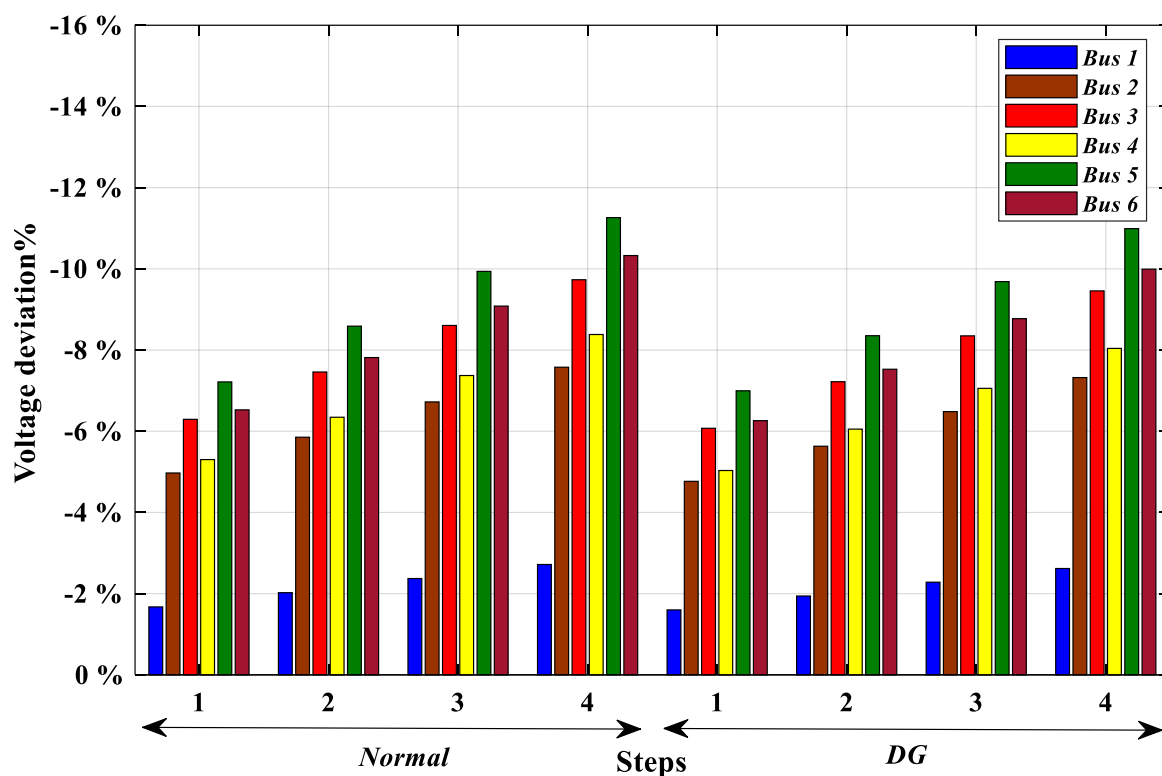


Figure 4.26 Voltage deviation % comparison between (normal) and (DG) cases for all busbars (5 m/s).

4.1.3.2 Sending voltage deviation % of transmission lines

In figure 4.27 we can see sending voltage deviation comparison between normal and controlled DG cases for wind speed 5 m/s. Results for this speed are similar to what we got for 10 and 15 m/s as the voltage deviation is decreased remarkably in the controlled case in compared to normal case. But, voltage deviation in the controlled case for this speed is higher than the other two high speeds for lines 2-3, 3-5, 3-4 and 4-6 and the magnitude of increase is (0.36% - 0.48%). For instance, sending voltage deviation for line 4-6 (step 4) increased from -1.4% (15 m/s) to 1.8% (10 m/s) and 2.28% (5 m/s).

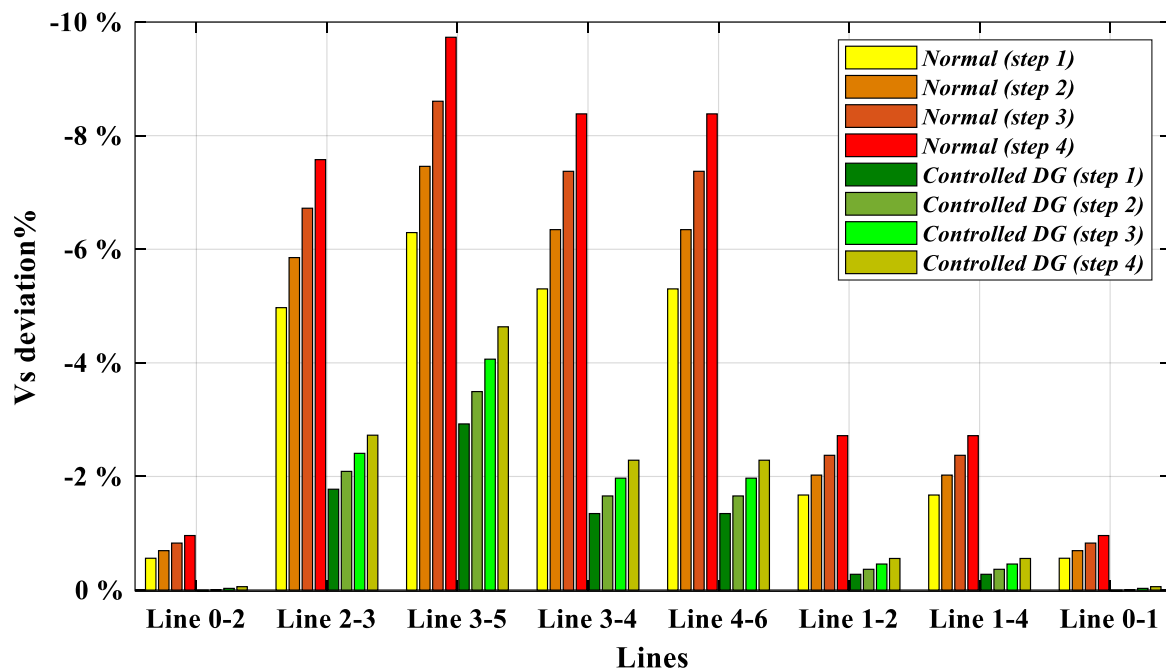


Figure 4.27 Sending voltage deviation % comparison between (normal) and (controlled DG) cases for all transmission lines(5 m/s).

Figure 4.28 shows a comparison between normal and DG cases in terms of sending voltage deviation for speed 5 m/s. The performance is similar to what we got for speed 10 m/s where the decreased generated active power from DG units cause to increase in the voltage deviation for lines especially 2-3, 3-5, 3-4 and 4-6 where the increment is between 0.82% and 1.13%. These results show that the impact of the decreased generated active power is bigger in the DG case with respect to the controlled DG case. Also, the controller still shows high efficiency in reducing voltage deviation.

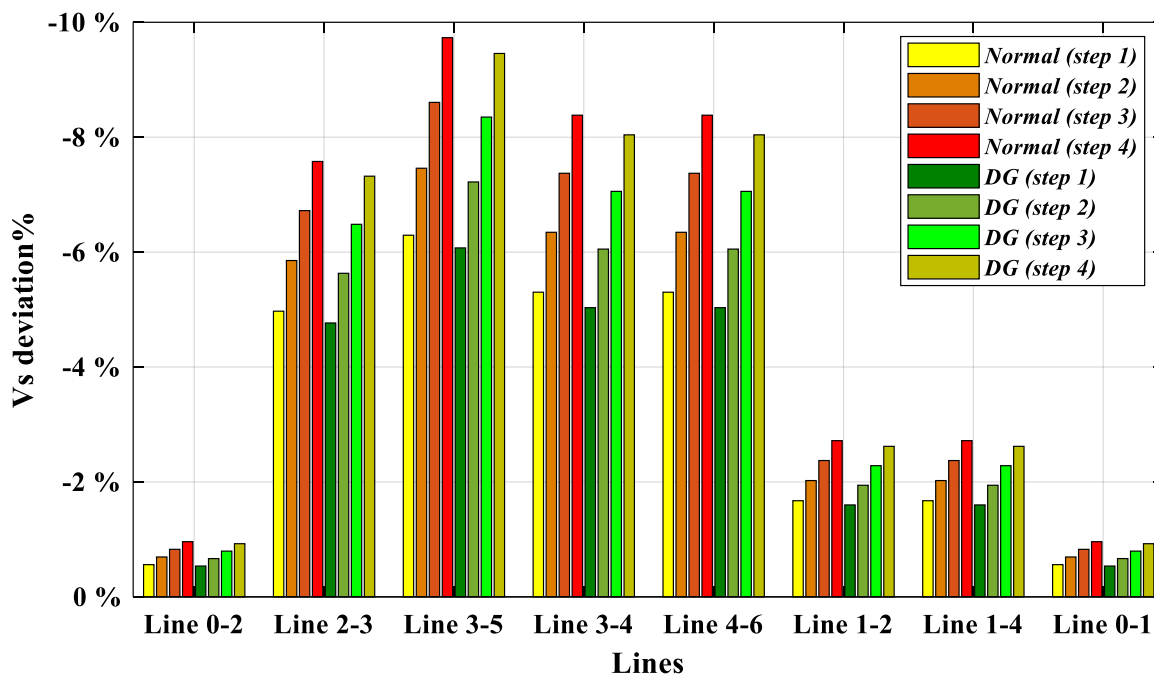


Figure 4.28 Sending voltage deviation % comparison between (normal) and (DG) cases for all transmission lines(5 m/s).

4.1.3.3 Receiving voltage deviation % of transmission lines

Figure 4.29 illustrates receiving voltage deviation % comparison between normal and controlled DG cases for wind speed 5 m/s. These results are similar to what we obtained for 10 m/s and 15 m/s where voltage deviation decreased remarkably in the controlled DG case with respect to the normal case. For instance, voltage deviation for line 4-6 (step 4) decreased from -10.3% in the normal case to -4.4% in the controlled DG case. Although, voltage deviation for this speed is slightly higher than the other two speeds and the difference is about (0.36% - 0.49%).

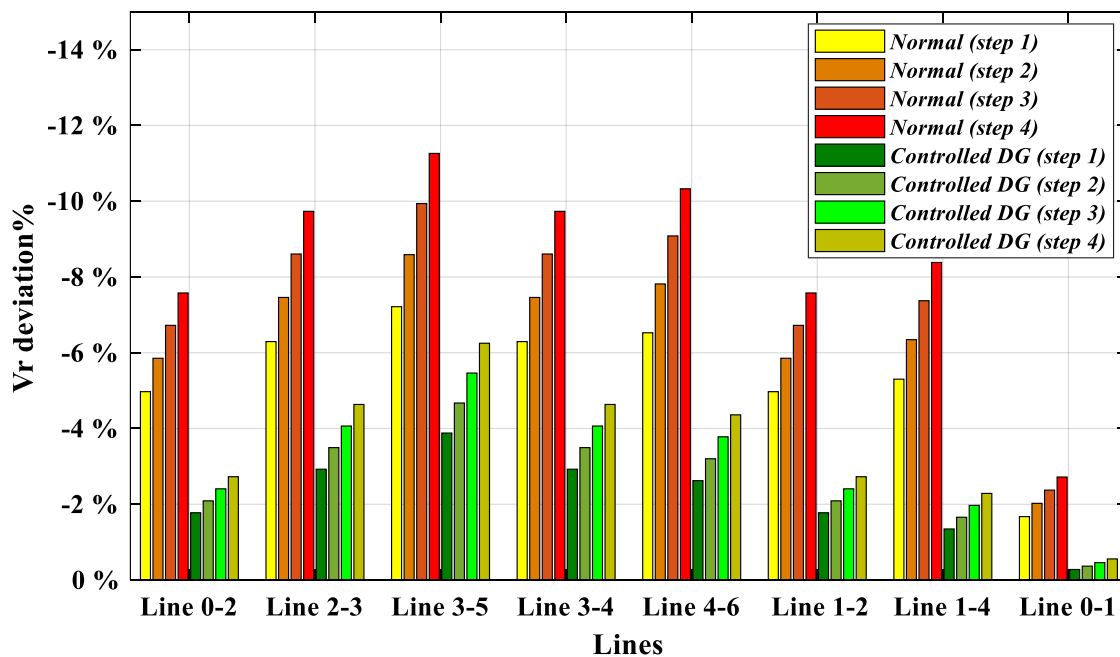


Figure 4.29 Receiving voltage deviation % comparison between (normal) and (controlled DG) cases for all transmission lines(5 m/s).

In figure 4.30 we can see the comparison between normal and DG cases in terms of receiving voltage deviation for speed 5 m/s. Similar to what we got for speed 10 m/s, the decreased generated active power from DG units led to voltage deviation increase in all lines. For instance, voltage deviation for line 4-6 (step 4) increased from -8.1% (15 m/s) to -8.9% (10 m/s) and -10% (5 m/s). Anyway, the controller still shows big impact on reducing voltage deviation even for low speeds.

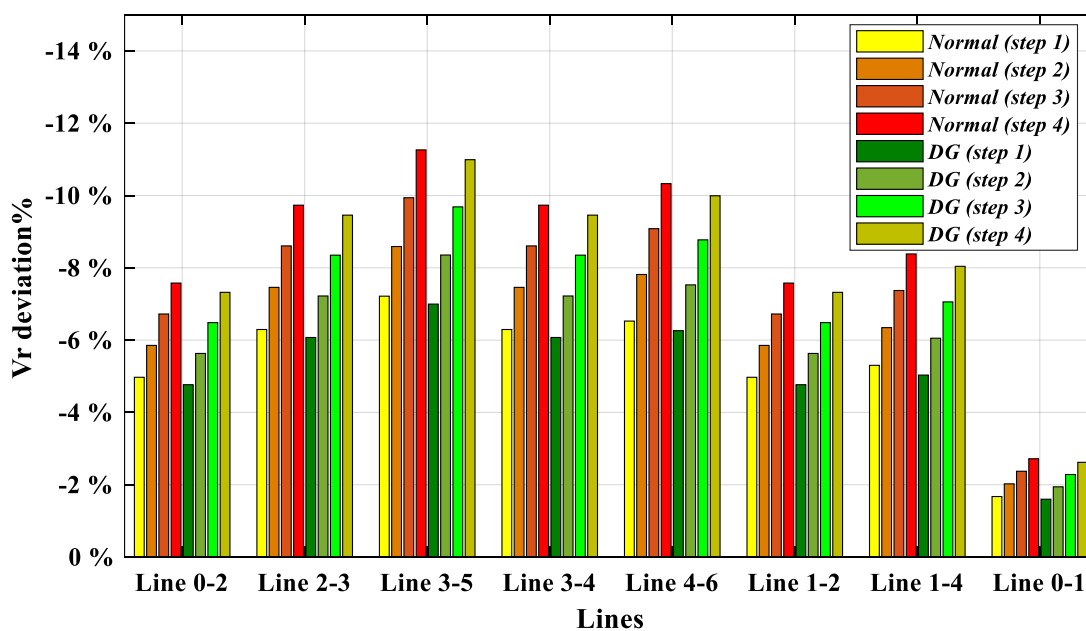


Figure 4.30 Receiving voltage deviation % comparison between (normal) and (DG) cases for all transmission lines(5 m/s).

4.1.3.4 Voltage drop % of transmission lines

In figure 4.31 we can see voltage drop % comparison between normal and controlled DG cases for wind speed 5 m/s. The obtained results are similar to what we got for the other two higher speeds where the controller reduced voltage drop especially for lines 0-1, 1-4, 1-2, and 0-2. For the other lines where we got higher voltage drops such as 3-5, 3-4, and 4-6, the reason is due to the fact that the controller increased voltage of the sending end more than voltage of the receiving end. The values of voltage drop are very close to the case of 15 m/s and 10 m/s for lines 2-3, 3-5, 3-4, 4-6, and 0-1. But for lines 0-2, 1-2, and 1-4, the values for speed 5 m/s are slightly higher than 10 m/s and the difference is about (0.34% - 0.43%).

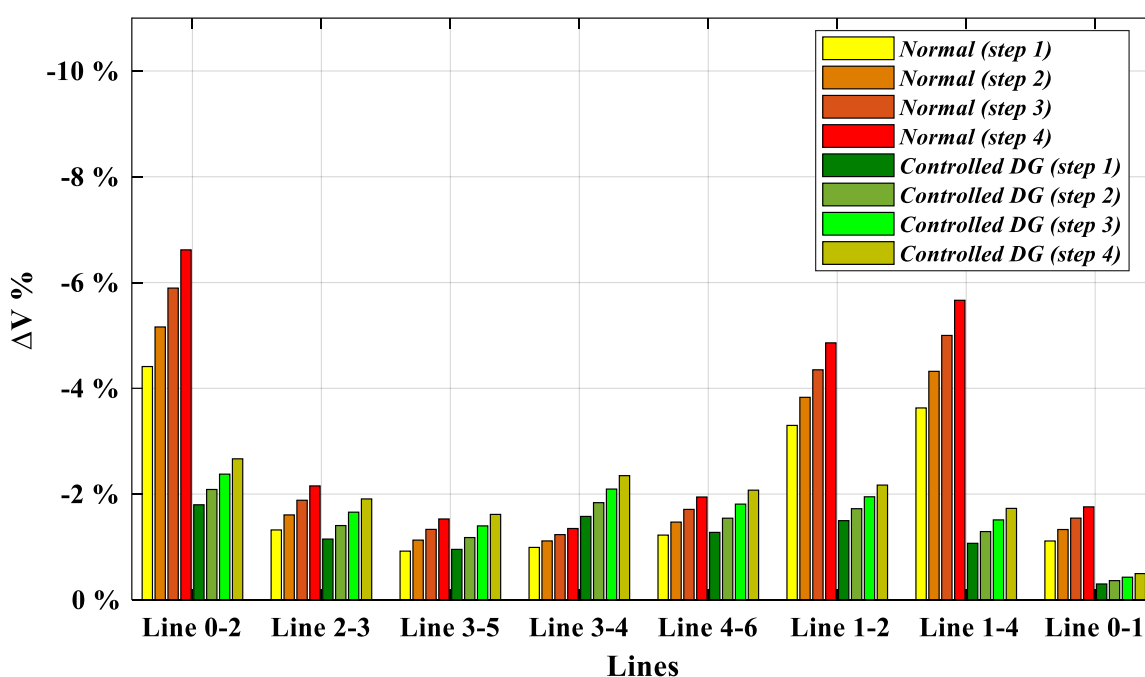


Figure 4.31 Voltage drop (%) comparison between (normal) and (controlled DG) cases for all transmission lines (5 m/s).

In figure 4.32, we can notice voltage drop comparison between normal and DG cases for speed 5 m/s. The low injected active power from DG units led to an get high voltage drop with respect to speed 15 m/s and 10 m/s. Actually, the voltage drop values for all lines are close to each other except lines 0-2, 1-2, and 1-4 where the voltage drop is slightly higher in case of 5 m/s with a difference (0.6% - 0.87%). For instance, voltage drop for line 0-2 (step 4) increased from 4.95% (15 m/s) to 5.56% (10 m/s) and 6.4% (5 m/s).

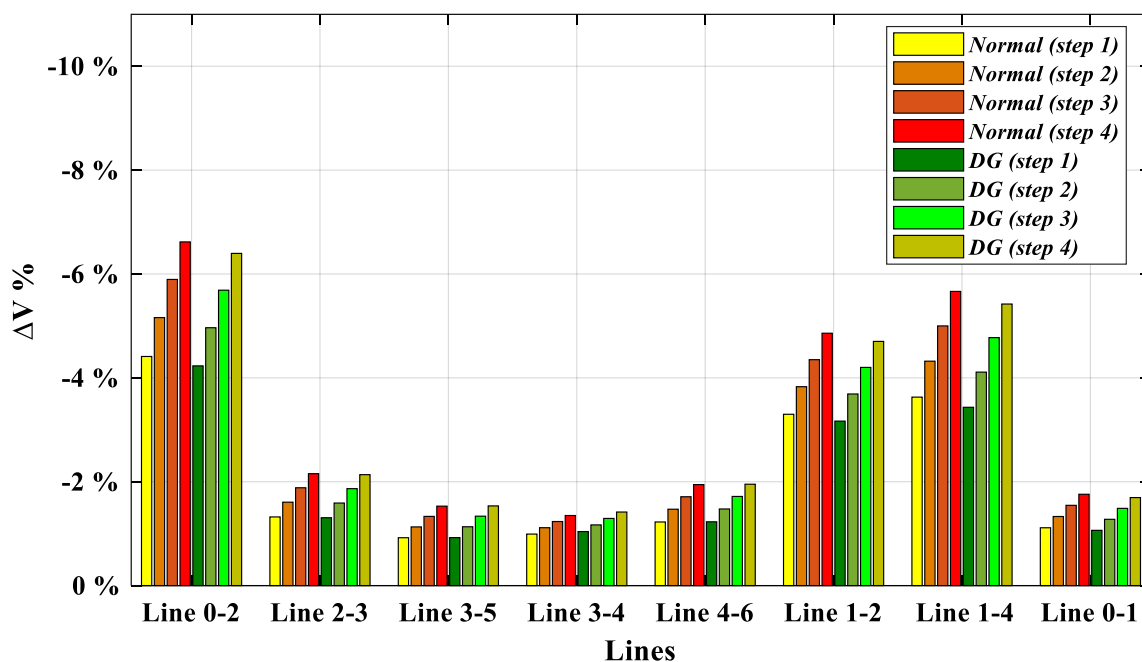


Figure 4.32 Voltage drop (%) comparison between (normal) and (DG) cases for all transmission lines (5 m/s).

4.1.3.5 Sending $\cos(\varphi)$ of transmission lines

Figure 4.33 shows sending $\cos(\varphi)$ comparison between normal and controlled DG cases for wind speed 5 m/s. The results here are similar to what we got for other higher speeds where the controller has some positive impact on improving $\cos(\varphi)$ especially lines 0-2, 1-2, and 1-4. But the decreased supplied active power from DG units cause decrement in $\cos(\varphi)$ for lines 0-1, 1-4, 1-2 and 3-4. The biggest decrease was for line 3-4 where the values of $\cos(\varphi)$ decreased from (0.94 - 0.98) for speed 15 m/s to (0.89 - 0.96) for speed 10 m/s to (0.79 - 0.89) for speed 5 m/s. The decrease of $\cos(\varphi)$ for the other lines is very small and the high decrease in line 3-4 is due to the fact this line transfers more reactive power to the loads when needed. Anyway, even for this low speed the controller still shows improvement in sending $\cos(\varphi)$ value.

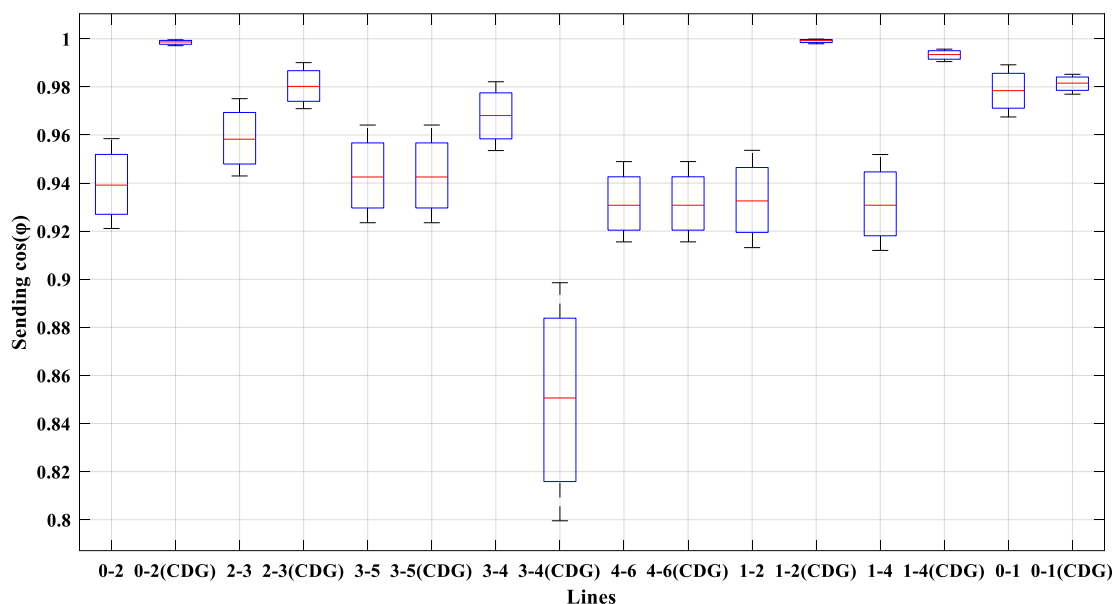


Figure 4.33 Sending $\cos(\varphi)$ comparison between (normal) and (controlled DG) cases for all transmission lines (5 m/s).

In figure 4.34, we can see the difference between normal and DG cases in terms of sending $\cos(\varphi)$ for wind speed 5 m/s. Results here shows that DG units have negative impact on sending $\cos(\varphi)$ for most of lines where its value is lower in the DG case for lines 0-1,0-2, 1-2, and 1-4 and this due to the low active power generation from DG units. For line 3-4, $\cos(\varphi)$ value increased slightly and for other lines there is no impact. By checking numerical results, we noticed that the reduced wind speed caused $\cos(\varphi)$ decrease in lines 0-2, 1-2, 1-4, and 0-1 and the difference is (0.04 – 0.08).

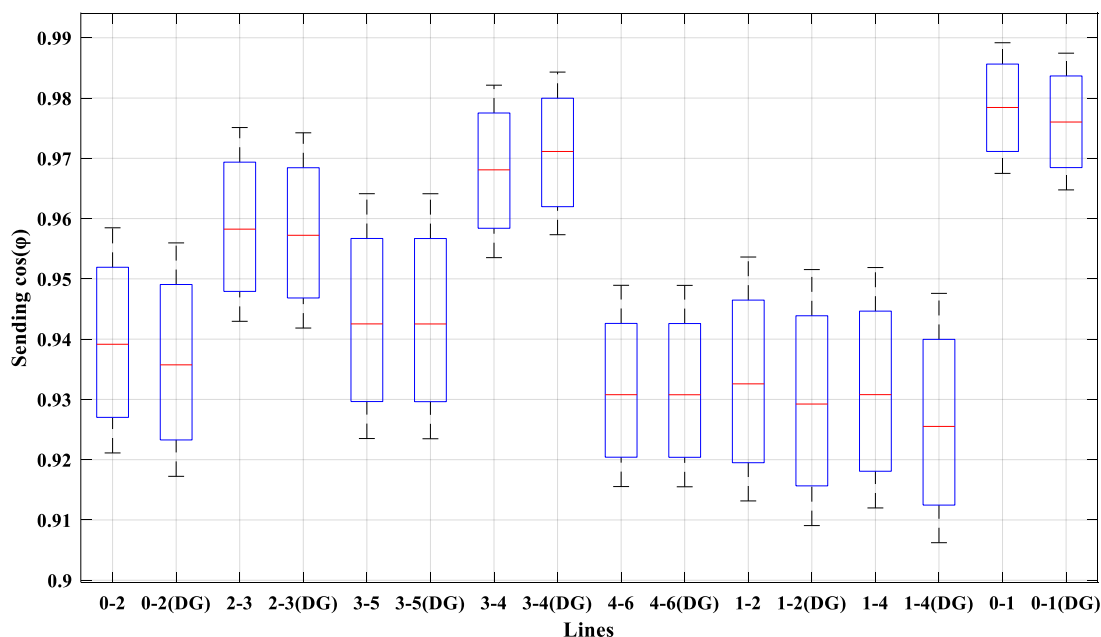


Figure 4.34 Sending $\cos(\varphi)$ comparison between (normal) and (DG) cases for all transmission lines (5 m/s).

4.1.3.6 Receiving $\cos(\varphi)$ of transmission lines

Figure 4.35 shows comparison between normal and controlled DG cases in regards to receiving $\cos(\varphi)$ for wind speed 5 m/s. Results show that for most of lines, the values of $\cos(\varphi)$ are very close to what we got for speed 10 m/s except line 3-4 which got lower $\cos(\varphi)$ for speed 5 m/s due to reduced transmitted active power through it. Anyway, the controller DG case still shows an improvement in the receiving $\cos(\varphi)$ in comparison to the normal case for lines 0-2, 2-3, 1-2, 1-4 and 0-1.

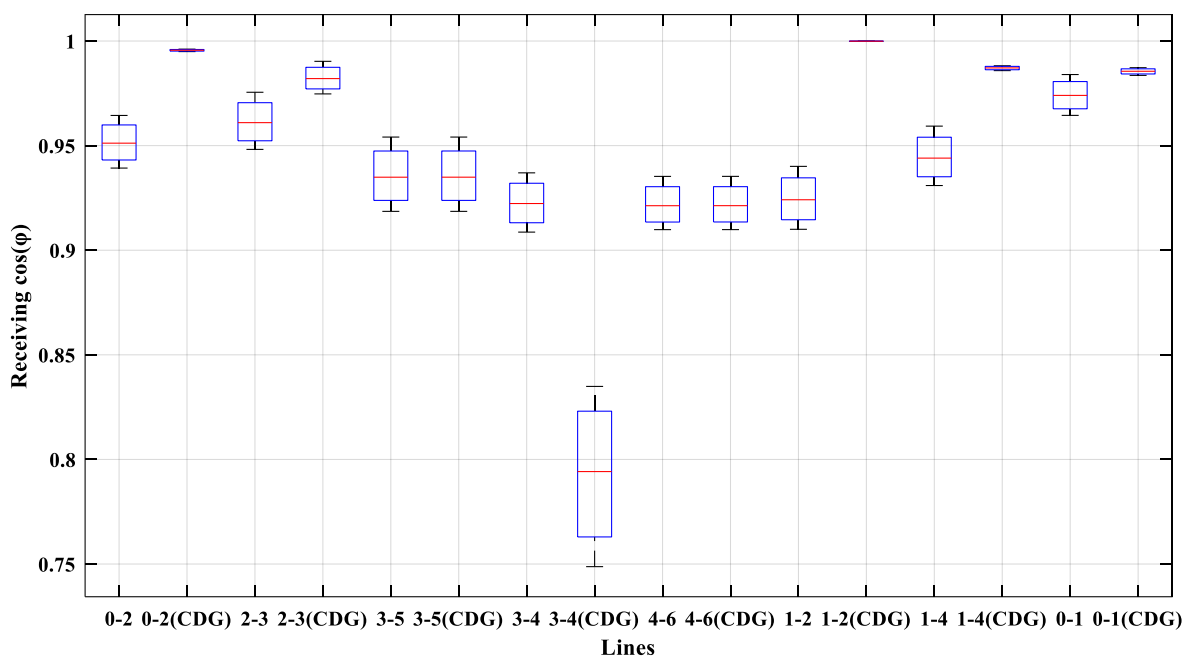


Figure 4.35 Receiving $\cos(\varphi)$ comparison between (normal) and (controlled DG) cases for all transmission lines (5 m/s).

In figure 4.36, we can notice receiving $\cos(\varphi)$ comparison between normal and DG cases for speed 5 m/s. As what we got for higher speeds, $\cos(\varphi)$ values decreased for lines 0-2, 2-3, 1-2, 1-4 and 0-1, but it increased for line 3-4 with respect to normal case. For the rest of lines, the values are very close to each other. If we want to compare the results for this speed with speed 10 m/s, we will notice that the low speed causes an increase in receiving $\cos(\varphi)$ for lines 0-2, 2-3, 1-2, 1-4, and 0-1. In general, the controller DG case showed the best performance in terms of receiving $\cos(\varphi)$.

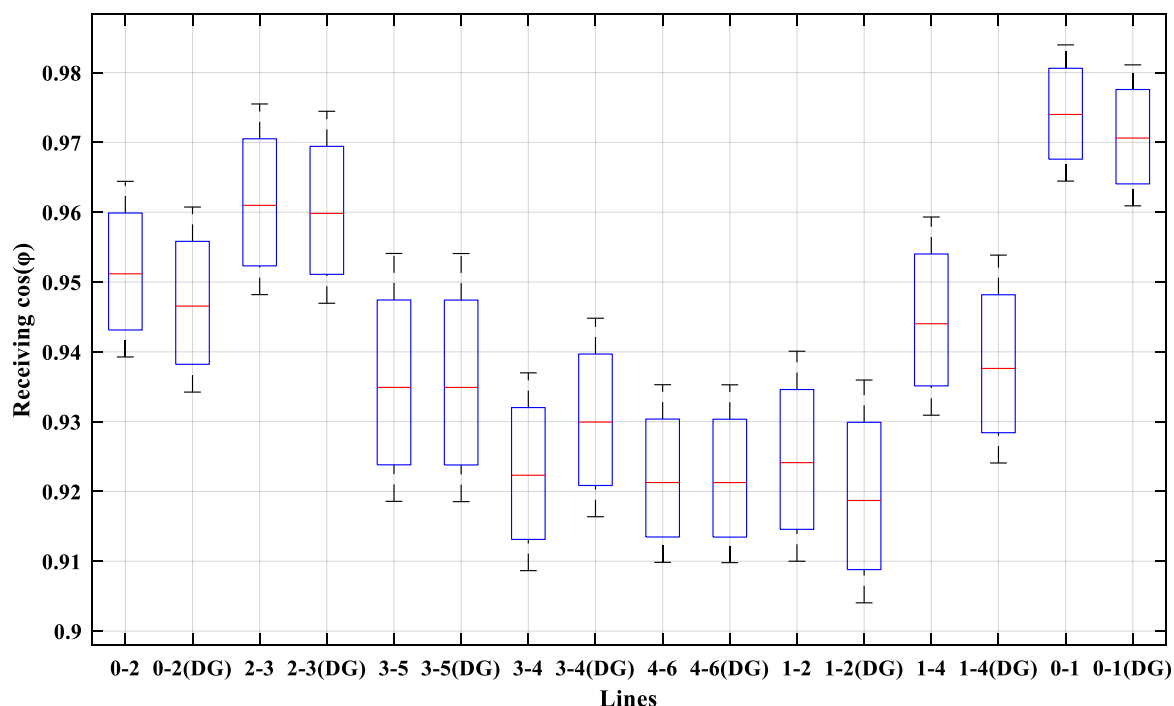


Figure 4.36 Receiving $\cos(\varphi)$ comparison between (normal) and (DG) cases for all transmission lines (5 m/s).

4.1.4 Fault Line 2-3 (speed 5 m/s)

4.1.4.1 Voltage deviation % of busbars

Figure 4.37 illustrates voltage deviation % comparison between normal and controlled DG cases for (Fault line 2-3, speed 5 m/s). The obtained results prove how the controller is able to reduce voltage deviation in efficient way even in case of faults and low active power generation. We can notice that the voltage deviation for busbars increased significantly when we faced the fault in line 2-3; where it increased from -11.3% before the fault to reach -20.3 % after the fault for busbar 5 (step 4). Also, the controller is capable to reduce the voltage deviation for all busbars to be in the range $\pm 10\%$ except busbar 5 (step 4). There is another difference with respect to the case before the fault which is getting higher voltage than the nominal voltage for busbar 2 due to the high reactive power generation to compensate the high voltage deviation that caused by the fault.

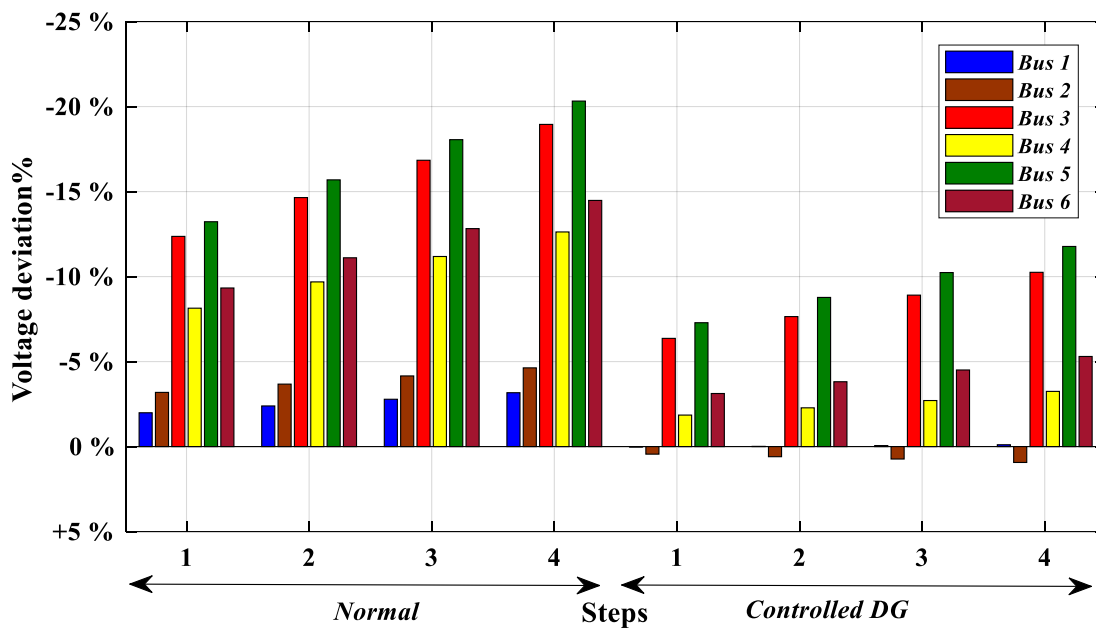


Figure 4.37 Voltage deviation % comparison between (normal) and (controlled DG) cases for all busbars (fault line 2-3, 5 m/s).

Figure 4.38 shows comparison between normal and DG cases in terms of voltage deviation for (Fault line 2-3, speed 5 m/s). The obtained results show that the DG units are able to reduce voltage deviation in a trivial way. For line 2-3 (step 4), voltage deviation decreased from -20.3% in the normal case to -18.6% in the DG case. Also, we can see that voltage deviation for busbars 3 and 5 is out of the allowed range $\pm 10\%$ even in the first step where we got (-12%) for busbar 3 and (-12.9%) for busbar 5.

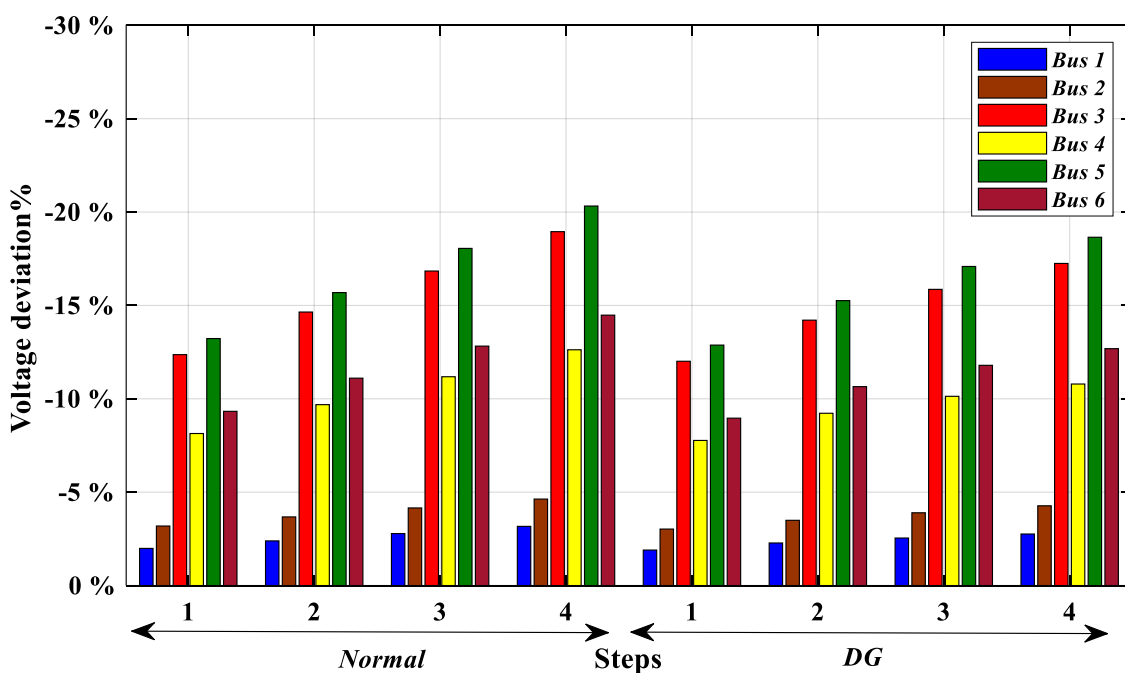


Figure 4.38 Voltage deviation % comparison between (normal) and (DG) cases for all busbars (fault line 2-3, 5 m/s).

4.1.4.2 Sending voltage deviation % of transmission lines

In figure 4.39, we can notice sending voltage deviation comparison between normal and controlled DG cases for (Fault line 2-3, speed 5 m/s). In the shown results we can see how the controller reduced voltage deviation remarkably for all lines. For instance, voltage deviation for line 3-5 (step 4) decreased from -18.95% at normal case to -10.25% at controlled DG case. The controller proves its high efficiency in terms of sending voltage deviation even in case of faults.

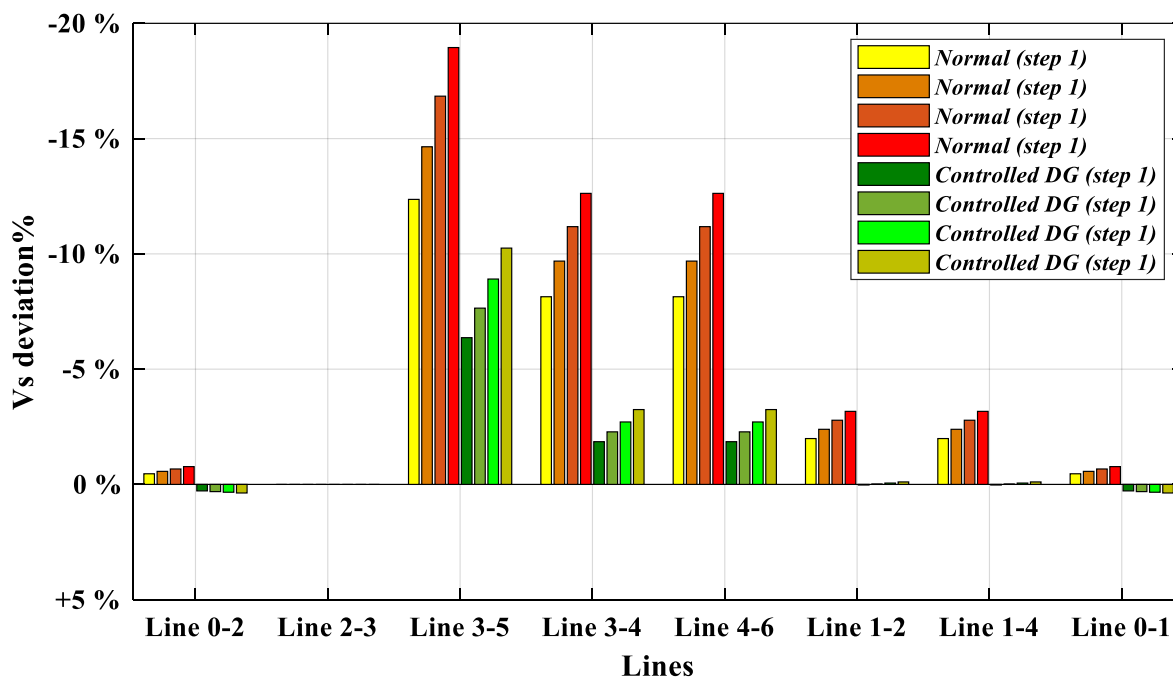


Figure 4.39 Sending voltage deviation % comparison between (normal) and (controlled DG) cases for all transmission lines (fault line 2-3, 5 m/s).

Figure 4.40 illustrates sending voltage deviation comparison between normal and DG cases for (Fault line 2-3, speed 5 m/s). The obtained results show that the existence of DG units has only a slight impact on reducing voltage deviation for sending ends. For example, voltage deviation for line 3-5 decreased from -18.95% at normal case to -17.25% at DG case. Also, the same behavior for the rest of lines and steps.

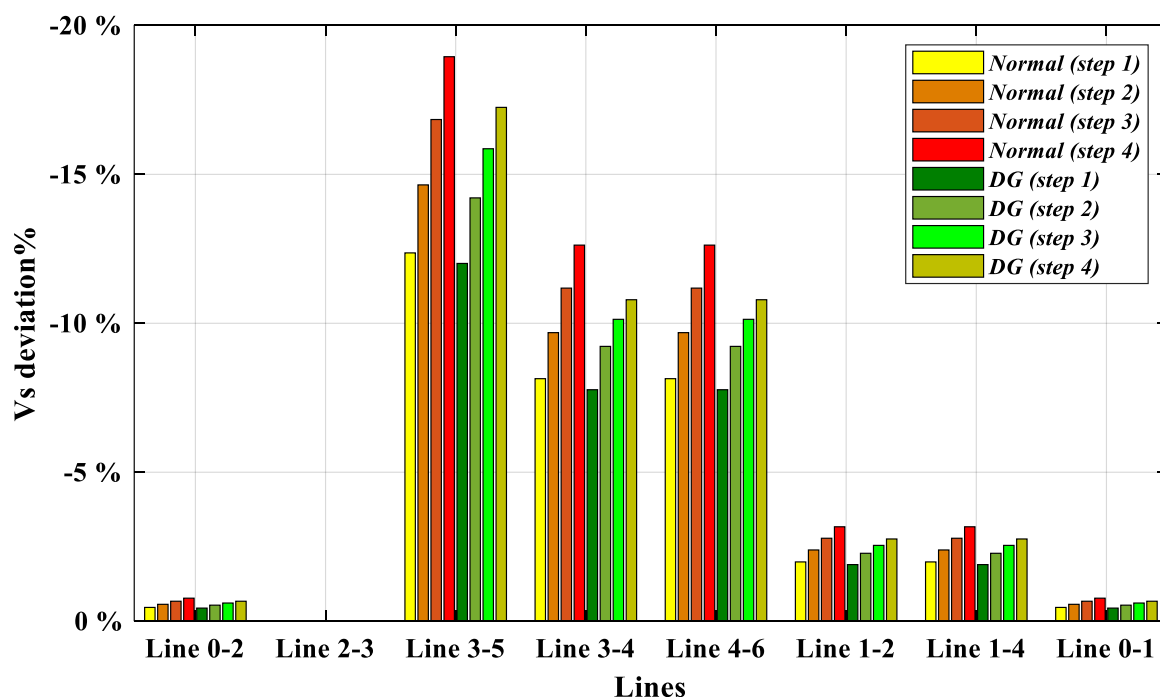


Figure 4.40 Sending voltage deviation % comparison between (normal) and (DG) cases for all transmission lines (fault line 2-3, 5 m/s).

4.1.4.3 Receiving voltage deviation % of transmission lines

In figure 4.41 we can see comparison between normal and controlled DG cases in terms of receiving voltage deviation for (Fault line 2-3, speed 5 m/s). For receiving ends, the controller shows big impact on improving voltage profile by reducing voltage deviation. This is obvious for all transmission lines. For example, voltage deviation for line 4-6 (step 4) decreased from -14.5% in the normal case to -5.3% at the controlled DG case, and for line 1-4 (step 4) it decreased from -12.6% to -3.2%. These results show that the controller played an important role in reducing voltage deviation values and narrowing the range of changes.

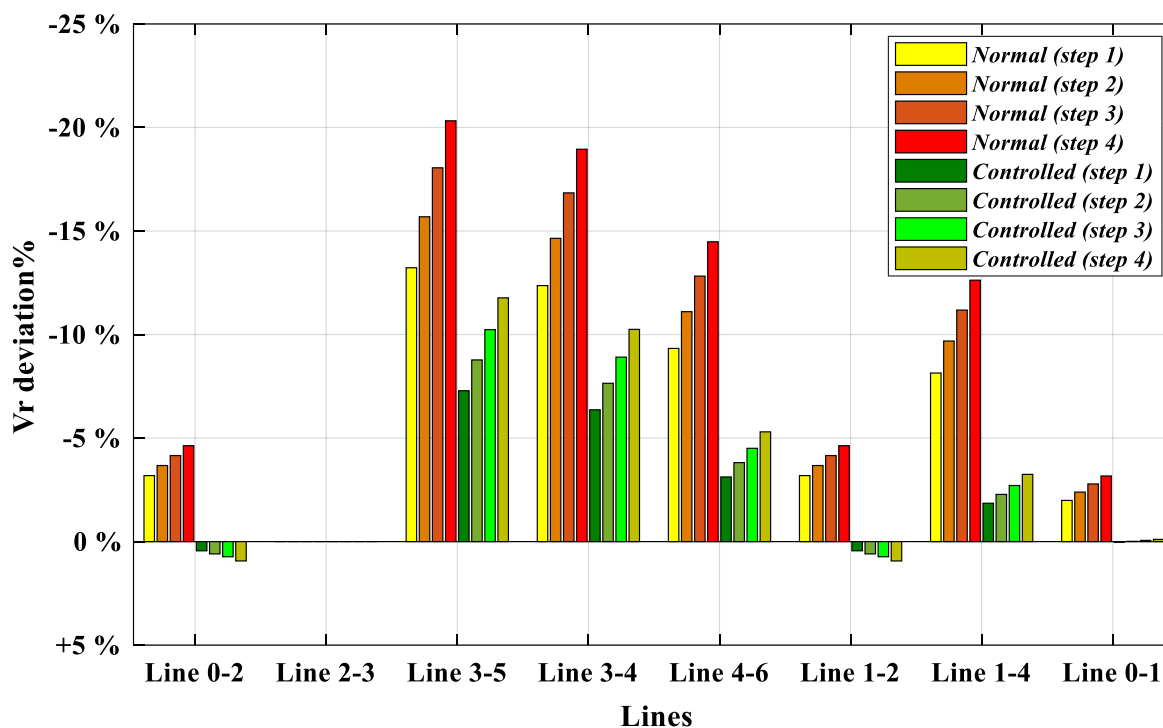


Figure 4.41 Receiving voltage deviation % comparison between (normal) and (controlled DG) cases for all transmission lines (fault line 2-3, 5 m/s).

Figure 4.42 shows receiving voltage deviation comparison between normal and DG cases for (Fault line 2-3, speed 5 m/s). The obtained results show that DG units are capable to reduce voltage deviation only by small magnitude for all lines. For instance, voltage deviation of line 4-6 (step 4) decreased from -14.5% to -12.7% at the DG case while it decreased to -5.3 at the controlled DG case.

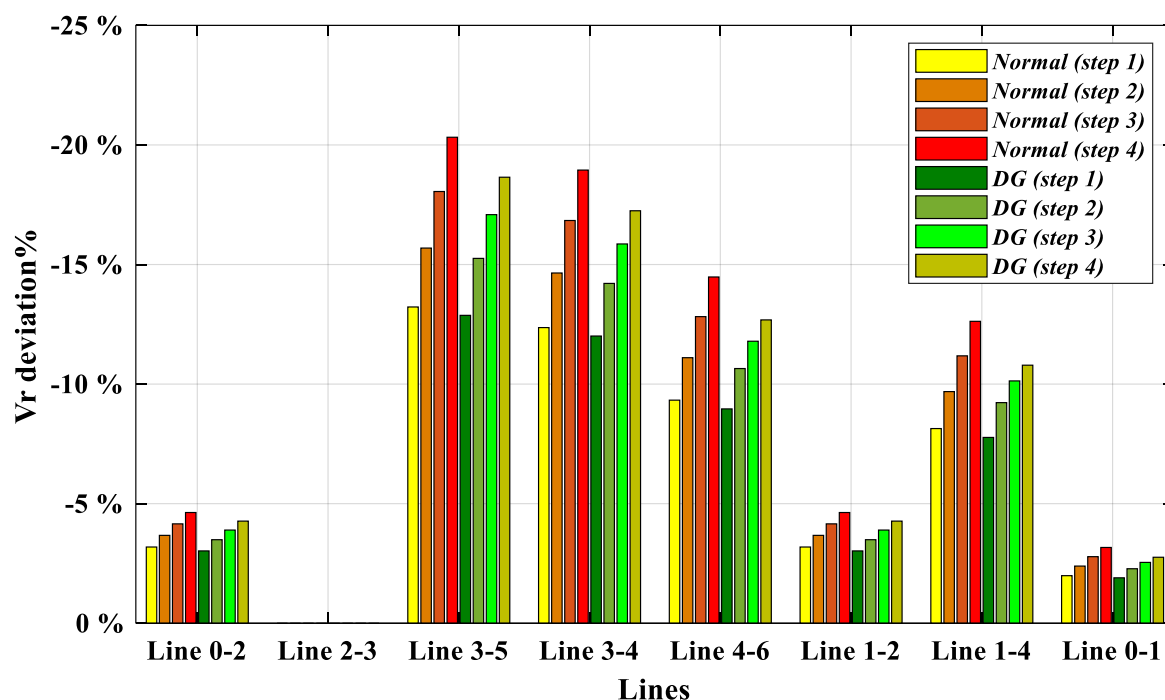


Figure 4.42 Receiving voltage deviation % comparison between (normal) and (DG) cases for all transmission lines (fault line 2-3, 5 m/s).

4.1.4.4 Voltage drop % of transmission lines

In figure 4.43, we can notice voltage drop comparison between normal and controlled DG cases for (Fault line 2-3, speed 5 m/s). The results here also show a big improvement for reducing voltage drop for lines 0-2, 1-2, 1-4, and 0-1 with respect to the normal case. Voltage drop for line 1-4 (step 4) reduced from 9.45% at the normal case to 3.14% at the controlled DG case. The slight increase in voltage drop for lines 3-5, 3-4, 4-6 is due to the fact that the increment in sending voltage is higher than receiving end. For example, sending voltage for line 3-4 (step 4) increased from 57.67 kV at the normal case to 63.86 kV at the controlled DG case (i.e. the increment is 6.19 kV), whereas the receiving voltage increased from 53.49 kV at normal case to 59.23 kV at the controlled DG case (i.e. the increment is 5.74 kV). We can see here some voltage values in positive area which means that change of the power flow direction such as lines 0-2 and 1-2.

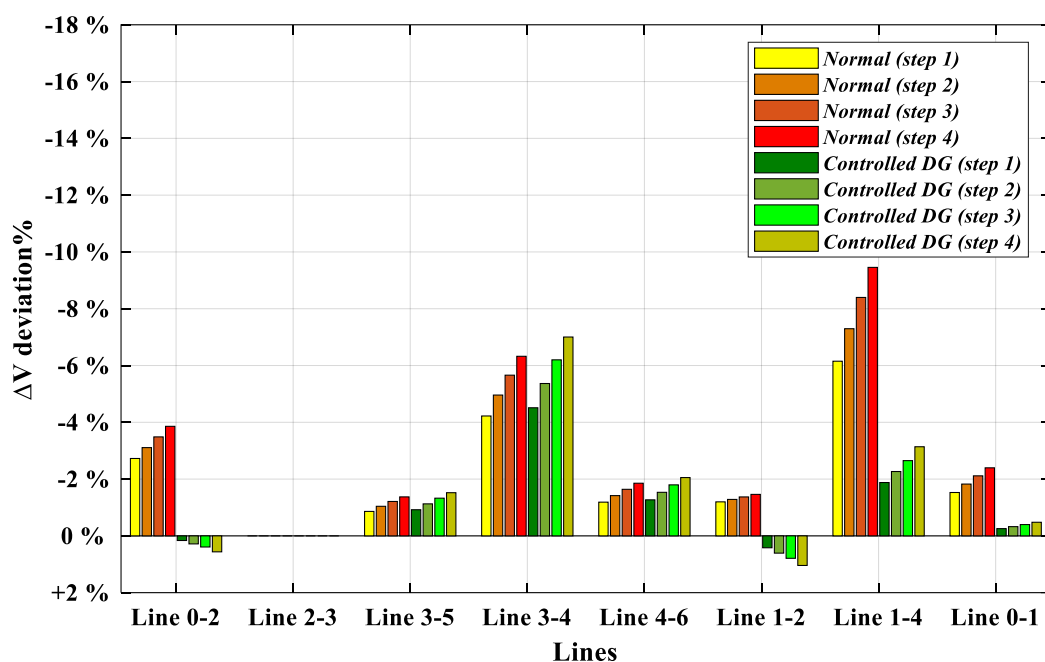


Figure 4.43 Voltage drop % comparison between (normal) and (controlled DG) cases for all transmission lines ((fault line 2-3, 5 m/s).

Figure 4.44 illustrates voltage drop comparison between normal and DG cases for (Fault line 2-3, speed 5 m/s). These results show that DG is able to reduce voltage drop for some lines only in a slight way. The improvement is not such a big difference if we compared it with the controller DG case. For instance, voltage drop for line 1-4 (step 4) reduced from 9.45% at the normal case to 3.14% at the controlled DG case and 8.03% at the DG case.

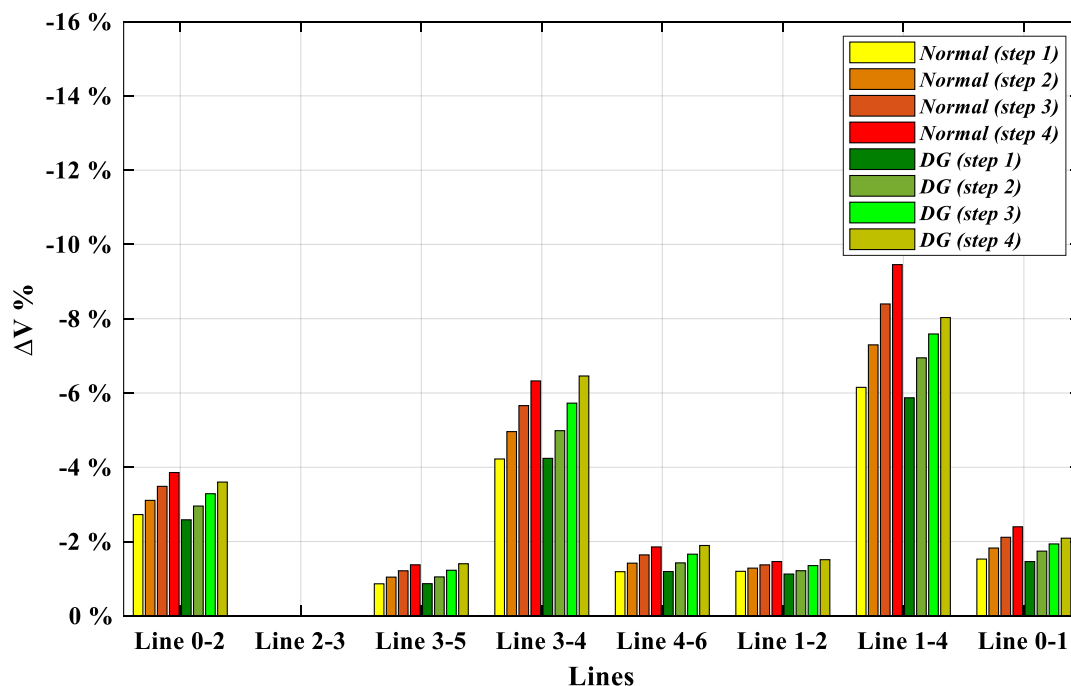


Figure 4.44 Voltage drop % comparison between (normal) and (DG) cases for all transmission lines ((fault line 2-3, 5 m/s).

4.1.4.5 Sending $\cos(\varphi)$ of transmission lines

In figure 4.45, we can see comparison between normal and controlled DG cases in terms of sending $\cos(\varphi)$ for (Fault line 2-3, speed 5 m/s). These results show that controller improved sending $\cos(\varphi)$ for lines 1-4 and 0-1. For lines 1-2 and 0-2 we can notice a decrease in the value of $\cos(\varphi)$ due to increased reactive power transferred through these lines. We can also notice that the value of $\cos(\varphi)$ kept its value without change for the rest of lines.

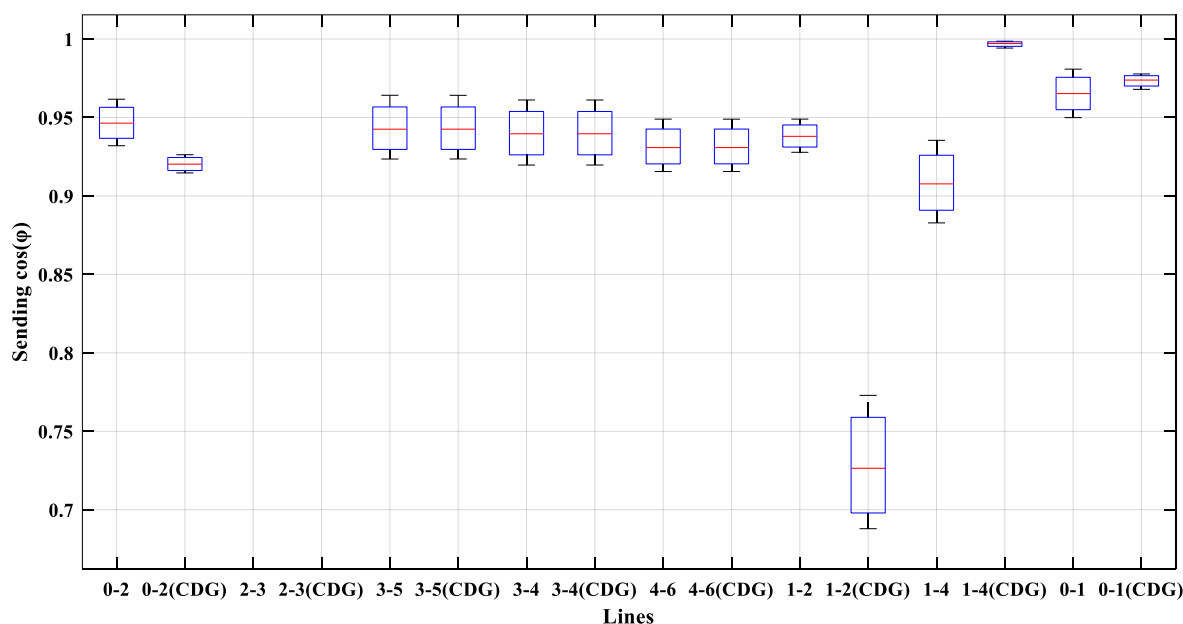


Figure 4.45 Sending $\cos(\varphi)$ comparison between (normal) and (controlled DG) cases for all transmission lines ((fault line 2-3, 5 m/s).

Figure 4.46 shows sending $\cos(\varphi)$ comparison between normal and DG cases for (Fault line 2-3, speed 5 m/s). The results here shows a narrower range of change for lines 0-1 and 1-4 with respect to the normal case but the improve is less than the controlled DG case where $\cos(\varphi)$ for line 1-4 improved from (0.88 – 0.93) at the normal case to (0.92- 0.93) at the DG case and 0.99 at the controlled DG case. For lines 0-2 and 1-2, we can see that the DG units have negative impact on $\cos(\varphi)$ value. Lines 3-5, 3-4 and 4-6 did not face any change in $\cos(\varphi)$ value in compared with normal case.

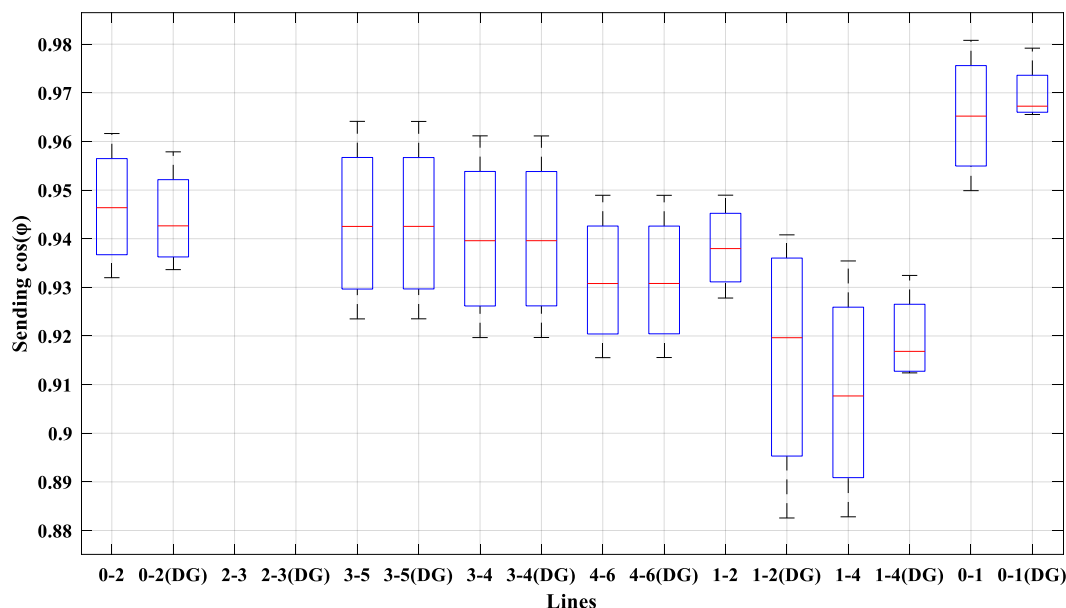


Figure 4.46 Sending $\cos(\varphi)$ comparison between (normal) and (DG) cases for all transmission lines ((fault line 2-3, 5 m/s).

4.1.4.6 Receiving $\cos(\varphi)$ of transmission lines

In figure 4.47, we can see the difference between normal and controlled DG cases in terms of receiving $\cos(\varphi)$ for (Fault line 2-3, speed 5 m/s). From the obtained results we can figure out that the we got an improvement in the controlled DG case in lines 0-1 and 1-4 with respect to the normal case. But we got lower values for $\cos(\varphi)$ in lines 0-2 and wider range of change in line 1-2 where it was (0.83 - 0.84) for the normal case and (0.77 - 0.89) for the controlled DG case. Values of $\cos(\varphi)$ for the rest of lines did not change and remained the same.

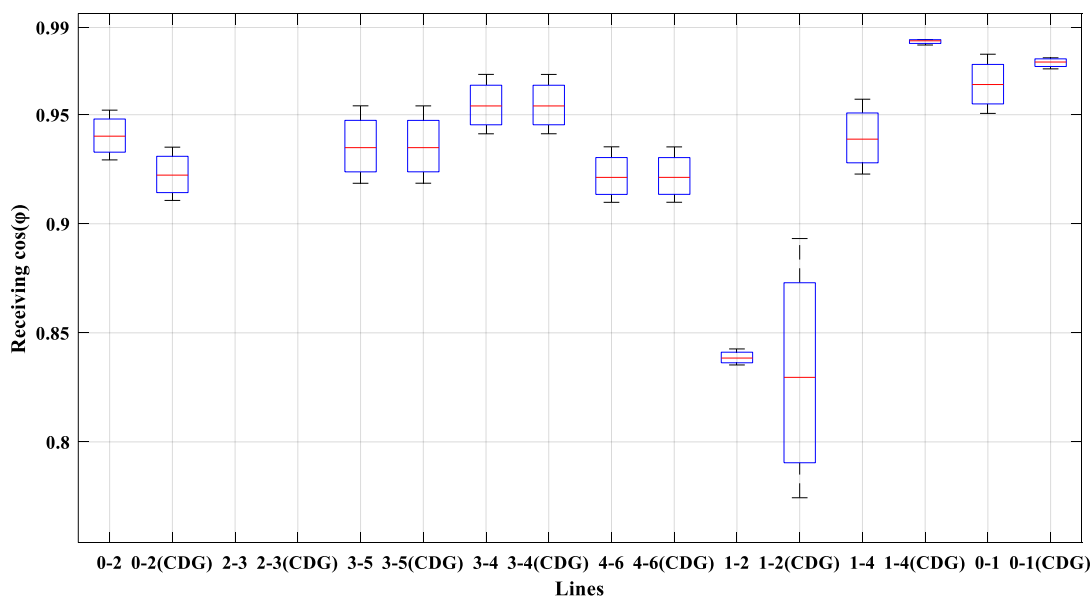


Figure 4.47 Receiving $\cos(\varphi)$ comparison between (normal) and (controlled DG) cases for all transmission lines ((fault line 2-3, 5 m/s).

Figure 4.48 shows receiving $\cos(\varphi)$ comparison between normal and DG cases for (Fault line 2-3, speed 5 m/s). These results show some improvement in the $\cos(\varphi)$ for lines 0-1 and 1-4 but less than what we got in the controlled DG case where $\cos(\varphi)$ for line 1-4 increased from (0.92 - 0.96) in the normal case to 0.95 in the DG case and 0.98 in the controlled DG case. Lines 0-2 and 1-2 got less values for $\cos(\varphi)$ in the DG case in compared with the normal case. Values of $\cos(\varphi)$ for lines 3-5, 3-4 and 4-6 remains without change.

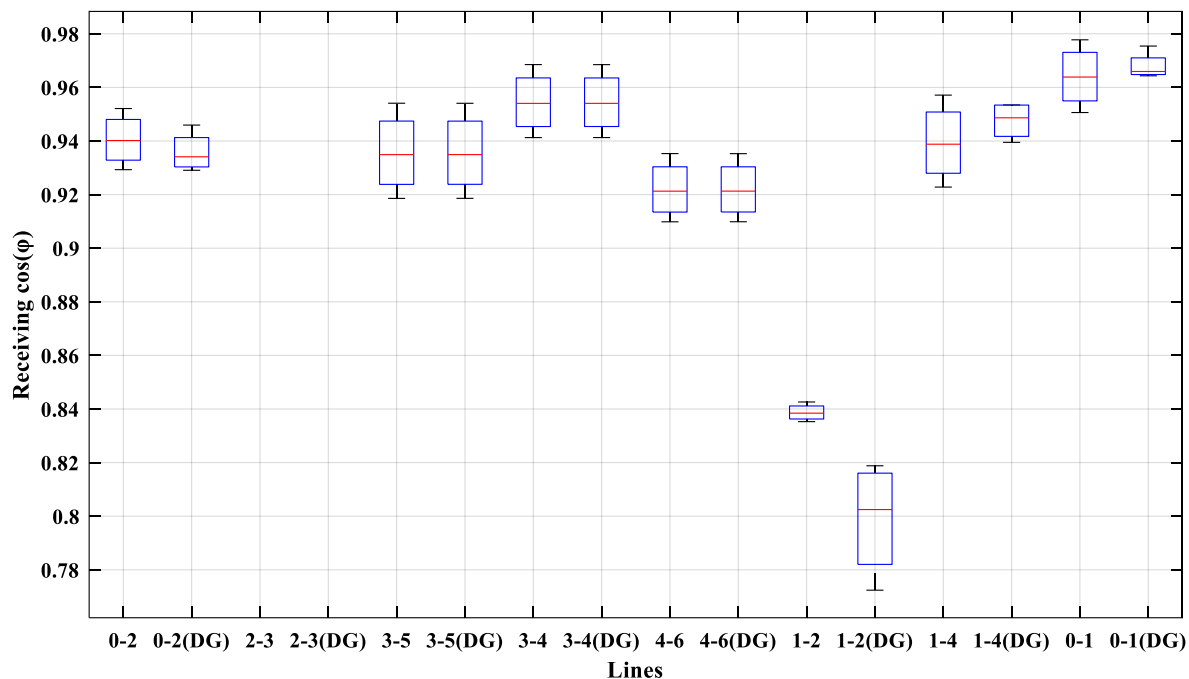


Figure 4.48 Receiving $\cos(\varphi)$ comparison between (normal) and (DG) cases for all transmission lines ((fault line 2-3, 5 m/s).

4.2 Power losses

4.2.1 Speed 15 m/s

In figure 4.49, we can notice the differences in total power losses for the whole system between normal and controlled DG cases for speed 15 m/s. The figure shows that the controlled DG case reduced power losses from 3.77 MW to 1.34 MW which means that reduction is about 64%. We can notice the same thing for all steps whereas total power losses changed from (2.05 MW - 3.77 MW) in the normal case to (0.51 MW – 1.34 MW) in the controlled DG case which corresponds reduction percentage (64% - 75%). Tables 4.1 and 4.2 show active power for sending and receiving ends for speed 15 m/s.

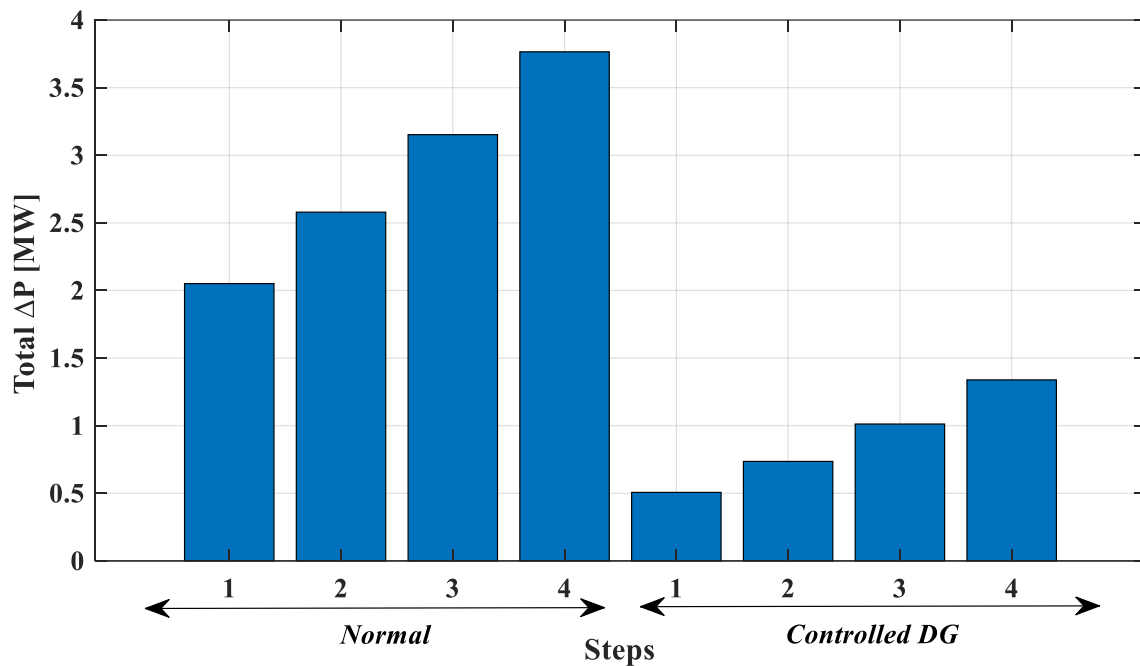


Figure 4.49 Total power losses comparison between (normal) and (controlled DG) cases (15 m/s).

Table 4.1 Sending active power values of lines for all steps (15 m/s) [kW].

Case		L 0-2	L 2-3	L 3-5	L 0-1	L 1-2	L 3-4	L 1-4	L 4-6
Normal	Step 1	25,789	20,517	10,093	13,509	14,686	5,594	28,999	10,313
	Step 2	28,222	22,810	11,313	14,959	15,977	5,854	32,174	11,630
	Step 3	30,523	24,947	12,424	16,348	17,188	6,090	35,166	12,850
	Step 4	32,699	26,937	13,432	17,677	18,325	6,301	37,984	13,979
Controlled DG	Step 1	8,532	17,476	10,976	2,824	5,690	10,924	4,159	11,363
	Step 2	11,403	20,307	12,474	4,340	7,321	11,298	8,053	13,026
	Step 3	14,188	23,035	13,888	5,824	8,894	11,650	11,833	14,627
	Step 4	16,879	25,643	15,208	7,273	10,406	11,973	15,491	16,154

Table 4.2 Receiving active power values of lines for all steps (15 m/s) [kW].

Case		L 0-2	L 2-3	L 3-5	L 0-1	L 1-2	L 3-4	L 1-4	L 4-6
Normal	Step 1	25,103	20,335	10,035	13,403	14,406	5,559	28,372	10,238
	Step 2	27,374	22,575	11,235	14,827	15,632	5,814	31,372	11,530
	Step 3	29,502	24,654	12,325	16,187	16,774	6,044	34,173	12,723
	Step 4	31,494	26,581	13,311	17,486	17,838	6,251	36,786	13,822
Controlled DG	Step 1	8,464	17,353	10,913	2,819	5,654	10,807	4,148	11,281
	Step 2	11,281	20,136	12,388	4,330	7,260	11,167	8,010	12,914
	Step 3	14,000	22,811	13,777	5,806	8,804	11,504	11,742	14,482
	Step 4	16,612	25,359	15,070	7,243	10,283	11,812	15,334	15,973

4.2.2 Speed 10 m/s

Figure 4.50 shows a comparison between normal and controlled DG cases in terms of total power losses for speed 10 m/s. For this speed we see also that the controller is capable to decrease total power losses. The total power losses decreased to about (0.98 MW - 2.22 MW) with reduction rate ranges between (41% to 52%). Tables 4.3 and 4.4 show active power for sending and receiving ends for speed 10 m/s.

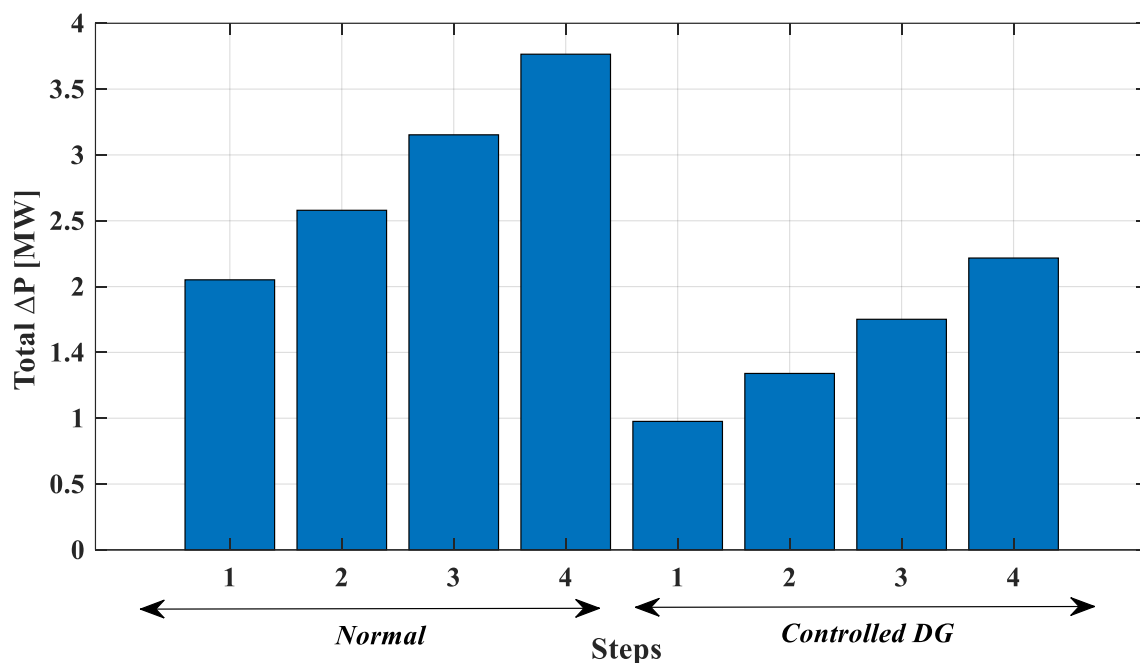


Figure 4.50 Total power losses comparison between (normal) and (controlled DG) cases (10 m/s).

Table 4.3 Sending active power values of lines for all steps (10 m/s) [kW].

Case		L 0-2	L 2-3	L 3-5	L 0-1	L 1-2	L 3-4	L 1-4	L 4-6
Normal	Step 1	25,789	20,517	10,093	13,509	14,686	5,594	28,999	10,313
	Step 2	28,222	22,810	11,313	14,959	15,977	5,854	32,174	11,630
	Step 3	30,523	24,947	12,424	16,348	17,188	6,090	35,166	12,850
	Step 4	32,699	26,937	13,432	17,677	18,325	6,301	37,984	13,979
Controlled DG	Step 1	16,979	19,507	10,917	7,637	10,311	8,733	16,465	11,293
	Step 2	19,876	22,315	12,404	9,173	11,950	9,106	20,398	12,942
	Step 3	22,691	25,023	13,806	10,678	13,535	9,458	24,226	14,531
	Step 4	25,434	27,631	15,125	12,154	15,075	9,783	27,970	16,058

Table 4.4 Receiving active power values of lines for all steps (10 m/s) [kW].

Case		L 0-2	L 2-3	L 3-5	L 0-1	L 1-2	L 3-4	L 1-4	L 4-6
Normal	Step 1	25,103	20,335	10,035	13,403	14,406	5,559	28,372	10,238
	Step 2	27,374	22,575	11,235	14,827	15,632	5,814	31,372	11,530
	Step 3	29,502	24,654	12,325	16,187	16,774	6,044	34,173	12,723
	Step 4	31,494	26,581	13,311	17,486	17,838	6,251	36,786	13,822
Controlled DG	Step 1	16,712	19,357	10,853	7,603	10,192	8,651	16,286	11,211
	Step 2	19,510	22,114	12,318	9,125	11,790	9,012	20,125	12,831

	Step 3	22,215	24,764	13,696	10,613	13,330	9,351	23,840	14,387
	Step 4	24,834	27,308	14,988	12,070	14,819	9,660	27,455	15,877

4.2.3 Speed 5 m/s

In figure 4.51 we can notice total power losses comparison between normal and controlled DG cases for wind speed 5 m/s. In this speed we can also notice that total power losses decreased for all steps to about (1.96 MW - 3.63 MW) whereas the reduction percentage is (3.4% to 4.3%). Tables 4.5 and 4.6 show active power for sending and receiving ends for speed 5 m/s.

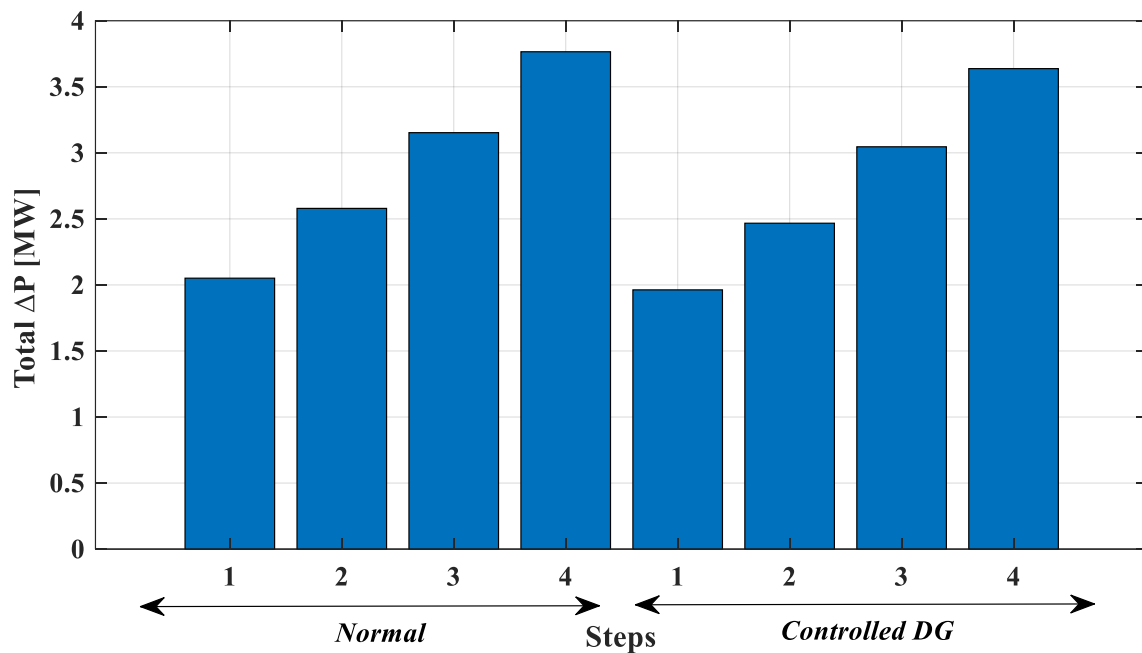


Figure 4.51 Total power losses comparison between (normal) and (controlled DG) cases (5 m/s).

Table 4.5 Sending active power values of lines for all steps (5 m/s) [kW].

Case		L 0-2	L 2-3	L 3-5	L 0-1	L 1-2	L 3-4	L 1-4	L 4-6
Normal	Step 1	25,789	20,517	10,093	13,509	14,686	5,594	28,999	10,313
	Step 2	28,222	22,810	11,313	14,959	15,977	5,854	32,174	11,630
	Step 3	30,523	24,947	12,424	16,348	17,188	6,090	35,166	12,850
	Step 4	32,699	26,937	13,432	17,677	18,325	6,301	37,984	13,979
Controlled DG	Step 1	26,111	21,713	10,828	12,896	15,264	6,301	29,873	11,189
	Step 2	29,038	24,315	12,300	14,379	16,951	6,853	33,547	12,822
	Step 3	31,853	27,127	13,683	15,935	18,508	7,057	37,641	14,384
	Step 4	34,540	29,775	14,990	17,421	19,994	7,322	41,439	15,894

Table 4.6 Receiving active power values of lines for all steps (5 m/s) [kW].

Case		L 0-2	L 2-3	L 3-5	L 0-1	L 1-2	L 3-4	L 1-4	L 4-6
Normal	Step 1	25,103	20,335	10,035	13,403	14,406	5,559	28,372	10,238
	Step 2	27,374	22,575	11,235	14,827	15,632	5,814	31,372	11,530

	Step 3	29,502	24,654	12,325	16,187	16,774	6,044	34,173	12,723
	Step 4	31,494	26,581	13,311	17,486	17,838	6,251	36,786	13,822
Controlled DG	Step 1	25,475	21,529	10,765	12,800	15,002	6,250	29,283	11,108
	Step 2	28,255	24,077	12,216	14,260	16,630	6,790	32,799	12,712
	Step 3	30,907	26,826	13,574	15,790	18,122	6,982	36,699	14,242
	Step 4	33,433	29,405	14,854	17,248	19,544	7,234	40,303	15,716

4.2.3 Fault Line 2-3 (speed 5 m/s)

Figure 4.52 shows comparison between normal and controlled DG cases in terms of total power losses for (fault line 2-3, 5 m/s). In the shown results, we can see a slight increase in power losses where total power losses increased (2.9 MW – 5.13 MW) to (3 MW - 5.6 MW). This increase happened due to the high injected reactive power in the network to regulate voltage for all busbars and keep it close to the nominal values. The high generated reactive power is due to the high voltage variations for busbars. Tables 4.7 and 4.8 show active power for sending and receiving ends for fault line 2-3 and speed 5 m/s.

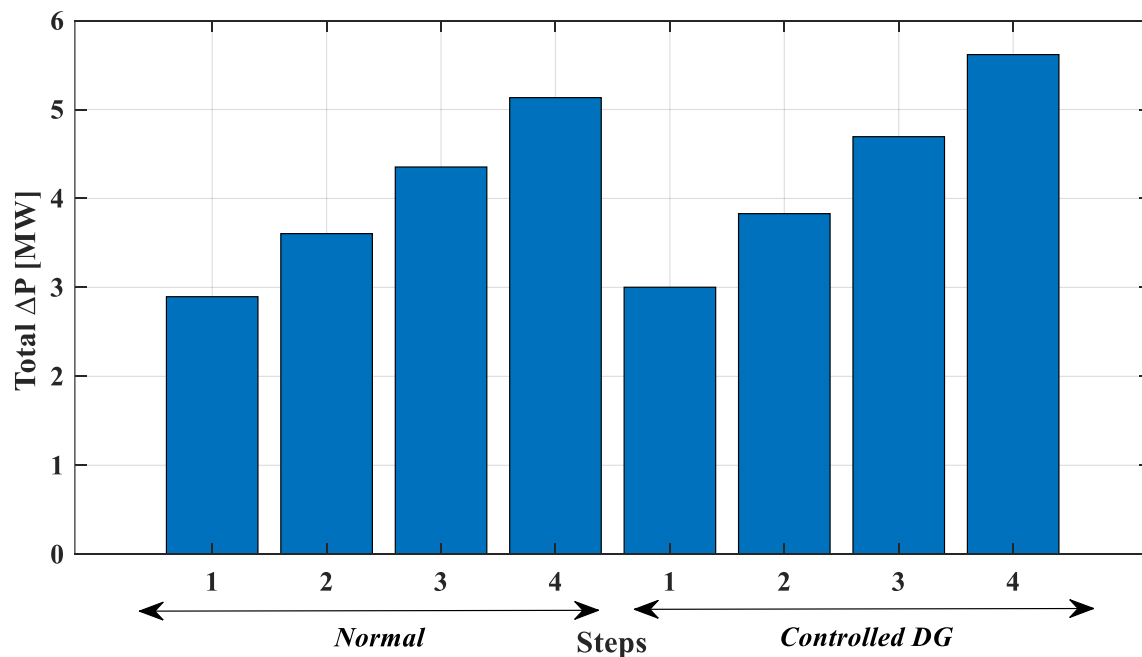


Figure 4.52 Total power losses comparison between (normal) and (controlled DG) cases (fault line 2-3, 5 m/s).

Table 4.7 Sending active power values of lines for all steps (fault line 2-3, 5 m/s) [kW].

Case		L 0-2	L 2-3	L 3-5	L 0-1	L 1-2	L 3-4	L 1-4	L 4-6
Normal	Step 1	15,585	-	8,828	17,142	4,405	23,300	46,403	9,704
	Step 2	16,866	-	9,624	18,858	4,607	24,949	50,779	10,815
	Step 3	18,090	-	10,286	20,461	4,818	26,365	54,744	11,815
	Step 4	19,260	-	10,829	21,959	5,035	27,572	58,335	12,714
Controlled DG	Step 1	15,519	-	10,086	16,899	4,389	26,620	50,745	11,087
	Step 2	17,359	-	11,265	19,059	4,804	29,205	57,420	12,660

	Step 3	18,844	-	12,333	21,033	5,014	31,611	63,590	14,167
	Step 4	20,482	-	13,311	22,927	5,387	33,890	69,523	15,628

Table 4.8 Receiving active power values of lines for all steps (fault line 2-3, 5 m/s) [kW].

Case		L 0-2	L 2-3	L 3-5	L 0-1	L 1-2	L 3-4	L 1-4	L 4-6
Normal	Step 1	15,334	-	8,777	16,969	4,377	22,648	44,733	9,634
	Step 2	16,565	-	9,558	18,644	4,576	24,151	48,678	10,722
	Step 3	17,736	-	10,204	20,203	4,783	25,415	52,186	11,698
	Step 4	18,850	-	10,731	21,655	4,996	26,469	55,300	12,572
Controlled DG	Step 1	15,270	-	10,027	16,733	4,359	25,875	49,073	11,006
	Step 2	17,042	-	11,188	18,849	4,765	28,269	55,279	12,551
	Step 3	18,463	-	12,234	20,778	4,966	30,473	60,958	14,026
	Step 4	20,034	-	13,190	22,626	5,329	32,534	66,366	15,452

4.5 Results Summary

From the results that we are obtained in the four cases above, we can figure out the following:

1. The controller played a vital role in improving voltage profile by reducing voltage deviation and voltage drop through reactive power generation control in all four cases.
2. When the drawn active and reactive load increases, the controller helped to achieve more stabilized voltage by narrowing the range of changes of voltage values in all cases.
3. The results of sending and receiving $\cos(\varphi)$ values after using the controller are better than the normal case.
4. The controller shows high efficiency for all the mesh grid parts including the radial ones.
5. The shown results prove that the controlled DG case is far better than the DG case and the normal one.
6. Low wind speed values led to a decrease in the capability of improving voltage profile and $\cos(\varphi)$ in both controlled DG and DG cases but the effect on controlled DG is very small with respect to the DG case which is very obvious in the case of speed 5 m/s.
7. The fault in the fourth case with low wind speed value (5 m/s) has big influence on the voltage deviation, voltage drop and $\cos(\varphi)$. The fault causes a high increase in voltage deviation and voltage drop. Also, it led to get low $\cos(\varphi)$ values.
8. The controller shows high efficiency in improving voltage profile and mitigating the negative effects of the fault even when the loads are high.
9. During the fault, the DG units could not reduce voltage deviation and voltage drop as needed. The slight improvement in the DG case with respect to the normal case was not sufficient.
10. The designed controller is a trustable and effective where shown results prove its capability in different cases from high speeds to low speeds and faults.

By comparing our method with [119], we can figure out the following:

1. Our method takes into account the distance between DG units and loads in addition to voltage deviations which means that each DG units will supply closer loads in effective

way more than far loads while this method uses only voltage values therefore the generation will be the same for close or far lines.

2. Our method could be used for one or more DG units while this method couldn't be used when there are many DG units because it will generate the same value of reactive power.
3. Our method couldn't lead to over voltage because the generation is related to the closer loads while this method could lead to over voltage at the node of injection because it the impact of voltage value for far transmission lines is the same like closer ones. Therefore, in case of high reactive loads or faults, this method will cause over voltage at the node of injection.

And if we compared our method with the used method in [120], we can find out that:

1. Our method works well and effective in decreasing voltage deviations even during line faults while this method doesn't work in such conditions where the voltage deviations increased.
2. Our method can adapt with the changes in the system topology (adding new loads or DG units) and loads changes as it will generate new values according the new values of admittance and voltage variations while any change in the topology of the system or big changes in power flow or faults will require new position of the STATCOM device.
3. In our method the reactive power generation will come from various DG units which means that it will not cause overloading of transmission lines while this method requires a very high reactive power injection (about 200 MVar) in one node which could cause overloading of the transmission.

Chapter 5

5 Conclusion

Renewable energy sources become an essential part of modern grids which leads to transformation from centralized generation to distributed generation. The high complexity of such grids and the increased needs to improve power quality is steering more research for more robust control of the DG units to achieve best performance.

DG units could be equipped with full scale converter, so they are capable to generate reactive power separately from active power which means that they can be used as a voltage control tool. DG units could be connected to the grid in many positions and new units could be added in the future. The topology of the electrical grid could be changed also by adding new loads or lines. The continues changes of consumed active and reactive power makes voltage control more complicated and this requires more robust control algorithm [118].

The designed controller uses the admittance matrix between each DG unit and all loads in addition to the voltage variation values as inputs of the controller. The controller is tested in four cases that include different wind speeds and fault occurrence. From these results, following points could be concluded [118]:

- The proposed control method is efficient at improving the voltage quality and power factor for mesh grids where we had significant improvements in the voltage variation for busbars, the variation of sending and receiving voltage, voltage drop, sending and receiving $\cos(\varphi)$.
- Using this method, we reduced voltage drops and, therefore, the power losses and the costs have been reduced too.
- Power flow through the lines has been reduced, which allows us to add new loads or to extend the distribution system.
- We can also conclude that it is important to use the admittance values between DG units and loads in order to coordinate the share of DG units in reactive power generation to maximize the benefits for all busbars and lines.
- It is also noticeable that the controller was efficient even for the busbars which are connected to the radial transmission lines.
- The shown results prove that the controller is effective in various cases even when there is a faults or low wind speed at the same time.
- Despite the fact that the improvements made in the voltage quality and power factor were more noticeable for the busbars and lines connected to the DG units, we had significant positive impacts on the remaining busbars and lines.
- The enormous advantage of this controller is that it uses admittance and voltage variation values as inputs, which makes it very efficient when we have load changes, faults, or any other unexpected case. Therefore, we obtain a better voltage quality and power factor in every case.

- Further, we can conclude the importance of DG units in improving the reliability of the electrical grid and improving the power quality of it [118].

This research can be used to design the control system of DG units, especially when we have many DG units in a small area. It could also be used as the core of a technique which is suitable to be used by distributed systems operators of radial, loop, and mesh grids [118].

Chapter 6

6 Literatures

6.1 References

- [1] European Commission, Roadmap, E., 2050., Brussels, 2011, pp. 1-20.
- [2] International Energy Agency. World Energy Outlook: Executive Summary, 2012, pp. 1-9.
- [3] <https://www.iea.org/>
- [4] International Energy Agency, Distributed generation in liberalised electricity markets. OECD Publishing, 2002.
- [5] Elmubarak, E.S. and Ali, A.M. Distributed generation: definitions, benefits, technologies & challenges. *Int. J. Sci. Res.(IJSR)*, Volume 5, 2016.
- [6] Fandi, G., Krepl, V., Ahmad, I., Igbinoia, F., Ivanova, T., Fandie, S., Muller, Z. and Tlusty, J. Design of an Emergency Energy System for a City Assisted by Renewable Energy, Case Study: Latakia, Syria. *Energies*, Volume 11, 2018, <https://doi.org/10.3390/en11113138>.
- [7] Shaw-Williams, D.; Susilawati, C.; Walker, G. Value of residential investment in photovoltaics and batteries in networks: A techno-economic analysis. *Energies*, Volume 11, 2018, <https://doi.org/10.3390/en11041022>.
- [8] Ghanbari, N.; Mokhtari, H.; Bhattacharya, S. Optimizing Operation Indices Considering Different Types of Distributed Generation in Microgrid Applications. *Energies*, Volume 11, 2018, <https://doi.org/10.3390/en11040894>.
- [9] Bhullar, S.; Ghosh, S. Optimal Integration of Multi Distributed Generation Sources in Radial Distribution Networks Using a Hybrid Algorithm. *Energies*, Volume 11, 2018, <https://doi.org/10.3390/en11030628>.
- [10] Doğanşahin, K.; Kekezoğlu, B.; Yumurtacı, R.; Erdiñç, O.; Catalão, J.P. Maximum Permissible Integration Capacity of Renewable DG Units Based on System Loads. *Energies*, Volume 11, 2018, <https://doi.org/10.3390/en11010255>.
- [11] El-Khattam, W. and Salama, M.M. Distributed generation technologies, definitions and benefits. *Electric power systems research*, 2004, Volume 71, pp.119-128.
- [12] European Commission, European technology platform smart grids: vision and strategy for Europe's electricity networks of the future, 2006.
- [13] Agarwal, V. and Tsoukalas, L.H. Smart grids: importance of power quality. In *International Conference on Energy-Efficient Computing and Networking*, Springer, Berlin, Heidelberg, 2010, pp. 136-143.
- [14] Prathibha, E. and Manjunath, A. An overview of power quality issues in smart grid. Dept., *International Journal of Innovative Research in Advanced Engineering (IJIRAE)*, Volume 1, 2014.
- [15] Saxena, D., Verma, K. and Singh, S. Power quality event classification: an overview and key issues. *International Journal of Engineering, Science and Technology*, 2010, Volume 2, pp.186-199.
- [16] Carriveau, R. *Advances in wind power*. IntechOpen Limited: London, UK, 2012.
- [17] Salman, S.K., 2017. *Introduction to the Smart Grid: Concepts, Technologies and Evolution* (Vol. 94). IET.
- [18] https://www.smartgrid.gov/files/Smart_grid_101_Everything_you_wanted_to_know_about_grid_mode_201112.pdf
- [19] Zeadally, S., Pathan, A.S.K., Alcaraz, C. and Badra, M., 2013. Towards privacy protection in smart grid. *Wireless personal communications*, 73(1), pp.23-50

- [20] Cespedes, R., Parra, E., Aldana, A. and Torres, C., 2010, November. Evolution of power to smart energy systems. In *2010 IEEE/PES Transmission and Distribution Conference and Exposition: Latin America (T&D-LA)* (pp. 616-621). IEEE.
- [21] https://www-pub.iaea.org/MTCD/Publications/PDF/TRS394_scr.pdf
- [22] KEMA research and analysis; U.S. Utilities: The implications of Carbon Legislation, Bernstein Research, October 2007, Scoping Plan, California Air Resources Board, Insights from Modeling Analyses of the Lieberman-Warner Climate Security Act (S. 2191) Pew Center for Global Climate Change.
- [23] <https://www.epa.gov/ghgemissions/global-greenhouse-gas-emissions-data>
- [24] https://www.ipcc.ch/site/assets/uploads/2018/02/ipcc_wg3_ar5_full.pdf.
- [25] Green Paper “Towards a European strategy for security of energy supply” European Communities 2001
- [26] Buchholz, B.M. and Styczynski, Z., 2014. *Smart grids-fundamentals and technologies in electricity networks* (Vol. 396). Heidelberg: Springer.
- [27] https://de.wikipedia.org/wiki/Fossile_Energie#Vorr.C3.A4tehttps://www.leifiphysik.de/themenbereiche/energieentwertung/ausblick#Reichweite
- [28] www.leifiphysik.de/themenbereiche/energieentwertung/ausblick#Reichweite
- [29] Makkonen H., Tikka V., Kaipia T., Lassila J., Partanen J., and Silventoinen P. Green Campus – Smart Grid [Online]. Available from http://www.google.co.uk/url?sa=t&rct=j&q=&esrc=s&frm=1&source=web&cd=1&ved=0CDEQFjAA&url=http%3A%2F%2Fwww.cleen.fi%2Fen%2FSitePages%2Fpublicdeliverables.aspx%3FfileId%3D1677%26webpartid%3Dg_e6ff1fc0_9a9440af_8aae_e1274f853ff6&ei=_K5vUvy3CYXwhQeC54HICg&usg=AFQjCNGT4o42-SJSpmY3Lf2A_AaPuBcFg&bvm=bv.55123115,d.d2k
- [30] Hashmi M. Survey of smart grids concepts worldwide [Online]. Finland: VTT Technical Research Centre of Finland; 2011. Available from <http://www.vtt.fi/inf/pdf/workingpapers/2011/W166.pdf>
- [31] Silberman S. *The energy web* [Online]. *Wired Magazine*. July 2001. Available from http://www.wired.com/wired/archive/9.07/juice_pr.html
- [32] Utility Standard board. *Smart Grid: interoperability and standards – an introductory review* [Online]. 2008. Available from http://xanthus-consulting.com/Publications/documents/Smart_Grid_Interoperability_and_Standards_White_Paper.pdf
- [33] Johnson A.P. ‘The history of the Smart Grid evolution at Southern California Edison’. *IEEE Conference on Innovative Smart Grid Technologies (ISGT)*; Gaithersburg, MD, 2010, pp. 1–3
- [34] European Commission (European Technology Platform). *SmartGrids: vision and strategy for Europe’s electricity networks of the future* [Online]. 2006. Available from http://ec.europa.eu/research/energy/pdf/smartgrids_en.pdf
- [35] European Technology Platform SmartGrids. *Strategic research agenda for Europe’s electricity networks of the future* [Online]. 2007. Available from ftp://ftp.cordis.europa.eu/pub/fp7/energy/docs/smartgrids_agenda_en.pdf
- [36] European Technology Platform. *SmartGrids: strategic deployment document for Europe’s electricity networks of the future* [Online]. 2010. Available from http://www.smartgrids.eu/documents/SmartGrids_SDD_FINAL_APRIL2010.Pdf.

- [37] Hashmi M. *Survey of smart grids concepts worldwide* [Online]. Finland: VTT Technical Research Centre of Finland; 2011. Available from <http://www.vtt.fi/inf/pdf/workingpapers/2011/W166.pdf>
- [38] Li J. *From strong to smart: the Chinese Smart Grid and its relation with the globe* [Online]. Asia Energy Platform – Article 00018602; 2009. Available from http://assets.fiercemarkets.net/public/smartgridnews/AEPN_Sept.pdf
- [39] Zpryme Research & Consulting. *China: rise of the smart grid – special report by Zpryme’s smart grid insights* [Online]. 2011. Available from https://www.smartgrid.gov/files/China_Rise_Smart_Grid_201103.pdf
- [40] IEEE. *China’s strengthened smart grid* [Online]. Available from <http://www.smartgrid.ieee.org/resources/public-policy/china>
- [41] Bipath M. *Proposed smart grid vision for South Africa* [Online]. 2012. Available from <http://africasmartgridforum2014.org/fr/expert/sessionb2/minnesh-bipath-sg-vision-presentation-to-the-asgf-en.pdf>
- [42] EU. *Background – SmartGrids: European technology platform* [Online]. Available from <http://www.smartgrids.eu/?q¼node/27>
- [43] U.S. Government. *H.R. 6 (110th): US Energy Independence and Security Act of 2007* [Online]. 2007. Available from <http://www.gpo.gov/fdsys/pkg/BILLS-110hr6enr/pdf/BILLS-110hr6enr.pdf>
- [44] Utility Standard Board. *Smart grid: interoperability and standards – an introductory review* [Online]. 2008. Available from http://xanthus-consulting.com/Publications/documents/Smart_Grid_Interoperability_and_Standards_White_Paper.pdf
- [45] ABB. *Towards a Smarter Grid, ABB’s vision for the power system of the future* [Online]. USA: ABB Inc. Report; 2009. Available from http://www02.abb.com/db/db0003/db002698.nsf/0/e30fc9d5f79d4ae8c12579e2002a4209/%24file/Toward_a_smarter_grid_Julþ09.pdf [Accessed 27 October 2015]
- [46] S. M. Amin and B. F. Wollenberg, “Toward a smart grid: power delivery for the 21st century,” *IEEE Power and Energy Magazine*, vol. 3, no. 5, pp. 34–41, Sep./Oct. 2005.
- [47] European Commission. *European smart grids technology platform: vision and strategy for Europe’s electricity networks of the future.* [Online]. Available: http://ec.europa.eu/research/energy/pdf/smartgrids_en.pdf.
- [48] U.S. National Energy Technology Laboratory. *Modern grid initiative: a vision for modern grid.* [Online]. Available: http://www.bpa.gov/energy/n/smart_grid/docs/Vision_for_theModernGrid_Final.pdf.
- [49] Zhou, J., He, L., Li, C., Cao, Y., Liu, X. and Geng, Y., 2013, December. What's the difference between traditional power grid and smart grid?—From dispatching perspective. In *2013 IEEE PES Asia-Pacific Power and Energy Engineering Conference (APPEEC)* (pp. 1-6). IEEE.
- [50] H. Farhangi, “The path of the smart grid,” *IEEE Transactions on Power and Energy*, vol. 8, no. 1, pp. 18-28, Feb. 2010.
- [51] Jain, A. and Mishra, R., 2016, December. Changes & challenges in smart grid towards smarter grid. In *2016 International Conference on Electrical Power and Energy Systems (ICEPES)* (pp. 62-67). IEEE.
- [52] Potocnik, J., 2006. *European technology platform smart grids: vision and strategy for Europe’s electricity networks of the future.*

- [53] Greer, C., Wollman, D.A., Prochaska, D.E., Boynton, P.A., Mazer, J.A., Nguyen, C.T., FitzPatrick, G.J., Nelson, T.L., Koepke, G.H., Hefner Jr, A.R. and Pillitteri, V.Y., 2014. Nist framework and roadmap for smart grid interoperability standards, release 3.0 (No. Special Publication (NIST SP)-1108r3).
- [54] NIST. NIST framework and roadmap for smart grid interoperability standards [Online]. 2010. Available from http://www.nist.gov/public_affairs/
- [55] Crape, M. ed., 2013. Electric power systems. John Wiley & Sons.
- [56] R. DE VRÉ, B. JACQUET, A. ROBERT, “Perturbations dans les installations électriques et électroniques Problèmes et solutions” (Disturbances in the electrical and electronic facilities – problems and solutions), Laborelec, Information note 52-4, August 1990.
- [57] <https://pdfs.semanticscholar.org/b80c/d53b4660dedf83fb6a928d7cba42c29433e1.pdf>
- [58] ETG-Task-Force: Versorgungsqualität im deutschen Stromversorgungssystem. Studie der Energietechnischen Gesellschaft im VDE (ETG), Frankfurt, Juli 2005
- [59] www.energy-regulators.eu
- [60] EN 50160:2011-02. Voltage characteristics of electricity supplied by public distribution networks.
- [61] Dugan, R.C., McGranaghan, M.F., Beaty, H.W. and Santoso, S., 1996. Electrical power systems quality.
- [62] IEEE Standard 100-1992, IEEE Standard Dictionary of Electrical and Electronic Terms.
- [63] Jenkins, N., Ekanayake, J.B. and Strbac, G., 2010. Distributed Generation, London, UK: Inst. Eng. Technol.
- [64] Momoh, J.A., 2017. Electric power distribution, automation, protection, and control. CRC press.
- [65] REN21. (Jan. 2017). Renewables 2016: Global Status Report (GSR). [Online]. Available: <http://www.ren21.net/>
- [66] Arefi, A., Shahnia, F. and Ledwich, G. eds., 2018. Electric distribution network management and control. Springer.
- [67] Blaabjerg, F. and Ma, K., 2017. Wind energy systems. Proceedings of the IEEE, 105(11), pp.2116-2131.
- [68] IRENA. (Jan. 2015). Renewable Power Generation Costs in 2014. [Online]. Available: <http://www.irena.org/>
- [69] GWEC. (Feb. 2017). Global Wind Statistics 2016. [Online]. Available: www.gwec.net
- [70] B. Wu, Y. Lang, N. Zargari, S. Kouro, Power Conversion and Control of Wind Energy Systems (Wiley, 2011).
- [71] (Jan. 2017). Website of MHI Vestas Offshore Wind. [Online]. Available: <http://www.mhivestasoffshore.com/>
- [72] UpWind Project. (Mar. 2011). Design Limits and Solutions for Very Large Wind Turbines. [Online]. Available: http://www.ewea.org/fileadmin/ewea_documents/documents/upwind/21895_UpWind_Report_low_web.pdf.
- [73] Fortmann, J., 2014. Modeling of wind turbines with doubly fed generator system. Springer.
- [74] Precup, R.E., Kamal, T. and Hassan, S.Z. eds., 2019. Advanced Control and Optimization Paradigms for Wind Energy Systems. Springer.

- [75] Clark K, Miller NW, Sanchez-Gasca JJ (2010) Modeling of GE wind turbine-generators for grid studies. Report, General Electric International, Inc., Apr 2010.
- [76] Tsourakis G, Nomikos BM, Vournas CD (2009) Effect of wind parks with doubly fed asynchronous generators on small-signal stability. *Electr Power Syst Res* 79(1):190–200
- [77] Errami, Y., Benchagra, M., Hilal, M., Maaroufi, M. and Ouassaid, M., 2012, May. Control strategy for PMSG wind farm based on MPPT and direct power control. In 2012 International Conference on Multimedia Computing and Systems (pp. 1125-1130). IEEE.
- [78] Di Tommaso, AO, Miceli, R, Galluzzo, G.R, Trapanese, M, "Optimum performance of permanent magnet synchronous generators coupled to wind turbines," Power Engineering Society General Meeting, IEEE, pp. I -7, 2007.
- [79] I. Erlich, J. Kretschmann, J. Fortmann, S. Engelhardt and H. Wrede, "Modeling of Wind Turbines based on Doubly-Fed Induction Generators for Power System Stability Studies", *IEEE Transactions on Power Systems*, Volume 22, Issue 3, Aug. 2007 Page(s):909 – 919
- [80] Timbus, A., Liserre, M., Teodorescu, R., Rodriguez, P. and Blaabjerg, F., 2009. Evaluation of current controllers for distributed power generation systems. *IEEE Transactions on power electronics*, 24(3), pp.654-664.
- [81] S. Fukuda and T. Yoda, "A novel current-tracking method for active filters based on a sinusoidal internal model", *IEEE Trans. Ind. Electron.*, vol. 37, no. 3, pp. 888-895, May/Jun. 2001.
- [82] Y. Sato, T. Ishizuka, K. Nezu and T. Kataoka, "A new control strategy for voltage-type PWM rectifiers to realize zero steady-state control error in input current", *IEEE Trans. Ind. Appl.*, vol. 34, no. 3, pp. 480-486, May/Jun. 1998.
- [83] X. Yuan, W. Merk, H. Stemmler and J. Allmeling, "Stationary-frame generalized integrators for current control of active power filters with zero steady-state error for current harmonics of concern under unbalanced and distorted operating conditions", *IEEE Trans. Ind. Appl.*, vol. 38, no. 2, pp. 523-532, Mar./Apr. 2002.
- [84] R. Teodorescu, F. Blaabjerg, U. Borup and M. Liserre, "A new control structure for grid-connected LCL PV inverters with zero steady-state error and selective harmonic compensation", *Proc. IEEE APEC 2004*, vol. 1, pp. 580-586.
- [85] R. Teodorescu and F. Blaabjerg, "Proportional-resonant controllers. A new breed of controllers suitable for grid-connected voltage-source converters", *Proc. OPTIM 2004*, vol. 3, pp. 9-14.
- [86] A. V. Timbus, M. Ciobotaru, R. Teodorescu and F. Blaabjerg, "Adaptive resonant controller for grid-connected converters in distributed power generation systems", *Proc. IEEE APEC 2006*, pp. 1601-1606.
- [87] M. Kazmierkowski and M. Dzieniakowski, "Review of current regulation methods for VS-PWM inverters", *Proc. ISIE 1993*, pp. 448-456.
- [88] S. Buso, L. Malesani and P. Mattavelli, "Comparison of current control techniques for active filter applications", *IEEE Trans. Ind. Electron.*, vol. 45, no. 5, pp. 722-729, Oct. 1998.
- [89] D. N. Zmood, D. G. Holmes and G. H. Bode, "Frequency-domain analysis of three-phase linear current regulators", *IEEE Trans. Ind. Appl.*, vol. 37, no. 2, pp. 601-610, Mar./Apr. 2001.
- [90] E. Twining and D. G. Holmes, "Grid current regulation of a three-phase voltage source inverter with an LCL input filter", *IEEE Trans. Power Electron.*, vol. 18, no. 3, pp. 888-895, May 2003.

- [91] S. Buso, S. Fasolo and P. Mattavelli, "Uninterruptible power supply multi-loop control employing digital predictive voltage and current regulators", Proc. IEEE APEC 2001, vol. 2, pp. 907-913.
- [92] Y. Ito and S. Kawauchi, "Microprocessor based robust digital control for UPS with three-phase PWM inverter", IEEE Trans. Power Electron., vol. 10, no. 2, pp. 196-204, Mar. 1995.
- [93] T. Kawabata, T. Miyashita and Y. Yamamoto, "Dead beat control of three phase PWM inverter", IEEE Trans. Power Electron., vol. 5, no. 1, pp. 21-28, Jan. 1990.
- [94] J. Kolar, H. Ertl and F. Zach, "Analysis of on- and off-line optimized predictive current controllers for PWM converter systems", IEEE Trans. Power Electron., vol. 6, no. 3, pp. 451-462, Jul. 1991.
- [95] P. Mattavelli, G. Spiazzi and P. Tenti, "Predictive digital control of power factor preregulators with input voltage estimation using disturbance observers", IEEE Trans. Power Electron., vol. 20, no. 1, pp. 140-147, Jan. 2005.
- [96] S.-G. Jeong and M.-H. Woo, "DSP-based active power filter with predictive current control", IEEE Trans. Ind. Electron., vol. 44, no. 3, pp. 329-336, Jun. 1997.
- [97] R. Wu, S. Dewan and G. Slemon, "Analysis of a PWM AC to DC voltage source converter under the predicted current control with a fixed switching frequency", IEEE Trans. Ind. Appl., vol. 27, no. 4, pp. 756-764, Jul./Aug. 1991.
- [98] K. Macken, K. Vanthournout, J. Van den Keybus, G. Deconinck and R. Belmans, "Distributed control of renewable generation units with integrated active filter", IEEE Trans. Power Electron., vol. 19, no. 5, pp. 1353-1360, Sep. 2004.
- [99] Blaabjerg, F. and Ma, K., 2013. Future on power electronics for wind turbine systems. IEEE Journal of emerging and selected topics in power electronics, 1(3), pp.139-152.
- [100] M. S. El-Moursi, B. Bak-Jensen, and M. H. Abdel-Rahman, "Novel STATCOM controller for mitigating SSR and damping power system oscillations in a series compensated wind park," IEEE Trans. Power Electron., vol. 25, no. 2, pp. 429-441, Feb. 2010.
- [101] J. Dai, D. D. Xu, and B. Wu, "A novel control scheme for currentsource-converter-based PMSG wind energy conversion systems," IEEE Trans. Power Electron., vol. 24, no. 4, pp. 963-972, Apr. 2009.
- [102] X. Yuan, F. Wang, D. Boroyevich, Y. Li, and R. Burgos, "DC-link voltage control of a full power converter for wind generator operating in weak-grid systems," IEEE Trans. Power Electron., vol. 24, no. 9, pp. 2178-2192, Sep. 2009.
- [103] P. Rodriguez, A. Timbus, R. Teodorescu, M. Liserre, and F. Blaabjerg, "Reactive power control for improving wind turbine system behavior under grid faults," IEEE Trans. Power Electron., vol. 24, no. 7, pp. 1798-1801, Jul. 2009.
- [104] A. Timbus, M. Liserre, R. Teodorescu, P. Rodriguez, and F. Blaabjerg, "Evaluation of current controllers for distributed power generation systems," IEEE Trans. Power Electron., vol. 24, no. 3, pp. 654-664, Mar. 2009.
- [105] M. Liserre, F. Blaabjerg, and S. Hansen, "Design and control of an LCLfilter-based three-phase active rectifier," IEEE Trans. Ind. Appl., vol. 41, no. 5, pp. 1281-1291, Sep./Oct. 2005.
- [106] P. Rodriguez, A. V. Timbus, R. Teodorescu, M. Liserre, and F. Blaabjerg, "Flexible active power control of distributed power generation systems during grid faults," IEEE Trans. Ind. Electron., vol. 54, no. 5, pp. 2583-2592, Oct. 2007.

- [107] R. Teodorescu, M. Liserre, and P. Rodriguez, *Grid Converters for Photovoltaic and Wind Power Systems*. New York, NY, USA: Wiley, 2011.
- [108] F. Blaabjerg, R. Teodorescu, M. Liserre, and A. V. Timbus, "Overview of control and grid synchronization for distributed power generation systems," *IEEE Trans. Ind. Electron.*, vol. 53, no. 5, pp. 1398–1409, Oct. 2006.
- [109] F. K. A. Lima, A. Luna, P. Rodriguez, E. H. Watanabe, and F. Blaabjerg, "Rotor voltage dynamics in the doubly fed induction generator during grid faults," *IEEE Trans. Power Electron.*, vol. 25, no. 1, pp. 118–130, Jan. 2010.
- [110] D. Santos-Martin, J. L. Rodriguez-Amendedo, and S. Arnaltes, "Providing ride-through capability to a doubly fed induction generator under unbalanced voltage dips," *IEEE Trans. Power Electron.*, vol. 24, no. 7, pp. 1747–1757, Jul. 2009.
- [111] Amaris, H., Alonso, M. and Ortega, C.A., 2013. Reactive Power Management. In *Reactive Power Management of Power Networks with Wind Generation* (pp. 97-115). Springer, London.
- [112] Anaya-Lara O, Jenkins N, Ekanayake J, Cartwright P, Hughes M (2011) *Wind energy generation: modelling and control*. Wiley, Chichester.
- [113] Hingorani NG, Gyugyi L (1999) *Understanding FACTS*. IEEE Press, New York.
- [114] Mithulananthan N, Canizares CA, Reeve J, Rogers GJ (2003) Comparison of PSS, SVC, and STATCOM controllers for damping power system oscillations. *IEEE Trans Power Syst* 18 (2):786–792.
- [115] Moore P, Ashmole P (1998) Flexible AC transmission systems. 4. Advanced FACTS controllers. *Power Eng J* 12(2):95–100.
- [116] Zhang X-P, Rehtanz C, Pal B (2006) *Flexible AC transmission systems: modelling and control*. Springer, Berlin.
- [117] Amaris H, Alonso M (2011) Coordinated reactive power management in power networks with wind turbines and FACTS devices. *Energy Convers Manage* 52(7):2575–2586.
- [118] Ahmad, I., Fandi, G., Muller, Z. and Tlustý, J., 2019. Voltage Quality and Power Factor Improvement in Smart Grids Using Controlled DG Units. *Energies*, 12(18), p.3433.
- [119] Fandi, G., 2017. *Intelligent Distribution Systems with Dispersed Electricity Generation*.
- [120] Tuzikova, V., *THE USE OF FACTS TECHNOLOGIES FOR MINIMIZING POWER LOSSES AND IMPROVEMENT OF POWER STABILITY IN ELECTRICAL GRIDS*.

6.2 Author's Publications

6.2.1 Publications in the Framework of the Thesis

6.2.1.1 Publications in Impact Factor Journals

1. Ahmad, I., Fandi, G., Muller, Z. and Tlustý, J., 2019. Voltage Quality and Power Factor Improvement in Smart Grids Using Controlled DG Units. *Energies*, 12(18), p.3433. (The shares of all co-authors are the same 25 %).
2. Igbinoia, F.O., Fandi, G., Ahmad, I., Muller, Z. and Tlustý, J., 2018. Modeling and simulation of the anticipated effects of the synchronous condenser on an electric-power network with participating wind plants. *Sustainability*, 10(12), p.4834. (The shares of all co-authors are the same 20 %).
3. Fandi, G., Ahmad, I., Igbinoia, F.O., Muller, Z., Tlustý, J. and Krepl, V., 2018. Voltage regulation and power loss minimization in radial distribution systems via reactive power injection and distributed generation unit placement. *Energies*, 11(6), p.1399. (The shares of all co-authors are the same 16.66 %).

6.2.1.2 Publications in Reviewed Journals

6.2.1.3 Patents

6.2.1.4 Publications in WoS and Scopus

1. Ahmad, I., Fandi, G., Müller, Z. and Tlustý, J., 2018, May. Improvement of voltage profile and mitigation of power losses in case of faults using DG units. In 2018 19th International Scientific Conference on Electric Power Engineering (EPE) (pp. 1-6). IEEE. (The shares of all co-authors are the same 25 %).
2. Fandi, G., Igbinoia, F.O., Ahmad, I., Svec, J. and Muller, Z., 2017, June. Modeling and simulation of a gearless variable speed wind turbine system with PMSG. In 2017 IEEE PES PowerAfrica (pp. 59-64). IEEE. (The shares of all co-authors are the same 20 %).

6.2.1.5 Publications are not in WoS and Scopus

1. AHMAD, I., 2018. Determination of Fault Location Effect on Voltage and Power Losses in Presence of DG Units. In Proceedings of the International Student Scientific Conference Poster–22/2018. Czech Technical University in Prague.
2. Fandi, G., Igbinoia, F.O. and Ahmad, I., 2018. Reactive power producing capability of wind turbine systems with IGBT power electronics converters. *Indian J. Eng*, 15, pp.198-208. (The shares of all co-authors are the same 33.33 %).

6.2.2 Other Publications

6.2.2.1 Publications in Impact Factor Journals

1. Fandi, G., Krepl, V., Ahmad, I., Igbinoia, F.O., Ivanova, T., Fandie, S., Muller, Z. and Tlustý, J., 2018. Design of an emergency energy system for a city assisted by

renewable energy, case study: Latakia, Syria. *Energies*, 11(11), p.3138. (The shares of all co-authors are the same 12.5 %).

6.2.2.2 Publications in Reviewed Journals

6.2.2.3 Patents

6.2.2.4 Publications in WoS and Scopus

6.2.2.5 Publications are not in WoS and Scopus

6.2.3 Submitted Publications

6.2.4 Awards

1. 1st place in the competition of ČEZ Group in June 2017

Chapter 7

7 Appendix

7.1 Transformers parameters

Table 7.1 Parameters of the three-phase 0.575/66 kV transformer of Wind farm A [118].

Transformer	Low Voltage Winding	High Voltage Winding
Connection type	Yg	Yg
V_{rms} (kV)	0.575	66
R (Ω)	1.749×10^{-5}	0.23048
L (H)	1.6705×10^{-6}	0.022009
Frequency f_n (Hz)	50	
Nominal Power S_n (MVA)	15.75	
Magnetization resistance R_m (Ω)	1.3829×10^5	
Magnetization inductance L_m (H)	Inf	

Table 7.2 Parameters of the three-phase 0.575/66 kV transformer of Wind farm B [118].

Transformer	Low Voltage Winding	High Voltage Winding
Connection type	Yg	Yg
V_{rms} (kV)	0.575	66
R (Ω)	1.0496×10^{-5}	0.13829
L (H)	1.0023×10^{-6}	0.013205
Frequency f_n (Hz)	50	
Nominal Power S_n (MVA)	26.25	
Magnetization resistance R_m (Ω)	82,971	
Magnetization inductance L_m (H)	Inf	

Table 7.3 Parameters of the three-phase 0.575/66 kV transformer of Wind farm A [118].

Transformer	Low Voltage Winding	High Voltage Winding
Connection type	Yg	Yg
V_{rms} (kV)	0.575	66
R (Ω)	7.4972×10^{-6}	0.098776
L (H)	7.1593×10^{-7}	0.0094324
Frequency f_n (Hz)	50	
Nominal Power S_n (MVA)	36.75	
Magnetization resistance R_m (Ω)	59,265	
Magnetization inductance L_m (H)	Inf	

7.2 Results for wind speed 15 m/s

Table 7.4 Voltage values of busbars for all steps and all cases (V) (15 m/s) [118].

Case	Bus 1	Bus 2	Bus 3	Bus 4	Bus 5	Bus 6
Normal Step 1	64,896	62,719	61,846	62,501	61,238	61,692

	Step 2	64,664	62,137	61,077	61,812	60,331	60,842
	Step 3	64,434	61,563	60,320	61,134	59,441	60,005
	Step 4	64,206	60,999	59,577	60,467	58,567	59,184
	Step 1	65,800	65,239	64,500	65,610	63,866	64,761
Controlled DG	Step 2	65,758	65,053	64,144	65,424	63,361	64,397
	Step 3	65,715	64,865	63,789	65,242	62,859	64,037
	Step 4	65,676	64,668	63,433	65,074	62,358	63,693
DG	Step 1	65,152	63,784	62,988	63,889	62,369	63,063
	Step 2	64,943	63,238	62,254	63,244	61,494	62,252
	Step 3	64,734	62,699	61,530	62,608	60,633	61,452
	Step 4	64,526	62,166	60,817	61,980	59,787	60,665

Table 7.5 Sending voltage values of lines for all steps and all cases (V) (15 m/s) [118].

Case		L 0-2	L 2-3	L 3-5	L 0-1	L 1-2	L 3-4	L 1-4	L 4-6
Normal	Step 1	65,630	62,719	61,846	65,630	64,896	62,501	64,896	62,501
	Step 2	65,542	62,137	61,077	65,542	64,664	61,812	64,664	61,812
	Step 3	65,454	61,563	60,320	65,454	64,434	61,134	64,434	61,134
	Step 4	65,366	60,999	59,577	65,366	64,206	60,467	64,206	60,467
Controlled DG	Step 1	65,939	65,239	64,500	65,939	65,800	65,610	65,800	65,610
	Step 2	65,932	65,053	64,144	65,932	65,758	65,424	65,758	65,424
	Step 3	65,923	64,865	63,789	65,923	65,715	65,242	65,715	65,242
	Step 4	65,913	64,668	63,433	65,913	65,676	65,074	65,676	65,074
DG	Step 1	65,663	63,784	62,988	65,663	65,152	63,889	65,152	63,889
	Step 2	65,586	63,238	62,254	65,586	64,943	63,244	64,943	63,244
	Step 3	65,508	62,699	61,530	65,508	64,734	62,608	64,734	62,608
	Step 4	65,430	62,166	60,817	65,430	64,526	61,980	64,526	61,980

Table 7.6 Receiving voltage values of lines for all steps and all cases (V) (15 m/s) [118].

Case		L 0-2	L 2-3	L 3-5	L 0-1	L 1-2	L 3-4	L 1-4	L 4-6
Normal	Step 1	62,719	61,846	61,238	64,896	62,719	61,846	62,501	61,692
	Step 2	62,137	61,077	60,331	64,664	62,137	61,077	61,812	60,842
	Step 3	61,563	60,320	59,441	64,434	61,563	60,320	61,134	60,005
	Step 4	60,999	59,577	58,567	64,206	60,999	59,577	60,467	59,184
Controlled DG	Step 1	65,239	64,500	63,866	65,800	65,239	64,500	65,610	64,761
	Step 2	65,053	64,144	63,361	65,758	65,053	64,144	65,424	64,397
	Step 3	64,865	63,789	62,859	65,715	64,865	63,789	65,242	64,037
	Step 4	64,668	63,433	62,358	65,676	64,668	63,433	65,074	63,693
DG	Step 1	63,784	62,988	62,369	65,152	63,784	62,988	63,889	63,063
	Step 2	63,238	62,254	61,494	64,943	63,238	62,254	63,244	62,252
	Step 3	62,699	61,530	60,633	64,734	62,699	61,530	62,608	61,452
	Step 4	62,166	60,817	59,787	64,526	62,166	60,817	61,980	60,665

Table 7.7 Voltage drop values of lines for all steps and all cases (V) (15 m/s) [118].

Case		L 0-2	L 2-3	L 3-5	L 0-1	L 1-2	L 3-4	L 1-4	L 4-6
Normal	Step 1	2,912	872	608	735	2,177	654	2,395	808
	Step 2	3,405	1,060	746	878	2,527	735	2,852	970

	Step 3	3,891	1,243	879	1,020	2,871	814	3,300	1,129
	Step 4	4,368	1,422	1,009	1,160	3,207	890	3,739	1,283
Controlled DG	Step 1	700	739	634	139	561	1,109	191	848
	Step 2	878	910	783	174	705	1,281	334	1,027
	Step 3	1,058	1,077	930	208	850	1,453	473	1,205
	Step 4	1,245	1,235	1,075	236	1,008	1,641	602	1,381
DG	Step 1	1,879	796	619	511	1,368	901	1,262	826
	Step 2	2,348	984	760	643	1,705	991	1,698	993
	Step 3	2,809	1,169	897	774	2,035	1,078	2,126	1,156
	Step 4	3,264	1,349	1,030	904	2,359	1,163	2,546	1,316

Table 7.8 Sending $\cos(\phi)$ values of lines for all steps and all cases (15 m/s) [118].

Case		L 0-2	L 2-3	L 3-5	L 0-1	L 1-2	L 3-4	L 1-4	L 4-6
Normal	Step 1	0.9585	0.9751	0.9641	0.9892	0.9536	0.9821	0.9519	0.9489
	Step 2	0.9454	0.9636	0.9493	0.9821	0.9393	0.9729	0.9374	0.9363
	Step 3	0.9329	0.9529	0.9358	0.9748	0.9258	0.9633	0.9242	0.9253
	Step 4	0.9211	0.9430	0.9235	0.9675	0.9132	0.9535	0.9120	0.9155
Controlled DG	Step 1	0.9981	0.9721	0.9641	0.9999	1.0000	0.9832	0.9978	0.9489
	Step 2	0.9985	0.9634	0.9493	0.9988	0.9997	0.9696	0.9987	0.9363
	Step 3	0.9984	0.9558	0.9358	0.9982	0.9992	0.9541	0.9992	0.9253
	Step 4	0.9979	0.9488	0.9235	0.9982	0.9984	0.9378	0.9998	0.9155
DG	Step 1	0.6992	0.9545	0.9641	0.6217	0.7561	0.9971	0.2613	0.9489
	Step 2	0.7221	0.9402	0.9493	0.7018	0.7562	0.9943	0.4395	0.9363
	Step 3	0.7330	0.9280	0.9358	0.7416	0.7536	0.9910	0.5280	0.9253
	Step 4	0.7376	0.9172	0.9235	0.7636	0.7495	0.9873	0.5767	0.9156

Table 7.9 Receiving $\cos(\phi)$ values of lines for all steps and all cases (15 m/s) [118].

Case		L 0-2	L 2-3	L 3-5	L 0-1	L 1-2	L 3-4	L 1-4	L 4-6
Normal	Step 1	0.9644	0.9755	0.9541	0.9840	0.9401	0.9370	0.9593	0.9353
	Step 2	0.9554	0.9655	0.9408	0.9773	0.9291	0.9270	0.9487	0.9254
	Step 3	0.9470	0.9564	0.9290	0.9707	0.9191	0.9176	0.9393	0.9171
	Step 4	0.9393	0.9482	0.9186	0.9645	0.9100	0.9087	0.9309	0.9098
Controlled DG	Step 1	0.9834	0.9700	0.9541	0.9709	0.9712	0.9659	0.9913	0.9353
	Step 2	0.9912	0.9630	0.9408	0.9934	0.9803	0.9500	0.9992	0.9254
	Step 3	0.9945	0.9570	0.9290	0.9983	0.9850	0.9334	0.9999	0.9171
	Step 4	0.9957	0.9516	0.9186	0.9995	0.9867	0.9168	1.0000	0.9098
DG	Step 1	0.6549	0.9520	0.9541	0.5521	0.6594	0.9881	0.2393	0.9353
	Step 2	0.6926	0.9397	0.9408	0.6478	0.6833	0.9842	0.4181	0.9254
	Step 3	0.7141	0.9294	0.9290	0.6998	0.6968	0.9801	0.5128	0.9171
	Step 4	0.7269	0.9205	0.9186	0.7305	0.7044	0.9760	0.5676	0.9098

7.3 Results for wind speed 10 m/s

Table 7.10 Voltage values of busbars for all steps and all cases (V) (10 m/s).

Case		Bus 1	Bus 2	Bus 3	Bus 4	Bus 5	Bus 6
Normal	Step 1	64,896	62,719	61,846	62,501	61,238	61,692
	Step 2	64,664	62,137	61,077	61,812	60,331	60,842

	Step 3	64,434	61,563	60,320	61,134	59,441	60,005
	Step 4	64,206	60,999	59,577	60,467	58,567	59,184
Controlled DG	Step 1	65,832	65,070	64,323	65,402	63,690	64,556
	Step 2	65,781	64,872	63,955	65,207	63,175	64,183
	Step 3	65,729	64,672	63,588	65,010	62,661	63,809
	Step 4	65,672	64,471	63,221	64,811	62,150	63,435
DG	Step 1	65,091	63,397	62,573	63,382	61,958	62,562
	Step 2	64,874	62,840	61,828	62,724	61,073	61,739
	Step 3	64,658	62,290	61,095	62,076	60,204	60,930
	Step 4	64,442	61,748	60,373	61,437	59,350	60,133

Table 7.11 Sending voltage values of lines for all steps and all cases (V) (10 m/s).

Case		L 0-2	L 2-3	L 3-5	L 0-1	L 1-2	L 3-4	L 1-4	L 4-6
Normal	Step 1	65,630	62,719	61,846	65,630	64,896	62,501	64,896	62,501
	Step 2	65,542	62,137	61,077	65,542	64,664	61,812	64,664	61,812
	Step 3	65,454	61,563	60,320	65,454	64,434	61,134	64,434	61,134
	Step 4	65,366	60,999	59,577	65,366	64,206	60,467	64,206	60,467
Controlled DG	Step 1	65,988	65,070	64,323	65,988	65,832	65,402	65,832	65,402
	Step 2	65,976	64,872	63,955	65,976	65,781	65,207	65,781	65,207
	Step 3	65,962	64,672	63,588	65,962	65,729	65,010	65,729	65,010
	Step 4	65,947	64,471	63,221	65,947	65,672	64,811	65,672	64,811
DG	Step 1	65,673	63,397	62,573	65,673	65,091	63,382	65,091	63,382
	Step 2	65,592	62,840	61,828	65,592	64,874	62,724	64,874	62,724
	Step 3	65,510	62,290	61,095	65,510	64,658	62,076	64,658	62,076
	Step 4	65,429	61,748	60,373	65,429	64,442	61,437	64,442	61,437

Table 7.12 Receiving voltage values of lines for all steps and all cases (V) (10 m/s).

Case		L 0-2	L 2-3	L 3-5	L 0-1	L 1-2	L 3-4	L 1-4	L 4-6
Normal	Step 1	62,719	61,846	61,238	64,896	62,719	61,846	62,501	61,692
	Step 2	62,137	61,077	60,331	64,664	62,137	61,077	61,812	60,842
	Step 3	61,563	60,320	59,441	64,434	61,563	60,320	61,134	60,005
	Step 4	60,999	59,577	58,567	64,206	60,999	59,577	60,467	59,184
Controlled DG	Step 1	65,070	64,323	63,690	65,832	65,070	64,323	65,402	64,556
	Step 2	64,872	63,955	63,175	65,781	64,872	63,955	65,207	64,183
	Step 3	64,672	63,588	62,661	65,729	64,672	63,588	65,010	63,809
	Step 4	64,471	63,221	62,150	65,672	64,471	63,221	64,811	63,435
DG	Step 1	63,397	62,573	61,958	65,091	63,397	62,573	63,382	62,562
	Step 2	62,840	61,828	61,073	64,874	62,840	61,828	62,724	61,739
	Step 3	62,290	61,095	60,204	64,658	62,290	61,095	62,076	60,930
	Step 4	61,748	60,373	59,350	64,442	61,748	60,373	61,437	60,133

Table 7.13 Voltage drop values of lines for all steps and all cases (V) (10 m/s).

Case		L 0-2	L 2-3	L 3-5	L 0-1	L 1-2	L 3-4	L 1-4	L 4-6
Normal	Step 1	2,912	872	608	735	2,177	654	2,395	808
	Step 2	3,405	1,060	746	878	2,527	735	2,852	970
	Step 3	3,891	1,243	879	1,020	2,871	814	3,300	1,129

	Step 4	4,368	1,422	1,009	1,160	3,207	890	3,739	1,283
Controlled DG	Step 1	918	747	632	156	761	1,079	430	846
	Step 2	1,104	916	781	194	910	1,252	574	1,024
	Step 3	1,290	1,084	927	233	1,057	1,422	719	1,200
	Step 4	1,476	1,250	1,071	274	1,202	1,590	862	1,376
DG	Step 1	2,276	824	615	582	1,693	808	1,709	820
	Step 2	2,752	1,012	755	718	2,034	896	2,149	985
	Step 3	3,221	1,195	891	853	2,368	981	2,582	1,146
	Step 4	3,681	1,375	1,023	986	2,695	1,064	3,005	1,304

Table 7.14 Sending $\cos(\varphi)$ values of lines for all steps and all cases (10 m/s).

Case		L 0-2	L 2-3	L 3-5	L 0-1	L 1-2	L 3-4	L 1-4	L 4-6
Normal	Step 1	0.9585	0.9751	0.9641	0.9892	0.9536	0.9821	0.9519	0.9489
	Step 2	0.9454	0.9636	0.9493	0.9821	0.9393	0.9729	0.9374	0.9363
	Step 3	0.9329	0.9529	0.9358	0.9748	0.9258	0.9633	0.9242	0.9253
	Step 4	0.9211	0.9430	0.9235	0.9675	0.9132	0.9535	0.9120	0.9155
Controlled DG	Step 1	0.9986	0.9830	0.9641	0.9814	0.9986	0.9600	0.9894	0.9489
	Step 2	0.9994	0.9752	0.9493	0.9845	0.9995	0.9379	0.9928	0.9363
	Step 3	0.9998	0.9680	0.9358	0.9868	0.9999	0.9145	0.9948	0.9253
	Step 4	1.0000	0.9614	0.9235	0.9887	1.0000	0.8908	0.9962	0.9156
DG	Step 1	0.9093	0.9668	0.9641	0.9462	0.9124	0.9929	0.8585	0.9489
	Step 2	0.8934	0.9537	0.9493	0.9359	0.8934	0.9881	0.8459	0.9363
	Step 3	0.8797	0.9420	0.9358	0.9270	0.8771	0.9827	0.8354	0.9253
	Step 4	0.8674	0.9315	0.9235	0.9190	0.8627	0.9770	0.8260	0.9155

Table 7.15 Receiving $\cos(\varphi)$ values of lines for all steps and all cases (10 m/s).

Case		L 0-2	L 2-3	L 3-5	L 0-1	L 1-2	L 3-4	L 1-4	L 4-6
Normal	Step 1	0.9644	0.9755	0.9541	0.9840	0.9401	0.9370	0.9593	0.9353
	Step 2	0.9554	0.9655	0.9408	0.9773	0.9291	0.9270	0.9487	0.9254
	Step 3	0.9470	0.9564	0.9290	0.9707	0.9191	0.9176	0.9393	0.9171
	Step 4	0.9393	0.9482	0.9186	0.9645	0.9100	0.9087	0.9309	0.9098
Controlled DG	Step 1	0.9997	0.9823	0.9541	0.9939	0.9984	0.9266	0.9920	0.9353
	Step 2	0.9996	0.9757	0.9408	0.9937	0.9986	0.9030	0.9930	0.9254
	Step 3	0.9996	0.9699	0.9290	0.9937	0.9987	0.8797	0.9935	0.9171
	Step 4	0.9996	0.9647	0.9186	0.9939	0.9987	0.8570	0.9939	0.9098
DG	Step 1	0.8983	0.9659	0.9541	0.9202	0.8692	0.9740	0.8485	0.9353
	Step 2	0.8888	0.9544	0.9408	0.9147	0.8585	0.9678	0.8428	0.9254
	Step 3	0.8808	0.9445	0.9290	0.9096	0.8493	0.9617	0.8379	0.9171
	Step 4	0.8736	0.9357	0.9186	0.9048	0.8410	0.9556	0.8333	0.9098

7.4 Results for wind speed 5 m/s

Table 7.16 Voltage values of busbars for all steps and all cases (V) (5 m/s).

Case		Bus 1	Bus 2	Bus 3	Bus 4	Bus 5	Bus 6
Normal	Step 1	64,896	62,719	61,846	62,501	61,238	61,692
	Step 2	64,664	62,137	61,077	61,812	60,331	60,842
	Step 3	64,434	61,563	60,320	61,134	59,441	60,005

	Step 4	64,206	60,999	59,577	60,467	58,567	59,184
Controlled DG	Step 1	65,817	64,828	64,070	65,111	63,440	64,269
	Step 2	65,759	64,621	63,694	64,906	62,916	63,887
	Step 3	65,698	64,411	63,317	64,700	62,394	63,505
	Step 4	65,633	64,200	62,941	64,491	61,875	63,122
DG	Step 1	64,944	62,854	61,992	62,678	61,382	61,868
	Step 2	64,718	62,283	61,234	62,005	60,487	61,032
	Step 3	64,493	61,721	60,489	61,342	59,607	60,210
	Step 4	64,271	61,168	59,758	60,693	58,746	59,405

Table 7.17 Sending voltage values of lines for all steps and all cases (V) (5 m/s).

Case		L 0-2	L 2-3	L 3-5	L 0-1	L 1-2	L 3-4	L 1-4	L 4-6
Normal	Step 1	65,630	62,719	61,846	65,630	64,896	62,501	64,896	62,501
	Step 2	65,542	62,137	61,077	65,542	64,664	61,812	64,664	61,812
	Step 3	65,454	61,563	60,320	65,454	64,434	61,134	64,434	61,134
	Step 4	65,366	60,999	59,577	65,366	64,206	60,467	64,206	60,467
Controlled DG	Step 1	66,015	64,828	64,070	66,015	65,817	65,111	65,817	65,111
	Step 2	65,998	64,621	63,694	65,998	65,759	64,906	65,759	64,906
	Step 3	65,980	64,411	63,317	65,980	65,698	64,700	65,698	64,700
	Step 4	65,960	64,200	62,941	65,960	65,633	64,491	65,633	64,491
DG	Step 1	65,646	62,854	61,992	65,646	64,944	62,678	64,944	62,678
	Step 2	65,560	62,283	61,234	65,560	64,718	62,005	64,718	62,005
	Step 3	65,475	61,721	60,489	65,475	64,493	61,342	64,493	61,342
	Step 4	65,389	61,168	59,758	65,389	64,271	60,693	64,271	60,693

Table 7.18 Receiving voltage values of lines for all steps and all cases (V) (5 m/s).

Case		L 0-2	L 2-3	L 3-5	L 0-1	L 1-2	L 3-4	L 1-4	L 4-6
Normal	Step 1	62,719	61,846	61,238	64,896	62,719	61,846	62,501	61,692
	Step 2	62,137	61,077	60,331	64,664	62,137	61,077	61,812	60,842
	Step 3	61,563	60,320	59,441	64,434	61,563	60,320	61,134	60,005
	Step 4	60,999	59,577	58,567	64,206	60,999	59,577	60,467	59,184
Controlled DG	Step 1	64,828	64,070	63,440	65,817	64,828	64,070	65,111	64,269
	Step 2	64,621	63,694	62,916	65,759	64,621	63,694	64,906	63,887
	Step 3	64,411	63,317	62,394	65,698	64,411	63,317	64,700	63,505
	Step 4	64,200	62,941	61,875	65,633	64,200	62,941	64,491	63,122
DG	Step 1	62,854	61,992	61,382	64,944	62,854	61,992	62,678	61,868
	Step 2	62,283	61,234	60,487	64,718	62,283	61,234	62,005	61,032
	Step 3	61,721	60,489	59,607	64,493	61,721	60,489	61,342	60,210
	Step 4	61,168	59,758	58,746	64,271	61,168	59,758	60,693	59,405

Table 7.19 Voltage drop values of lines for all steps and all cases (V) (5 m/s).

Case		L 0-2	L 2-3	L 3-5	L 0-1	L 1-2	L 3-4	L 1-4	L 4-6
Normal	Step 1	2,912	872	608	735	2,177	654	2,395	808
	Step 2	3,405	1,060	746	878	2,527	735	2,852	970
	Step 3	3,891	1,243	879	1,020	2,871	814	3,300	1,129
	Step 4	4,368	1,422	1,009	1,160	3,207	890	3,739	1,283

Controlled DG	Step 1	1,187	759	630	198	988	1,041	706	842
	Step 2	1,378	927	778	240	1,138	1,213	852	1,019
	Step 3	1,569	1,094	923	283	1,286	1,383	998	1,195
	Step 4	1,760	1,259	1,066	328	1,432	1,550	1,142	1,369
DG	Step 1	2,792	862	610	702	2,090	686	2,266	810
	Step 2	3,277	1,049	748	842	2,435	771	2,713	974
	Step 3	3,754	1,232	882	981	2,773	853	3,151	1,133
	Step 4	4,222	1,409	1,012	1,118	3,103	935	3,578	1,288

Table 7.20 Sending $\cos(\varphi)$ values of lines for all steps and all cases (5 m/s).

Case		L 0-2	L 2-3	L 3-5	L 0-1	L 1-2	L 3-4	L 1-4	L 4-6
Normal	Step 1	0.9585	0.9751	0.9641	0.9892	0.9536	0.9821	0.9519	0.9489
	Step 2	0.9454	0.9636	0.9493	0.9821	0.9393	0.9729	0.9374	0.9363
	Step 3	0.9329	0.9529	0.9358	0.9748	0.9258	0.9633	0.9242	0.9253
	Step 4	0.9211	0.9430	0.9235	0.9675	0.9132	0.9535	0.9120	0.9155
Controlled DG	Step 1	0.9971	0.9901	0.9641	0.9770	0.9979	0.8986	0.9905	0.9489
	Step 2	0.9983	0.9834	0.9493	0.9802	0.9989	0.8691	0.9925	0.9363
	Step 3	0.9991	0.9771	0.9358	0.9830	0.9996	0.8322	0.9944	0.9253
	Step 4	0.9996	0.9710	0.9235	0.9852	0.9999	0.7996	0.9957	0.9156
DG	Step 1	0.9560	0.9742	0.9641	0.9874	0.9515	0.9843	0.9476	0.9489
	Step 2	0.9422	0.9626	0.9493	0.9799	0.9362	0.9756	0.9323	0.9363
	Step 3	0.9293	0.9518	0.9358	0.9722	0.9222	0.9666	0.9187	0.9253
	Step 4	0.9172	0.9418	0.9235	0.9648	0.9091	0.9573	0.9062	0.9155

Table 7.21 Receiving $\cos(\varphi)$ values of lines for all steps and all cases (5 m/s).

Case		L 0-2	L 2-3	L 3-5	L 0-1	L 1-2	L 3-4	L 1-4	L 4-6
Normal	Step 1	0.9644	0.9755	0.9541	0.9840	0.9401	0.9370	0.9593	0.9353
	Step 2	0.9554	0.9655	0.9408	0.9773	0.9291	0.9270	0.9487	0.9254
	Step 3	0.9470	0.9564	0.9290	0.9707	0.9191	0.9176	0.9393	0.9171
	Step 4	0.9393	0.9482	0.9186	0.9645	0.9100	0.9087	0.9309	0.9098
Controlled DG	Step 1	0.9949	0.9903	0.9541	0.9836	0.9998	0.8349	0.9858	0.9353
	Step 2	0.9954	0.9846	0.9408	0.9849	0.9999	0.8112	0.9867	0.9255
	Step 3	0.9958	0.9795	0.9291	0.9862	0.9999	0.7772	0.9876	0.9171
	Step 4	0.9961	0.9747	0.9186	0.9872	1.0000	0.7487	0.9882	0.9099
DG	Step 1	0.9607	0.9745	0.9541	0.9811	0.9360	0.9448	0.9539	0.9353
	Step 2	0.9509	0.9644	0.9408	0.9740	0.9239	0.9346	0.9425	0.9254
	Step 3	0.9422	0.9552	0.9290	0.9672	0.9136	0.9253	0.9328	0.9171
	Step 4	0.9342	0.9470	0.9185	0.9609	0.9040	0.9164	0.9241	0.9098

7.5 Results for fault L 2-3, wind speed 5 m/s

Table 7.22 Voltage values of busbars for all steps and all cases (V) (Fault line 2-3, 5 m/s).

Case		Bus 1	Bus 2	Bus 3	Bus 4	Bus 5	Bus 6
Normal	Step 1	64,687	63,896	57,840	60,627	57,271	59,843
	Step 2	64,422	63,575	56,334	59,607	55,646	58,671
	Step 3	64,163	63,257	54,885	58,620	54,085	57,538
	Step 4	63,909	62,944	53,493	57,668	52,587	56,444

Controlled DG	Step 1	66,017	66,293	61,799	64,777	61,192	63,939
	Step 2	65,991	66,393	60,954	64,495	60,210	63,483
	Step 3	65,961	66,483	60,120	64,212	59,244	63,026
	Step 4	65,929	66,617	59,235	63,857	58,231	62,502
DG	Step 1	64,746	64,004	58,074	60,872	57,503	60,085
	Step 2	64,496	63,695	56,621	59,911	55,930	58,971
	Step 3	64,321	63,428	55,533	59,312	54,723	58,217
	Step 4	64,179	63,181	54,616	58,878	53,691	57,628

Table 7.23 Sending voltage values of lines for all steps and all cases (V) (Fault line 2-3, 5 m/s).

Case		L 0-2	L 2-3	L 3-5	L 0-1	L 1-2	L 3-4	L 1-4	L 4-6
Normal	Step 1	65,695	-	57,840	65,695	64,687	60,627	64,687	60,627
	Step 2	65,627	-	56,334	65,627	64,422	59,607	64,422	59,607
	Step 3	65,558	-	54,885	65,558	64,163	58,620	64,163	58,620
	Step 4	65,490	-	53,493	65,490	63,909	57,668	63,909	57,668
Controlled DG	Step 1	66,186	-	61,799	66,186	66,017	64,777	66,017	64,777
	Step 2	66,206	-	60,954	66,206	65,991	64,495	65,991	64,495
	Step 3	66,224	-	60,120	66,224	65,961	64,212	65,961	64,212
	Step 4	66,245	-	59,235	66,245	65,929	63,857	65,929	63,857
DG	Step 1	65,710	-	58,074	65,710	64,746	60,872	64,746	60,872
	Step 2	65,645	-	56,621	65,645	64,496	59,911	64,496	59,911
	Step 3	65,598	-	55,533	65,598	64,321	59,312	64,321	59,312
	Step 4	65,558	-	54,616	65,558	64,179	58,878	64,179	58,878

Table 7.24 Receiving voltage values of lines for all steps and all cases (V) (Fault line 2-3, 5 m/s).

Case		L 0-2	L 2-3	L 3-5	L 0-1	L 1-2	L 3-4	L 1-4	L 4-6
Normal	Step 1	63,896	-	57,271	64,687	63,896	57,840	60,627	59,843
	Step 2	63,575	-	55,646	64,422	63,575	56,334	59,607	58,671
	Step 3	63,257	-	54,085	64,163	63,257	54,885	58,620	57,538
	Step 4	62,944	-	52,587	63,909	62,944	53,493	57,668	56,444
Controlled DG	Step 1	66,293	-	61,192	66,017	66,293	61,799	64,777	63,939
	Step 2	66,393	-	60,210	65,991	66,393	60,954	64,495	63,483
	Step 3	66,483	-	59,244	65,961	66,483	60,120	64,212	63,026
	Step 4	66,617	-	58,231	65,929	66,617	59,235	63,857	62,502
DG	Step 1	64,004	-	57,503	64,746	64,004	58,074	60,872	60,085
	Step 2	63,695	-	55,930	64,496	63,695	56,621	59,911	58,971
	Step 3	63,428	-	54,723	64,321	63,428	55,533	59,312	58,217
	Step 4	63,181	-	53,691	64,179	63,181	54,616	58,878	57,628

Table 7.25 Voltage drop values of lines for all steps and all cases (V) (Fault line 2-3, 5 m/s).

Case		L 0-2	L 2-3	L 3-5	L 0-1	L 1-2	L 3-4	L 1-4	L 4-6
Normal	Step 1	1,799	-	569	1,008	791	2,787	4,060	784
	Step 2	2,052	-	688	1,204	847	3,273	4,815	936
	Step 3	2,301	-	800	1,396	905	3,735	5,542	1,082

	Step 4	2,546	-	906	1,582	965	4,174	6,241	1,224
Controlled DG	Step 1	-108	-	608	169	-277	2,978	1,240	838
	Step 2	-187	-	744	215	-401	3,542	1,496	1,013
	Step 3	-259	-	876	263	-521	4,092	1,749	1,186
	Step 4	-371	-	1,004	317	-688	4,622	2,072	1,355
DG	Step 1	1,706	-	571	964	742	2,798	3,874	787
	Step 2	1,951	-	691	1,149	801	3,290	4,585	941
	Step 3	2,170	-	810	1,277	892	3,780	5,009	1,095
	Step 4	2,377	-	925	1,379	997	4,262	5,301	1,250

Table 7.26 Sending $\cos(\varphi)$ values of lines for all steps and all cases (Fault line 2-3, 5 m/s).

Case		L 0-2	L 2-3	L 3-5	L 0-1	L 1-2	L 3-4	L 1-4	L 4-6
Normal	Step 1	0.9616	-	0.9641	0.9808	0.9490	0.9612	0.9354	0.9489
	Step 2	0.9513	-	0.9493	0.9704	0.9415	0.9465	0.9164	0.9363
	Step 3	0.9414	-	0.9358	0.9600	0.9345	0.9327	0.8989	0.9253
	Step 4	0.9320	-	0.9235	0.9499	0.9278	0.9197	0.8828	0.9155
Controlled DG	Step 1	0.9263	-	0.9641	0.9679	0.7729	0.9611	0.9942	0.9489
	Step 2	0.9227	-	0.9493	0.9721	0.7449	0.9465	0.9964	0.9363
	Step 3	0.9178	-	0.9358	0.9755	0.7080	0.9327	0.9978	0.9253
	Step 4	0.9147	-	0.9235	0.9777	0.6879	0.9197	0.9986	0.9156
DG	Step 1	0.9579	-	0.9641	0.9792	0.9408	0.9611	0.9324	0.9489
	Step 2	0.9464	-	0.9493	0.9680	0.9312	0.9465	0.9124	0.9363
	Step 3	0.9389	-	0.9358	0.9655	0.9080	0.9327	0.9131	0.9253
	Step 4	0.9336	-	0.9235	0.9665	0.8826	0.9197	0.9206	0.9156

Table 7.27 Receiving $\cos(\varphi)$ values of lines for all steps and all cases (Fault line 2-3, 5 m/s).

Case		L 0-2	L 2-3	L 3-5	L 0-1	L 1-2	L 3-4	L 1-4	L 4-6
Normal	Step 1	0.9521	-	0.9541	0.9777	0.8426	0.9685	0.9571	0.9353
	Step 2	0.9440	-	0.9408	0.9684	0.8396	0.9586	0.9445	0.9254
	Step 3	0.9364	-	0.9290	0.9593	0.8373	0.9495	0.9331	0.9171
	Step 4	0.9293	-	0.9186	0.9506	0.8353	0.9413	0.9228	0.9098
Controlled DG	Step 1	0.9351	-	0.9541	0.9710	0.8932	0.9685	0.9820	0.9353
	Step 2	0.9267	-	0.9408	0.9732	0.8527	0.9586	0.9834	0.9254
	Step 3	0.9179	-	0.9291	0.9751	0.8065	0.9495	0.9844	0.9171
	Step 4	0.9107	-	0.9186	0.9761	0.7744	0.9413	0.9844	0.9099
DG	Step 1	0.9459	-	0.9541	0.9754	0.8188	0.9685	0.9533	0.9353
	Step 2	0.9366	-	0.9408	0.9653	0.8133	0.9586	0.9395	0.9254
	Step 3	0.9316	-	0.9291	0.9643	0.7916	0.9495	0.9439	0.9171
	Step 4	0.9291	-	0.9186	0.9666	0.7724	0.9413	0.9534	0.9099

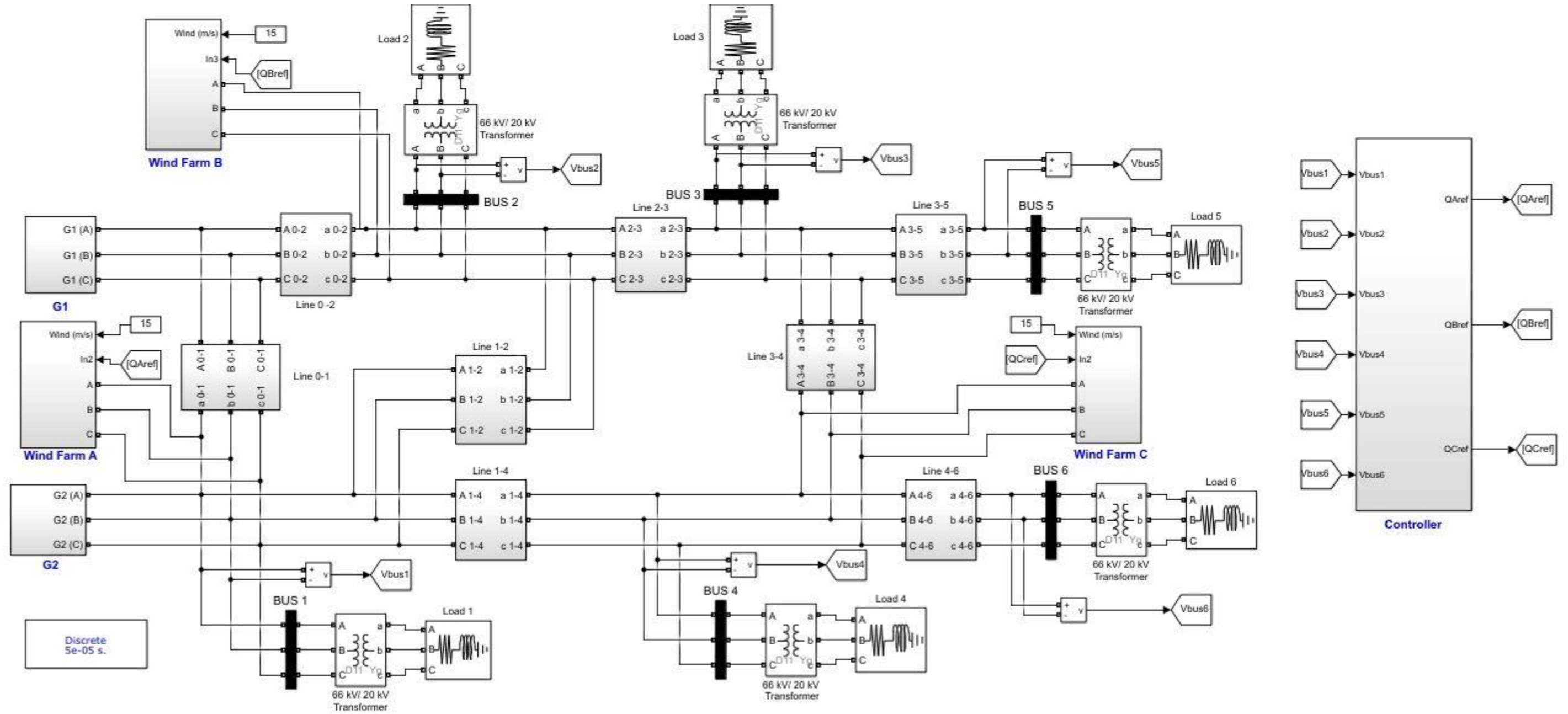


Figure 7.1 MATLAB Simulink model of the electrical system.

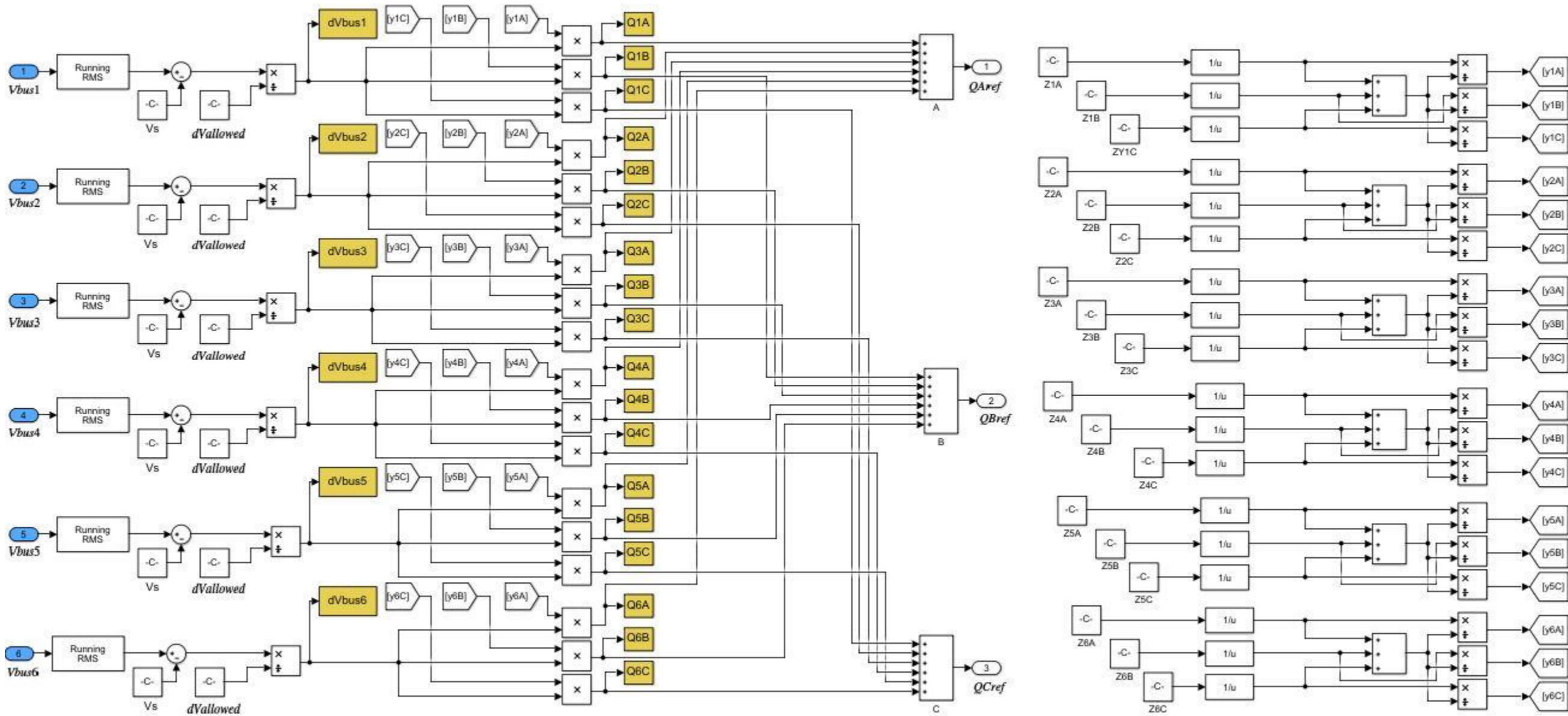


Figure 7.2 MATLAB Simulink model of the controller (Busbars voltage inputs).

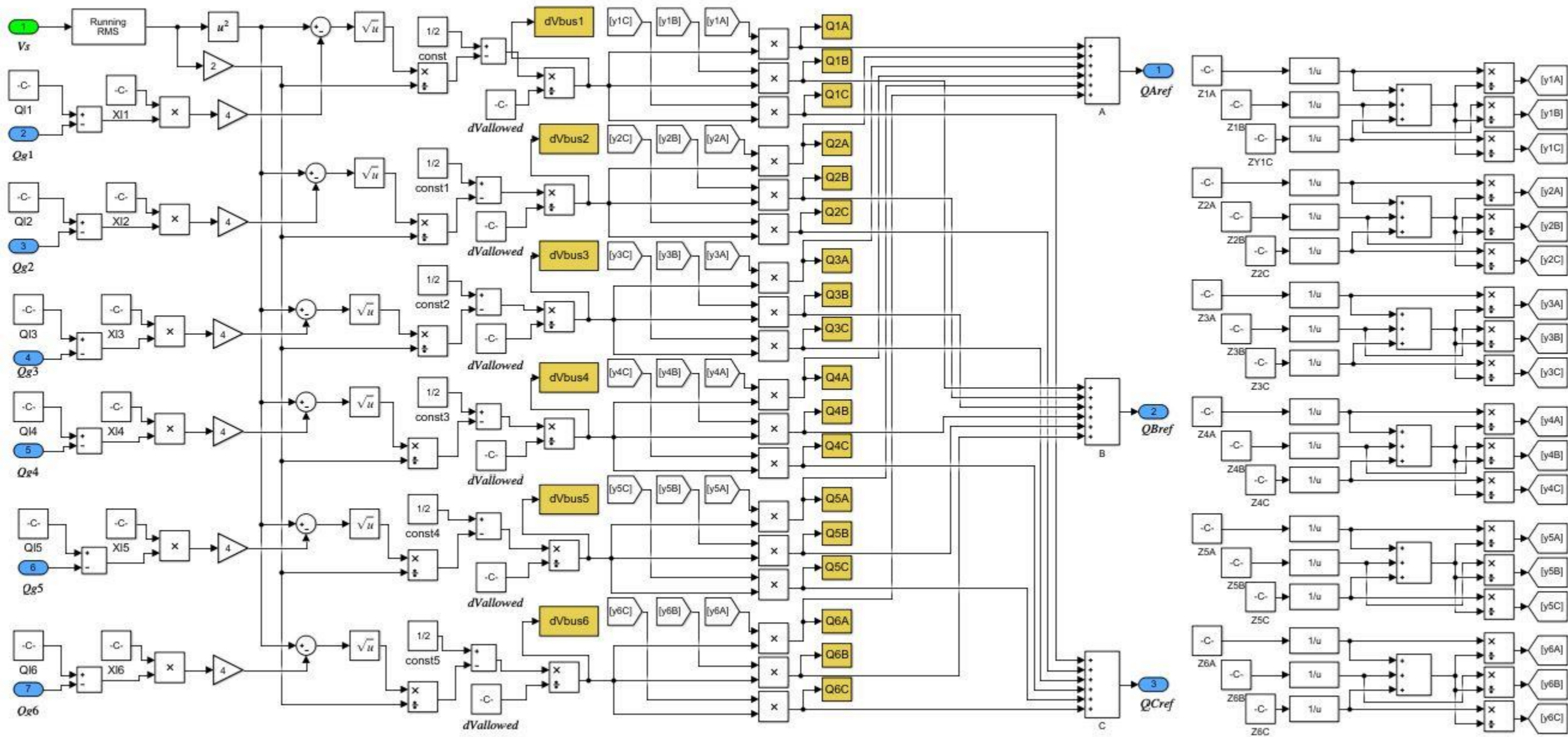


Figure 7.3 MATLAB Simulink model of the controller (Reactive power inputs).